January 2015

Finite Element Analysis of the Equine Distal Limb Transfixation Cast

Timothy B. Lescun
Purdue University

Graduate School Form 30
Updated 1/15/2015

PURDUE UNIVERSITY
GRADUATE SCHOOL
Thesis/Dissertation Acceptance

This is to certify that the thesis/dissertation prepared

By Timothy B. Lescun

Entitled
Finite Element Analysis of the Equine Distal Limb Transfixation Cast

For the degree of Doctor of Philosophy

Is approved by the final examining committee:

Gert J. Breur
Co-chair

Eric A. Nauman
Co-chair

Srinivasan Chandrasekar

Stephen B. Adams

To the best of my knowledge and as understood by the student in the Thesis/Dissertation Agreement, Publication Delay, and Certification Disclaimer (Graduate School Form 32), this thesis/dissertation adheres to the provisions of Purdue University's "Policy of Integrity in Research" and the use of copyright material.

Approved by Major Professor(s): Gert J. Breur

Approved by: J. Catharine Scott-Moncrieff 11/25/2015

Head of the Departmental Graduate Program Date

FINITE ELEMENT ANALYSIS OF THE EQUINE DISTAL LIMB TRANSFIXATION CAST

A Dissertation

Submitted to the Faculty

of

Purdue University

by

Timothy B. Lescun

In Partial Fulfillment of the

Requirements for the Degree

of

Doctor of Philosophy

December 2015

Purdue University

West Lafayette, Indiana

For Heidi and Lili. Your love, support and understanding means everything to me.

For my parents. Thank you for giving me the gift of education and for showing me the value of hard work and perseverance.

ACKNOWLEDGEMENTS

I would like to thank Dr. Gert Breur for his guidance, support and expertise during my graduate training and in the completion of this work. The stimulating discussions and challenging of ideas were invaluable to me throughout the process. I would like to thank Dr. Eric Nauman for providing thought provoking ideas, encouragement and expertise in the concepts and practice of modeling biologic phenomena. I would also like to thank Dr. Stephen Adams, for his continued support of my education and for constantly challenging me to make discoveries that are clinically relevant and that can contribute to the art and science of equine surgery. I would like to thank Dr. Srinivasan Chandrasekar, for showing me how engineering concepts can be applied to biologic phenomena, for enhancing my understanding of material behavior and for providing access to technical support throughout this work.

I would like to thank Dr. Russell Main for his support and assistance in this work as well as Kari Jensen, Anirban Mahato, Haisheng Yang and Max Gallant for their technical assistance. I would like to acknowledge my faculty colleagues Dr. Jan Hawkins and Dr. Nickie Baird for their support throughout this process. I would especially like to thank and acknowledge the support of Dr. Peter Constable, for encouraging and assisting me to undertake graduate studies as a faculty member, and Dr. Catharine Scott-Moncrieff for her continued support of this process.

I would like to acknowledge and thank Jim, Angus, Geoff, Steve, Scott, Jan, Jack, Gert and Dave, for their mentorship over the years of my professional career, providing me with unique perspectives on research and veterinary surgery, and instilling in me the passion to pursue ideas and seek answers.

TABLE OF CONTENTS

Page

Page

LIST OF TABLES

Table Page

LIST OF FIGURES

Figure Page

Figure Page

Figure Page

LIST OF ABBREVIATIONS

BPI = Bone-pin interface

CPI = Cast-pin interface

CT = Computed tomography

ESF = External skeletal fixator

FE = Finite element

GPa = Gigapascals

Kg = kilograms

MC3 = Third metacarpal bone

mm = millimeters

MPa = Megapascals

MT3 = Third metatarsal bone

N = Newtons

PMMA = Polymethylmethacrylate

ABSTRACT

Lescun, Timothy B. Ph.D., Purdue University, December 2015. Finite Element Analysis of the Equine Distal Limb Transfixation Cast. Major Professors: Gert Breur and Eric Nauman.

Transfixation casting is a method of managing distal limb fractures in the horse. It has similarities to external skeletal fixation including the use of transcortical pins and the complications that occur as a result of concentrated stresses at the bone-pin interface. Currently, the major challenges facing equine surgeons when using a transfixation cast are pin loosening, secondary pin hole fracture and excessive stress reduction distal to the transcortical pins during healing. The equine distal limb transfixation cast was modeled from a computed tomography scan of a representative third metacarpal bone of the horse. Finite element analysis was performed to evaluate the impact of pin parameters on bone-pin interface stresses and strains. The parameters were pin diameter, number, type (half or full, threaded or smooth), spacing, orientation, location within the bone and pin material. The model was also used to determine the effect of the cast-pin interface attachment, and to determine the effect of increasing fracture tissue stiffness or external foot contact pressure, on bone-pin interface stresses. A general approach to transcortical pin selection was developed based on the total pin area moment of inertia of pins in the cast. Pin diameter and pin number had the most profound influence on bone-pin interface stresses. Cast-pin interface attachment influenced the bone-pin interface stresses and modeling a fixed pin end position underestimated bone-pin interface stresses. Increasing distal contact pressure and tissue modulus decreased bone-pin interface stresses and their distribution around pin holes. The results of this study will assist equine surgeons in improving transfixation casting in the horse by employing methods that help to minimize complications associated with the bone-pin interface that are currently limiting the clinical success of this technique.

CHAPTER 1. INTRODUCTION

1.1 Introduction

Fractures in the horse are difficult to treat successfully. Public perception of the current capability to treat a major equine fracture is that it is extremely challenging, frequently impossible and often humane euthanasia is the most appropriate course of action available. This perception has been reinforced in recent times by the occurrence of catastrophic (fatal) fractures during nationally televised Thoroughbred racing events and other high profile equestrian sports. Injuries to Kentucky Derby winner Barbaro in the 2006 Preakness Stakes, and the 3-year-old filly Eight Belles immediately after crossing the finish line 2nd during the 2008 Kentucky Derby both resulted in euthanasia of the horse involved. Treatment of Eight Belles' injuries was not attempted; however Barbaro was treated by world-renowned equine veterinary surgeons and support team, in state-of-the-art facilities, with essentially no financial constraints. These events highlight the challenge that these major injuries present for the veterinarian. While current public perception may, at least clinically, under-represent the potential for surgical repair, the reality is that fracture treatment in the horse, despite many advances, remains a challenging undertaking plagued by life-threatening complications and co-morbidities. Improvements are needed in our capability to treat major musculoskeletal injuries in the horse.

The domesticated horse is an animal which retains a strong "flight" instinct in response to danger and is consequently prone to traumatic injuries. Injuries or trauma were estimated to be responsible for 16 – 24% of equine fatalities in a national survey conducted by the United States Department of Agriculture in 2005.[1] Fractures accounted for approximately

9% of all equine cases seen by U.S. veterinary medical teaching hospitals as well as 10% of all equine mortality insurance claims in a survey in France.[2,3] Fractures occurred in approximately 7% of foals during the first year of life in an Irish survey conducted on Thoroughbred breeding farms, accounting for 14% of total foal mortalities.[4] Catastrophic musculoskeletal injuries also result in significant losses in the racing industry, estimated to occur at a rate of approximately 5 per 1000 race starts by the California Postmortem Program when both racing and training injuries are included.[5] Fractures are a significant cause of both morbidity and mortality in the horse.

Commonly employed methods of fracture fixation used in humans and other species, such as internal plate and lag screw fixation, intra-medullary pinning techniques (including intra-medullary nails), and external fixation have been utilized in the horse. Each has demonstrated specific advantages and disadvantages in the treatment of equine fractures. Repair methods that have greater biomechanical stability have generally been most successful in the horse. When compared to humans and other lighter weight animals, the large bodyweight and fractious nature of the horse, the stress that immediate post-operative weight bearing places on the fracture fixation and the requirement for early patient comfort on the fractured limb post-operatively are unique factors which influence the choice of repair method. However, no one bone fixation method can be applied to all fracture types and locations. Equine fractures often involve multiple bone pieces and significant soft-tissue injury, making reconstructive efforts with internal fixation challenging and in some cases futile.

Several complications are known to limit the success of fracture repair in horses, with implant failure, supporting limb laminitis and infection being the most significant.[6–10] Implant failure is a well-recognized limitation of equine internal fixation, particularly in fractures where complete bone reconstruction is not possible.[6] Horses are also susceptible to secondary complications when the non-injured opposite limb and foot is overloaded due to ongoing pain and instability in the injured limb. Excessive weight-bearing on the opposite foot can result in support limb laminitis, a condition where the laminar

attachments between the hoof wall and the distal phalanx separate over time.[11] Laminitis is itself associated with severe pain and permanent damage to the laminar junction. Laminitis is a major complication of fracture treatment in the horse and has been a significant hindrance to success,[7,8] as it was during the treatment of Barbaro. Another of the unique challenges presented by the equine fracture patient is the sparse soft tissue coverage of bones in the distal limb. This feature results in a high rate of fractures that are open or where skin overlying the bone becomes severely traumatized.[3,9,12] Osteomyelitis and implant-associated infections are serious complications associated with treatment of these fractures using internal fixation and contribute to treatment failure.[10] Improvement in equine fracture repair requires consideration of the spectrum of challenges that these injuries present and of the various fixation methods that are available.

External skeletal fixation has been used with good success in humans and small animals to overcome some of the disadvantages associated with internal fixation for fracture repair.[13] External fixation achieves fracture stabilization through the placement of transcortical pins across intact segments of bone adjacent to the fracture site, which are then connected to each other externally using sidebars and clamps. External fixation is particularly well suited to highly comminuted or open fractures, and those fractures associated with extensive soft-tissue or vascular damage, as it allows limb stabilization without requiring complete bone reconstruction and without surgically exposing the fracture site. However, premature pin loosening and pin hole infections are common complications associated with external fixation.[14–16] An additional drawback to the use of external fixation in the horse has been the occurrence of secondary fracture through a pin hole, which significantly complicates further treatment and often results in euthanasia.[6,12,15,17–19] Stress protection during external fixation in the horse can also have adverse effects on both fracture healing and the bone strength of the protected region of the limb.[17,18]

Transfixation casting is a modified form of external skeletal fixation that has been used to treat complicated distal limb fractures, such as those which are open or highly

comminuted, in the horse.[6,12,15,17,18] Transcortical pins placed through the bone, proximal to the fracture site, are incorporated into a distal limb cast which encompasses the foot **(Figure 1.1)**. The cast acts as the sidebars of a traditional external fixator and weight-bearing loads are transferred from the bone, through the pins and cast to the ground. Significant reductions in bone strain and of fracture collapse in the proximal phalanx were found when a transfixation cast with pins in the **third metacarpal bone (MC3)** was compared to a standard half limb cast.[20–23] Horses wearing transfixation casts are normally comfortable and able to use the fractured limb while the construct remains stable.[15,16] A significant limitation, however, is that transfixation pins, similar to external fixation pins, invariably loosen over time due to osteoclastic bone resorption and fibrous tissue formation at the **bone-pin interface (BPI)**.[24] This occurs more rapidly in the presence of high bending loads and local stresses, such as those resulting from the weight bearing of an adult horse.[14,15,24,25] A review of fractures treated using transfixation casting revealed that 68% of cases suffered premature pin loosening, 68% of cases also had radiographic evidence of osteopenia distal to the pins, and 14% of cases suffered from secondary complete fracture through a pin hole.[18] Loose pins have been theorized to result in higher local stresses in the bone surrounding the pin,[26] which may result in both a vicious cycle of loosening and increased local bone stress at the BPI, and a greater risk of bone failure with complete fracture through the pin hole. The high rate of premature pin loosening, the degree of stress protection present within the transfixation cast, and the occurrence of serious pin associated complications such as secondary pin hole fracture, are the key limitations of an otherwise rational approach to the treatment of complicated distal limb fractures in the horse.

The weak link of both transfixation casting in the horse, and traditional external fixation used in other species, including humans, is the BPI.[6,27,28] Bone resorption and pin loosening result from mechanical and thermal damage to bone tissue during hole drilling and pin insertion, as well as cyclic loading during limb use. Pin hole infections also contribute to the breakdown of BPI stability,[29] although it has been proposed that these infections are simply coincidental with pin loosening and are not always causal.[30,31]

Regardless, pin loosening and infection contribute to patient morbidity through pain, loss of fracture stability, increased risk of catastrophic bone failure through an enlarged pin hole and an eventual requirement for additional surgery to replace pins, debride infected pin holes or reconfigure fracture fixation. Premature pin loosening would be eliminated by avoiding local bone resorption at the BPI and enhancing pin stability within the bone. The occurrence of pin associated complications such as secondary pin hole fracture may also be reduced with enhanced pin stability and lower local BPI stress. In addition, a stable BPI may allow implementation of approaches to control the stress environment within a transfixation cast, matching gains in fracture stability with reductions in stress protection and BPI stress, which could ultimately reduce the morbidity associated with this form of fracture treatment.

There is ongoing concern among equine surgeons that the risk of secondary pin hole fracture due to transcortical pins is too high to justify their use in the horse. Despite an improvement in the rate of pin hole fractures observed with transfixation casting,[18] currently greater than 10% of adult horses treated using transfixation casting methods are likely to suffer a pin hole fracture. This rate is unacceptably high considering the consequence is often euthanasia due to the added financial burden and reduced prognosis involved in treating a second fracture in the same horse.[18,30] Additional concerns among equine surgeons include early pin and fixation instability that occurs as a consequence of pin loosening.[9] In the absence of improvements in external fixation methods, we will continue to see life-threatening complications of fracture treatment, such as implant failure, infection, laminitis and pin hole fractures limit success. The ability to improve the range of treatments available for horses suffering potentially catastrophic fractures depends upon developing innovative solutions to address these current limitations in external fixation approaches when applied to the horse.

Finite element (FE) modeling is a powerful technique that has been used for the investigation of various orthopedic problems, including the BPI and the equine MC3.[26,32–36] The technique allows for the simulation of mechanical behavior based on mathematical

models and their solutions using numerical methods within defined model conditions. Output field variables (such as stress and strain values) are obtained following input of specific geometric configurations, constitutive parameters, loading and boundary conditions, and mesh generation.[37] Applying the FE method to a specific biomechanical problem can reduce the number and enhance the value of animal experiments by optimizing the conditions which are ultimately studied *in vivo*.[37] In addition, the FE method can reduce the time necessary to refine an orthopedic approach *in vivo* by providing an advanced starting point that has already undergone preliminary development through simulated testing and optimization. Using the FE method to model the equine distal limb transfixation cast may allow an improved approach to fracture fixation in the horse to be developed.

1.2 Research Goals

Based on the need to advance the capability of veterinarians to treat major equine fractures, the ***long term goal*** of this area of study is to improve the safety and reliability of transfixation casting methods in the horse and ultimately reduce the morbidity and mortality due to fractures and complications associated with their treatment. The ***central hypothesis*** is that the safety and reliability of equine transfixation casting with transcortical implants placed in the MC3 will be improved through the use of specific preferred pin configurations, the promotion of pin stability within the cast, and an approach to control the stress environment within the cast. To test this central hypothesis 4 specific research goals have been developed:

Research goal #1: To utilize FE models of the equine distal limb transfixation cast to determine transcortical pin configurations which result in BPI stress predictions below the expected yield stress of the equine MC3.

To achieve this goal the bones of the distal limb of the adult horse will be characterized, in terms of mechanical and biologic features, in order to create a range of representative FE models which will be employed to optimize transcortical pin configuration(s) for use

in transfixation casting. Model validation will be performed through *ex vivo* testing and comparisons will be made with previous analyses of bone-pin interface stresses to support the findings.

Research goal #2: To develop a general approach for determining preferred transcortical pin configurations in anatomic locations other than the MC3 of horses.
To achieve this goal, a combination of finite element models and previously published parametric analyses will be applied to the general situation of transcortical pin configuration with particular reference to specific measurable bone parameters which can guide pin size and number selection and positioning for external skeletal fixation.

Research goal # 3: To determine, using preferred transcortical pin configurations, the effect of cast-pin interface stability on BPI stresses in the equine third metacarpal bone.
To achieve this goal, the previously developed FE models with preferred pin configurations will be analyzed with different cast-pin interface parameters applied. Mechanical properties of cast material from available literature will be used and the appropriate boundary conditions for the cast-pin interface will be applied to the models. Local BPI stresses will be evaluated to determine whether altered cast-pin interface stability could improve transfixation casting methods by reducing local BPI stresses.

Research goal #4: To determine, using an FE model of the equine distal limb transfixation cast, how changing the loading conditions within the cast distal to the transcortical pins will affect local stresses at the BPI.
To achieve this goal, an FE model of the equine distal limb transfixation cast will be constructed and appropriate boundary conditions applied to simulate cast and pin attachments. Increasing tissue stiffness below the transcortical pins and increasing contact pressure beneath the foot will be simulated within the model to determine whether local BPI stresses and bone stresses distal to the transcortical pins are impacted during weight-bearing.

1.3 List of References

1. USDA:APHIS:VS. Equine 2005, Part I: Baseline reference of equine health and management, 2005. Fort Collins, CO: United States Department of Agriculture. 2006:139.
2. Leblond A, Villard I, Leblond L, et al. A retrospective evaluation of the causes of death of 448 insured French horses in 1995. *Vet Res Commun* 2000; 24:85–102.
3. McClure SR, Watkins JP, Glickman NW, et al. Complete fractures of the third metacarpal or metatarsal bone in horses: 25 cases (1980-1996). *J Am Vet Med Assoc* 1998;213:847–850.
4. Galvin N, Corley K. Causes of disease and death from birth to 12 months of age in the Thoroughbred horse in Ireland. *Ir Vet J* 2010;63:37–43.
5. Stover SM, Murray A. The California postmortem program: leading the way. *Vet Clin North Am Equine Pract* 2008;24:21–36.
6. Nunamaker D. Orthopedic implant failure. In: AJ Nixon ed. *Equine Fracture Repair*. Philidelphia: WB Saunders Co.; 1996;350–353.
7. Van Eps A, Collins SN, Pollitt CC. Supporting limb laminitis. *Vet Clin North Am Equine Pract* 2010;26:287–302.
8. Nixon AJ. Laminitis and contracture deformity. In: AJ Nixon ed. *Equine Fracture Repair*. Philidelphia: WB Saunders Co.; 1996;367–370.
9. Bischofberger AS, Fürst A, Auer J, et al. Surgical management of complete diaphyseal third metacarpal and metatarsal bone fractures: clinical outcome in 10 mature horses and 11 foals. *Equine Vet J* 2009;41:465–473.
10. Ahern BJ, Richardson DW, Boston RC, et al. Orthopedic infections in equine long bone fractures and arthrodeses treated by internal fixation: 192 cases (1990-2006). *Vet Surg* 2010;39:588–593.
11. Peloso JG, Cohen ND, Walker MA, et al. Case-control study of risk factors for the development of laminitis in the contralateral limb in Equidae with unilateral lameness. *J Am Vet Med Assoc* 1996;209:1746–1749.

12. Kraus BM, Richardson DW, Nunamaker DM, et al. Management of comminuted fractures of the proximal phalanx in horses: 64 cases (1983-2001). *J Am Vet Med Assoc* 2004;224:254–263.
13. Lewis DD, Cross AR, Carmichael S, et al. Recent advances in external skeletal fixation. *J Small Anim Pract* 2001;42:103–112.
14. Clary E, Roe S. Enhancing external skeletal fixation pin performance - consideration of the pin-bone interface. *Vet Comp Orthop Traumat* 1995;8:6–13.
15. McClure S, Honnas CM, Watkins JP. Managing equine fractures with external skeletal fixation. *Comp Cont Educ Pract Vet* 1995;17:1054–1063.
16. Auer JA. Principles of fracture treatment. In: Auer JA and Stick JA eds. *Equine Surgery*. 3rd ed. Saint Louis, MO: Saunders Elsevier; 2006:1000–1029.
17. Joyce J, Baxter GM, Sarrafian TL, et al. Use of transfixation pin casts to treat adult horses with comminuted phalangeal fractures: 20 cases (1993-2003). *J Am Vet Med Assoc* 2006;229:725–730.
18. Lescun TB, McClure SR, Ward MP, et al. Evaluation of transfixation casting for treatment of third metacarpal, third metatarsal, and phalangeal fractures in horses: 37 cases (1994-2004). *J Am Vet Med Assoc* 2007;230:1340–1349.
19. Nunamaker DM. A new external skeletal fixation device that allows immediate full weightbearing application in the horse. *Vet Surg* 1986;15:345–355.
20. Hopper SA, Schneider RK, Ratzlaff MH, et al. Effect of different full-limb casts on in vitro bone strain in the distal portion of the equine forelimb. *Am J Vet Res* 1998;59:197–200.
21. Hopper SA, Schneider RK, Johnson CH, et al. In vitro comparison of transfixation and standard full-limb casts for prevention of displacement of a mid-diaphyseal third metacarpal osteotomy site in horses. *Am J Vet Res* 2000;61:1633–1635.
22. McClure SR, Watkins JP, Bronson DG, et al. In vitro comparison of the standard short limb cast and three configurations of short limb transfixation casts in equine forelimbs. *Am J Vet Res* 1994;55:1331–1334.

23. Schneider RK, Ratzlaff MC, White KK, et al. Effect of three types of half-limb casts on in vitro bone strain recorded from the third metacarpal bone and proximal phalanx in equine cadaver limbs. *Am J Vet Res* 1998;59:1188–1193.
24. Aro HT, Markel MD, Chao EY. Cortical bone reactions at the interface of external fixation half-pins under different loading conditions. *J Trauma* 1993;35:776–785.
25. McDuffee LA, Stover SM, Coleman K. Limb loading activity of adult horses confined to box stalls in an equine hospital barn. *Am J Vet Res* 2000;61:234–237.
26. Huiskes R, Chao EY, Crippen TE. Parametric analyses of pin-bone stresses in external fracture fixation devices. *J Orthop Res* 1985;3:341–349.
27. Moroni A, Aspenberg P, Toksvig-Larsen S, et al. Enhanced fixation with hydroxyapatite coated pins. *Clin Orthop Relat Res* 1998:171–177.
28. McClure SR, Watkins JP, Hogan HA. In vitro evaluation of four methods of attaching transfixation pins into a fiberglass cast for use in horses. *Am J Vet Res* 1996;57:1098–1101.
29. DeJong ES, DeBerardino TM, Brooks DE, et al. Antimicrobial efficacy of external fixator pins coated with a lipid stabilized hydroxyapatite/chlorhexidine complex to prevent pin tract infection in a goat model. *J Trauma* 2001;50:1008–1014.
30. Nunamaker DM, Nash RA. A tapered-sleeve transcortical pin external skeletal fixation device for use in horses: development, application, and experience. *Vet Surg* 2008;37:725–732.
31. Bowman KF, Leitch M, Nunamaker DM, et al. Complications during treatment of traumatic disruption of the suspensory apparatus in Thoroughbred horses. *J Am Vet Med Assoc* 1984;184:706–715.
32. Wullschleger L, Weisse B, Blaser D, et al. Parameter study for the finite element modelling of long bones with computed-tomography-imaging-based stiffness distribution. *Proc Inst Mech Eng H* 2010;224:1095–1107.
33. Capper M, Soutis C, Oni OO. Comparison of the stresses generated at the pin-bone interface by standard and conical external fixator pins. *Biomaterials* 1994;15:471–473.
34. Götzen N, Cross AR, Ifju PG, et al. Understanding stress concentration about a nutrient foramen. *J Biomech* 2003;36:1511–1521.

35. Les CM, Keyak JH, Stover SM, et al. Development and validation of a series of three-dimensional finite element models of the equine metacarpus. *J Biomech* 1997;30:737–742.
36. Oni OO, Capper M, Soutis C. Factors which may increase stresses at the pin-bone interface in external fixation: a finite element analysis study. *Afr J Med Med Sci* 1999;28:13–15.
37. Huiskes R, Hollister SJ. From structure to process, from organ to cell: recent developments of FE-analysis in orthopaedic biomechanics. *J Biomech Eng* 1993;115:520–527.

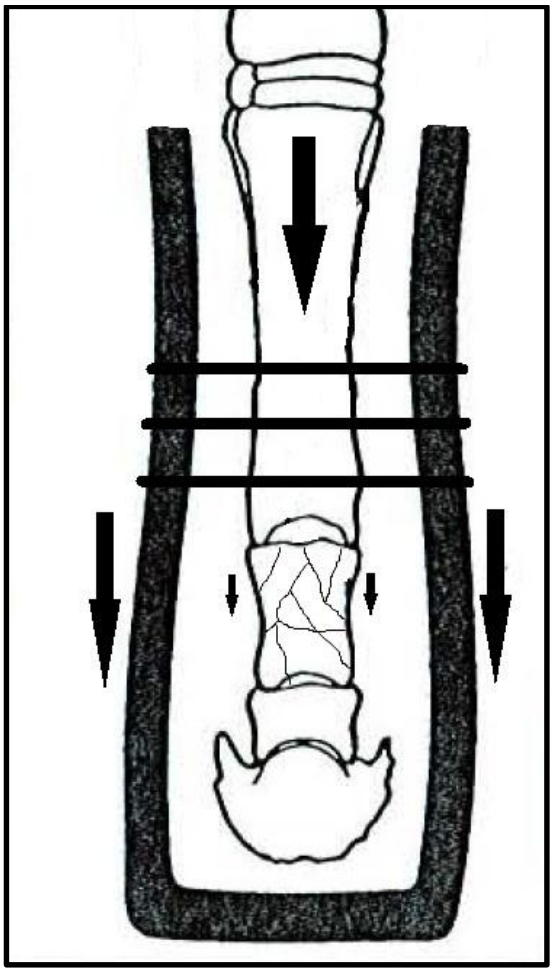

Figure 1.1 Illustration showing the concept of the distal limb transfixation cast used in the horse. The transcortical pins are positioned within the third metacarpal bone and are incorporated into a distal limb cast. The fractured proximal phalanx is protected from approximately 80% of the weight bearing loads (depicted by the arrows) providing axial stabilization and preventing significant fracture collapse. (Adapted from: Brommer et al. In vitro determination of equine third metacarpal bone unloading, using a full limb cast and a walking cast. *Am J Vet Res*,1996; 57:1386-1389).

CHAPTER 2. LITERATURE REVIEW

2.1 Introduction

A range of methods of fracture fixation have been utilized in the horse.[1] Both internal and external fixation have demonstrated particular advantages and disadvantages when applied to the equine fracture patient. Biomechanically stable methods of fixation tend to be most successful due to the comparatively large bodyweight and the stress that immediate post-operative weight bearing places on any fracture fixation. No one bone fixation method can be applied to all fractures and having a range of treatment options available is essential for the equine surgeon to be successful in managing the range of fractures encountered.

Internal fixation, particularly using compression plates and/or bone screws, has become the most commonly employed method of fracture repair in the horse since its adoption in the early 1970's.[1] Internal fixation was recently reported to result in hospital discharge of 82% of treated horses presenting with a broad range of fracture types and injuries.[2] The principle advantage of internal fixation is early mobilization of the affected limb, which avoids complications associated with cast immobilization; so called "cast disease".[1] Achieving compression between bone fragments during repair adds stability to the fixation. Friction present between the bone fragments allows effective load transfer through the fractured bone during weight bearing and re-establishment of skeletal integrity during the healing process. Accurate anatomic alignment of fractured bone fragments is generally necessary in adult horses for internal fixation to be successful. During long bone fracture repair, cortical defects or malalignment, particularly of the compression surface of the bone, can result in excessive cycling of the implant and

early failure prior to bone healing.[1,3] Early return to function of the fractured limb results in greater joint mobility, reduced loss of articular cartilage proteoglycan, less joint stiffness, less muscle wasting and soft tissue laxity, and avoids loss of bone density and development of osteopenia, when compared to limb immobilization with external coaptation.[1]

A disadvantage of internal fixation is the soft tissue dissection and periosteal disruption that may be required for the application of implants. The use of locking compression plates or limited contact dynamic compression plates can reduce the need for periosteal disruption during bone plating.[1] Soft tissue dissection can also be minimized with the use of minimally invasive plate fixation, although currently this approach has only been reported for non-displaced, incomplete fracture repair and arthrodesis in the horse.[4] An additional disadvantage of internal fixation is the introduction of foreign material in the form of a metallic implant at the fracture site. This is least desirable when the fracture is open or potentially contaminated. Metallic implants provide foreign material for bacterial colonization and the formation of surface biofilms, which make treatment of infection particularly challenging.[5,6] The infection rate following fracture repair with internal fixation in horses was recently reported to be 28% (53/192) overall, with 57% of open fractures and 24% of closed fractures developing a post-operative infection.[2] Open fractures, accounting for 11% of cases treated, were 4.2 times more likely to become infected and 4.5 times less likely to be discharged from the hospital than closed fractures. Approximately one-third of long bone fractures in the horse are **third metacarpal (MC3)** or **third metatarsal (MT3)** fractures. Between 36 and 71% of complete, unstable MC3 or MT3 fractures were classified as open at presentation from several reports.[2,7–9] Combining data from 2 studies with available information on complete MC3 or MT3 fractures, 63% (20/32) of open fractures became infected, while 15% (2/13) of closed fractures became infected when internal fixation was used.[7,8] These high rates of infection in both open and closed MC3 or MT3 fractures in the horse illustrate the need for alternative approaches in the treatment of equine fractures to enable the surgeon to select the most appropriate treatment modality for the specific injury presented. External

skeletal fixation allows fracture stabilization without the need to disrupt the soft tissues at the fracture site. It can also avoid placement of implants in open and contaminated wounds thereby minimizing the risk of implant associated infection following fracture repair.

The equine distal limb transfixation cast is a modified form of **external skeletal fixator (ESF)** that is used to treat distal limb fractures in the horse. This review of the literature presents the principles and use of the transfixation cast within the broader context of external skeletal fixation. As the **bone-pin interface (BPI)** plays a central and limiting role in the application of external skeletal fixation and the transfixation cast, the mechanical and biological factors that contribute to BPI stresses, bone resorption and ultimately pin loosening during external fixation will be reviewed along with strategies that have been employed to negate these factors. The review will also explore the unique factors applicable to the equine distal limb transfixation cast which may influence BPI stresses. Finally, a review of the **finite element (FE)** method and how it has been used to characterize both the BPI and the equine MC3 with specific reference to the parameters that will be used in the FE models developed for this thesis will be presented.

2.2 External Skeletal Fixation

External skeletal fixation utilizes percutaneous transcortical pins placed in intact bone and clamped to a connecting rod adjacent to the limb, to effect stabilization of a fractured segment of bone.[10,11] In contrast to internal fixation, this approach avoids invasion of the fracture site and has been used with good success in humans and small animal patients to overcome some of the disadvantages associated with internal fixation for fracture repair.[10–13] External skeletal fixation provides an alternative approach to internal fixation of certain fractures by exploiting its inherent advantages, namely minimizing implants at the fracture site and providing sufficient fracture stabilization often without perfect fracture reconstruction. The primary indications for use of ESFs are highly comminuted or open fractures, and those fractures associated with extensive concurrent soft-tissue or

vascular injury.[11] A variety of construct designs have been developed with variations in pin type, construct configuration, and the connections used.[10,11]

2.2.1 Classification, terminology and general use

External skeletal fixators are classified based upon the pins, their configuration and their connectors. A variety of ESF pins have been developed and used clinically. Pins may be threaded or smooth. Threads may be negative profile (where threads are cut into the pin leaving the core diameter of the threaded region smaller than the diameter of the remaining smooth pin section and outer thread diameter) or positive profile (where the threads are formed to extend above the core diameter of the pin, so that the outer thread diameter is greater than the core diameter of the pin). There is a known stress riser effect and subsequent weakness at the junction of the threaded and smooth portion of negative profile pins.[14] Positive profile pins are not prone to this weakness and are generally preferred for this reason.[15] Pins which are threaded on one end are designed for insertion into the far cortex of the bone and not beyond. These are called half pins. Pins which are threaded in their central portion are designed for insertion through the far cortex, and the soft tissue and skin, leaving the threaded portion positioned within both bone cortices. These are termed full pins and a series of them are typically connected independently on each end by connecting rods (also termed sidebars) or formed acrylic bars. Threaded pins offer the inherent advantage of remaining more stable to movement within the bone along the pins axis compared to smooth pins, and their insertion is facilitated by the threads which enable a gradual and controlled passage of the pin into the bone through a pre-drilled and often pre-tapped pilot hole.[15,16] Current recommendations for transcortical pin use in small animal ESF construction are; to choose a size of pin based on the dorsal-palmar diameter of the bone and not to exceed 25% of this dimension; to use positive profile pins; to position 3-4 pins on either side of the fractured bone region whenever possible; to pre-drill holes in the bone that are 0.1 mm smaller than the core pin diameter being used; to distribute pins evenly along main fracture segments; to avoid critical anatomic structures by positioning pins within known safe zones of the limb; and to

create wide soft tissue corridors for pins to avoid morbidity associated with soft tissue interference by pins.[15]

A wide range of ESF frame configurations are possible, including linear, circular and hybrid combinations. The primary method of pin connection is through the use of a connecting rod, which can be made from various materials including stainless steel, titanium, aluminum or carbon fiber composite. Pins are connected to the rod by specialized clamps which are adjustable in positioning along the length of the rod and somewhat in their alignment with the pin once positioned on the connecting rod. An alternative form of connection between pins is with the use of an acrylic bar. The formation of an acrylic bar involves initially positioning flexible plastic tubing over the ends of a series of pins and capping one end of the tubing to allow the acrylic to be poured into the tubing prior to setting up. The acrylic hardens within the tubing over each of the pin ends, effectively creating pin to pin and pin to bar connections, equivalent in principle to connecting rod and clamp connections. The acrylic bar system provides some flexibility in pin alignment when compared to traditional connecting rods. **Polymethylmethacrylate (PMMA)** is the most commonly used acrylic and it has been compared to stainless steel connecting rods in several studies. The PMMA acrylic bar system of connection has been shown to have similar stiffness and other mechanical properties to the stainless steel connecting rods.[17,18] An acrylic connecting bar is able to be enlarged by using a greater diameter of plastic tubing during the formation process. This results in relatively greater axial and bending stiffness of the bar.[17]

External skeletal fixator frame configurations have been classified to help clinicians conceptualize the range of possibilities that can be constructed.[14,15] In principle, greater construct stiffness is achieved with greater complexity of ESF configuration. A type-1 ESF consists of half pins exiting the bone from only one side. A series of half pins connected by a single connecting rod or bar in the same plane is classified as a type-1a ESF. This is the least rigid fixator configuration possible.[14] A second group of half pins positioned adjacent to but in a different plane to the first, and connected to each other and

the first connecting rod adds stiffness to the construct and is classified as a type-1b ESF. Multiplanar configurations provide greater stability than equivalent uniplanar configurations. Full transcortical pins which traverse through the soft tissue and skin and are connected at both ends by two rods or bars in the same plane are classified as type-2 ESFs. Additional half pins can be added to this configuration in an additional plane to construct a type-3 ESF. These basic linear ESF constructs are shown in **Figure 2.1**. The progression of complexity in ESFs results in increasing overall construct stiffness.[14,15,19,20] In addition to linear bars connecting pins along the long axis of the bone, circular ESFs have been developed which connect pins within the same transverse axis of the bone and are also connected to each other along the long axis of the bone by threaded rods. Circular ESF constructs are generally based on the principles of Ilizarov, who developed the circular transfixation-wire ESF construct for orthopedic applications, including limb lengthening procedures, in the 1950's.[21–23] Transcortical wires of relatively small diameter, compared to standard ESF pins, are tensioned along their long axis across the ring. The tension in the wire increases its stiffness and resistance to bending during loading. Hybrid ESF constructs have also been developed where a combination of conventional, circular and hemicircular constructs are used depending upon their ability to be applied to the relevant anatomy and fracture configuration.[15] Many of the current manufacturers of ESF systems include both linear and circular ESF hardware which is cross compatible to allow easy hybrid ESF construction in sizes suitable for small animals and humans.

There are limitations and disadvantages to the use of ESFs. Principle among these are the limitations of the pins and their stability within the bone. Pin loosening is a frequent occurrence during the use of ESFs and requires pin removal or revision surgery. In addition, pin site infections add morbidity to the fracture healing process and can rarely result in fulminant osteomyelitis. Pain associated with soft tissue impingement by the pin has also added to the morbidity of using ESFs.[15] Maintenance of ESFs requires daily pin and wound care which may not be possible in all circumstances. Some comminuted fracture configurations may not allow stable pin positioning to achieve a solid construct

using ESFs. External fixation is not as stable as internal fixation in most circumstances and so its use may be limited in clinical fracture presentations which demand a high degree of post-operative stability.

2.2.2 External skeletal fixation in the horse

The clinical use of conventional ESFs in the horse has primarily been reported for non-weight bearing applications such as mandibular and maxillary fractures, or in lighter weight animals such as foals, miniature horses and donkeys.[24–29] There are reports describing the use of external fixation to treat mandibular and maxillary disorders in the horse.[24,26,30,31] Mandibular fractures are well suited to the use of external fixation. Mandibular fractures have a high potential to be open within the oral cavity or have significant mucosal compromise, both leading to bacterial contamination of the fracture site.[30] External fixation allows flexibility of pin positioning within areas of the mandible or maxilla that can avoid the tooth roots. Internal fixation using standard plating techniques limits this flexibility due to the fixed position of screw holes within the plates. An additional reason why external fixation is suited to mandibular fractures in the horse is that it allows sufficient biomechanical stabilization for a wide variety of fracture configurations. External fixation can be readily combined with intraoral wiring or splinting methods to compliment fixation.[30,32] However, when tested and compared biomechanically, external fixation was less rigid than dynamic compression plating for interdental space fractures of the mandible.[32] Specific pin types have ranged from smooth Steinmann pins to threaded pins and large (5.5 mm) cortical bone screws. Methods of connection have included standard connecting rods, PMMA acrylic bars or fiberglass casting material. In contrast to its use in these non-weight bearing applications, external fixation using standard connections such as rods or acrylic bars, in linear, circular or hybrid configurations has not attained widespread use in fracture repair of weight bearing bones in the adult horse due to inadequate strength of the construct.[1]

In the foal, weight bearing fractures have been treated using conventional ESFs, however reports are limited to single cases.[25,33,34] There are additional case reports of the use of ESFs to treat limb deformity in a foal and a Miniature donkey.[28,35] There is a detailed report on the results of treating tibial osteotomies in foals with either a type-2 or a type-3 ESF frame configuration.[29] In that study, a standard rod and clamp apparatus was combined with 3 Steinman pins (6.35 mm diameter) positioned both proximal and distal to a midshaft tibial osteotomy in foals. Despite the lighter weight of the foals treated (less than 150 kg) compared to an adult horse, treatment of the tibial osteotomies using an ESF was found to result in significant morbidity. All 6 foals treated using the type-2 ESF suffered pin loosening within 5-6 weeks of surgery. The pin loosening corresponded with the onset of greater reluctance of foals to use the treated limb. Four of the 6 foals treated using the type-2 ESF healed the osteotomy and were comfortable long term. However, 2 foals were euthanized due to complications during treatment. One suffered a secondary fracture through the proximal pin hole within 1 week of surgery, while the other foal had acute displacement of the original fragments at the osteotomy site 6 weeks following surgery followed by further progressive fragment displacement resulting in euthanasia of the foal at 12 weeks. Foals treated with the type-3 ESF were initially more reluctant to bear weight on the limb than foals treated with the type-2 ESF and their use of the limb decreased further 2-3 weeks following surgery. Subsequently the original study protocol was not completed in these 5 foals. Overall, 4 of 11 treated foals suffered from a cortical fracture associated with one of the pin holes.[29]

A customized external skeletal fixation device was developed for an adult horse by Nunamaker and his colleagues for the treatment of distal limb orthopedic conditions, including fractures.[27,36] The device used large transcortical pins (9.6 mm diameter) with a negative thread profile attached to a polyurethane-metal composite sidebar which extended to a steel foot plate.[27] The transcortical pins were positioned 5 cm apart in the frontal plane of the MC3 and subsequently connected in a type-2 ESF configuration. The foot plate contacted the ground surface and the foot was attached to the plate using a bar shoe with screws. The device essentially suspended the distal part of the limb below the

transcortical pins. A major limitation to the clinical use of external skeletal fixation in the adult horse has been the occurrence of secondary pin hole fractures, which significantly complicate further treatment.[16,27,37–40] The original Nunamaker external skeletal fixation device has been modified in an attempt to address this problem by reducing the size of the pins down to 7.9 mm in diameter and adding a tapered pin sleeve that inserts over the pin ends to modify the contact point between the pins and the bone.[41,42]

External skeletal fixation methods that have been evaluated for the adult horse ex vivo to determine if they are mechanically feasible for stabilization of limb fractures include a circular ESF using Ilizarov rings with pins and a circular ESF using transosseous wire ropes.[43,44] Cervantes et al. applied a 4-ring multiplanar circular ESF to the MC3 using 3 different pin sizes (1/8" [3.2 mm], 3/16" [4.8 mm] and ¼" [6.4 mm] diameter) and tested the configuration in bending, torsion and axial compression.[43] Four pins were placed on either side of a mid-MC3 osteotomy in cadaveric bone, with each pair of pins attached to a ring fixator in a crossed fashion through cannulated fixation bolts. The transfixation pins were not pre-tensioned along their axis, in contrast to the described Ilizarov technique, and the stiffness of the construct was found to be inadequate to withstand the weight bearing load expected with an unstable MC3 fracture.[43] Mechanical testing of a system of transosseous wire ropes attached in a ring fixator configuration was performed in an attempt to apply the Ilizarov principles of pre-tensioned wires for application in large animals.[44] The ropes consisted of 19 separate stainless steel strands combined to create a 6.4-mm nominal diameter rope. Methods of attachment to the ring fixator were evaluated to maximize the applied pre-tension. Three different transosseous rope configurations were also evaluated. This apparatus, using 2 ropes separated by 60-degrees at each ring and a total of 4 circular rings, resulted in 2 mm of axial displacement at a load of 1730 N. As a result, it was concluded that this apparatus was unsuitable for the fixation of unstable fractures in large animals.[44]

There have been several studies both evaluating ESFs and applying them clinically in large animal species other than the horse. In cattle, reports of successful treatment of long

bone fractures using external fixation techniques are more numerous than in the horse.[45–53] This may be due to the less fractious nature of cattle, their tendency to lay down more during the post-operative recovery period, a lesser requirement of limb use for their intended purposes following treatment and a difference in susceptibility to laminitis in the opposite limb. Regardless, clinical treatment of a variety of fractures using ESFs in calves and young cattle has been performed and the complications reported using these techniques tend to be similar to, but often less consequential, than those encountered in horses. These complications primarily relate to the BPI and the transfixation pins.[49]

2.2.3 Equine distal limb transfixation cast

A method of treating major distal limb fractures in the horse using the principles of external skeletal fixation, known as transfixation casting, has gained greater interest among equine surgeons.[37–39,54–57] Transfixation (transcortical) pins placed transversely through intact bone proximal to the fracture site, are incorporated into a distal limb cast which encompasses the foot (**Figure 2.2**). The cast functions as the connecting rods and clamps of a conventional ESF and weight bearing loads are transferred from intact bone proximal to the fracture site, through the pins and cast to the ground. Although possible in MC3 fractures, pins are not typically placed distal to the fracture site in proximal phalanx fractures due to limited access to the middle phalanx. Without distal pins, the bottom of the cast enclosing the foot is the primary point of load transfer from the proximal transfixation pins to the ground.[37,38] Early reports of transfixation casting techniques in the horse were sporadic but emerged in the 1950's.[40,58] The technique is similar in principle to the walking cast methods initially developed for fracture treatment in large animals in the 1970's by Nemeth and Back.[40] The walking cast incorporated 2 aligned transcortical pins positioned proximal to the fracture site into a metal U-bar which extended beneath the hoof. Plaster cast material was applied to the limb and the metal U-bar was positioned within the cast layers during application. The cast material did not extend below the foot in the walking cast, and so load transfer from the pins to the ground surface was achieved through the metal bar. More recently, improvements in

casting material strength, with the transition from plaster of Paris to fiberglass casting tape in clinical practice, as well as other improvements in application technique have improved clinical outcomes when transfixation casting was used in horses.[37,38,59,60] Within the transfixation cast, significant reductions in both bone strain below the pins and osteotomy displacement in the proximal phalanx have been confirmed experimentally when the distal limb transfixation cast was compared to a standard half limb cast.[55,57,61] Similar findings have been reported, in terms of bone strain reduction and osteotomy displacement, for full limb transfixation casting with transcortical pins located in the distal radius.[55,62] Horses wearing a transfixation cast are typically comfortable and able to have full weightbearing on the fractured limb while the construct remains stable.[1,16] Gradual pin loosening has been shown to coincide with greater reluctance to use the limb in horses wearing a transfixation cast.[16,37,63]

2.2.3.1 Conventional external skeletal fixation and transfixation casting

The introduction of fiberglass casting material for clinical use resulted in four primary differences between conventional ESFs, such as the Nunamaker device, and the transfixation cast as it could subsequently be applied in the adult horse. First, the superior strength of fiberglass casting material compared to plaster of Paris allowed the cast alone to support transfixation pins without the need for a metal support bar (such as in the walking cast) without a detrimental loss of axial stability.[57,60] Second, fiberglass casting material constructions are lightweight in comparison to sufficiently sized conventional ESFs when applied in the adult horse. Third, the distance between the outer bone contact point of a transcortical pin and the inner contact point of the pin with the cast material, also known as the working length of the pin, is less than for a conventional ESF. The shorter working length of the pin allows smaller diameter transcortical pins to be used in a transfixation cast compared to a conventional ESF. The shorter working length proportionally reduces the bending moment acting on the pin since the bending moment is equal to the product of the load applied to the pin and the working length. The smaller bending moment thereby reduces the stress at the BPI resulting from an equivalent

diameter pin.[19,64] Alternatively, a smaller pin diameter can be expected to have similar BPI stresses when the pin working length is reduced. Currently, 6.35 mm transcortical pins are used for a transfixation cast in the adult horse whereas 7.9 mm pins are used for the Nunamaker equine skeletal fixation device. Finally, since casting material acts as the connecting rods and clamps of the ESF, exact pin alignment is no longer necessary since pin ends are incorporated into the transfixation cast during application. Consequently, a transfixation cast has become more straightforward to apply when compared to the pin alignment requirements of both the walking cast and the Nunamaker device.[16,27,39,59] Offsetting pin alignment was also shown to result in less weakening of the bone in torsion following transfixation pin placement.[59] An additional difference between the conventional ESF and the transfixation cast is the lack of access to the pin sites (and wounds) beneath a transfixation cast. Despite this apparent disadvantage of the transfixation cast, there has been greater clinical use observed in recent years, likely due to the biomechanical advantages outlined previously and a lack of detrimental effect observed when managing open wounds and orthopedic infections within a cast.[37–39,65,66] In support of this contention, there is growing evidence in humans that regular ESF pin site care has no effect on the pin tract infection rate observed clinically.[67,68]

2.2.3.2 Clinical results and indications for transfixation casting

There are 5 recent reports on the clinical outcome of fractures treated using current transfixation casting methods in the horse.[8,37–39,65] Joyce et al. reported on the treatment of 20 phalangeal fractures using a transfixation cast, including 14 middle phalanx fractures and 6 proximal phalanx fractures.[38] Overall, 14 fractures healed (70%) and the horses were discharged from the hospital. Lescun et al. reported on the treatment of 37 fractures using transfixation casts, including MC3 or MT3, proximal phalanx or middle phalanx fractures.[37] Treatment of this series of fractures using transfixation casts resulted in 77% of fractures healing. This included successful treatment of 10 of 15 (67%) MC3 or MT3 fractures, 11 of 12 (92%) proximal phalanx fractures and 6 of 8 (75%) middle phalanx fractures. More recently, Rossignol et al. reported on the outcome of treatment in

11 horses with comminuted proximal phalanx fractures using some minor modifications of the previously described transfixation casting technique.[65] Nine of the 11 (82%) fractures healed. The overall treatment success using transfixation casting was equivalent or superior to internal fixation methods for the fracture types treated in these studies.[37,38] A previous study on the treatment of comminuted proximal phalanx fractures reported a survival rate of 23% of horses when no intact strut of bone was present between the metacarpophalangeal and proximal interphalangeal joint.[69] In addition to these 3 studies evaluating transfixation casting, there are 2 recent case series of distal limb fractures which include a sub-group of horses treated by transfixation casting.[8,39] Within a series of 64 comminuted proximal phalanx fractures in the horse, Kraus et al. reported on the treatment of 6 severely comminuted fractures using a transfixation cast.[39] Four (66%) of the fractures were treated successfully and ultimately healed. Bischofberger et al. reported on the results of treating MC3 or MT3 fractures in 10 foals and 11 adult horses. Three adult horses in this study were treated using a transfixation cast. One fracture healed and the horse survived. This horse also had a single dynamic compression plate applied to assist fracture fixation.[8]

The most common reason for treatment failure in these case series has been secondary pin hole fractures, accounting for 8 of 21 (38%) non-survivors from a total of 77 horses treated using a transfixation cast. Two other non-survivors were euthanized due to complications directly related to the transfixation cast, one with bent pins and an unstable fixation and the other from biaxial proximal sesamoid bone fractures secondary to severe osteopenia below the pins. Four of the non-survivors were euthanized due to complications related to the fracture itself (2 distal limb ischemia and necrosis, 1 fracture collapse and 1 osteomyelitis with non-union). Four horses were euthanized due to laminitis and 3 horses were euthanized due to gastrointestinal complications. Across all 5 of these studies, 56 horses (62%) survived and their fracture healed.

The concept of using internal fixation in combination with external fixation has been reported in the treatment of challenging radial and tibial fractures in humans with

encouraging results.[12,70] Similarly, the combination of transfixation casting with internal fixation methods was reported in 4 of these 5 recent studies.[8,37,38,65] Lag screw fixation was primarily used in the reported cases to complement the transfixation cast and establish fracture fragment realignment or joint congruity when possible. This approach has been found not to adversely affect clinical outcomes in the horse and has been recommended where possible to realign fracture fragments and encourage load sharing between the fractured bone and the transcortical pins.[37,38]

The primary indications for the selection of transfixation casting for fracture treatment in the horse are highly comminuted fractures and open fractures. In addition, for some fractures in which either a distal or proximal location of the fracture on a long bone makes application of adequate internal fixation impossible, a transfixation cast combined with lag screws may be indicated to achieve fracture realignment and axial stability through the combination of fixation methods. Highly comminuted fractures of the proximal phalanx are the best example of where transfixation casting in the horse is indicated. From the recent reports on the use of transfixation casting, there were a total of 28 comminuted proximal phalanx fractures identified in which the outcome was reported, of which 23 (82%) fractures healed and horses survived.[37,39,65] This success rate compares very favorably to the previously reported survival rate for comminuted proximal phalanx fractures treated using open reduction and internal fixation, where only 3 of 11 (27%) horses treated survived.[69] Both Markel et al. and Kraus et al., who reported on the treatment of a total of 94 comminuted first phalanx fractures from the same institution over successive time periods spanning a total of approximately 25 years, highlight the distinction between comminuted proximal phalanx fractures that contain an intact strut of bone between the metacarpophalangeal and proximal interphalangeal joints, and those that do not.[39,69] Without this strut of bone, preventing continued axial collapse of the fracture is an important goal for fixation. Transfixation casting has proven to be more effective than internal fixation at achieving axial stability and subsequently successful outcomes in these highly comminuted proximal phalanx fractures. In contrast, comminuted proximal phalanx fractures in which an intact strut of bone is present can be

successfully treated using lag screw fixation alone in most cases.[39] Similar advantages and indications for transfixation casting exist for other long bone fractures in which comminution is present and jeopardizes adequate reconstruction using internal fixation, such as MC3 or MT3 fractures.[37,40]

Transfixation casting is also indicated for the treatment of open fractures.[14,15] In the report by Lescun et al, 9 open MC3 or MT3 fractures were treated using transfixation casting, of which only 1 (11%) developed osteomyelitis which could not be controlled and which ultimately affected case outcome (amputation).[37] In a series of 192 long bone fractures treated using internal fixation or arthrodeses, 21 fractures were open at hospital admission, of which 12 (57%) developed post-operative infection and/or osteomyelitis which affected case outcome.[2] Similarly in the study by Bischofberger et al. 17 MC3 or MT3 fractures were treated using internal fixation alone, 12 of which were classified as open fractures at hospital admission. Of these 12 fractures, 6 (50%) developed clinical signs of infection, with 5 (42%) of these cases ultimately euthanized.[8] In a previous study by Beinlich and Bramlage, a total of 15 axially unstable and open MC3 or MT3 fractures were treated using plate fixation and in 6 cases (40%) treatment was unsuccessful.[9] Finally, in a study by McClure et al, 7 of 17 (41%) fractures of the MC3 or MT3 that were open at admission and treated using internal fixation became infected and did not heal.[7] The ability to achieve axial stability without requiring implants be inserted into a contaminated fracture site is a strong indication for the use of transfixation casting in the treatment of open distal limb fractures in the horse.

2.2.3.3 Major complications of transfixation casts

A recent review of fractures treated using transfixation casting revealed that 68% of cases (25 of 37) suffered premature pin loosening, 68% (25 of 37) of cases had radiographic evidence of osteopenia distal to the pins, and 14% of cases (5 out of 37) suffered from a secondary fracture through a pin hole.[37] In another case series of transfixation casting of phalangeal fractures, 60% of cases (12 out of 20) had radiographic evidence of lysis

around the pins, 15% of cases (3 of 20) had premature pin loosening which resulted in early pin removal, all cases showed some degree of osteopenia distal to the transfixation pins and 20% of cases (4 of 20) suffered a secondary complete fracture through the pin hole.[38] There were a total of 8 complete pin hole fractures in these 2 case series, of which 7 (88%) occurred through the proximal pin hole. The high rate of pin complications and the mortality associated with secondary pin hole fractures are the biggest limitations of an otherwise rational approach to treatment of complex distal limb fractures in the horse. As outlined previously, transfixation cast related complications such as secondary pin hole fracture, distal limb osteopenia and pin bending or failure, account for almost half of the treatment failures reported for transfixation casting in the horse. Pin loosening is a direct consequence of bone resorption at the BPI. The details of this process will be a major focus of this review and covered in subsequent sections. The occurrence of secondary fractures through the pin hole will also be discussed in subsequent sections as it is very likely to be interrelated with pin hole size, pin diameter and the mechanics of external fixator pins. The remainder of this section will discuss the development of osteopenia distal to the pins as a complication of transfixation casting and its impact on clinical case management as it relates to fracture healing.

2.2.3.3.1 Disuse osteopenia

Osteopenia is defined as the loss of bone mass. Skeletal disuse osteopenia can arise for a number of underlying reasons, all related to a reduction in loading of the specific region of the skeleton affected.[71] The effects of space-flight on astronauts and of bed rest on the skeleton of someone seriously injured, ill or paralyzed, are the most well-known examples of disuse osteopenia in humans. Disuse osteopenia has also been studied in mammals that hibernate to elucidate the existence of novel protective mechanisms against severe bone loss.[72] Cast application has long been known to cause osteopenia in humans as well as animals, and several studies have examined the effects of cast immobilization on the lower limb in horses.[71,73–76] At a basic level, the maintenance of bone mass requires a stimulus in the form of mechanical loading. The normal balance

between bone formation and bone resorption is altered towards greater bone resorption when the mechanical stimulus is lost or reduced.[77] It is beyond the scope of this review to examine the various pathways through which mechanoregulation of bone is proposed to occur. However, current theories propose that fluid flow through canaliculi in response to mechanical loading results in the required stimulus at the osteocyte cell membrane to regulate molecular signaling of effector cells for bone formation (osteoblasts) or bone resorption (osteoclasts).[77–79]

The effect of forelimb cast immobilization on MC3 bone quality in the horse was studied by Buckingham and Jeffcott over a period of 8 weeks within the cast and 12 weeks following cast removal.[74] They found that both the cast limb and the opposite forelimb had reductions in bone mineral content, bone mineral density and elastic modulus, with the cast limb generally having more profound reductions. During remobilization of the limb following cast removal recovery of bone mineral content, bone mineral density and elastic modulus were observed. Van Harreveld et al performed a similar study in horses whereby a cast was applied for 7 weeks followed by 8 weeks of remobilization using a controlled, gradually increasing treadmill exercise program.[75,76] Radiographically detectable osteopenia was observed in all immobilized limbs at cast removal and had not fully resolved by the end of the study period. The change in bone density was most prominent in the proximal sesamoid bones and the joint margins of the proximal phalanx and MC3. These findings were confirmed using microradiography to study several regions of the metacarpophalangeal joint. There was also a significant difference in the bone volume fraction (bone volume/tissue volume), measured using dual energy x-ray absorptiometry, between immobilized and non-immobilized bones despite the 8 week remobilization period.[75,76] Delguste et al studied the effect of using a bisphosphonate drug, tiludronate, to ameliorate disuse osteopenia during cast immobilization in the horse.[73] Cast immobilization was performed for 8 weeks, remobilization following cast removal for 4 weeks and active training for a further 8 weeks. Tiludronate treatment was performed at the time of cast application and after 4 weeks. A reduction from baseline in the serum biochemical marker C-telopeptide of type-1 collagen cross-links, which

reflects bone resorption, was seen through the first 5 weeks of the study in tiludronate treated horses, while placebo-treated control horses' values were increased above baseline. Bone mineral density, as measured by dual energy x-ray absorptiometry, was reduced to 90% of initial values in the control horses immobilized MC3 by the end of the study. There was also an increase in bone mineral density observed in treated horses' immobilized MC3 by the end of the casting period and a higher bone mineral density when compared to the control horses by the end of the study. However, measurements of bone mineral density at the time of cast removal were thought to be falsely increased by limb edema overlying the measurement locations. In support of this, in the control group, bone mineral density measurements at the time of cast removal were higher in the immobilized MC3 compared to the opposite MC3, which is contrary to previous studies.[74–76] These findings all support the occurrence of disuse osteopenia in the equine MC3 both due to stall confinement and additionally due to cast immobilization.

The effect of the transfixation cast on bone strain below the pins has been well documented and compared to the effect of a standard limb cast.[55,57,61,62] In a study by Schneider et al, axial bone strain measured in the proximal phalanx during loading was reduced by 84% compared to a reduction of 61% observed with a standard half limb cast.[61] McClure et al showed that osteotomy displacement in the proximal phalanx was significantly reduced in the distal limb transfixation cast when compared to a standard half limb cast.[57] Hopper et al also found significant reductions in axial bone strain in the proximal phalanx with a full limb transfixation cast when compared to a standard full limb cast.[62] In addition, osteotomy displacement was observed to be reduced over a range of loading levels by a factor of approximately 10 in a full limb transfixation cast when compared to a standard full limb cast.[55] These findings all support the clinical and experimental observations made in regards to the development of disuse osteopenia when transfixation casts are used in the horse.[37,38,63] While a direct comparison of the osteopenia which develops within a cast and a transfixation cast has not been made, it seems reasonable to speculate that the degree of osteopenia which develops within a transfixation cast will be more profound than that observed in a standard cast. Recently, a

linear relationship between strain stimulus and bone mass and strength has been proposed,[79] and it has been shown that the mechanical load and strain experienced below the transfixation pins is lower than in a standard cast. In addition, the occurrence of secondary proximal sesamoid bone fractures following transfixation cast removal was thought to be a result of the profound disuse osteopenia observed in 2 clinical cases.[37,38] Taken together, these studies show that stall confinement alone can have an effect on measures of bone quality in the horse while cast immobilization has an additional negative effect. Transfixation casting has a more profound effect on strain reduction in the lower limb than casting alone and there is clinical evidence that disuse osteopenia from transfixation casting develops rapidly and puts horses at risk for secondary fracture.

2.3 The Bone-Pin Interface

During external fixation, the BPI is the critical link between the bone and the fixation construct. The biologic response of bone to a metallic implant as well as the mechanical behavior of external fixation pins and constructs have been examined in a range of animal species relative to their use in humans and small animals.[80–85] The majority of the available information on the BPI comes from these non-equine studies and some extrapolation to transfixation casting in horses is necessary. The specific assumptions made when modeling approaches have been used or the testing conditions utilized to examine the BPI should be scrutinized for their specific applicability to the horse. Maintaining BPI integrity is essential for continued pin stability and longevity. Bone-pin interface integrity is also critical for overall construct stability which contributes to both patient comfort and satisfactory fracture healing. Three key factors determine the ongoing integrity of the BPI; the preparation of the pin hole and insertion of the pin, local stresses within the bone due to cyclic pin loading, and infection of the pin tract.[83,86,87] These factors will be reviewed in detail following an overview of the expected biologic response of bone during external fixation and the mechanical aspects of external fixation constructs which affect the BPI.

2.3.1 Biologic response at the BPI

The biologic response of bone at the BPI is similar to the response to any implant, and is largely determined by the initial and ongoing mechanical environment that exists at the interface.[88–90] However, other factors such as sepsis, chronic inflammation and the surface characteristics of the implant can also influence the type of tissue that forms at this critical junction.[86,89,91,92] Initial bone damage incurred during implantation (both mechanical and thermal) stimulates local bone resorption and its replacement with new tissue at the implant interface.[93–95] The amount of bone resorption is representative of the degree of damage incurred.[90,96] The regeneration of bone tissue around an implant has been described as being akin to fracture healing,[88–90] and the replacement tissue that fills the interface will vary from bone to fibrous connective tissue.[92,96,97] An early examination of the response of bone to a long term implant was reported by Cameron and Fornasier,[98] who performed microradiography and histology on bone surrounding stainless steel and cobalt-chrome implants following up to 10 years of implantation in human patients. A range of tissue types were observed surrounding the implants, progressing from bone to cartilage or fibrocartilage, fibrovascular tissue and a layer of synovial-like lining cells closest to the implant. Hemosiderin found in the fibrovascular layer was thought to be indicative of ongoing trauma sustained by this layer in response to implant loading during activity.[98] The cancellous bone surrounding the implants was observed to take on an appearance similar to a subchondral bone plate, termed a “peri-implant bone plate” by these researchers. It has since been proposed that the type of tissue that forms is determined primarily by the type of strain field present at the interface of the implant.[88,99] In contrast to the early findings with stainless steel implants, the long term bone response to titanium implants was shown to result in direct bone to implant contact even when examined down to the electron microscopic level.[100] This intimate bone-implant contact was termed osseointegration and was thought to be a function of the response of bone to the titanium, including the surface chemistry of its titanium oxidation layer.[101]

The type of implant material used, its mechanical properties, the implant geometry, and surface chemistry and topography can all influence the biologic response of bone to an implant, along with the mechanical environment.[89,101] If there is relative motion between an implant and the bone, a layer of fibrous connective tissue is expected to form.[102] Recently, it has been proposed that this relative motion, or more specifically the interfacial strain resulting from micromotion at the implant interface, has a threshold level, above which fibrous tissue will form and below which bone healing and formation will occur.[92,103] This notion was previously proposed by Simmons et al when studying the effect of implant surface geometry on bone formation. A strain value of 8% was predicted to result in bone formation at the implant interface, whereas a strain value of 3% was predicted to result in de novo bone formation within healing tissue.[104] These findings suggest that there is a higher likelihood of fibrous encapsulation at implant locations that are more mechanically demanding, such as the interface between external fixation pins and bone, as has been observed, but that bone formation at the BPI is possible if the interfacial strain is kept below a certain critical value.[85,97] However, as stated previously, the mechanical environment at the BPI is not the only factor determining local tissue formation. Successful osseointegration of external fixation pins has been achieved through surface modification of titanium pins and the use of hydroxyapatite pin coatings to encourage early bone ongrowth at the pin surface.[105,106] From a biomechanical standpoint, initial pin stability appears to be a vital factor in the ongoing and long term stability of a pin.[85,97] Assuming that the rate of pin loosening is a function of the initial pin stability, greater initial stability will prolong the time for pins to become loose.[63,82,97] In addition, reducing the initial interfacial strain present between the pin and bone during loading by increasing initial pin stability will reduce the likelihood of fibrous tissue formation around the pin.[85] Critical to this notion is the bone response to any damage incurred during drilling, tapping and pin insertion. Significant bone resorption as a result of initial bone damage will negate the effects of an initially stable BPI as the pin becomes loose, the interfacial strain at the BPI increases and fibrous encapsulation becomes more likely. This concept of a cycle of bone resorption resulting in increasing interfacial and local tissue strains stimulating further bone resorption and continued deterioration of BPI

stability, has been proposed by other investigators in the context of hip replacement implants and cortical bone screws.[107]

The effect of different loading conditions has also been examined to determine the biologic response of bone to an external fixation pin.[84,85] Pettine et al examined external fixation pins inserted into canine tibiae and maintained for 40 days under 4 different loading conditions; 1) control pins with no external fixator frame attachment, 2) pins loaded in compression through the external fixator frame but without an osteotomy, 3) pins loaded by stabilizing an osteotomy with a gap, and 4) pins loaded by stabilizing an osteotomy in compression using the external fixator frame.[85] At the completion of the study, loose pins, defined as "easily pulled out by hand", had more bone resorption, less new bone formation and less original bone present at the BPI than tight pins. Radiolucency of greater than 1 mm around a pin at both the entry and exit cortex was a strong indicator of gross pin loosening. These investigators were able to determine an optimum initial insertion torque for tibial pins above which <10% of the pins became grossly loose and below which almost 70% of the pins became grossly loose in the 40 days of the study. Insertion technique and establishing an initially tight pin at insertion had an important effect on pin loosening. The pins which stabilized an unstable osteotomy gap also had a higher incidence of gross loosening than pins without an osteotomy, suggesting that greater local stresses at the BPI influenced pin loosening. Grossly loose pins were often observed to have an infiltrate of granulation tissue interposed between the pin and the cortical bone.[85] These findings appear to support the recent proposal by Wazen et al that a threshold interfacial strain may exist above which bone tissue will not form at the BPI.[92]

The influence of implantation time was examined in a study of the BPI performed in a sheep tibial osteotomy model by Schell et al.[97] This study included assessments at 3, 6 and 9 weeks of observation time, evaluating pin insertion and extraction torque as well as histology of the BPI and microbiologic culture. Contrary to their initial hypothesis that increased pin loosening and pin tract infection would occur over time, these investigators

found that there was not an increase in loosening following the 3 week time point. There was also a low infection rate reported with 2 of 24 pins (8%) culturing greater than 1000 colony forming units of the same bacterial species (criteria for excluding contamination during removal), both at 6 weeks. Histologically, the periosteal callus area measured surrounding pin tracts decreased from 3 to 9 weeks while the density of the periosteal callus increased, indicating maturation of the periosteal new bone. Endosteal callus area around the pins increased from 3 to 9 weeks while the density of the endosteal new bone decreased over this time frame. Interestingly, the density of the cortical bone surrounding the pins also decreased significantly from 3 to 6 weeks post-implantation.[97] The low infection rate and lack of progressive pin loosening beyond 3 weeks in this study was attributed to careful bone thread preparation and pin insertion as well as a vigilant pin care and cleaning routine. However, similar to previous studies using stainless steel pins[108,109] extraction torque measurements were lower than insertion torque measurements overall, and histologic grades progressively showed greater amounts of fibrous tissue present at later time points.

2.3.2 External fixator mechanics and the BPI

There are five main factors which influence the biomechanical performance at the BPI. These are the pin geometry and thread design, bone thread preparation, pin insertion technique, pin-bone stress and the overall external fixation rigidity.[81,83] The first 4 factors are specific to the pin and are discussed elsewhere in this review, this section will address how overall external fixation rigidity influences the performance of the BPI. Three key factors which contribute to the rigidity of external fixation are the effect of weight bearing, the configuration of the fixation device and the degree of fracture reduction and/or load sharing that is present.[83] In horses, weight-bearing immediately following fracture repair is desirable to avoid secondary complications in the opposite limb, such as support limb laminitis.[110] The weight-bearing loads in the metacarpus of a 500 kg horse can be calculated to be 1,470 N during standing with even weight bearing among limbs. At the walk, loads have been estimated to be 7,500 N.[111] As stated previously, high local

stresses and strains at the BPI, which will be present with large weight bearing loads or unstable fracture reductions, result in local bone yielding, bone resorption and ultimately pin loosening due to failure of the bone at the interface.[81,83,85] Bone failure at the interface ultimately results in fibrous tissue formation around the pin. The type of fracture and consequently the amount of cortical contact present following fracture reduction are critical for the axial rigidity of the external fixator construct.[81] In turn, the overall rigidity of the fixation contributes to the stresses transferred through the BPI in any construct. In an experimental canine tibial osteotomy model, the incidence of pin loosening was shown to be higher in a less rigid external fixation configuration.[112] Increasing the rigidity of a fixation construct can be achieved by increasing pin diameter, increasing pin number, decreasing the distance from the outer bone cortex to the connecting bar (the working length), decreasing pin separation, increasing pin-group separation on either side of the fracture and applying pins in multiple planes.[19,81,83]

2.3.2.1 Pin diameter

The diameter of the external fixation pin plays a critical role in the rigidity of the ESF.[19,64] The area moment of inertia of the pin is proportional to the pin diameter raised to the fourth power. The area moment of inertia of the pin describes the contribution of its shape towards the bending resistance of the pin to an applied moment force. The moment force of the pin has been estimated to contribute to greater than 90% of the pin-bone interface stresses during external fixation, with the transverse loading force contributing the remainder.[64] The pin diameter and the pin material are the only factors that can be varied to alter the resistance to bending (rigidity) of the pin. The larger the pin, the greater the resistance to bending and the more rigid the fixation, when all other factors are equal.[19] Considering the impact that fixation rigidity has on the BPI it is logical to consider the upper and lower limits of pin diameter that can be used in external fixation. The upper limit to pin diameter will be determined by the bone into which it is placed for fixation. A larger pin will result in a larger defect in the bone cortex and

greater loss of bone strength.[113–116] The lower limit of pin size will be determined by the likelihood of a pin bending or breaking under the expected load.

2.3.2.1.1 Upper limit of pin diameter

Currently, there is no consensus on what the optimum pin diameter is that will avoid complications due to loss of bone strength following insertion. A common guideline used for ESFs in humans and small animals has been to use a ratio of pin diameter to dorsal-palmar bone diameter that is approximately 0.2 or 20%.[15,114,115] Due to the requirement to support large weight-bearing loads early in the post-operative period this guideline was surpassed in early attempts at external fixation in the horse, reaching a pin diameter to bone diameter ratio over 0.3.[27] It is known that any sized bone defect will create a stress concentration at the edge of the defect, where the resulting bone stress present is higher than it would normally be under the same load without the defect being present.[113] Several investigators have attempted to quantify or model the strength reductions expected in a long bone as a result of cortical defects, both for the purposes of determining an appropriate pin size as well as to predict what size or shape of bone defect may require prophylactic fixation to avoid pathologic bone fracture following tumor removal or biopsy.[113–118] There have been fewer studies examining the effect of hole size on bone strength in the horse, although the findings have been comparable with the studies in smaller animals.[119,120] Unfortunately, the studies performed have used a variety of methods, such as different animal species, different bones, testing and failure criteria, and different hole sizes and number of cortices, making direct comparison or corroboration of the findings difficult. However, some general guidelines can be assembled from the various studies. Brooks et al evaluated 2 commonly used hole sizes in the humerus and femur of dogs with a hole diameter to bone diameter ratio ranging from 0.12 to 0.28. Holes were drilled through both cortices and bones were tested in torsion to failure. No difference was observed in failure energy between the hole sizes tested. There was a significant difference in failure energy between intact and drilled bones with drill holes reducing failure energy by up to 59%. The calculated stress

concentration factor averaged 1.6 over all bones tested.[117] In an effort to expand on these findings and to develop prediction models of bone failure following drilling, McBroom et al used cadaveric testing in canine femora along with beam theory calculations and FE models to provide guidelines for fracture risk in bones with diaphyseal holes.[113] Unicortical holes were created at the femoral midshaft with hole to bone diameter ratios ranging from 0.1 to 0.8. Bones were tested to failure in 4-point bending with the hole positioned to undergo tensile loading. Mean loss of strength as calculated from failure load was 38% for holes with a hole to bone diameter ratio of 0.2, and 70% for holes with a ratio of 0.8. The progressive reduction in strength did not follow a linear pattern when the hole to bone diameter ratio was considered, however when the cross-sectional area of cortical bone loss was examined for each hole, a linear relationship with loss of strength was apparent.[113] The stress concentration factors calculated in this study, which were based on the models and predicted stress at the hole cross-section, ranged from 2.3 to 2.6, with lower values present in the larger holes examined. Edgerton et al performed a study in sheep femora evaluating the effect of unicortical holes in the posterior (caudal) cortex on bone strength during torsion to failure.[114] There was no difference detected between intact and drilled bone for ultimate failure torque or failure energy for defects with a hole to bone diameter ratio up to 0.1. Similar to McBroom et al, defects with a hole to bone diameter ratio from 0.1 to 0.2 resulted in a large reduction in the measured parameters when compared to intact bones. For a hole to bone diameter ratio of 0.2, ultimate failure torque was 36% lower than the control, while ultimate failure energy was 60% lower than control. The reduction in failure torque and energy for hole to bone diameter ratios from 0.2 to 0.6 was more gradual and linear. Interestingly, despite gradual reductions in failure characteristics for hole to bone diameter ratios ranging from 0.1 to 0.6, there was no significant change in stiffness calculated for any of the bone specimens with defects in this study.[114] Hipp et al expanded on the findings of Edgerton et al in sheep femora by using the *in vitro* data they generated to create FE models of the unicortical defects and study the effect of varying different bone parameters.[115] Using this numerical approach and expanding to bicortical holes several material and geometric parameters were investigated, including bone material properties, hole size, cortical wall thickness, long

bone curvature and defect length. Cortical thickness and defect length were found to have significant effects on torsional strength whereas long bone curvature had a minor effect. Interestingly, in contrast to previous *in vitro* results, the models predicted a rapid drop in torsional strength up to a hole to bone diameter ratio of 0.1, with a more gradual drop between a ratio of 0.1 and 0.6.[114,115] Expanding on these findings, Kuo et al addressed the issue of the location of the maximum stress relative to the bone defect size using an acrylic tubular model of bone and a combination of experimental data and FE modeling.[116] Similar to previous studies, a large decrease in torsional strength was observed for a hole to bone diameter ratio of 0.1 showing a 43% loss of strength. A less dramatic and more linear reduction in strength was observed beyond this point with a loss of 69% of failure torque at a hole to bone diameter ratio of 0.6. Higher hole to bone diameter ratios also resulted in a shift of the fracture helix path that initiated at the edge of the hole. This was consistent with a shift in the location of the maximum stress for larger defects compared to smaller defects. The other finding of note by Kuo et al was that when single and double cortex holes were compared the overall stress concentration factors were found to be similar, which is in line with observations between studies examining unicortical and bicortical holes, where absolute loss of bone strength were similar despite different bone hole locations and animal species used.[114,116,117] Several studies have reported that the failure mode in bones with drilled holes displays less comminution than intact control bones.[113,117,119] This observation is consistent with the finding that a bone with a drilled hole has a lower failure energy with less stored energy released upon fracture.

In horses, 2 studies have attempted to address the question of whether hole size affects bone strength.[119,120] Seltzer et al compared the torsional mechanical properties of equine third metacarpal bones with no holes, 5/16” (7.9 mm) holes and 3/8” (9.5 mm) holes drilled at the midpoint of the diaphysis in a bicortical medial to lateral direction. These hole sizes ranged from 22 to 33% of the dorsal-palmar bone diameter and were chosen to be clinically relevant for the current state of practice for external fixation in horses at the time of the study. Similar to Edgerton et al, these investigators did not observe a change

in bone stiffness between the 3 groups. However, as the hole to dorsal-palmar bone diameter ratio increased the yield and failure torques and energies decreased. The hole to bone diameter ratio only accounted for up to 30% of the variability in the mechanical properties data overall, suggesting that factors other than the hole to bone diameter ratio contribute to reductions in mechanical properties in drilled bones. Interestingly, there was failure of all specimens with 3/8" (9.5 mm) holes at the yield point, with no plastic deformation occurring in these bones. The authors hypothesized that this lack of post yield behavior, with enough stress concentration to result in bone failure upon yielding, could be clinically relevant. The larger hole size may result in horses failing to protect the limb prior to reaching this yield point stress as pain associated with plastic deformation and damage accumulation may not be experienced during use of the limb.[119] In comparing the findings of Seltzer et al to studies in other species, the reduction in failure strength ranged from 13 to 22%, somewhat lower than observed by Edgerton et al (unicortical holes in sheep tested in torsion), Brooks et al (bicortical holes in dogs tested in torsion) and McBroom et al (unicortical holes in dogs tested in 4-point bending). Despite this, Seltzer et al concluded that both hole sizes reduced all torsional structural properties of the bone, excluding stiffness, and so would presumably put horses at risk of catastrophic fracture through the hole during use of the limb.[119] In a study evaluating hole size in the equine radius, Hopper et al found a 13% lower mean torsional breaking strength for a 9.5 mm hole when compared to a 6.35 mm hole drilled in the distal radius.[120]

Despite the range of methods and findings presented in these studies, the following conclusions can be applied to the question of a safe upper limit hole size that can be used in the application of transcortical pins in the horse; 1) any size of hole is expected to result in a stress concentration in the bone; 2) larger hole sizes result in larger reductions in expected failure load and failure energy than smaller hole sizes; 3) a hole to bone diameter ratio greater than 0.3 can result in changes in failure characteristics (no plastic deformation) in equine bone; 4) a hole to bone diameter ratio of greater than 0.5 can result in changes in the expected location of maximum stress at the hole edge; 5) similar

loss of strength is expected for unicortical and bicortical holes; and 6) there are factors other than hole size which will contribute to a loss of bone strength, such as cortical thickness and hole elongation. One final consideration is the effect of the presence of the pin within the hole and the effect this may have on BPI stress, compared to the effect of an empty bone defect on bone strength.

2.3.2.1.2 Lower limit of pin diameter

Pin bending and pin breakage have both been reported as complications of transfixation casting in the horse.[37,38,40] There are a range of factors which determine the lower limit of pin size that can be used for external fixation. These can be divided into factors related to the pin itself and those factors which determine the stresses on the pin during loading. Properties of the pin itself which are important to consider include the yield strength, ultimate strength and the fatigue properties of the pin material in addition to pin size. Implant mechanical properties are dependent on both the type of metal used and the manufacturing methods used to produce the implant. There are a range of manufacturing methods that can alter the yield and strength properties of a metal.[121–123] Yield strength is the stress at which plastic deformation of the pin begins to occur. The yield strength of medical grade 316L stainless steel, which is the most widely used metal in external skeletal fixation applications, is reported to range from 23 to 767 MPa.[121] Values around 170 - 190 MPa have been reported from steel manufacturers and in the medical literature for stainless steel used in orthopedic implants.[122,124] The ultimate strength of the pin material is the stress at which monotonic or single cycle failure of the pin occurs.[123] The ultimate tensile strength of stainless steel is reported as between 341 and 1000 MPa.[121] Values of 485 and 490 MPa have been reported from steel manufacturers and in the medical literature for stainless steel used in implants.[122,124] In theory, if an implant is not loaded beyond its elastic limit (beyond the yield stress) it would have an infinite lifespan. In reality, additional factors such as corrosion and material imperfections contribute to eventual material failure.[122,123] However, the yield stress can be used as a conservative guide for an implant stress that could avoid fatigue failure. The fatigue properties of an

implant can also be determined experimentally through the construction of an S-N curve, on which loading stress (S) is plotted against the number of cycles (N) to failure of an implant.[123] Loads which are close to the ultimate strength of the implant will result in fatigue failure after relatively few cycles, whereas loading at stress levels much lower than the ultimate stress (but higher than the yield stress) will result in the implant withstanding a much larger number of cycles prior to failure. Experimental determination of the number of cycles to failure at a fixed stress level and mode of loading allows a curve to be generated from several (usually at least 6 or 7) points of stress and corresponding number of cycles to complete material failure. There is a stress level, known as the endurance limit or the fatigue strength, which can be extrapolated from an S-N curve as the asymptote of the curve below which an implant will endure a very large number of cycles (typically greater than 10^7) without failure.[122,123] The fatigue strength of 316L stainless steel is reported to range from 256 MPa to 307 MPa,[121] although in the recent review by Chen and Thouas a lower value of 200 MPa was reported when testing was performed in phosphate buffered saline.[122] Another method to estimate a "safe" stress level that avoids fatigue failure for ductile metals can be made using 35 to 60% of the ultimate tensile strength.[125] For 316L stainless steel this would be approximately 172 to 294 MPa. Considering the different methods of manufacture and modes of testing used to determine fatigue limits, all of these estimates can only be used as a guide in the determination of the lower limit of pin size for use in transfixation casting. The large range of values reported serve to illustrate that no single "safe" stress level can be assigned to the use of transcortical pins in the horse considering the upper limit of pin size as determined by the bone as has been outlined previously. Other factors, such as pin manufacturing processes, stress concentrators and the pin stress level itself, as determined by pin number, configuration, axial load and pin working length, will be important determinants of the likelihood of pin failure.

The number of cycles a transfixation pin will be required to withstand can be estimated from a knowledge of normal bone healing, previous studies on the clinical use of transfixation casting for fracture treatment and the activity level of a horse confined to a

stall during hospitalization. It has been reported that in the stress protected environment of the transfixation cast, fracture healing and particularly callus mineralization appear to be delayed and that radiographic healing may not be detected prior to pin removal.[37,38] In the adult horse, recent retrospective studies have shown that fracture management is most successful when the duration of transfixation casting is 6-8 weeks.[37,38,65] McDuffee et al previously determined that a hospitalized horse takes approximately 200 steps per hour over a 24 hour period, or 4800 steps per day when confined to a box stall.[126] The range among horses in this study by McDuffee et al was from 64 to 502 steps per hour. Therefore, an approximate range in the number of implant cycles during transfixation casting (using upper and lower values for both time and step rate) can be calculated as between 64,512 and 672,000 based on these estimates. An intermediate value would be 235,200 cycles using 200 steps per hour for 7 weeks. This number of implant cycles is small compared to the expectation for a permanent implant and well below the 10^7 cycles which are used to determine the fatigue strength of an implant material.[122,123]

Factors which determine the stress in the pin itself during external fixation were systematically explored by Huiskes and Chao.[19] The maximum pin stresses are predicted to occur at the level of the outer margin of the bone cortex. The determinants of the pin stress include the axial loading force, the diameter of the pin, the working length of the pin, the total number of pins and connecting rods in the fixator system and the pin area moment of inertia.[19,64] Apart from the axial loading force, which may vary from 1,470 N in an evenly weight bearing, 500 kg standing horse to 7,500 N at the walk,[111] and which may be reduced by load sharing through the fracture, the other determinants of pin stress also play a role in determining overall construct rigidity.

2.3.2.2 Pin number

Assuming that the axial load is supported somewhat evenly among each pin within a construct, the number of pins has a direct effect on construct rigidity, pin stress and BPI stress.[19] A common recommendation for the ideal number of pins to be used in a

conventional ESF is 3 or 4 pins on each side of the fracture.[10,15] This recommendation balances the greater construct stability afforded by a larger number of pins with the space limitations within fractured bone segments and reasonable spacing between pins. Pin stress and BPI stress are inversely proportional to both pin number and the number of connecting rods present in an ESF, while construct rigidity is directly proportional to these factors.[19] Therefore, increasing the number of pins and connecting rods increases construct rigidity and reduces both pin stress and BPI stress. Since transfixation pins are not typically placed distal to the fracture site and are often positioned in an intact bone above the fracture, a different set of limitations on the number of pins used during transfixation casting exist compared to conventional external fixation. From 2 to 5 transfixation pins have been used in clinical transfixation cast cases.[37] Several authors have also cautioned against placing transfixation pins close to the top of the cast due to a greater occurrence of secondary fracture through the top pin hole.[16,37,40] Pin number is also determined in part by pin spacing in a particular bone. Nunamaker et al, in their original description of the equine external skeletal fixation device used a pin spacing of 5-cm between pins in the third metacarpal and third metatarsal bones.[27] Pin spacing used for transfixation casts has been approximately 2 to 2.5 cm.[16,37,127]

2.3.2.3 Pin working length

The pin working length is the distance along the pin from the outer cortical surface, where the pin exits the bone, to the point of contact with the connecting clamp, or in the case of a transfixation cast to the point of contact with the cast material. According to Huiskes and Chao, the rigidity of an external fixation construct is inversely proportional to the working length of the pins raised to the third power.[19] This relationship assumes an absolutely rigid fixation point between the connecting rod and pins as well as a connecting rod that does not bend. In the case of a unilateral ESF these assumptions do not hold and experimental data for rigidity matched poorly with the parametric models proposed.[19] However, for bilateral fixators the symmetric arrangement results in a more accurate approximation of rigidity by the parametric model. Regardless, a shorter pin

working length results in a considerably more rigid construct. In addition, the assumption of rigid fixation between pins and a transfixation cast, which may be unreasonable, could affect the construct rigidity. This concept will be explored and addressed further in a subsequent chapter.

The working length of the pins also has a directly proportional effect on both the maximal pin stress and pin-bone interface stress.[19,64] There have been several efforts to improve the mechanics of external fixation in the horse through manipulation of the pin working length present using conventional ESF. The most basic of these efforts, the transfixation or walking cast concept, has been extensively discussed as it is a focus of this review, where the pin working length is minimized by the use of a cast over the pins rather than connecting rod attachments. Two other methods to improve the mechanics of external fixation in horses have been the tapered-sleeve concept and the pin-sleeve concept.[41,42,128,129] The tapered-sleeve concept was first proposed by Nash et al, as a way to reduce the working length of the pin by placing a tapered-sleeve over the transfixation pin and tightening the sleeve down to the bone using threads on the pin.[42] The tapered-sleeve extended from the bone to the sidebar. It was hypothesized that since the load was transferred from the tapered-sleeve to the pin immediately adjacent to the bone surface, the transcortical pin was loaded in shear rather than bending as expected in a conventional ESF. This concept substantially increased the load to yielding and the construct stiffness compared to conventional pins for 3 different pin sizes tested.[42] A modification of this concept was tested by using the tapered-sleeve pins with a cast rather than a sidebar. Elce et al evaluated this concept and compared a standard transfixation pin cast to a tapered-sleeve transfixation pin cast in a distal radial osteotomy model in adult horses.[128] Higher mean load to failure was reported for the tapered-sleeve transfixation pin cast.

The pin-sleeve concept for external fixation involves placing a sleeve within the bone which has two ridges on its internal surface for contact with the transfixation pin. The transfixation pin is then retained within an external ring embedded in the cast.[129,130] The

pin was tensioned within the ring to improve its stiffness and bending resistance under load as a smaller pin size (5 mm diameter compared to 6.3 mm transfixation pin) was required to fit within the sleeve (8mm diameter). The working length of this pin-sleeve system is actually larger than the standard transfixation pin because the pin contact points of the sleeve are inside the bone cortical edge and the cast attachment remains at a similar distance. However, the bending of the pin occurs within the sleeve during loading and so not all stresses as a result of the bending moment are transferred to the bone. Brianza et al showed a large reduction in bone stress and strain in an FE model of this concept.[129] While these methods of BPI stress reduction and fixation construct rigidity improvement have been explored experimentally, the transfer of these concepts to clinical use has been challenging.[41,131]

2.3.2.4 Connecting rods, clamps and fiberglass cast material

The significant impact that fiberglass casting material has had on improving transfixation casting compared to plaster of Paris used in the walking cast was described earlier in this chapter.[16,40] One unique aspect of transfixation casting which cannot be readily extrapolated from previous studies of the mechanics of external fixators is the effect of using fiberglass cast material in place of connecting rods and clamps for the fixation construct. Increasing the number of external fixation connecting rods increases construct rigidity,[19,64] and using additional rods between connecting rods also improves fixator rigidity.[10,14,15] Using cast material, which encompasses all pins within the transfixation cast construct, in effect creates as many connecting rods as would be possible for the pin configuration selected. The substitution of cast material for connecting rods into existing parametric models of external fixation mechanics,[19,64] introduces further uncertainty about the validity of the ESF models. An additional factor to consider is the attachment of transfixation pins to the cast material. As stated earlier, it is often assumed that fixation between the pin and the connecting rod is perfectly rigid in idealized models of external fixation and that the connecting rod does not bend. It is known that these assumptions are violated and that in the case of a unilateral fixator the effect of connecting rod bending

results in inaccuracy of the predictions sufficient to warrant an alternative, more complicated model to improve prediction of construct stiffness by accounting for connecting rod bending.[19] Making the assumption that the transfixation pin attachment to the cast and the cast material itself will be perfectly rigid is more questionable than it is for external fixators, where current connecting rods and clamps have evolved to be strong and stable for their purpose.[15] The effect of the stability of the pin attachment to the clamp and connecting rod was evaluated experimentally by Egkher et al as it applies to external fixation.[132] These investigators altered the amount of pin positioned within the clamp to simulate altering a theoretical bearing factor parameter on pin displacement during loading. The bearing factor could vary from a value of 1 (perfectly rigid connection) to a value of 4 (single point support of the pin). It was found that an intermediate value of 2.5 should be assumed for most fixators based on their experimental data.[132] McClure et al showed that the attachment of transfixation pins to fiberglass casting material was primarily limited by the strength of the cast material itself in axial loading.[60] Four different methods of attachment were assessed. A washer and nut on the pin within the cast material, attachment of the pin to a steel halo outside the cast using the washer and nut, a combination of washers within the cast and an attached steel halo outside the cast, and simple incorporation of pins directly by the cast material. There was no difference in stiffness modulus between methods of pin attachment under compressive loading to failure or following cyclic loading. In addition, the presence of pins within the cast material, regardless of attachment method, reduced the stiffness of the construct compared to cast material alone.[60] As a result of this study, the simplest method of direct incorporation of the pins into the cast has generally been adopted in clinical practice with minor modifications.[16,37,38,65] Interestingly in the study by Elce et al, where tapered-sleeve pins in the radius were incorporated into casting material and compared to standard transfixation pins, constructs from both groups failed exclusively through buckling and delamination of the cast material with dorsal bending at the carpus.[128] Failure occurred at a mean load of 35,814N for the tapered-sleeve pins and at a mean load of 22,344N for the standard transfixation pins. None of the constructs failed through the bone or from pins bending or breaking. The authors stated that neither

fixation method provided sufficient dorsal-palmar stability but did not speculate on the reason for the difference in constructs beyond suggesting that the tapered-sleeve resulted in pin loading in shear rather than bending.[128] Considering failure for all constructs was in the cast material and not at the BPI, the higher loads to failure found in the tapered-sleeve pin group may indicate that the attachment of the cast to the larger diameter sleeve influences the behavior of the cast pin construct under large compressive loads compared to standard pins.

As the cast was found to be the weakest link in these 2 studies of cast-pin interface attachment and the transfixation cast technique using tapered-sleeve pins, an examination of the properties of fiberglass cast materials is warranted.[60,128] Fiberglass cast material properties have been examined by several investigators,[133–140] including studies that have compared fiberglass casts to plaster of Paris.[136–139] There is no standardized testing established for cast materials and most investigators have examined a range of features including both material property tests, such as uniaxial tensile testing, as well as structural tests such as a cylinder bending test. Callahan et al published details of 3 separate cast strength tests which have been adopted by others in the testing of cast materials.[133] These authors argued that because casts can fail in any number of ways a series of tests is preferable over one single standardized test of cast material. They described a 3-point bending test performed on a cast cylinder applied over a Styrofoam form (structural test), a 3-point bending test performed on a beam of cast material (material test) and a diametral compression test, or Brazilian test, which was performed by placing a compressive load across a disc of cast material (material test). Tests used by other investigators to examine cast strength have included a cast cylinder compression test, cyclic deflection test, uniaxial tension test, lamination strength build up test, water immersion test and an impact strength test. Additional tests have been developed to examine properties such as exothermicity, permeability, radiolucency, roughness and wear resistance of cast materials. Studies have found minor differences between the different brands of fiberglass casting material and no single brand appears to be superior across the range of tests employed. The polyurethane resin impregnated fiberglass cast

materials have, however, been shown to be generally 2-3 times stronger than plaster of Paris across the range of tests applied.[136–139] The directional properties of the different types of cast materials have been shown to vary; fiberglass cast materials were stronger in bending and tension transversely (across the material roll) while plaster of Paris was stronger longitudinally.[137] The effect of water on the strength of cast materials has also been examined.[137,139] Plaster of Paris loses almost 60% of its strength when wet, whereas fiberglass materials lose between 13 and 41% of their strength when they are wet and return to 70-93% of their original strength when they are subsequently dried.[139] These findings may be relevant to the cast pin interface of the transfixation cast if discharge around the pin results in moisture wicking through to the cast material itself. Interestingly, plaster of Paris has been shown to have bilinear load/displacement behavior under tension with higher initial stiffness due to the plaster material and a longer lower stiffness due to the bandage material. Fiberglass cast materials respond to loading in a linear elastic manner with an elastic modulus calculated to be 316 MPa.[136] The strongest fiberglass casting material found in the initial studies performed by Callahan et al failed in compression at a mean load of 13,941 N[134] The mean ultimate failure load of the strongest material under tensile testing from the study by Bartels et al was 1,561 N/cm.[135]

2.3.2.5 Pin elastic modulus

The material used for an external fixation pin determines, along with the size of the pin, its ability to resist bending and consequently the stiffness of the fixation construct. For specific metals, the modulus of elasticity (or Young's modulus) of the material reflects this property. The two most commonly used metals for orthopedic implants are 316L stainless steel, which has an elastic modulus of 200GPa, and titanium alloy (Ti-6Al-4V) which has an elastic modulus of 110GPa.[122] The elastic modulus of the pin has a proportional relationship with construct stiffness and an inversely proportional relationship with the expected BPI stresses.[19,64] A higher pin modulus will result in a higher construct stiffness and lower BPI stresses. Stainless steel has several disadvantages when compared to titanium alloys if used for long term implantation

within the body, including corrosion and fatigue failure.[122] However, for short term implantation as an external fixation pin, the mechanical properties of stainless steel are superior to titanium in terms of construct stiffness and expected BPI stresses. There are two factors however, which may result in an advantage of titanium alloy over stainless steel for external fixation pins. The first is the ability of bone to form in close apposition with the titanium alloy surface (osseointegration). This attachment could alter the way in which stresses are transferred to the bone from the pin during loading by transferring both tensile as well as compressive loads as was postulated by Huiskes and Chao.[19,64] In this situation, it is conceivable that BPI stresses may be reduced by up to 50% for a fully integrated pin compared to a pin in which only compressive loads are transferred to the bone. The second potential advantage of titanium alloy over stainless steel is the fact that its elastic modulus is closer to that of cortical bone than stainless steel.[122] The elastic modulus of cortical bone typically falls in the range of 10-20 GPa. It has been suggested that the lower elastic modulus of titanium alloy compared to stainless steel can result in less stress shielding and pain associated with implant loading. Titanium alloy also has a considerably higher strength to weight ratio than other metals used for implants.[122,141] Titanium alloy yield strength (828MPa) is over 4 times higher than implant grade stainless steel, its ultimate strength (895MPa) is almost 2 times higher than stainless steel, while its density (4.43 g/cm^3) is almost half that of stainless steel (8.0 g/cm^3). These advantages may outweigh the disadvantage in terms of construct stiffness for external fixation pins due to the lower elastic modulus compared to stainless steel if smaller diameter pins (and hence pin holes) are able to be used in equine transfixation casting.

2.3.3 Pin hole preparation and the BPI

The stability of the BPI requires ongoing intimate bone contact with the pin surface. As outlined earlier, local bone resorption around the pin and its replacement with fibrous tissue is the underlying process by which pin loosening occurs during external fixation. Bone resorption can be a result of ongoing local stresses which exceed the yield limit of the bone,[81,85] infection of the pin tract,[67,68] or bone damage at the time of pin insertion.[142–

[144] Local bone damage from the process of pin hole preparation and pin insertion into the bone can be conceptually divided into thermal and mechanical bone damage, although these phenomena are closely linked in the pin hole preparation process.

2.3.3.1 Thermal bone damage

Thermal bone damage has long been recognized as a potential source of complications following bone drilling in orthopedic procedures.[96,145–149] In vitro evaluation of the effects of heat shock on osteoblasts found that irreversible disruption of cytoskeletal elements and activation of cellular processes leading to apoptosis or necrosis occurred at 48°C.[150] In early work evaluating the effect of heat on the viability of bone tissue in vivo, a threshold temperature of 47°C was proposed based upon experiments evaluating the effect of both time and temperature on bone tissue during vital microscopic observations in rabbits.[96,147] The distance of detectable bone damage from the heat source, as determined by histochemical diaphorase staining methods, was found to increase linearly with increasing exposure time, while it increased exponentially with increased temperature.[96] In bone exposed to 47°C for 1 minute, detectable resorption was observed 2-3 weeks following the heating event in 40% (2/5) of animals.[147] When the temperature was increased to 50°C for 1 minute, or the time increased to 5 minutes at 47°C, all bones underwent observable resorption and replacement with fat.[147] In an earlier study, at a bone temperature of 60°C for 30 seconds, bone damage was detected up to 0.2 mm from the heat source, while at a temperature of 80°C for 5 seconds bone damage was detected up to 0.4 mm from the heat source.[96] In the case of severe thermal damage, bone tissue resorption may extend beyond 1 mm from the heat source.[96] These findings serve to illustrate the important interplay between bone temperature and exposure time as well as the significant impact, in terms of the resorption zone, that thermal damage can have in the early post-operative period following pin insertion. As a result of bone resorption from thermal damage and its replacement with fibrous connective tissue, the extraction force of an implant was also shown to be significantly reduced.[96]

Pin hole preparation has evolved in response to complications arising from thermal bone damage.[86,142,151] While it is feasible to place pointed external fixation pins in small animals and humans without creating a pilot hole,[86] reduced bone damage and enhanced pin stability results when pilot holes are drilled prior to pin placement.[86,143,144,152] Wikenheiser et al found elevated bone and pin temperatures measured during the insertion process of half pins examined in their study despite using manufacturer recommendations for pilot hole drilling. There was also a correlation between pin torque during insertion and the heat generated.[153] Pre-drilling holes for pin placement is therefore currently recommended in small animals.[15,86] In horses and other large animals, due to the thickness and density of the cortical bone, it is not possible to place transcortical pins without drilling a pilot hole. Some investigators have examined the feasibility of using self-tapping pins in the equine MC3 as a way to simplify pin insertion.[142,154] Morisset et al evaluated a self-drilling, self-tapping transfixation pin in the diaphysis of the equine MC3 and found that the mean temperature of both the drill point on the pin and the pin thread exceeded 70°C when placement was performed with saline irrigation at 20°C. The mean temperature of the drill tip in the non-self-drilling non-self-tapping group of this study, in which drilling, tapping and pin insertion were performed as separate steps for pin placement, exceeded 60°C.[142] Bubeck et al evaluated a self-tapping transfixation pin in equine MC3's and found mean temperature elevations of over 20°C in the bone at a location 1 mm from the pin threads. At the trans cortex, these temperature elevations were greater than 10°C for over 1 minute.[154] The results of both of these studies illustrate that in dense equine cortical bone, the use of self-tapping transfixation pins results in temperature elevations that are likely to result in considerable thermal damage to the pin hole and these types of pins are not recommended for use in the horse.

An examination of methods to reduce bone temperatures while drilling pilot holes in equine MC3's has been performed by several investigators.[151,155–158] The use of a sequential over drilling method to create a 6.2 mm diameter hole has been shown to result in lower temperature elevations within the bone surrounding the drill hole when

compared to a single drill hole method.[151,158] Lower drill speed and higher feed rate during drilling have also been shown to reduce the maximum bone temperature attained during drilling the equine MC3.[157] McClure et al found no difference between drilling the diaphysis and the metaphysis of MC3 in terms of maximum temperature measured on the drill bit, pin tap or pin threads.[156] Application of a hard-carbon nanofilm to the surface of the drill bit to reduce its co-efficient of friction resulted in lower mean temperatures and reduced drilling time when compared to standard stainless steel drill bits.[155] In spite of these methods to improve drilling the equine MC3, at least in cadaveric testing, none of the temperatures reported would be considered to fall into the "safe" temperature of being less than 47°C for less than 1 minute immediately at the BPI. Several studies showed temperature elevations of less than 10°C at distances of 1 mm from the hole margin. However, when either the hardware temperature within the hole or extrapolation of the expected bone temperature at the hole margin from the measured temperature at a known distance from the hole is considered, thermal bone damage is likely to occur when transfixation pins are placed in the equine MC3 using best practices pilot hole drilling.[157] How these studies performed in cadaveric equine bones compare to the in vivo drilling situation is unknown. The effect of local blood flow in dissipating heat from the bone during drilling has not been examined directly. However, in human patients, Eriksson et al found in vivo drilling temperatures up to 89°C at 0.5 mm from the hole margin and observed that the temperatures were higher in bones with a larger cortical thickness.[145] Baker et al also found temperatures up to 89°C in human patients during femoral head resurfacing procedures and concluded that up to 1/3 of patients in their study likely suffered from thermal osteonecrosis based on the in vivo temperatures recorded.[94] It is also unknown how the thermal effects of bone drilling and pin placement procedures may alter the immediate mechanical properties at the BPI prior to any biologic response in the form of bone resorption or regeneration. In a study evaluating the effect of conventional bone cutting compared to laser cutting of the murine tibial cortex, collagen denaturation due to thermal damage was observed and resulted in delayed bone matrix deposition and healing time due to a prolonged inflammatory response.[93] Heat denaturation of the organic matrix proteins present in bone may also play a role in directly altering the

mechanical properties of bone.[159] This alteration is distinct but closely related to the direct mechanical bone damage that results from drilling, tapping and insertion of transfixation pins.

2.3.3.2 Mechanical bone damage

Drilling a pilot hole, tapping threads along the hole and inserting a transfixation pin into the threaded hole can all contribute to mechanical bone damage at the BPI.[142,143,153,154,156] In addition, Field and Sumner-Smith documented vascular damage with perfusion impairment in the cortical bone surrounding a drill hole in sheep.[160] Removing bone by drilling or tapping is a bone cutting process during which bone chips are formed at the cutting edge of the drill bit or tap thread. Chip formation, being essentially a controlled fracture process, results in microdamage to the remaining bone surface (the hole) as well as the chip (swath) itself.[161,162] Wikenheiser et al showed that microdamage is expected to result from each of the phases of pin hole preparation and pin insertion in sheep tibiae.[153] McClure et al found that cortical microfractures occurred primarily during drilling and tapping of holes in the equine MC3 while pin placement did not add significantly to the damage already present.[156] Clary and Roe found that microfracture around the pin hole and threads was minimized by drilling a pilot hole that is close (within 0.1 mm) to the core diameter of the pin being inserted.[143] Bilouris et al have questioned the use of a radial preload for initial pin stability. They found varying degrees of gross and microscopic damage associated with preloads up to 1 mm in human cadaveric tibia.[144] Morisset et al found greater damage in self-drilling self-tapping pins when compared to non-self-drilling non-self-tapping transfixation pins in the equine MC3,[142] while Bubeck et al found no difference between bone damage scores between non-self-tapping pins and self-tapping pins.[154] From these studies it is clear that mechanical bone damage occurs at the time of pin hole creation and that creating a pilot hole that is very close to the core diameter of the pin is preferred to minimize this damage. Additional local vascular damage may also compromise the bone surrounding the pin that constitutes the BPI. The degree of damage, both thermal and mechanical, will impact the initial and the ongoing

stability of the BPI as well as the bone remodeling response which will follow pin insertion.[97] In addition, these changes in the BPI over time will be impacted by the local stresses experienced by the bone through pin loading.

2.3.4 Local stresses at the BPI

Local BPI stresses, primarily a result of cyclic pin loading during weight bearing, play a central role in changes which occur at the BPI during external fixation. These changes are attributable to the effect of these stresses on the bone material immediately surrounding the pin. As was previously discussed, the bone immediately surrounding the pin is initially at risk of thermal and mechanical bone damage at the time of surgery for pin placement. This damage may alter the mechanical properties of the local bone tissue. In addition, bone resorption at the pin hole can result in a change in the local stresses as the support for the pin and integrity of the BPI is lost, the effective pin working length is increased and pin stability decreases. Huiskes and Chao proposed that, in an idealized model of a type-2 ESF, the BPI stresses are dependent upon several parameters related to both the bone dimensions, and the pin and fixator mechanics that determine the pin bending moment. Specifically, they considered the cortical width and the intramedullary width of the bone along with pin diameter, pin working length, transverse (loading) force, pin area moment of inertia and the pin elastic modulus to formulate their guidelines for determining the BPI stresses using a combination of FE and analytical methods.[19,64]

Several investigators have attempted to determine the local stress or strain limits of cortical bone which may predict yielding and local failure and ultimately result in bone resorption and / or replacement with fibrous tissue instead of bone. Wazen et al. suggested that interfacial strain plays a key role in the biologic response to an implant at the BPI.[92] Using pin and screw shaped implants in mice tibiae under different implant stability and loading conditions, they showed that bone regeneration at the BPI was disrupted where high strain concentrations were present. Manley et al showed that an elastomeric coating placed on the outer surface of the pin may reduce stresses in the

cortical bone (due to transverse compressive loading) by up to 50%. Their study did not evaluate the effect on bending load and the bending moment of the pin, which is thought to contribute approximately 90% of the cortical bone stress at the BPI.[163] Hyldahl et al compared bone resorption around transfixation pins in sheep and showed that a radial preload was superior to a bending preload for minimizing bone resorption around the pins.[84] Capper et al showed that the stresses in the bone surrounding the pin are expected to increase as the pilot hole size created prior to pin insertion decreases.[164] Capper et al also evaluated bone stresses associated with standard and conical external fixation half pins using FE analysis. They found that the stresses were maximum at the pin entry cortex of the bone and reduced to almost zero within a distance of 20 mm from the outer cortex (approximately one-third of the distance across the bone). In addition, they found that the stresses increased focally around pin threads, which is also supported by the work of Wazen et al.[92,165] These findings support earlier work from Huiskes et al and Huiskes and Chao who determined that the pattern of local bone stresses surrounding an external fixation pin were greatest at the outer bone cortex and reduced as the distance from the outer cortex increased into the bone.[19,64] More recently, this pattern of local bone stress distribution during weight bearing in external fixation and transfixation casting was reported by Donaldson et al and Brianza et al.[129,166]

2.3.4.1 Cortical bone response to cyclic loading

Since cyclic stresses experienced at the BPI during transfixation casting or external fixation contribute to bone resorption and pin loosening, the question of how cortical bone responds to loading becomes a critical factor to consider. Direct loading of the bone through the pin is primarily compressive at the BPI when the pin and bone are not bonded, which would be expected for pins immediately following insertion and in which osseointegration does not occur.[64] The fatigue response of bone to cyclic loading has been examined using 2 primary measures; loss of mechanical properties, principally elastic modulus, and microdamage, most notably in the form of microcracks in the cortical bone. It has been shown that cortical bone responds differently under

compressive compared to tensile loads, including the mechanisms of failure observed.[167–169] Zioupos et al studied the patterns of microcracking during bone failure in both compression and tension.[169] They found, similar to previous investigators, that the elastic modulus was higher when bone was tested along the osteonal "grain" or longitudinal direction compared to transverse or radial directions. In addition, testing in compression resulted in a higher yield stress than testing in tension and microcrack formation began to be detected at a load corresponding to the yield point during uniaxial mechanical testing. The patterns of microcrack formation around a circular hole were best predicted by the use of a failure based criterion for anisotropic materials rather than principal stress, von Mises stress or the strain energy density function, which had often been used to predict bone fracture.[169] The mechanical properties of cortical bone have also been shown to differ depending upon the mode of habitual loading the cortex has experienced.[170–172] A bone cortex that is primarily loaded in compression during use, more readily resists failure in compression than a cortex loaded primarily in tension.[168] Reilly and Currey quantified the degree of microcracking in bone specimens from the cranial and caudal cortices of the equine radius under both compressive and tensile loading. Cranial bowing of the equine radius results in the cranial cortex being primarily under tension during loading and the caudal cortex primarily under compression. Tensile microcracks were diffuse, began to appear at a strain of 0.4% and showed considerable growth at strain values beyond 0.8%. Compressive microcracks were larger, straighter and less diffuse, first appearing at a strain of 0.8% and increasing beyond a strain value of 1%.[168] In a study of canine femurs, Burr et al reported similar findings in terms of a large number of diffuse microcracks forming in tensile cortices and greater individual crack growth appearing in compressive cortices.[173] A loss of approximately 15% in elastic modulus was documented to occur before cortical microdamage became visible in their study. Pattin et al had similar findings when examining the loss of mechanical properties of human femurs during cyclic loading and established that a threshold strain of 0.25% in tension and 0.4% in compression had to be exceeded before modulus degradation was detected.[174] In the equine MC3, it has been shown that the fatigue life under cyclic loading differs between the dorsal, medial and lateral cortices.[175] However, in contrast to

human and canine cortical bone, a clear reduction in elastic modulus and residual strength following cyclic loading was not observed by Martin et al when studying equine MC3's.[176] Cortical beams from these bones were cycled 100,000 times between 0 and 0.5% strain (5000 microstrain) and then tested monotonically to failure to determine yield and post-yield mechanical properties. This same research group did however, find an increase in microcracks in equine MC3 cortical bone following both monotonic loading to failure and cyclic fatigue loading when values of 1% strain were used for cyclic testing.[177] Taken together, these findings suggest that in equine MC3's, a threshold level of compressive strain between 0.5 and 1% may exist, above which a reduction in mechanical properties of the cortical bone of the BPI and detectable microdamage could occur over the course of repeated cyclic loading. This is considerably higher than the threshold suggested in other species. However, Nunamaker et al and Davies have shown that in vivo strain values achieved in the equine MC3 often exceed 0.5% during galloping exercise, which is also higher than in vivo strain values observed in other species.[178,179]

The preceding review of the impact of mechanical loading on cortical bone ignores the effect of any biologically driven response of the bone to loading and the pin. It has been suggested that in terms of fatigue failure of equine bone, the consequences of remodeling in response to loading damage may be more important than the immediate mechanical effects.[176] Cardoso et al showed that osteocyte apoptosis is key in the initiation of bone remodeling in response to fatigue induced bone microdamage.[180] Kennedy et al, building on this initial work, showed that the remodeling response to microdamage induced apoptosis of osteocytes involved both the apoptotic cells as well as surrounding viable osteocytes which upregulate production of osteoclastogenic cytokines.[181,182] Interestingly, Herman et al were able to distinguish that the stimulus from diffuse microdamage (sub-lamellar or less than 1-2 micron length) did not induce osteocyte apoptosis while larger microcracks (10 – 100 microns in length) did stimulate the resorption process.[183] Once initiated, the process of bone resorption following osteocyte apoptosis is a well-regulated series of events, coupled with new bone formation that results in remodeling of targeted areas of the bone cortex. This remodeling process is achieved through the formation of

basic (bone) multicellular units comprising osteoclastic removal of bone and osteoblast formation of new bone around a centrally formed blood vessel. This unit results in the formation of new osteons in a coordinated manner within cortical bone.[77,184] The time taken for bone resorption to occur is approximately 3 weeks, while the time taken for osteoblast matrix deposition to be completed and substantial mineralization to occur is around 3-4 months, although complete mineralization can take up to 1 year.[77] The consequence of this delay between resorption and formation is an increase in bone porosity for a period of time if the activation of these events (microdamage) occurs within a spatial or temporal cluster, such as occurs with pin insertion and loading.

Considering this process of bone remodeling and the mechanical stimulus that results in bone microdamage at the BPI it is apparent that cyclic loading of pins has a cumulative effect on the adjacent bone. Schell et al showed that the cortical bone density adjacent to external fixation pins decreased from 3 - 6 weeks following implantation,[97] while Donaldson et al have shown that increased overall bone porosity (as a proxy for old age in humans) is predicted to result in a significant increase in yielded bone volume over time surrounding the pin.[166] These series of events again culminate in a viscous cycle of local bone microdamage, stimulation of local resorption and remodeling through the process of osteocyte apoptosis and local cytokine upregulation, with progressive reduction in mechanical bone properties of the cortex due to increased porosity and reduced bone density, resulting in a greater susceptibility to the effects of cyclic loading of the bone and further microdamage. These biologic events coincide with the mechanical effects described above, in which microdamage and loss of bone material properties at the BPI are also predicted to occur as a result of cyclic loading at the BPI.

2.3.5 Pin tract infections and the BPI

Pin tract infections are the most common complication observed during the use of external fixation pins.[67] There is ongoing debate as to the significance of pin tract infections and a large range reported for the infection rate associated with external

fixation pins.[67] The reason for this large range of reported infection rates is likely due to the inconsistent definitions applied between studies for a pin tract infection. One distinction has been made between pin tract reaction (within 72 hours of pin insertion), pin colonization (presence of bacteria along the pin tract) and infection (presence of purulent drainage) of the pin tract. Another distinction made is the presence of minor (manageable without pin removal) and major (which necessitate pin removal) pin tract infections. Despite this inconsistency among definitions and between studies, pin tract infections certainly result in a high level of morbidity in patients undergoing external fixation,[15,68] including horses treated using transfixation casts.[37,38] Some investigators consider the development of pin tract infections an inevitability and so prefer to assess the degree of clinical impact on the patient rather than the presence or absence of infection.[67,68,87,185,186] The available information regarding the role of pin tract infections on the integrity of the BPI is mixed in its conclusions. Local osteomyelitis and bone resorption around the pin can dramatically reduce the stability of an external fixation pin.[29,37,68,185] There is some evidence that the process of pin loosening is largely unaffected by the external care of the pin tract skin wounds,[67,68] although this is not a universally held view.[97,185]

The pathophysiology of pin tract infections has been examined. Clasper et al showed that external fluid accumulation around the BPI resulted in rapid translocation of bacteria along the pin and into the medulla of the bone within 1 hour. This process was independent of pin loosening which occurred within the first 24 hours of external fixation pin placement in some cases.[87] This same study observed that cortical bone damage was present along the pin tract and may have been an explanation for why a watertight seal along the pin tract was not achieved. Others have documented bone microdamage during all stages of pin placement, including drilling, tapping and pin insertion itself.[153] These findings support the notion that pin tract infections may contribute to pin loosening in combination with mechanical and thermal bone damage at the time of pin insertion. More recently, Schell et al observed no progressive loosening of external fixation pins in sheep over a 9 week implantation period and suggested that pin loosening may not be as

prevalent when the incidence of pin tract infections is low.[97] Due to the nature of the external fixation pin, with both the requirement to be percutaneous and the unavoidable occurrence of microscopic bone damage of the pin tract during hole creation and pin insertion, it is difficult to separate the significance of pin tract infection, initial bone microdamage and ongoing pin loading effects on the process of pin loosening. In horses, it has been suggested that pin tract infections can contribute to progressive pin loosening, pin hole osteolysis and cortical ring sequestrum formation and result in pin hole enlargement and an increased risk of secondary fracture through the pin hole.[1,16,27]

2.4 The Finite Element Method

The FE method is used to solve, using numerical approximation, physical (or other) phenomena such as a stress response in objects that make the use of purely analytical approaches difficult or impossible. This method has been used widely in engineering fields since the 1960's to understand the physical behavior of objects under differing stress conditions, as well as chemical, electromagnetic, thermal and other complex problems.[187]

2.4.1 Basic concepts

The FE method divides objects up into individual elements which are connected at nodes.[187] A mesh is generated which closely approximates the original object geometry to be examined. The mesh is made up of a finite number of elements which are connected by nodes in a defined manner depending on the element type being used. The more complex the mesh and the more elements that are used to represent the object, the closer the approximation to the actual object. The generated mesh, elements and nodes are used to solve the problem being considered. The unknown being solved for is the value of interest (output variable) at each of the nodes which interconnect the mesh. Using input data for known values in the system, such as a material property or length, as well as constitutive laws of physical behavior, such as Hooke's law, a series of linear algebraic

equations are solved simultaneously for the nodal values. For any system with a large number of elements (and nodes) the computational power of a computer becomes an essential tool to generate these solutions. It has been shown that as the number of elements increase within a problem, the solution will converge on the solution obtained from partial differential equations.[187] While a larger number of elements and a more complex mesh result in a more accurate solution, the direct tradeoff is computational time and computing capacity.

Stress analysis requires input of the geometry of objects in the system as well as their intrinsic material properties such as density, modulus of elasticity and Poisson's ratio, which determine how an object responds to an applied force. In addition, any interactions that occur between objects need to be defined. Other input variables include any externally applied force(s) acting on the object and the boundary conditions of the system. Boundary conditions define the restraints placed on the system and result in additional known values in the series of equations constructed to solve the problem. The output variable in a stress analysis is the displacement of each node. Additional variables at each node can be derived such as principal and axis stresses, strains and other relevant data such as von Mises stress criterion.

2.4.2 The equine third metacarpal bone

The FE method has been used in a range of equine applications including teeth, hooves, joints, bones and airflow.[188–193] The MC3 specifically has been the subject of several studies due to its importance as a site of injury in the horse.[111,129,192,194–197] Les et al, developed subject-specific FE models of the equine metacarpus with the aid of **computed tomography (CT)** studies.[192] Bone material properties for the FE models were assigned using a calibration phantom to determine the relationship between radiographic density and elastic modulus for equine bone.[198] While the elastic modulus was varied throughout the model based on the CT data, isotropic material properties for each element were used. These models were validated by comparing surface strains generated by the model with

those measured by strain gauges during both axial loading and 4-point bending tests of the bones.[192]

Gotzen et al used FE modeling of the equine MC3 at a microstructural level to examine any reduction of stress concentration observed around a nutrient foramen. The bone material properties were derived using a combination of bone mineral content, bone volume fraction, architecture index and osteonal orientation around the foramen as determined by histological analysis.[195] This information was combined with a previously developed multivariate regression function for compact bone[199] to calculate elastic moduli in 3 principal axes.

The mechanical loading components of the MC3 have been examined using FE analysis at both the walk and the trot.[196,197] These studies compared an FE analysis to a mathematical modeling approach using mechanical theories of beams and shafts. The mathematical model made several simplifying assumptions about the behavior of the MC3, including ignoring the inertial forces present during the stride (quasi-static equilibrium modeling), using transversely orthotropic bone material properties based on a single CT slice of the mid-diaphysis of the bone and making the assumption that the bending moment about the distal end of the bone in the sagittal plane was zero.[196] The FE model was generated from the single CT slice of the mid-diaphysis by extrusion of the cross sectional geometry. These simplified models were used to predict the loading components of the MC3 during walking and trotting but were not directly validated through in vitro testing of the bone from the horse used to obtain the original strain data. However, additional kinematic and force plate loading data were incorporated into the final models and showed good agreement with the simplified models developed. Overall, these models found that at both the walk and the trot the predominant loading of the MC3 in the horse is axial compression during the stance phase of the stride. A peak force of approximately 20 N/kg was reported at the walk and 35 N/kg at the trot.[196,197]

In an earlier study, Les et al used ex vivo loading conditions to simulate in vivo strain distributions previously reported in the equine MC3 for the purposes of providing realistic input data for specific FE and other modeling approaches.[111] These investigators concluded that the load conditions at the walk were well simulated by a 7500 N distributed load on the proximal metacarpus. Harrison et al. developed a detailed subject-specific model of the metacarpophalangeal joint of a horse, which included the distal portion of the MC3, as a method for evaluating the distribution of load across the articular surfaces.[190] Due to the focus on articular cartilage loading, bone in this FE model was represented as non-deformable shell elements rather than solid 3-dimensional elements.

One previous study utilized FE analysis to evaluate the equine MC3 and transfixation pin concepts. Brianza et al. used an FE model to examine a novel pin-sleeve combination for external fixation in the horse.[129] Primary FE models were constructed using known geometric and material properties of a bone substitute material which was used for in vitro testing of the concept. A secondary analysis was performed on an anatomically correct model constructed from computed tomographic data of an MC3. Isotropic bone material properties (elastic modulus of 20 GPa, Poisson's ratio of 0.3) were assigned in this model to 4-node linear tetrahedral elements. A 5000 N distributed axial loading condition on the proximal joint surface was used for evaluation of the stresses associated with a standard transfixation pin and the novel pin-sleeve combination, using a simulated comminuted fracture with a tissue stiffness of 0.5 GPa.[129]

2.4.3 Bone-pin interface

The FE method has been used to specifically evaluate the BPI in several studies. Huiskes et al used stress data generated from an FE model of a single BPI to develop an analytical model of the pin-bone configuration and develop a subsequent parametric analysis for a complete ESF.[64] The 2 models compared well in terms of the stresses predicted about the BPI in the 2 dimensions of the frontal plane. Stresses were found to be highest at the

outer cortical bone margin and were also predicted to return to nominal levels of stress at a distance of approximately 10 mm from the pin.[64] This study by Huiskes et al provided the basis for additional studies to examine the BPI in more detail as it pertains to external fixators and their clinical application.[19,80–83,85,200] Capper et al evaluated the effect of a conical pin shape on predicted bone stresses using FE analysis by comparing it to a standard cylindrical half-pin.[165] Higher bone stresses along the axis of the pin were associated with the pin thread troughs at the BPI, while higher bone stresses were observed at the tips of the threads in the loading axis across the pin. Similar to Huiskes et al, the highest stress values were found at the pin entry site at the outer cortex. In addition, the conical pin had higher stresses than the larger of the 2 standard half-pin sizes evaluated.[165] Oni et al evaluated the effect of a flanged pin on its bending stiffness using FE analysis.[201] A flange located at the outer cortical contact point of the pin was able to increase the bending stiffness of the pin when compared to standard cylindrical pins. Donaldson et al used a strain based yielding criterion in their FE model of the human tibia to evaluate the effect of age-related bone material properties, pin number and pin material on half-pin loosening.[166] It was concluded that bone material properties profoundly affect pin loosening with 3 times the yielded bone volume present in ‘old’ versus ‘young’ bone around the pin. In addition, yielded bone volume was 80% lower when 3 pins were used compared to 2 pins and titanium pins resulted in greater yielded bone volume than stainless steel.[166] Karunratanakul et al used a combination of FE analysis and mechanical testing to show that the contact conditions at the BPI are critical to the accuracy of the FE predictions in a unilateral fixator model of the rabbit tibia.[202,203] Contact conditions of the FE model were refined by applying the results of mechanical testing of individual components to better capture the effect of BPI interactions. Significant improvements in the predicted stiffness of the fixator were realized when these contact conditions were included in the model.[202,203] These studies have shown that the bone stresses surrounding a pin can be reasonably predicted using FE methods and these predictions compare well to a simpler parametric model when applied in 2 dimensions. The stresses are expected to be higher at the outer cortex during pin loading and alteration of the pin in this location may increase the bending stiffness of the pin.

There is also evidence from these studies that a strain based assessment at the BPI can be a good predictor of bone yielding and subsequent pin loosening. The studies also highlight the potential sensitivity of an FE analysis to the contact condition at the BPI and raise the question of whether other factors may alter the accuracy of the FE analysis predictions.

2.4.4 Element selection

The elements used for FE modeling can take a variety of forms. A commonly used element form for biomechanics problems is a continuum or solid element. Others include shell, beam, truss, membrane and rigid elements, although there are a large number of other element forms available for use within commercial software programs. The choice of element is generally based on the type of analysis being performed. Simplifying a problem down to the least complex element form allows for more efficient computational performance. Symmetry can often be used to reduce a problem along an axis or 3-dimensional problems can be reduced to simpler 2-dimensional problems when the primary focus of the study is within a single plane. Solid elements are used for analysis of more complex 3-dimensional problems. Apart from the form of the element to be used, other factors determine the element type, including the degrees of freedom, the number of nodes in each element, the formulation defining an elements behavior and the method of integration used for each element.

2.5 List of References

1. Auer JA. Principles of fracture treatment. In: Auer JA and Stick JA eds. *Equine Surgery*. 3rd ed. Saint Louis, MO: Saunders Elsevier; 2006:1000–1029.

2. Ahern BJ, Richardson DW, Boston RC, et al. Orthopedic infections in equine long bone fractures and arthrodeses treated by internal fixation: 192 cases (1990-2006). *Vet Surg* 2010;39:588–593.

3. Nunamaker D. Orthopedic implant failure. In: Nixon AJ ed. *Equine Fracture Repair*. Philidelphia: WB Saunders Co.; 1996:350–353.

4. James FM, Richardson DW. Minimally invasive plate fixation of lower limb injury in horses: 32 cases (1999-2003). *Equine Vet J* 2006;38:246–251.

5. Schneider RK. Synovial and osseous infections. In: Auer JA and Stick JA eds. *Equine Surgery*. 3rd ed. St. Louis, MO: Saunders Elsevier; 2006:1121–1130.

6. Trampuz A, Zimmerli W. Diagnosis and treatment of infections associated with fracture-fixation devices. *Injury* 2006;37 Suppl 2:S59–66.

7. McClure SR, Watkins JP, Glickman NW, et al. Complete fractures of the third metacarpal or metatarsal bone in horses: 25 cases (1980-1996). *J Am Vet Med Assoc* 1998;213:847–850.

8. Bischofberger AS, Fürst A, Auer J, et al. Surgical management of complete diaphyseal third metacarpal and metatarsal bone fractures: clinical outcome in 10 mature horses and 11 foals. *Equine Vet J* 2009;41:465–473.

9. Beinlich CP, Bramlage LR. Results of plate fixation of third metacarpal and metatarsal diaphyseal fractures. *Proc Am Assoc Equine Pract* 2002;48:247–248.

10. Kraus KH, Toombs JP, Ness MG. Basics of external fixation. In: Kraus KH, Toombs JP, Ness MG eds. *External fixation in small animal practice*. Oxford: Blackwell Science; 2003:1–8.

11. Piermattei D, Flo GL, DeCamp CE. Fractures: Classification, diagnosis, and treatment. In: Piermattei D, Flo GL, DeCamp CE eds. *Brinker, Piermattei, and Flo's handbook of small animal orthopedics and fracture repair*. 4th ed. St. Louis Mo.: Saunders/Elsevier; 2006:25–159.

12. Kádas I, Magyari Z, Vendégh Z, et al. Changing the treatment to reduce complication rate in open tibial fractures. *Int Orthop* 2009;33:1725–1731.
13. Tejwani NC, Achan P. Staged management of high-energy proximal tibia fractures. *Bull Hosp Jt Dis* 2004;62:62–66.
14. Lewis DD, Cross AR, Carmichael S, et al. Recent advances in external skeletal fixation. *J Small Anim Pract* 2001;42:103–112.
15. Palmer RH. External fixators and minimally invasive osteosynthesis in small animal veterinary medicine. *Vet Clin North Am Small Anim Pract* 2012;42:913–934.
16. McClure S, Honnas CM, Watkins JP. Managing equine fractures with external skeletal fixation. *Comp Cont Educ Pract Vet* 1995;17:1054–1063.
17. Willer RL, Egger EL, Histand MB. Comparison of stainless steel versus acrylic for the connecting bar of external skeletal fixators. *J Am Anim Hosp Assoc* 1991;27:541–548.
18. Wells KL, Pardo AD, Parrott MB, et al. A comparison of the mechanical properties of two external fixator designs for transarticular stabilization of the canine hock. *Vet Comp Orthop Traumatol* 1997;10:54–59.
19. Huiskes R, Chao EY. Guidelines for external fixation frame rigidity and stresses. *J Orthop Res* 1986;4:68–75.
20. Brinker WO, Verstraete MC, Soutas-Little RW. Stiffness studies on various configurations and types of external fixators. *J Am Anim Hosp Assoc* 1985;21:801–808.
21. Ilizarov GA. Clinical application of the tension-stress effect for limb lengthening. *Clin Orthop Relat Res* 1990:8–26.
22. Jordan CJ, Goldstein RY, McLaurin TM, et al. The evolution of the Ilizarov technique: part 1: the history of limb lengthening. *Bull Hosp Jt Dis* 2013;71:89–95.
23. Goldstein RY, Jordan CJ, McLaurin TM, et al. The evolution of the Ilizarov technique: part 2: the principles of distraction osteosynthesis. *Bull Hosp Jt Dis* 2013;71:96–103.
24. Belsito KA, Fischer AT. External skeletal fixation in the management of equine mandibular fractures: 16 cases (1988-1998). *Equine Vet J* 2001;33:176–183.

25. Eggleston RB, Mueller PO, Chambers JN, et al. Use of an external ring fixator for correction of an acquired angular limb deformity in a donkey. *J Am Vet Med Assoc* 2000;217:1186–1190.
26. Klaus CS, Hertsch BW, Höppner S, et al. Long term outcome after surgical correction of mandibular brachygnathia with unilateral type-1 external skeletal fixation. *Vet Surg* 2013;42:979–983.
27. Nunamaker DM. A new external skeletal fixation device that allows immediate full weightbearing application in the horse. *Vet Surg* 1986;15:345–355.
28. Porter EG, Cuddy LC, Graham AS, et al. Hinged circular fixator construct for correction of congenital metatarsal deformity in a foal. *Vet Comp Orthop Traumatol* 2014;27:74–79.
29. Sullins KE, McIlwraith CW. Evaluation of 2 types of external skeletal fixation for repair of experimental tibial fractures in foals. *Vet Surg* 1987;16:255–264.
30. Auer JA. Craniomaxillofacial disorders. In: Auer JA and Stick JA eds. *Equine Surgery*. 3rd ed. St. Louis, MO: Saunders Elsevier; 2006:1341–1362.
31. Cousty M, Haudiquet P, Geffroy O. Use of an external fixator to correct a wry nose in a yearling. *Equine Vet Educ* 2010;22:458–461.
32. Peavey CL, Edwards RB, Escarcega AJ, et al. Fixation technique influences the monotonic properties of equine mandibular fracture constructs. *Vet Surg* 2003;32:350–358.
33. Leroux AJ, Moll HD, Modransky PM, et al. Repair of an open fracture in a foal using a modified external fixator. *Equine Pract* 1992;14:7–10.
34. De Godoy RF, Filgueiras RR, Gontijo LA, et al. Treatment of a periarticular tibial fracture in a foal with a hybrid external fixator. *Vet Surg* 2009;38:650–653.
35. Whitehair KJ, Adams SB, Toombs JP, et al. Arthrodesis for congenital flexural deformity of the metacarpophalangeal and metatarsophalangeal joints. *Vet Surg* 1992;21:228–233.
36. Richardson DW, Nunamaker DM, Sigafoos RD. Use of an external skeletal fixation device and bone graft for arthrodesis of the metacarpophalangeal joint in horses. *J Am Vet Med Assoc* 1987;191:316–321.

37. Lescun TB, McClure SR, Ward MP, et al. Evaluation of transfixation casting for treatment of third metacarpal, third metatarsal, and phalangeal fractures in horses: 37 cases (1994-2004). *J Am Vet Med Assoc* 2007;230:1340–1349.
38. Joyce J, Baxter GM, Sarrafian TL, et al. Use of transfixation pin casts to treat adult horses with comminuted phalangeal fractures: 20 cases (1993-2003). *J Am Vet Med Assoc* 2006;229:725–730.
39. Kraus BM, Richardson DW, Nunamaker DM, et al. Management of comminuted fractures of the proximal phalanx in horses: 64 cases (1983-2001). *J Am Vet Med Assoc* 2004;224:254–263.
40. Nemeth F, Back W. The use of the walking cast to repair fractures in horses and ponies. *Equine Vet J* 1991;23:32–36.
41. Nunamaker DM, Nash RA. A tapered-sleeve transcortical pin external skeletal fixation device for use in horses: development, application, and experience. *Vet Surg* 2008;37:725–732.
42. Nash RA, Nunamaker DM, Boston R. Evaluation of a tapered-sleeve transcortical pin to reduce stress at the bone-pin interface in metacarpal bones obtained from horses. *Am J Vet Res* 2001;62:955–960.
43. Cervantes C, Madison JB, Miller GJ, et al. An in vitro biomechanical study of a multiplanar circular external fixator applied to equine third metacarpal bones. *Vet Surg* 1996;25:1–5.
44. Rapoff AJ, Markel MD, Vanderby R. Mechanical evaluation of transosseous wire rope configurations in a large animal external fixator. *Am J Vet Res* 1995;56:694–699.
45. Aithal HP, Singh GR, Hoque M, et al. The use of a circular external skeletal fixation device for the management of long bone osteotomies in large ruminants: an experimental study. *J Vet Med A Physiol Pathol Clin Med* 2004;51:284–293.
46. Aithal HP, Amarpal N, Kinjavdekar P, et al. Management of fractures near the carpal joint of two calves by transarticular fixation with a circular external fixator. *Vet Rec* 2007;161:193–198.
47. Singh GR, Aithal HP, Amarpal N, et al. Evaluation of two dynamic axial fixators for large ruminants. *Vet Surg* 2007;36:88–97.

48. Aithal HP, Kinjavdekar P, Amarpal N, et al. Management of tibial fractures using a circular external fixator in two calves. *Vet Surg* 2010;39:621–626.
49. Vogel SR, Anderson DE. External skeletal fixation of fractures in cattle. *Vet Clinics North Am, Food Anim Pract* 2014;30:127–142.
50. Bilgili H, Kurum B, Captug O. Use of a circular external skeletal fixator to treat comminuted metacarpal and tibial fractures in six calves. *Vet Rec* 2008;163:683–688.
51. Aithal HP, Singh GR, Kinjavdekar P, et al. Hybrid construct of linear and circular external skeletal fixation devices for fixation of long bone osteotomies in large ruminants. *Indian J Anim Sci* 2007;77:1083–1090.
52. Yardimci C, Ozak A, Nisbet HO. Treatment of unusual congenital flexural and torsional limb deformities with circular external skeletal fixation system in two calves. *Proc World Vet Orthop Congr* 2010:702.
53. Yardimci C, Ozak A, Nisbet O. Correction of severe congenital flexural carpal deformities with semicircular external skeletal fixation system in calves. *Vet Comp Orthop Traumatol* 2012;25:518–523.
54. Easter JL, Schumacher J, Watkins JP. Transfixation cast technique for arthrodesis of the distal interphalangeal joint of horses. *Vet Comp Orthop Traumatol* 2011;24:62–67.
55. Hopper SA, Schneider RK, Johnson CH, et al. In vitro comparison of transfixation and standard full-limb casts for prevention of displacement of a mid-diaphyseal third metacarpal osteotomy site in horses. *Am J Vet Res* 2000;61:1633–1635.
56. Lescun TB, Morisset SM, Fugaro MN, et al. Facilitated ankylosis of the distal interphalangeal joint in a foal. *Aust Vet J* 2004;82:282–285.
57. McClure SR, Watkins JP, Bronson DG, et al. In vitro comparison of the standard short limb cast and three configurations of short limb transfixation casts in equine forelimbs. *Am J Vet Res* 1994;55:1331–1334.
58. Grossman BS, Nickels FA. Repair of metatarsal fractures with transfixation pins and plaster casts. *Equine Pract* 1979;1:13–16.
59. McClure SR, Watkins JP, Ashman RB. In vitro comparison of the effect of parallel and divergent transfixation pins on breaking strength of equine third metacarpal bones. *Am J Vet Res* 1994;55:1327–1330.

60. McClure SR, Watkins JP, Hogan HA. In vitro evaluation of four methods of attaching transfixation pins into a fiberglass cast for use in horses. *Am J Vet Res* 1996;57:1098–1101.
61. Schneider RK, Ratzlaff MC, White KK, et al. Effect of three types of half-limb casts on in vitro bone strain recorded from the third metacarpal bone and proximal phalanx in equine cadaver limbs. *Am J Vet Res* 1998;59:1188–1193.
62. Hopper SA, Schneider RK, Ratzlaff MH, et al. Effect of different full-limb casts on in vitro bone strain in the distal portion of the equine forelimb. *Am J Vet Res* 1998;59:197–200.
63. Lescun TB, Baird DK, Oliver LJ, et al. Comparison of hydroxyapatite-coated and uncoated pins for transfixation casting in horses. *Am J Vet Res* 2012;73:724–734.
64. Huiskes R, Chao EY, Crippen TE. Parametric analyses of pin-bone stresses in external fracture fixation devices. *J Orthop Res* 1985;3:341–349.
65. Rossignol F, Vitte A, Boening J. Use of a modified transfixation pin cast for treatment of comminuted phalangeal fractures in horses. *Vet Surg* 2014;43:66–72.
66. Janicek JC, McClure SR, Lescun TB, et al. Risk factors associated with cast complications in horses: 398 cases (1997-2006). *J Am Vet Med Assoc* 2013;242:93–98.
67. Camathias C, Valderrabano V, Oberli H. Routine pin tract care in external fixation is unnecessary: a randomised, prospective, blinded controlled study. *Injury* 2012;43:1969–1973.
68. Lethaby A, Temple J, Santy-Tomlinson J. Pin site care for preventing infections associated with external bone fixators and pins. *Cochrane Database Syst Rev* 2013;12:CD004551:1-50.
69. Markel M, Richardson D, Nunamaker D. Comminuted first phalanx fractures in 30 horses. Surgical vs. nonsurgical treatments. *Vet Surg* 1985:135–140.
70. Rogachefsky RA, Lipson SR, Applegate B, et al. Treatment of severely comminuted intra-articular fractures of the distal end of the radius by open reduction and combined internal and external fixation. *J Bone Joint Surg Am* 2001;83-A:509–519.
71. Bloomfield SA. Disuse osteopenia. *Curr Osteoporos Rep* 2010;8:91–97.

72. McGee-Lawrence ME, Carey HV, Donahue SW. Mammalian hibernation as a model of disuse osteoporosis: the effects of physical inactivity on bone metabolism, structure, and strength. *Am J Physiol Regul Integr Comp Physiol* 2008;295:R1999–2014.
73. Delguste C, Amory H, Doucet M, et al. Pharmacological effects of tiludronate in horses after long-term immobilization. *Bone* 2007;41:414–421.
74. Buckingham SH, Jeffcott LB. Osteopenic effects of forelimb immobilisation in horses. *Vet Rec* 1991;128:370–373.
75. Van Harreveld PD, Lillich JD, Kawcak CE, et al. Clinical evaluation of the effects of immobilization followed by remobilization and exercise on the metacarpophalangeal joint in horses. *Am J Vet Res* 2002;63:282–288.
76. Van Harreveld PD, Lillich JD, Kawcak CE, et al. Effects of immobilization followed by remobilization on mineral density, histomorphometric features, and formation of the bones of the metacarpophalangeal joint in horses. *Am J Vet Res* 2002;63:276–281.
77. Allen MR, Burr DB. Bone modeling and remodeling. In: Burr DB and Allen MR eds. *Basic and Applied Bone Biology*. London: Elsevier Inc; 2014:75–90.
78. Bonewald LF, Johnson ML. Osteocytes, mechanosensing and Wnt signaling. *Bone* 2008;42:606–615.
79. Sugiyama T, Meakin LB, Browne WJ, et al. Bones' adaptive response to mechanical loading is essentially linear between the low strains associated with disuse and the high strains associated with the lamellar/woven bone transition. *J Bone Miner Res* 2012;27:1784–1793.
80. Aro HT, Kelly PJ, Lewallen DG, et al. The effects of physiologic dynamic compression on bone healing under external fixation. *Clin Orthop Relat Res* 1990:260–273.
81. Aro HT, Chao EY. Biomechanics and biology of fracture repair under external fixation. *Hand Clin* 1993;9:531–542.
82. Aro HT, Markel MD, Chao EY. Cortical bone reactions at the interface of external fixation half-pins under different loading conditions. *J Trauma* 1993;35:776–785.
83. Chao EY, Aro HT, Lewallen DG, et al. The effect of rigidity on fracture healing in external fixation. *Clin Orthop Relat Res* 1989:24–35.

84. Hyldahl C, Pearson S, Tepic S, et al. Induction and prevention of pin loosening in external fixation: an in vivo study on sheep tibiae. *J Orthop Trauma* 1991;5:485–492.
85. Pettine KA, Chao EY, Kelly PJ. Analysis of the external fixator pin-bone interface. *Clin Orthop Relat Res* 1993:18–27.
86. Clary E, Roe S. Enhancing external skeletal fixation pin performance - consideration of the pin-bone interface. *Vet Comp Orthop Traumatol* 1995;8:6–13.
87. Clasper JC, Cannon LB, Stapley SA, et al. Fluid accumulation and the rapid spread of bacteria in the pathogenesis of external fixator pin track infection. *Injury* 2001;32:377–381.
88. Carter DR, Beaupré GS. Skeletal Tissue Regeneration. In: Carter DR, Beaupré GS eds. *Skeletal function and form : mechanobiology of skeletal development, aging, and regeneration*. Cambridge ; New York: Cambridge University Press; 2001:161–200.
89. Mavrogenis AF, Dimitriou R, Parvizi J, et al. Biology of implant osseointegration. *J Musculoskelet Neuronal Interact* 2009;9:61–71.
90. Goodman SB. The biologic response to orthopaedic implants. In: O'Keefe RJ, Jacobs JJ, Chu CR, et al., eds. *Orthopaedic basic science : foundations of clinical practice*. 4th ed. Rosemont, Ill: American Academy of Orthopaedic Surgeons; 2013:341-352.
91. Simon U, Augat P, Ignatius A, et al. Influence of the stiffness of bone defect implants on the mechanical conditions at the interface--a finite element analysis with contact. *J Biomech* 2003;36:1079–1086.
92. Wazen RM, Currey JA, Guo H, et al. Micromotion-induced strain fields influence early stages of repair at bone-implant interfaces. *Acta Biomater* 2013;9:6663–6674.
93. Leucht P, Lam K, Kim J-B, et al. Accelerated bone repair after plasma laser corticotomies. *Ann Surg* 2007;246:140–150.
94. Baker R, Whitehouse M, Kilshaw M, et al. Maximum temperatures of 89°C recorded during the mechanical preparation of 35 femoral heads for resurfacing. *Acta Orthop* 2011;82:669–673.
95. Li C, Kotha S, Mason J. Evaluation of the effects of implant materials and designs on thermal necrosis of bone in cemented hip arthroplasty. *Biomed Mater Eng* 2003;13:419–428.

96. Lundskog J. Heat and bone tissue. An experimental investigation of the thermal properties of bone and threshold levels for thermal injury. *Scand J Plast Reconstr Surg* 1972;9:1–80.
97. Schell H, Reuther T, Duda GN, et al. The pin-bone interface in external fixator: a standardized analysis in a sheep osteotomy model. *J Orthop Trauma* 2011;25:438–445.
98. Cameron HU, Fornasier VL. The bone-metal interface following hip nailing. *J Biomed Mater Res* 1976;10:769–776.
99. Simmons CA, Meguid SA, Pilliar RM. Differences in osseointegration rate due to implant surface geometry can be explained by local tissue strains. *J Orthop Res* 2001;19:187–194.
100. Albrektsson T, Brånemark PI, Hansson HA, et al. Osseointegrated titanium implants. Requirements for ensuring a long-lasting, direct bone-to-implant anchorage in man. *Acta Orthop Scand* 1981;52:155–170.
101. Dohan Ehrenfest DM, Coelho PG, Kang B-S, et al. Classification of osseointegrated implant surfaces: materials, chemistry and topography. *Trends Biotechnol* 2010;28:198–206.
102. McKoy B, An YH, Friedman RJ. Factors affecting the strength of the bone-implant interface. In: An YH, Draughn RA, eds. *Mechanical testing of bone and the bone-implant interface.* Boca Raton: CRC Press; 2000:439–462.
103. Szmukler-Moncler S, Salama H, Reingewirtz Y, et al. Timing of loading and effect of micromotion on bone-dental implant interface: review of experimental literature. *J Biomed Mater Res* 1998;43:192–203.
104. Simmons CA, Meguid SA, Pilliar RM. Mechanical regulation of localized and appositional bone formation around bone-interfacing implants. *J Biomed Mater Res* 2001;55:63–71.
105. Moroni A, Toksvig-Larsen S, Maltarello MC, et al. A comparison of hydroxyapatite-coated, titanium-coated, and uncoated tapered external-fixation pins. An in vivo study in sheep. *J Bone Joint Surg Am* 1998;80:547–554.

106. Moroni A, Cadossi M, Romagnoli M, et al. A biomechanical and histological analysis of standard versus hydroxyapatite-coated pins for external fixation. *J Biomed Mater Res Part B Appl Biomater* 2008;86B:417–421.
107. Weinans H, Huiskes R, Grootenboer HJ. Quantitative analysis of bone reactions to relative motions at implant-bone interfaces. *J Biomech* 1993;26:1271–1281.
108. Moroni A, Faldini C, Pegreffi F, et al. Fixation strength of tapered versus bicylindrical hydroxyapatite-coated external fixation pins: an animal study. *J Biomed Mater Res* 2002;63:61–64.
109. Augat P, Claes L, Hanselmann KF, et al. Increase of stability in external fracture fixation by hydroxyapatite-coated bone screws. *J Appl Biomater* 1995;6:99–104.
110. van Eps A, Collins SN, Pollitt CC. Supporting limb laminitis. *Vet Clin North Am Equine Pract* 2010;26:287–302.
111. Les CM, Stover SM, Taylor KT, et al. Ex vivo simulation of in vivo strain distributions in the equine metacarpus. *Equine Vet J* 1998;30:260–266.
112. Wu JJ, Shyr HS, Chao EY, et al. Comparison of osteotomy healing under external fixation devices with different stiffness characteristics. *J Bone Joint Surg Am* 1984;66:1258–1264.
113. McBroom RJ, Cheal EJ, Hayes WC. Strength reductions from metastatic cortical defects in long bones. *J Orthop Res* 1988;6:369–378.
114. Edgerton BC, An KN, Morrey BF. Torsional strength reduction due to cortical defects in bone. *J Orthop Res* 1990;8:851–855.
115. Hipp JA, Edgerton BC, An KN, et al. Structural consequences of transcortical holes in long bones loaded in torsion. *J Biomech* 1990;23:1261–1268.
116. Kuo RF, Chao EY, Rim K, et al. The effect of defect size on the stress concentration and fracture characteristics for a tubular torsional model with a transverse hole. *J Biomech* 1991;24:147–155.
117. Brooks DB, Burstein AH, Frankel VH. The biomechanics of torsional fractures. The stress concentration effect of a drill hole. *J Bone Joint Surg Am* 1970;52:507–514.

118. Olcay E, Allahverdi E, GüLmez T, et al. Evaluation of the effects of holes of various sizes on fracture rates in sheep femurs. *Kafkas Univ Vet Fak Derg* 2013;19(Suppl-A):A49-A53.
119. Seltzer KL, Stover SM, Taylor KT, et al. The effect of hole diameter on the torsional mechanical properties of the equine third metacarpal bone. *Vet Surg* 1996;25:371–375.
120. Hopper SA, Schneider RK, Ratzlaff MH, et al. Effect of pin hole size and number on in vitro bone strength in the equine radius loaded in torsion. *Am J Vet Res* 1998;59:201–204.
121. Narayan, RJ Materials for medical devices. In: Narayan, RJ ed. *ASM Handbook. Vol 23*. ASM International; 2012:368.
122. Chen Q, Thouas GA. Metallic implant biomaterials. *Mater Sci Eng R* 2015;87:1–57.
123. Saunders MM. Mechanical testing for the biomechanical engineer: a practical guide. *Synth Lect Biomed Eng* 2015;9:1-276.
124. Atlas specialty metals. Stainless steel - Grade 316L - Properties, fabrication and applications. 2013. Available at: http://www.azom.com/.
125. Campbell FC. Fatigue. In: Campbell FC ed. *Elements of Metallurgy and Engineering Alloys*. Materials Park, OH. ASM International; 2008.
126. McDuffee LA, Stover SM, Coleman K. Limb loading activity of adult horses confined to box stalls in an equine hospital barn. *Am J Vet Res* 2000;61:234–237.
127. Williams JM, Elce YA, Litsky AS. Comparison of 2 equine transfixation pin casts and the effects of pin removal. *Vet Surg* 2014;43:430–436.
128. Elce YA, Southwood LL, Nutt JN, et al. Ex vivo comparison of a novel tapered-sleeve and traditional full-limb transfixation pin cast for distal radial fracture stabilization in the horse. *Vet Comp Orthop Traumatol* 2006;19:93–97.
129. Brianza S, Brighenti V, Lansdowne JL, et al. Finite element analysis of a novel pin-sleeve system for external fixation of distal limb fractures in horses. *Vet J* 2011;190:260–267.
130. Brianza S, Brighenti V, Boure L, et al. In vitro mechanical evaluation of a novel pin-sleeve system for external fixation of distal limb fractures in horses: a proof of concept study. *Vet Surg* 2010;39:601–608.

131. Vogel S, Desrochers A, Brianza S, et al. Evaluation of a novel pin-sleeve and ring system for transfixation casting in a neonatal calf model. *Proc Am Coll Vet Surg Ann Symp*. Chicago, IL: American College of Veterinary Surgeons; 2011:E49–E50.
132. Egkher E, Martinek H, Wielke B. How to increase the stability of external fixation units. Mechanical tests and theoretical studies. *Arch Orthop Trauma Surg* 1980;96:35–43.
133. Callahan DJ, Daddario N, Williams S, et al. Three experimental designs testing orthopedic casting material strength. *Orthopedics* 1986;9:673–675.
134. Callahan DJ, Carney DJ, Daddario N, et al. A comparative study of synthetic cast material strength. *Orthopedics* 1986;9:679–681.
135. Bartels KE, Penwick RC, Freeman LJ, et al. Mechanical testing and evaluation of eight synthetic casting materials. *Vet Surg* 1985;14:310–318.
136. Mihalko WM, Beaudoin AJ, Krause WR. Mechanical properties and material characteristics of orthopaedic casting material. *J Orthop Trauma* 1989;3:57–63.
137. Wytch R, Mitchell CB, Wardlaw D, et al. Mechanical assessment of polyurethane impregnated fibreglass bandages for splinting. *Prosthet Orthot Int* 1987;11:128–134.
138. Martin PJ, Weimann DH, Orr JF, et al. A comparative evaluation of modern fracture casting materials. *Eng Med* 1988;17:63–70.
139. Berman AT, Parks BG. A comparison of the mechanical properties of fiberglass cast materials and their clinical relevance. *J Orthop Trauma* 1990;4:85–92.
140. Wilson DG, Vanderby R Jr. An evaluation of six synthetic casting materials: strength of cylinders in bending. *Vet Surg* 1995;24:55–59.
141. Karachalios T and Koutalos A. The biology of aseptic loosening. In: Karachalios T ed. *Bone-implant interface in orthopedic surgery : basic science to clinical applications*. London, Springer-Verlag. 2014:139-159.
142. Morisset S, McClure SR, Hillberry BM, et al. In vitro comparison of the use of two large-animal, centrally threaded, positive-profile transfixation pin designs in the equine third metacarpal bone. *Am J Vet Res* 2000;61:1298–1303.
143. Clary EM, Roe SC. In vitro biomechanical and histological assessment of pilot hole diameter for positive-profile external skeletal fixation pins in canine tibiae. *Vet Surg* 1996;25:453–462.

144. Biliouris TL, Schneider E, Rahn BA, et al. The effect of radial preload on the implant-bone interface: a cadaveric study. *J Orthop Trauma* 1989;3:323–332.
145. Eriksson AR, Albrektsson T, Albrektsson B. Heat caused by drilling cortical bone. Temperature measured in vivo in patients and animals. *Acta Orthop Scand* 1984;55:629–631.
146. Eriksson RA, Albrektsson T, Magnusson B. Assessment of bone viability after heat trauma. A histological, histochemical and vital microscopic study in the rabbit. *Scand J Plast Reconstr Surg* 1984;18:261–268.
147. Eriksson AR, Albrektsson T. Temperature threshold levels for heat-induced bone tissue injury: a vital-microscopic study in the rabbit. *J Prosthet Dent* 1983;50:101–107.
148. Eriksson A, Albrektsson T, Grane B, et al. Thermal injury to bone. A vital-microscopic description of heat effects. *Int J Oral Surg* 1982;11:115–121.
149. Matthews LS, Hirsch C. Temperatures measured in human cortical bone when drilling. *J Bone Joint Surg Am* 1972;54:297–308.
150. Li S, Chien S, Brånemark PI. Heat shock-induced necrosis and apoptosis in osteoblasts. *J Orthop Res* 1999;17:891–899.
151. Lescun TB, Frank EA, Zacharias JR, et al. Effect of sequential hole enlargement on cortical bone temperature during drilling of 6.2-mm-diameter transcortical holes in the third metacarpal bones of horse cadavers. *Am J Vet Res* 2011;72:1687–1694.
152. Heidemann W, Gerlach KL, Gröbel KH, et al. Influence of different pilot hole sizes on torque measurements and pullout analysis of osteosynthesis screws. *J Craniomaxillofac Surg* 1998;26:50–55.
153. Wikenheiser MA, Markel MD, Lewallen DG, et al. Thermal response and torque resistance of five cortical half-pins under simulated insertion technique. *J Orthop Res* 1995;13:615–619.
154. Bubeck KA, García-Lopez JM, Jenei TM, et al. In vitro comparison of two centrally threaded, positive-profile transfixation pin designs for use in third metacarpal bones in horses. *Am J Vet Res* 2010;71:976–981.
155. Gasiorowski JC, Richardson DW, Boston RC, et al. Influence of a resilient, hard-carbon thin film on drilling efficiency and thermogenesis. *Vet Surg* 2011;40:875–880.

156. McClure SR, Hillberry BM, Fisher KE. In vitro comparison of metaphyseal and diaphyseal placement of centrally threaded, positive-profile transfixation pins in the equine third metacarpal bone. *Am J Vet Res* 2000;61:1304–1308.
157. Toews AR, Bailey JV, Townsend HG, et al. Effect of feed rate and drill speed on temperatures in equine cortical bone. *Am J Vet Res* 1999;60:942–944.
158. Bubeck KA, García-López J, Maranda LS. In vitro comparison of cortical bone temperature generation between traditional sequential drilling and a newly designed step drill in the equine third metacarpal bone. *Vet Comp Orthop Traumatol* 2009;22:442–447.
159. Yamashita J, Li X, Furman BR, et al. Collagen and bone viscoelasticity: a dynamic mechanical analysis. *J Biomed Mater Res* 2002;63:31–36.
160. Field JR, Sumner-Smith G. Bone blood flow response to surgical trauma. *Injury* 2002;33:447–451.
161. Sugita N, Osa T, Aoki R, et al. A new cutting method for bone based on its crack propagation characteristics. *CIRP Annals - Manufac Techn* 2009;58:113–118.
162. Jacobs CH, Pope MH, Berry JT, et al. A study of the bone machining process-orthogonal cutting. *J Biomech* 1974;7:131–136.
163. Manley MT, Hurst L, Hindes R, et al. Effects of low-modulus coatings on pin-bone contact stresses in external fixation. *J Orthop Res* 1984;2:385–392.
164. Capper M, Soutis C, Oni OO. Pin-hole shear stresses generated by conical and standard external fixation pins. *Biomaterials* 1993;14:876–878.
165. Capper M, Soutis C, Oni OO. Comparison of the stresses generated at the pin-bone interface by standard and conical external fixator pins. *Biomaterials* 1994;15:471–473.
166. Donaldson FE, Pankaj P, Simpson AHRW. Bone properties affect loosening of half-pin external fixators at the pin-bone interface. *Injury* 2012;43:1764–1770.
167. Ebacher V, Tang C, McKay H, et al. Strain redistribution and cracking behavior of human bone during bending. *Bone* 2007;40:1265–1275.
168. Reilly GC, Currey JD. The development of microcracking and failure in bone depends on the loading mode to which it is adapted. *J Exp Biol* 1999;202:543–552.

169. Zioupos P, Currey JD, Mirza MS, et al. Experimentally determined microcracking around a circular hole in a flat plate of bone: comparison with predicted stresses. *Philos Trans R Soc Lond, B, Biol Sci* 1995;347:383–396.
170. Mason MW, Skedros JG, Bloebaum RD. Evidence of strain-mode-related cortical adaptation in the diaphysis of the horse radius. *Bone* 1995;17:229–237.
171. Skedros JG, Mason MW, Nelson MC, et al. Evidence of structural and material adaptation to specific strain features in cortical bone. *Anat Rec* 1996;246:47–63.
172. Skedros JG, Dayton MR, Sybrowsky CL, et al. The influence of collagen fiber orientation and other histocompositional characteristics on the mechanical properties of equine cortical bone. *J Exp Biol* 2006;209:3025–3042.
173. Burr DB, Turner CH, Naick P, et al. Does microdamage accumulation affect the mechanical properties of bone? *J Biomech* 1998;31:337–345.
174. Pattin CA, Caler WE, Carter DR. Cyclic mechanical property degradation during fatigue loading of cortical bone. *J Biomech* 1996;29:69–79.
175. Gibson VA, Stover SM, Martin RB, et al. Fatigue behavior of the equine third metacarpus: mechanical property analysis. *J Orthop Res* 1995;13:861–868.
176. Martin RB, Gibson VA, Stover SM, et al. Residual strength of equine bone is not reduced by intense fatigue loading: implications for stress fracture. *J Biomech* 1997;30:109–114.
177. Martin RB, Stover SM, Gibson VA, et al. In vitro fatigue behavior of the equine third metacarpus: remodeling and microcrack damage analysis. *J Orthop Res* 1996;14:794–801.
178. Davies HMS. Ex vivo calibration and validation of in vivo equine bone strain measures. *Equine Vet J* 2009;41:225–228.
179. Nunamaker DM, Butterweck DM, Provost MT. Fatigue fractures in thoroughbred racehorses: relationships with age, peak bone strain, and training. *J Orthop Res* 1990;8:604–611.
180. Cardoso L, Herman BC, Verborgt O, et al. Osteocyte apoptosis controls activation of intracortical resorption in response to bone fatigue. *J Bone Miner Res* 2009;24:597–605.

181. Kennedy OD, Herman BC, Laudier DM, et al. Activation of resorption in fatigue-loaded bone involves both apoptosis and active pro-osteoclastogenic signaling by distinct osteocyte populations. *Bone* 2012;50:1115–1122.
182. Kennedy OD, Laudier DM, Majeska RJ, et al. Osteocyte apoptosis is required for production of osteoclastogenic signals following bone fatigue in vivo. *Bone* 2014;64:132–137.
183. Herman BC, Cardoso L, Majeska RJ, et al. Activation of bone remodeling after fatigue: differential response to linear microcracks and diffuse damage. *Bone* 2010;47:766–772.
184. Smit TH, Burger EH, Huyghe JM. A case for strain-induced fluid flow as a regulator of BMU-coupling and osteonal alignment. *J Bone Miner Res* 2002;17:2021–2029.
185. DeJong ES, DeBerardino TM, Brooks DE, et al. Antimicrobial efficacy of external fixator pins coated with a lipid stabilized hydroxyapatite/chlorhexidine complex to prevent pin tract infection in a goat model. *J Trauma* 2001;50:1008–1014.
186. Perry EL, Beck JP, Williams DL, et al. Assessing peri-implant tissue infection prevention in a percutaneous model. *J Biomed Mater Res Part B Appl Biomater* 2010;92:397–408.
187. Fish J, Belytschko T. Introduction. In: Fish J, Belytschko T eds. *A first course in finite elements*. Hoboken, NJ. John Wiley; 2007:1-9.
188. Cordes V, Gardemin M, Lüpke M, et al. Finite element analysis in 3-D models of equine cheek teeth. *Vet J* 2012;193:391–396.
189. Newlyn HA, Collins SN, Cope BC, et al. Finite element analysis of static loading in donkey hoof wall. *Equine Vet J Suppl* 1998:103–110.
190. Harrison SM, Chris Whitton R, Kawcak CE, et al. Evaluation of a subject-specific finite-element model of the equine metacarpophalangeal joint under physiological load. *J Biomech* 2014;47:65–73.
191. O'Hare LMS, Cox PG, Jeffery N, et al. Finite element analysis of stress in the equine proximal phalanx. *Equine Vet J* 2013;45:273–277.

192. Les CM, Keyak JH, Stover SM, et al. Development and validation of a series of three-dimensional finite element models of the equine metacarpus. *J Biomech* 1997;30:737–742.
193. Rakesh V, Datta AK, Ducharme NG, et al. Simulation of turbulent airflow using a CT based upper airway model of a racehorse. *J Biomech Eng* 2008;130:031011.
194. Skedros JG, Dayton MR, Sybrowsky CL, et al. Are uniform regional safety factors an objective of adaptive modeling/remodeling in cortical bone? *J Exp Biol* 2003;206:2431–2439.
195. Götzen N, Cross AR, Ifju PG, et al. Understanding stress concentration about a nutrient foramen. *J Biomech* 2003;36:1511–1521.
196. Merritt JS, Burvill CR, Pandy MG, et al. Determination of mechanical loading components of the equine metacarpus from measurements of strain during walking. *Equine Vet J Suppl* 2006:440–444.
197. Merritt JS, Pandy MG, Brown NAT, et al. Mechanical loading of the distal end of the third metacarpal bone in horses during walking and trotting. *Am J Vet Res* 2010;71:508–514.
198. Les CM, Keyak JH, Stover SM, et al. Estimation of material properties in the equine metacarpus with use of quantitative computed tomography. *J Orthop Res* 1994;12:822–833.
199. Currey JD. The effect of porosity and mineral content on the Young's modulus of elasticity of compact bone. *J Biomech* 1988;21:131–139.
200. Markel MD, Wikenheiser MA, Chao EY. A study of fracture callus material properties: relationship to the torsional strength of bone. *J Orthop Res* 1990;8:843–850.
201. Oni OO, Capper M, Soutis C. An investigation of the bending stiffness of and the plane stresses generated by a flanged external fixator pin. *J Orthop Trauma* 1995;9:83–88.
202. Karunratanakul K, Kerckhofs G, Lammens J, et al. Validation of a finite element model of a unilateral external fixator in a rabbit tibia defect model. *Med Eng Phys* 2013;35:1037–1043.

203. Karunratanakul K, Schrooten J, Van Oosterwyck H. Finite element modelling of a unilateral fixator for bone reconstruction: Importance of contact settings. *Med Eng Phys* 2010;32:461–467.

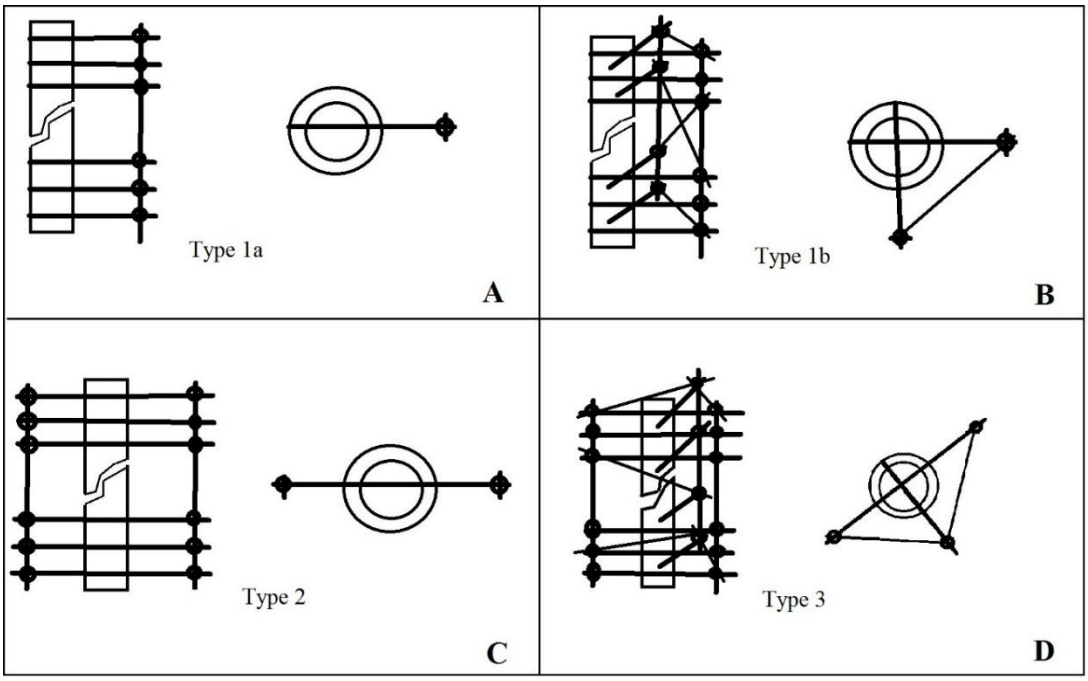

Figure 2.1 Schematic illustration of external skeletal fixator types showing the pin, clamp and connecting rod positioning relative to the fractured bone. A. Type 1a fixators are unilateral configurations with only one connecting rod. B. Type 1b fixators employ multiple unilateral half pin configurations. C. Type 2 fixators employ full pins in a biplanar configuration. D. Type 3 fixators employ both full pins and half pins in a multiplanar configuration.

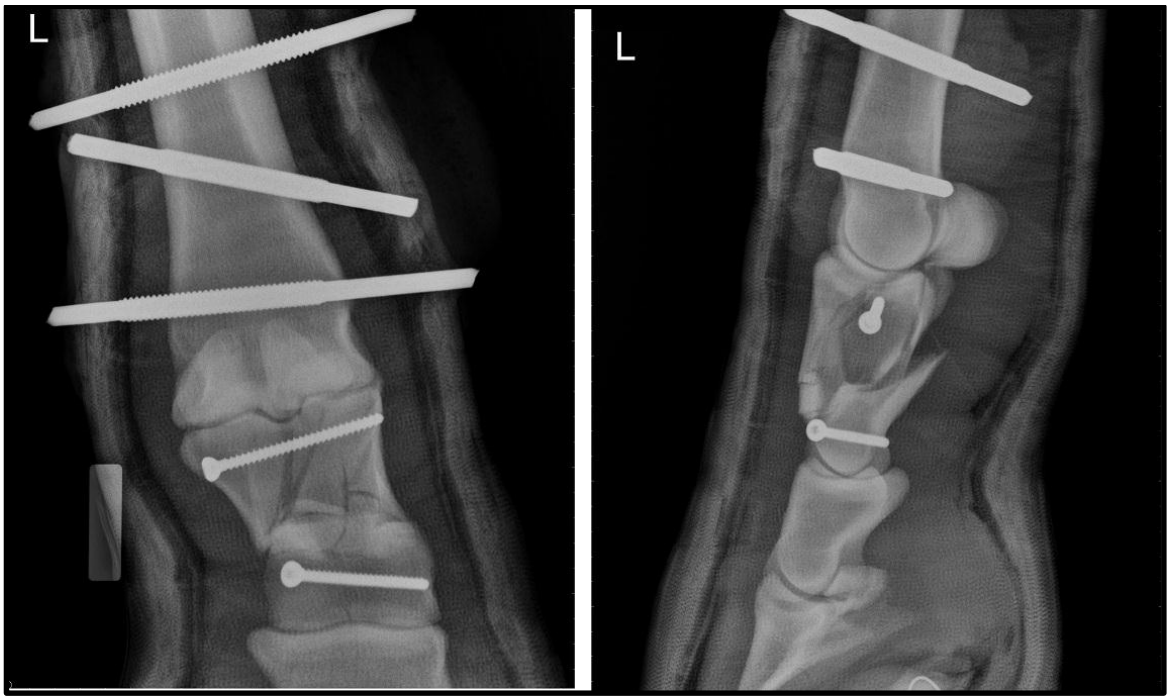

Figure 2.2 Dorsal-palmar (left) and lateral-medial (right) radiographs of a highly comminuted proximal phalanx fracture in a horse treated using a distal limb transfixation cast. This is the typical fracture configuration amenable to repair using a transfixation cast in the horse. Three offset transcortical pins are present in the distal third metacarpal bone and have been incorporated into the distal limb cast which encompasses the foot. Two 4.5 mm lag screws have been positioned to provide some fracture alignment during healing.

CHAPTER 3. FINITE ELEMENT ANALYSIS OF THE EFFECT OF TRANSCORTICAL PIN PARAMETERS ON BONE-PIN INTERFACE STRESSES IN THE EQUINE THIRD METACARPAL BONE

3.1 Introduction

Transfixation casting has improved the success of treating complex distal limb fractures in the horse, particularly comminuted fractures of the proximal phalanx.[1–4] However, complications associated with transfixation casting, such as early pin loosening and secondary pin hole fractures, continue to frustrate surgeons due to their common occurrence and potentially devastating consequences. The basic concepts of transfixation casting are similar to external skeletal fixation, although important differences exist. Similar to external fixation, transfixation casting utilizes multiple transcortical pins placed through intact bone and a rigid external connection between them, to provide stabilization of a specific segment of the skeleton.[5] The fundamental reliance of both methods of fixation on the stability of the transcortical pin within the bone results in comparable limitations related to the **bone-pin interface (BPI)**.[2,5,6] Loss of stability of the pin within the bone is a result of bone resorption at the BPI.[7,8] Resorption is initiated by thermal and mechanical bone damage at the time of pin insertion, and progresses due to cyclic loading of the pin during weight bearing.[6–8] Local bone damage occurs during cyclic loading when bone yield thresholds are exceeded at the BPI.

Pin loosening is the most common complication of both external fixation and transfixation casting.[1,2,9–11] An additional, often devastating complication observed in the horse is the occurrence of secondary pin hole fractures.[1–4,11–13] Both of these complications constitute a form of BPI failure, either insidiously in the form

of pin loosening, or acutely in the case of secondary pin hole fracture. A number of studies have evaluated specific pin modifications in the horse aimed at addressing BPI complications, although these modifications have yet to be widely adopted.[14–19] Clinical improvements in outcome with the use of transfixation casting are unlikely without comprehensively addressing the underlying issues associated with BPI failure.

The biomechanics of external skeletal fixation and the BPI have been studied extensively.[20–27] The effect of altering various parameters of external fixation on BPI stresses, fixator rigidity and the fracture healing process has been examined using analytical, finite element, ex vivo and in vivo methods.[7,8,20,22,23,25–28] Parameters such as pin size, pin number, pin separation distance, pin material, pin working length, sidebar size and number, and number of fixator planes have all been evaluated and recommendations made for clinicians applying external skeletal fixation for fracture repair in humans and small animals.[9,21,27,29] While some of these recommendations have been translated from external fixation to transfixation casting, not all findings or recommendations are directly applicable due to differences between the two techniques. Ex vivo studies have been performed specifically on transfixation casts to evaluate parameters such as pin size, pin number, pin orientation, transcortical hole size, methods of cast attachment to pins and staged pin removal.[30–34] These studies have addressed specific questions related to the transfixation casting method and help to guide current clinical practice.[1,2,4] However, pin number and pin size were evaluated in the radius, while transcortical hole size, pin orientation and staged pin removal were all evaluated in the **third metacarpal bone (MC3)**. None of these studies examined the range of parameters and parameter values that can be altered in the transfixation cast. A systematic evaluation of transfixation casting parameters would provide clinicians with information on the effect of specific pin parameters on BPI stresses and fixation rigidity. Ideally, guidelines that could predict an optimal transcortical pin configuration that would minimize BPI stresses could be developed from a systematic evaluation of pin parameters. Considering the high rate of pin loosening and devastating nature of secondary pin hole fractures, a transcortical pin configuration that reduces BPI stresses below bone yield

threshold levels could improve the safety and reliability of transfixation casting in the horse by reducing these BPI related complications.

Bone yield stress and strain values have been examined for the equine MC3 in both compression and tension during monotonic loading to failure.[35–39] Reported yield stress values range from 147 to 186 MPa in compression and from 64 to 148 MPa in tension. Yield strain values range from -1.44 to -1.76% in compression and from 0.39 to 1.0% in tension. However, under cyclic loading conditions, Martin et al reported that cyclic loading from 0 - 5,000 microstrain (0.5%) in tension over 100,000 cycles resulted in detectable changes in post-yield properties and fatigue damage in the bone.[40] Gibson et al showed that cyclic loading from 0 - 10,000 microstrain in tension resulted in fatigue failure in under 2,000 cycles.[41] Considering these findings, compressive yield strain values of -1% (-10,000 microstrain) and tensile yield strain values of 0.5% (5,000 microstrain) for equine MC3 would be conservative values for a yield strain threshold. Compressive yield stress of -175 MPa and tensile stress of 75 MPa would be considered conservative stress values.

Finite element analysis has been increasingly utilized in orthopedic biomechanics prior to or in parallel with ex vivo and in vivo testing.[42,43] Finite element analysis can be used to model physical phenomena and with rapid improvements in computing power has been increasingly utilized to address complex questions related to orthopedic implants.[44] Finite element analysis utilizes numerical methods for solving large equation sets which are generated based upon a specific assembly of object geometries, constitutive relationships and material properties.[45] The geometry of the object(s) to be studied is represented by an interconnected mesh constructed from discrete elements. Each element contains a defined number of nodal points at which the equations of interest are solved, thereby providing information regarding the entire object through the generation of specific output for each node. Utilizing finite element analysis, a range of parameters could be evaluated to determine an optimal pin configuration for the equine distal limb transfixation cast. Reducing BPI stresses below bone yield threshold levels has the potential to reduce

secondary fractures and premature pin loosening during transfixation casting in the horse. Therefore, the first objective of this study was to develop FE models representative of the equine distal limb transfixation cast to determine which transcortical pin configurations result in BPI stress and strain predictions below expected yield stress and strain values for the equine MC3. The second objective of this study was to determine, from these models, an optimal transcortical pin configuration which would minimize both bone removal for pin placement and BPI stresses in the equine MC3. The third objective of this study was to validate the developed FE models through ex vivo compression testing and surface strain measurement around the pin holes at 3 distinct load levels. The results of this study will allow recommendations to be made regarding specific pin parameters which reduce BPI stresses when a distal limb transfixation cast is used in clinical practice.

3.2 Materials and Methods

3.2.1 Study design

The study was conducted in 3 phases. Initially, geometrically constructed FE models of diaphyseal cortical bone were used to examine the effect of a range of pin parameters on BPI stress and strain. Next, a more complex FE model, having both cortical and cancellous bone regions, was constructed to expand and support the initial findings of the cortical model. Stress and strain predictions from the corticocancellous model were then used to determine preferred bone-pin configurations by using yield stress and strain threshold values combined with calculating the amount of bone removed for pin placement in each model. Finally, validation of the models was performed by comparing FE analysis results with measured surface strain values during ex vivo testing through a range of applicable loads on a single MC3 pin configuration. The bone models were developed from a CT scan of the right forelimb of a 10 year old Quarter Horse gelding weighing 465 kg. A scan was performed of the forelimb from the carpus distally using a 64 slice helical scanner (Lightspeed VCT, General Electric, Milwaukee, WI) at a slice thickness of 3.75mm.

3.2.2 Parameters

Seven parameters of transfixation pins and their placement in the equine MC3 were examined. The parameters were pin diameter, pin type, pin number, pin location, pin spacing, pin orientation and pin material. The parameters were examined by using conventional pin configurations as the primary comparison. In this manner, the effect of parameters such as pin spacing, pin type and pin orientation were evaluated using a single 6.3 mm pin diameter. Therefore, not all of the possible 12,960 parameter combinations were modeled explicitly in this study.

3.2.2.1 Pin diameter

Pin diameters ranging from 4.0 mm through to 9.5 mm were evaluated in this study. Pins ranging in size from 4.7 mm to 9.5 mm in diameter have been used clinically. Larger pin diameters are more resistant to bending and are expected to result in reduced BPI stress.[20] However, they require larger holes in the cortex for insertion which has been shown to reduce the breaking strength of bone.[34,46,47] Pin hole fractures have been reported with 6.3 mm diameter pins and larger in the adult horse, primarily in diaphyseal regions of the MC3.[1,2,4,11,12] A 9.5 mm (3/8”) diameter hole resulted in equine MC3 failure at the yield point during torsional testing, reflecting a lack of plastic deformation of the bone with a mid diaphyseal hole of this size.[34]

3.2.2.2 Pin type

External fixation pins can be either full (completely traverse the bone and externally attached at both ends) or half pins (engaging both cortices of bone but externally attached only at one end). Half pins have not been evaluated in adult horses, either experimentally or clinically. Their inclusion in the study was based upon both the lack of access to the palmar surface of the MC3 in the horse due to major soft tissue structures and the desire

to fully explore any novel transfixation pin configurations that may reduce BPI stresses. Combinations of full pins and half pins were included in the analysis and compared to models with an equivalent number of full pins. Half pins were expected to encounter higher pin stresses and higher bone stresses at the near cortex than full pins.[20]

The effect of pin threads was examined to determine their impact on local stresses and strains at the BPI compared to smooth pins. Smooth pins were used to evaluate all other parameter combinations to reduce geometry complexity of the pins and improve the consistency of results between model comparisons. Threaded pins have been predicted to result in high principal and loading axis stresses and strains at the thread tips and low stresses and strains in the thread troughs.[48,49]

3.2.2.3 Pin number

A range from 1 to 6 pins was evaluated. The number of pins used clinically for transfixation casting has ranged from 2 to 5. Currently 2 or 3 pins are most commonly used.[1,2,4] There are anatomic limits to the number of pins that can be placed within a bone. The pin number is also determined by pin size, pin spacing and pin location parameters. A larger number of pins is expected to reduce BPI stresses.[20]

3.2.2.4 Pin location

A previous recommendation made from clinical observations has been to place pins as far from the top of the cast as possible to avoid secondary pin hole fractures.[2,11] This approach results in pins located in the distal metaphysis of the MC3 in most clinical cases. Pin locations in both the diaphysis and metaphysis were analyzed due to the differences in cortical thickness between these regions, the presence of cancellous bone in the metaphysis and the possibility that factors other than proximity to the top of the cast are

responsible for the occurrence of previously observed secondary pin hole fractures in pins positioned in the diaphysis.[2]

3.2.2.5 Pin spacing

Pin spacing of 10, 20, 25, 30 and 40 mm was evaluated. Clinically, pin spacing of approximately 25 mm is used between transfixation pins in the adult horse.[2,5] An analysis of pin spacing between 2 pins was used to determine if changes in spacing would result in an interaction of the stresses between 2 pins, a stress concentration between pins or an increase in the maximum stresses observed in the models.

3.2.2.6 Pin orientation

A previous ex vivo study has shown that a parallel pin orientation reduced bone strength more than a divergent orientation when tested in torsion.[31] However, clinical studies have failed to detect a difference in secondary pin hole fracture or pin loosening between a divergent pin orientation and a parallel pin orientation.[1,2] For the current study, orientation relative to the frontal plane was varied within the anatomic limits of the metacarpal region to examine this parameter. To determine a feasible degree of offset (or divergence) for pins, these anatomic limits were calculated from CT images of the metacarpus for pin sizes of 4 mm, 6 mm and 8 mm. The anatomic limits of pin placement were defined to avoid removing part of the dorsal cortex during hole creation due to concerns that this may weaken the bone.[12] The limits were: 1) the second or fourth metacarpal bones on the palmar aspect, and 2) the dorsal medial or dorsal lateral cortex of the MC3 on the dorsal aspect **(Figure 3.1)**. An angle of 20 degrees from the frontal plane was chosen for positioning pins in an offset or divergent orientation. This was based on the range of safe pin orientations determined from the CT images. For a 3 pin model with offset, the distal pin was positioned within the frontal plane, the next proximal pin was positioned with 20 degrees of rotation in a clockwise direction (when viewed from above)

and the next proximal pin was rotated 20 degrees in a counterclockwise direction. This orientation resulted in a total of 40 degrees of offset between the proximal two pins and was designated a positive offset model based on the direction of rotation of the pin adjacent to the most distal pin in the bone (**Figure 3.2**). The direction of rotation was reversed for each pin to compare the opposite orientation which was designated a negative offset. A series of 5 different models with various pin diameter and pin number combinations were created to evaluate the effect of an offset pin orientation.

3.2.2.7 Pin material

Currently, 316L stainless steel is used almost exclusively in equine transfixation pins. Titanium alloy pins (most commonly Ti-6Al-4V) are available for use in human orthopedics and small animal practice. The elastic modulus of titanium (110 GPa) is approximately half that of stainless steel (200 GPa) and closer to the elastic modulus of equine MC3 cortical bone (15-20 GPa). Titanium alloy yield strength (828 MPa) is over 4 times higher than implant grade stainless steel (190 MPa), its ultimate strength (895MPa) is almost 2 times higher than stainless steel (490 MPa), while its density (4.43 g/cm^3) is almost half that of stainless steel (8.0 g/cm^3). Stainless steel and titanium alloy pins were evaluated. It was expected from previous studies that stainless steel would result in lower BPI stresses than titanium alloy.[20]

3.2.3 Finite element models

Models of the equine MC3 (described below) and transfixation pins were constructed within an FE software program (Abaqus, v.6.12, Dassault Systemes Simulia Corp, RI, USA) to examine the parameters of interest. In all models, the x-axis represented the medial to lateral direction across the bone, the y-axis represented the dorsal to palmar direction of the bone and the z-axis the proximal to distal or longitudinal direction of the bone. Smooth transfixation pins were constructed directly within the software program. Threaded pins were constructed by adding a helical revolution path of the pin thread

profile sketch around a smooth pin core, thus creating a positive profile threaded pin. Threaded pins had a pitch of 1 mm and thread height of 1 mm. All pins were constructed to be 70 mm in length. Pins were positioned within bone models and Boolean operations used to create pin holes using the intended pin positioning. A 15 mm distance from the outer cortical bone margin to the fixed pin end within the cast (pin working length) was used based on review of radiographs of 6 recent clinical cases of transfixation casting. The pin working length measurements from these 6 cases had a mean and median of 17 mm across all pins, regardless of site within the MC3. Both static analyses and quasi-static analyses were used to examine the initial model, assessing both the expected standing load (static) and walking load (quasi-static) in the adult equine MC3. To simulate standing and weight shifting, a 2500 N distributed axial compressive load was applied over the proximal surface of the bone. This load approximates a 500 kg adult horse shifting its weight onto the transfixation casted limb by lifting the opposite forelimb while standing. To simulate walking, a 7500 N distributed axial compressive load was applied to the proximal surface of the bone. This load and distribution was previously found to approximate the in vivo mid-diaphyseal surface strains of the MC3 when applied during ex vivo testing.[50] The material properties of the bone and pins used for the models were based on previous studies and reference data obtained from metal suppliers for pins **(Table 3.1)**.[51–54] Free meshing algorithms were used for meshing procedures. All models were meshed using solid quadratic tetrahedral elements (C3D10I). These elements allow accurate surface stress predictions due to integration points being located at the nodes and enforcing pressure continuity across material boundaries. This element type is also less likely to result in inaccuracies than a linear tetrahedral element when complex geometries are modeled. Adaptive remeshing was performed to refine the mesh for each individual model based upon the output variable von Mises stress. Remeshing was continued until there was a maximum of 2% change in von Mises stress when compared to the previous mesh. The cast was not modeled specifically for this portion of the study; pin attachment to the cast was included in the model by restraining the end of each pin in all 3 axes as a boundary condition.[19] The distal end of the bone was unrestrained in the longitudinal direction (z-axis) in order to simulate a complete, axially

unstable fracture within the cast distal to the pins. However it was fully constrained in both the lateral to medial (x-axis) and dorsal to palmar (y-axis) directions. Non-linear surface to surface contact stiffness was used at the BPI for all models. This allowed separation of surfaces after contact, sliding between surfaces and prevented overclosure of surfaces under pressure. These conditions would be representative of the BPI immediately after pin insertion. Friction was not included in the contact interaction properties due to the predominantly normal direction of the axial loading forces relative to the pin surface and the restraint of the pin ends in the x-axis. It has been shown that a fully bonded interface will result in an overestimation of the fixator stiffness and that these contact settings are important in the overall accuracy of the model.[55,56] Global seeds were set for the creation of each mesh, with approximate element sizes ranging from 4 to 6 mm. A virtual topology feature was used prior to meshing to combine faces of the more complex geometries and avoid generation of small or unusable elements at the vertices of segments within the individual models.

3.2.3.1 Cortical diaphysis model

The cortical diaphysis model was constructed using geometric information from the CT scan. The entire metacarpus was made up of 62 slices, with 19 slices comprising the diaphysis where the medullary canal was free of cancellous bone. This segment of bone was designated for the cortical diaphysis model. The slice images generated of the diaphysis were imported into image processing software (Image J, v1.46r, National Institutes of Health, http://imagej.nih.gov/ij) to perform measurements and shape fitting procedures on each slice. The thickness of the dorsal, palmar, medial and lateral cortices were measured and recorded. The total bone width and medullary canal width from lateral to medial and from dorsal to palmar were measured and recorded. An ellipse was visually fit to the outer and inner cortical surfaces of the MC3 for each slice image and the dimensions of the best fitting ellipse was recorded. The second and fourth metacarpal bones were not included in this shape fitting process. The final outer cortex ellipse had a lateral to medial dimension of 40 mm and a dorsal to palmar dimension of 30 mm. The

final medullary canal ellipse had a lateral to medial dimension of 16 mm and a dorsal to palmar dimension of 12 mm **(Figure 3.3)**. Cortical thickness measurements were used to determine positioning of the medullary canal within the outer cortical shape. The geometric data obtained from the slice images was used to construct the shape of the diaphysis directly within the FE software program using geometric part construction features and Boolean operations. An elliptic cylinder was created by extrusion of the 2 dimensional shape within the xy plane a distance of 70 mm along the z-axis. This initial elliptic cylinder was flattened slightly on the palmar surface at an angle of 2.5 degrees from the x-axis from lateral to medial. The angle of flattening was approximated from the CT slice images of the diaphyseal bone segment to account for the degree of rotation and palmar flattening observed about the long axis of the MC3 previously described to occur over the full length of MC3 in the horse.[57] The cortical diaphysis model was retained as a part within the model database and separate pin parameters were applied (eg pin diameter) to generate individual bone-pin models by combining pins with this initial bone segment. Contact interactions, load and boundary conditions, meshing and remeshing were then performed on each model as described previously.

3.2.3.2 Corticocancellous model

The corticocancellous model was constructed from the additional 20 CT slices distal to the cortical diaphysis, ending at the physeal scar of distal MC3 just above the metacarpal condyles. The construction approach was similar to the cortical diaphysis model with 2 modifications. First, since bone cross sectional shape changed more rapidly in the metaphyseal region, a lofting procedure was used to connect multiple cross sectional sketches. Cross sectional sketches matching the slice images from the original CT scan of the metaphysis were constructed for every 3rd slice, upon which lofting between slices was used to connect them in sequence and create a 3 dimensional geometry. Second, the cancellous portion of the metaphysis was formed using Boolean operations following creation of the cortical portion of the metaphysis. The metaphysis and diaphysis were combined to form the final corticocancellous model. Similar to the cortical diaphysis

model, this bone segment was retained as a part in the model database to allow it to be used repeatedly for creation of additional bone pin constructs.

3.2.4 Model validation

Model validation was performed by comparing measured surface strain values during ex vivo testing of the original bone with values obtained from FE analysis. This was performed for both the cortical diaphysis model and the corticocancellous model. Loads of 2500, 5000 and 7500N were applied sequentially in axial compression to the proximal end of MC3 for all validation tests. A material testing system (Qtest/50LP, MTS, Eden Prairie, MN) capable of loading up to 50 kN was used to provide axial compression. A custom jig was constructed to accommodate the dimensions of the bone within the materials testing system. The jig consisted of adjustable side walls to enable accurate positioning of the pin. The pin was positioned through a bushing of matching inner diameter to the pin core diameter. The bushing was located within the sidewalls to minimize movement at the pin attachment site and was stabilized using a set screw. Side wall brackets were reinforced to minimize movement of the jig in the lateral to medial direction. A steel cap measuring 70 mm in diameter and 25 mm deep was used to contact the proximal bone surface. To accommodate the proximal bone surface, a 5 mm deep, 45 mm diameter circular depression was created on the lower surface of the steel cap. A solid steel cylinder 25 mm in length and 12 mm in diameter was positioned in a corresponding depression on the upper surface of the steel cap to enable even loading across the proximal bone surface **(Figure 3.4)**.

Each bone model segment was tested separately. A single smooth 6.35 mm diameter pin was centered 35 mm from the bottom of the cortical diaphysis segment and 41 mm from the bottom of the corticocancellous bone segment. The tests were performed sequentially, with the corticocancellous bone segment tested first. The cortical diaphysis segment was then removed by cutting with a saw at the appropriate level of the distal diaphysis. Two rosette strain gauges (FRA-2-11, Texas Measurements, College Station, TX) were

attached approximately 5 mm from the hole margin at a proximal and a dorsal position for both the lateral and medial holes. A single axis strain gauge (FLA-2-11, Texas Measurements, College Station, TX) was placed in a palmar position 5 mm from the hole margin for both lateral and medial holes. Single axis strain gauges were also positioned 20 mm from the pin center both proximally and distally on the dorsal midline. All single axis gauges were visually aligned in the longitudinal (z-axis) bone direction. The rosette gauges were aligned around the medial and lateral holes of each of the bone segments being tested **(Figure 3.5)**. The exact position of each gauge relative to the pin hole was determined by caliper measurement following attachment to the bone. Values used for validation were taken from the center of the strain gauges based on the measurements from the pin hole edge and markers present on the gauge denoting its axis and center. Strain values in the longitudinal axis were obtained directly from the corresponding FE model and compared to those recorded during ex vivo testing. Maximum and minimum principal strain values were calculated from the results of the rosette gauges proximal to the medial and lateral pin holes[58] and compared to corresponding values from the FE model. Longitudinal strain values were compared directly.

Strain gauge attachment was performed by first removing all soft tissue covering the bone surface in the designated strain gauge areas. The cleaned surface was then defatted and dried using 2-butanone (Sigma-Aldrich, St. Louis, MO). Cyanoacrylate was used to attach gauges to the bone, ensuring that a solid surface attachment had been achieved. The gauge lead wires were soldered to a microconnector (4-103240-0, Digi-Key., Thief River Falls, MN) which was plugged into a cable connected to a signal amplifier (2110B, Vishay Precision Instruments, Raleigh, NC). Amplified strain signals were sampled at 100 Hz through an A/D converter and converted to microstrain ($\mu\varepsilon$, strain x 10^{-6}) within the manufacturer's software (Labchart7, ADInstruments, Dunedin, New Zealand). Testing was performed at a loading rate of 6 mm/min. The testing was performed twice at each load level to enable data collection for both medial and lateral pin holes by attaching the appropriate microconnectors to the cable. Each cycle of testing was determined to be

within the linear elastic range of the bone from the load deformation curves generated by the materials testing system and recorded on the dedicated computer.

3.2.4.1 Output variables and preferred pin configuration selection

The output variables specifically recorded and compared for each model were the cortical bone von Mises stress, maximum (tensile) and minimum (compressive) principal cortical bone stress, maximum (tensile) and minimum (compressive) principal cortical bone strain, cortical bone volume removed and longitudinal cortical bone stress and strain values. Maximum pin von Mises stress was also recorded for each model. Output database files were generated for each model and could be reviewed to retrieve a complete data set for the models as necessary. Von Mises stress was used to report single parameter comparisons and highlight general trends within these comparisons as it was generally representative of the overall findings when compared to the other output variables examined.

The principal stress and strain values were used in preference to von Mises stress to perform model selection. The model selection process was based upon bone yield thresholds as these values have been previously measured in equine bone,[35,37] whereas von Mises stress has been shown not to be a good predictor of yielding around circular holes in bone.[59] Principal tensile stress threshold was set at 75 MPa, principal stress threshold in compression was set at -175 MPa, principal tensile strain threshold was set at 0.5% strain (5,000 microstrain), and principal compressive strain threshold was set at -1% strain (-10,000 microstrain). For each model, the stress and strain values were recorded and those falling under all of the bone yield threshold values were selected as preferred bone pin configurations.

3.3 Results

3.3.1 Finite element models

The finite element models constructed from both the cortical diaphysis and the corticocancellous region of the bone were successfully used to assess the range of pin parameters examined. The number of elements in the models ranged from approximately 25,000 to 175,000, largely dependent upon the number of pins evaluated and the amount of remeshing of the model required to achieve convergence within the stated 2% limit for von Mises stress values.

3.3.2 Parameters

3.3.2.1 Pin diameter

Pin diameter had a predictable effect on cortical bone von Mises stress, as well as principal stresses and strains, when examined in isolation. Smaller pin sizes resulted in higher stresses at the BPI. Maximum values were invariably observed at the outer proximal margin of the pin hole consistent with previous studies.[20] Values for cortical bone von Mises stress reduced sharply both from the outer cortex towards the inner cortex and radially away from the pin hole (**Figure 3.6**). The relationship between pin diameter and cortical bone von Mises stress fitted negative power law equations for one, two, three and four pin models (**Figure 3.7**). Similar relationships were also observed for the principal stress and strain values. Maximum principal stress and strain and minimum principal stress and strain, along with maximum von Mises stress for the range of pin diameters examined in one, two, three and four pin models are presented in **Tables 3.2 – 3.5,** respectively. In models with only one pin, the cortical bone yield thresholds were exceeded for maximum principal stress and maximum principal strain for all pin diameters examined. The smallest pin diameter for which all maximum and minimum principal stress and strain values were below the yield threshold values was 8 mm in the

two pin models, 7 mm in the three pin models and 6 mm in the four pin models. This applied to both the cortical diaphysis model and the corticocancellous model.

3.3.2.2 Pin type

The effect of the addition of a half pin was examined in both the cortical diaphysis model and the corticocancellous model. The half pin resulted in a maximum cortical bone von Mises stress approximately midway between the respective full pin models (**Figures 3.8 and 3.9**). A threaded pin was examined using the cortical diaphysis bone model and compared directly to a smooth pin of the same core diameter. Patterns of stress concentration were apparent at the thread peaks present in the bone, making direct comparison of maximum values difficult **(Figure 3.10)**. The maximum von Mises stress recorded for the threaded pin occurred in the proximal outer cortex of the bone, similar to the smooth pin, however the magnitude of the maximum peak was 14,420 MPa compared to the smooth pin which had a maximum von Mises stress of 429.8 MPa. In an effort to remove the effect of large stress singularities arising from the fine remeshing process which occurred around the threads, the 95^{th} percentile of the von Mises stress was compared between these models. The threaded pin model 95^{th} percentile of von Mises stress in the cortical bone was 645.5 MPa, while the smooth pin model value was 209.9 MPa. The von Mises cortical bone stress was also compared between the threaded and smooth pin by examining the stresses at a set distance from the pin core diameter. This was performed at 1 mm from the pin (core) proximal edge. The maximum von Mises cortical bone stress for the threaded pin was 275.8 MPa and for the smooth pin was 208.7 MPa (**Figure 3.11**).

3.3.2.3 Pin number

Increasing the number of pins in the cortical diaphysis bone model resulted in a predictable reduction in the maximum cortical bone von Mises stress. Similar to the

different pin number models for a specific pin diameter comparison, the different pin diameter models for a specific pin number comparison show that a consistent relationship exists across different pin diameters (**Figure 3.12**). Increasing the number of pins resulted in a greater reduction in maximum cortical bone von Mises stress for smaller pin diameters compared to larger pin diameters. A similar relationship was observed in the corticocancellous model and with maximum cortical bone strain values (**Figure 3.13**).

3.3.2.4 Pin location

Pin location was examined by comparing the results from single pins in the cortical diaphysis model (**Table 3.2**), with single pins placed in the metaphysis of the corticocancellous model (**Table 3.6**). The pin location affected the maximum cortical bone von Mises stress values, with higher stress values present in the metaphyseal region compared to the diaphyseal region of bone. This was more evident for smaller pin diameters (**Figure 3.14**). There were only small differences observed between bone locations for maximum principal stress or maximum principal strain values, while minimum principal stress and strain values were lower in the metaphyseal region (ie. higher compressive stress and strain) when compared to the diaphyseal region.

3.3.2.5 Pin spacing

Pin spacing was varied from 10 mm to 40 mm between pin edges in the cortical diaphysis model. There were only small differences between maximum cortical bone von Mises stress values ranging from 247.7 MPa to 257.2 MPa across the different spacing distances. Maximum and minimum principal stress and strain values were also similar among spacing distances. Qualitative examination of the stress and strain patterns surrounding the pin holes did not show stress concentrations between or around pins for the spacing distances evaluated.

3.3.2.6 Pin orientation

Comparisons were made between pins oriented in a divergent position from the frontal plane (offset) and pins oriented solely within the frontal plane (inline). The maximum angle that pins could be offset from the frontal plane was determined from the CT images and calculated for each slice (**Figure 3.15**). The maximum angle possible within the defined anatomic limits increased from proximal to distal locations in the bone and was larger in 4 mm pins, ranging from 48 to 72 degrees. For 6 mm pins the maximum angle ranged from 35 to 59 degrees and for 8 mm pins the maximum angle ranged from 28 to 48 degrees.

In the cortical diaphysis model, offsetting the pin orientation in 2 and 3 pin models using 6.3 mm diameter pins resulted in similar values for cortical bone von Mises stress. However, maximum (and minimum) principal stresses and strains were generally higher (and lower) in the offset models. The exception was for the maximum principal strain value for the 2 pin model with a positive offset of the second pin (**Table 3.7**).

In the corticocancellous model, offsetting the pin orientation resulted in lower maximum principal strain values in the 3 pin model using 7 mm diameter pins compared to an inline orientation (**Table 3.8**). However in the 4 pin model using 7 mm diameter pins, no decrease in stress or strain values were observed when offsetting was used. In a 6 pin model with 5.5 mm diameter pins an offset orientation of pins resulted in lower maximum principal strain compared to an inline orientation, while other stress and strain values were similar between orientations. The reduction in maximum principal strain for an offset orientation was approximately 5% for the 6 pin model and 8% for the 3 pin model (**Table 3.8**). Overall, no consistent pattern of stress reduction or stress concentration was observed as a result of diverging the pin orientation from the frontal plane.

3.3.2.7 Pin material

Stainless steel and titanium alloy pins were compared using single pins positioned in the distal metaphysis of the corticocancellous bone model **(Figure 3.16)**. A range of pin sizes from 5 mm to 9 mm were examined and maximum von Mises stress was compared for both cortical bone (**Figure 3.17**) and the pins (**Figure 3.18**). Maximum cortical bone stress was lower for stainless steel pins across the range of pin sizes examined, while maximum pin von Mises stress was lower for the titanium alloy pins.

3.3.2.8 Preferred pin configurations

An optimal pin configuration from the analysis of parameters in the present study was determined by comparing model results with the yield threshold values for principal tensile (maximum values) and compressive (minimum values) stress and strain within the corticocancellous bone models generated. Since there was a large influence of both pin diameter and pin number across the range of models evaluated in this study (**Figures 3.7 and 3.12**), the smallest pin size for each evaluated number of pins was determined as the preferred pin configuration within each pin number group. None of the single pin models had maximum stress and strain values below the yield threshold values. Two pin models using 9 mm diameter pins were below all threshold values, while two 8 mm diameter pins were below the threshold for all outcome variables except for maximum strain (5099 microstrain). Three pin models using 7 mm diameter pins were below yield threshold values for all 4 outcome variables. Four pin models using 6.3 mm diameter pins were also below bone yield threshold for all 4 outcome variables. Five pin models using a 6 mm diameter pin were below threshold while six pin models with 5.5 mm pins were below the threshold values of outcome variables used for selection.

3.3.3 Model validation

The surface strain measurements recorded during loading of each model were compared to the FE models at the corresponding locations based on the gauge position measurements. Longitudinal strain values for the corticocancellous model varied from the corresponding measured values by 1.3 – 16.9%. Maximum and minimum principal strain values calculated from rosette gauges varied from the corresponding FEM values in the corticocancellous model by 1.5 – 23.9% (**Table 9**). A similar linear response between the load levels was seen in both the FE models and the tested bone-pin constructs. The mean percentage difference between the FE model and ex vivo testing strain values was 5.9% for the longitudinal strain, 10% for the maximum principal strain and 7.3% for the minimum principal strain comparisons. The comparison between the modeled and the measured strain values are illustrated in **Figure 3.19**. The results for the longitudinal strain in the cortical diaphysis model ranged from 22.4 – 62.7% difference between the ex vivo measurements and the FE model. The pin placement for the ex vivo testing in this bone segment was unintentionally angled by 6 degrees proximal-medial to distal-lateral. Technical issues with poor wire contact from the strain gauges resulted in an incomplete data collection on the cortical diaphysis model. The strain gauges also did not lie completely flat on the curved surface of the cortical bone and so the reliability of the data collected from the cortical diaphysis model is unclear.

3.4 Discussion

The results of this study show that the number of pins used, and their diameter, had a predictable and profound effect on the BPI stresses and strains obtained in the FE models evaluated. The trends seen in these results are consistent with previous studies examining external fixation parameters.[20,21] In contrast, the spacing between pins and their orientation about the frontal plane each had only minor influence on the predicted BPI stresses and strains. Threaded pins were predicted to have higher local stresses and strains associated with the threads when compared to smooth pins, which is also consistent with

previous studies.[48] Half pins resulted in load sharing and a stress reduction of approximately 50% of that expected for an additional full pin without any decrease in the bone volume removed for pin placement. Stainless steel pins resulted in lower BPI stresses due to their higher stiffness, however titanium alloy pin stresses were marginally lower than stainless steel pins and as such titanium alloy pins may be less likely to fail during cyclic loading, particularly since their yield stress value is higher than equivalent diameter stainless steel pins. Pins located in the metaphyseal region of the bone resulted in higher compressive stresses and strains than pins located in the diaphysis of the bone. The optimal pin configurations proposed from these results should be further evaluated in ex vivo and in vivo testing to verify these initial findings beyond the individual horse used to validate the FE models in the current study.

The overall goal of this study was to systematically evaluate pin and pin positioning parameters relevant to the clinical use of the distal limb transfixation cast in the horse to determine which parameter combination(s) would result in BPI stresses and strains below bone yield thresholds for equine bone. Finite element analysis was chosen to perform this evaluation because of its ability to utilize information on the mechanical conditions of a system, calculate predictions regarding the overall stress and strain environment of that system and provide data on specific models that can be further developed and refined, either with further FE analysis or in cadaveric or in vivo testing. This method of screening pin parameters avoided the use of a large number of animals or cadaver limbs to gain preliminary information regarding the pin parameters of interest.

The FE models developed were deliberately simple in their geometric design to facilitate performing a large number of specific model constructions without the complexity of strict anatomic reproduction. Modeling techniques used to convert anatomic data such as CT images into a mesh available for FE analysis typically employ smoothing and simplifying algorithms to minimize the sharp features of a bone and the negative impact they can have on the generation of a suitable mesh.[60] The approach used in the current study converted the CT slice geometry of the diaphysis and metaphysis into a part

directly within the FE software that could be fully manipulated to position pins and undergo mesh generation in a repeatable and consistent manner from one pin combination to the next. The use of quadratic solid tetrahedral elements with accurate transmission of pressure between bone and pin surfaces was possible with this geometry. Previous studies have utilized linear tetrahedral elements when evaluating the BPI in the horse which do not provide the same degree of accuracy when modeling at an interface or when fine meshes are required.[19] Validation of the current method was performed through comparison to the ex vivo testing performed on the corticocancellous bone segment. The differences between the models were generally low, with only 4 specific comparisons being greater than 10%, and the mean percentage differences across each of the strain measures analyzed less than or equal to 10%. These comparisons were made not only for measured longitudinal strain values but also calculated principal strain values and across 3 different loading levels to provide information on the validity of the model over the different strain directions and different weight bearing loads in the horse. These robust validation findings support that the simplified approach had good agreement with the ex vivo testing. While it has been shown that the generation of subject-specific FE models from CT data of human long bones can give accurate information regarding stresses and bone failure,[60–62] several investigators have used simplified models of the equine MC3 and also shown good agreement with ex vivo results.[50,63–65] The simple shape of the equine MC3 allows good reproduction of its mechanical performance using the simplified modeling approach adopted and the objectives of the current study were more readily achieved with this approach.

Current limitations of transfixation casting in the horse are primarily related to the BPI.[1,2] Two key limitations are pin loosening due to chronic local bone failure and subsequent bone resorption, and secondary pin hole fracture due to acute bone failure at the pin hole. As a result, the focus of the output variables evaluated in this study was the maximum (tensile) and minimum (compressive) principal stresses and strains, which consistently occurred at the BPI. The threshold yield criteria used to evaluate the models were based on previous studies evaluating equine MC3 cyclic bone failure.[35,37] The loading

conditions applied for each model were aimed at mimicking a worst case scenario within the transfixation cast. A 7500 N load applied to the proximal bone surface has been shown to be representative of the ex vivo load which reproduces in vivo bone strain at the walk in an adult horse.[50] The boundary condition of the distal end of the bone was set to be unrestrained in the longitudinal axis, as may be the case in a complete, axially unstable fracture immediately following transfixation cast application. These loading conditions would be expected to be less severe for a fracture configuration in which partial load transfer occurs through the fractured bone ends and at times when the horse is not walking.[26–28] In addition, soft tissue and distal limb contact with the cast material in a distal limb transfixation cast would be expected to provide further reductions in the actual load transfer applicable to the BPI in the MC3.

The approach used to determine the preferred pin configurations was applied for each individual pin number, since this parameter had a profound influence on the BPI stresses observed. Currently, the most common configuration of pin number and diameter used clinically is 2 or 3 threaded pins of 6.3 mm diameter. Based on the results of this study, these pin configurations would be expected to result in tensile strains at the BPI over the 5,000 microstrain threshold set in this study for bone failure and over the 10,000 microstrain threshold for compressive strain. These results are also comparable to a previous finite element analysis of transcortical pins in the equine MC3.[19] As is observed clinically, local bone failure at the BPI with bone resorption and pin loosening would be expected to occur when 2 or 3 pins of 6.3 mm diameter are used in a distal limb transfixation cast. The results suggest that 4 pins of 6.3 mm diameter would reduce the expected BPI stresses and strains below the threshold values set in this study and may reduce pin loosening resulting from cyclic loading.

Huiskes and Chao developed a predictive formula for peak compressive stress at the BPI.[20,21] They did not evaluate tensile stresses and strains. Schileo et al have shown that a maximum principal strain criterion is superior to von Mises stress and maximum principal stress in predicting bone failure in the human femur.[62] In our selection process

for preferred pin diameter and number combinations, the tensile strain yield threshold was consistently the last criteria met as pin diameter and pin number in the models increased.

The selection of the parameters to evaluate in this study was made based on current clinical practices. A range of pin diameters have been used in the adult horse for transfixation casting and external fixation. Increasing pin diameter increases the resistance of the pin to bending under load. The area moment of inertia of the pin increases with the fourth power of the diameter. The relationship demonstrated between pin diameter and maximum von Mises stress for a single pin appears to be consistent with the influence that pin area moment of inertia is expected to have on bending stiffness of the pin and consequently BPI stress, with a power law exponent of 3.18 **(Figure 3.7)**. It is evident from examining pin diameter against maximum cortical bone von Mises stress in models with increasing numbers of pins that the influence of pin diameter lessens as the number of pins in the model increases. This effect is reflected in the lower exponent in the power law relationships that exist for each curve based on different pin numbers. From these results it is evident that further evaluation of the relationship between the area moment of inertia of the pin and the pin number is warranted to examine the overall effect of both parameters together, which were found to have the greatest influence on BPI stresses and strains in this study.

The examination of pin orientation in this study failed to show a clear advantage to this method of pin positioning in the equine MC3. However, our analysis used only an axial compressive load, while a previous study evaluating pin orientation ex vivo tested bones in torsion.[31] We elected to test in compression because the predominant loading of the MC3 in the horse is compressive.[50] The results of the current study agree with the clinical findings of retrospective studies where neither pin loosening nor secondary pin hole fracture were found to be affected by an offset (divergent) pin orientation relative to an inline (parallel) orientation.

There are several limitations of this study that merit discussion. The accuracy of any analysis is dependent on the accuracy of the input data. Finite element analysis for mechanical behavior requires the input of material information such as bone density and elastic modulus. Bone is an anisotropic material and its density varies depending on the type of bone and its degree of porosity. A relationship between bone density and elastic modulus can be used to provide detailed material information on an elemental level to increase the accuracy of a model.[62] However, this method of material assignment increases the computational complexity of the model substantially. In addition to the variability in bone material that was not accounted for in this study, the material properties of metals, while more consistent than bone, can vary due to different manufacturing and processing procedures. Another model assumption used in this study was that the distal end of the bone segment was restrained in the transverse (x and y) axes. This assumption is unlikely to be fully reflective of the true situation, however, movement within a cast in the transverse axes relative to the longitudinal axis is expected to be minimal. The assumption that the pin ends are completely fixed is also unlikely to reflect the true situation within a cast. Further evaluation of the effect of this assumption on the results of these models is warranted. Another limitation of the modeling approach in this study was the fact that the BPI contact conditions were simplified by not accounting for friction that undoubtedly occurs as part of the true situation and interaction of a pin within the bone. Friction would be expected to have an effect on sliding of the pin even though the major loading direction was normal to the pin surface, and lateral to medial sliding was not permitted due to restraining the pin ends.

An advantage that using the simplified modeling approach provided was our ability to make multiple comparisons across different pin parameters. The fixed length of the pin allowed for rapid and accurate alignment of the pins within the bone model which was consistent from one model to the next. Coupled with validation of the corticocancellous model, the findings allow us to further investigate specific aspects of the distal limb transfixation cast which are likely to have the greatest influence on BPI stresses and strains using further ex vivo and in vivo testing.

3.5 List of References

1. Joyce J, Baxter GM, Sarrafian TL, et al. Use of transfixation pin casts to treat adult horses with comminuted phalangeal fractures: 20 cases (1993-2003). *J Am Vet Med Assoc* 2006;229:725–730.

2. Lescun TB, McClure SR, Ward MP, et al. Evaluation of transfixation casting for treatment of third metacarpal, third metatarsal, and phalangeal fractures in horses: 37 cases (1994-2004). *J Am Vet Med Assoc* 2007;230:1340–1349.

3. Kraus BM, Richardson DW, Nunamaker DM, et al. Management of comminuted fractures of the proximal phalanx in horses: 64 cases (1983-2001). *J Am Vet Med Assoc* 2004;224:254–263.

4. Rossignol F, Vitte A, Boening J. Use of a modified transfixation pin cast for treatment of comminuted phalangeal fractures in horses. *Vet Surg* 2014;43:66–72.

5. McClure S, Honnas CM, Watkins JP. Managing equine fractures with external skeletal fixation. *Comp Cont Educ Pract Vet* 1995;17:1054–1063.

6. Clary E, Roe S. Enhancing external skeletal fixation pin performance - consideration of the pin-bone interface. *Vet Comp Orthop Traumatol* 1995;8:6–13.

7. Aro HT, Markel MD, Chao EY. Cortical bone reactions at the interface of external fixation half-pins under different loading conditions. *J Trauma* 1993;35:776–785.

8. Pettine KA, Chao EY, Kelly PJ. Analysis of the external fixator pin-bone interface. *Clin Orthop Relat Res* 1993:18–27.

9. Palmer RH. External fixators and minimally invasive osteosynthesis in small animal veterinary medicine. *Vet Clin North Am Small Anim Pract* 2012;42:913–934.

10. Moroni A, Vannini F, Mosca M, et al. State of the art review: techniques to avoid pin loosening and infection in external fixation. *J Orthop Trauma* 2002;16:189–195.

11. Nemeth F, Back W. The use of the walking cast to repair fractures in horses and ponies. *Equine Vet J* 1991;23:32–36.

12. Nunamaker DM. A new external skeletal fixation device that allows immediate full weightbearing application in the horse. *Vet Surg* 1986;15:345–355.

13. Sullins KE, McIlwraith CW. Evaluation of 2 types of external skeletal fixation for repair of experimental tibial fractures in foals. *Vet Surg* 1987;16:255–264.
14. Nash RA, Nunamaker DM, Boston R. Evaluation of a tapered-sleeve transcortical pin to reduce stress at the bone-pin interface in metacarpal bones obtained from horses. *Am J Vet Res* 2001;62:955–960.
15. Nunamaker DM, Nash RA. A tapered-sleeve transcortical pin external skeletal fixation device for use in horses: development, application, and experience. *Vet Surg* 2008;37:725–732.
16. Zacharias JR, Lescun TB, Moore GE, et al. Comparison of insertion characteristics of two types of hydroxyapatite-coated and uncoated positive profile transfixation pins in the third metacarpal bone of horses. *Am J Vet Res* 2007;68:1160–1166.
17. Lescun TB, Baird DK, Oliver LJ, et al. Comparison of hydroxyapatite-coated and uncoated pins for transfixation casting in horses. *Am J Vet Res* 2012;73:724–734.
18. Brianza S, Brighenti V, Boure L, et al. In vitro mechanical evaluation of a novel pin-sleeve system for external fixation of distal limb fractures in horses: a proof of concept study. *Vet Surg* 2010;39:601–608.
19. Brianza S, Brighenti V, Lansdowne JL, et al. Finite element analysis of a novel pin-sleeve system for external fixation of distal limb fractures in horses. *Vet J* 2011;190:260–267.
20. Huiskes R, Chao EY, Crippen TE. Parametric analyses of pin-bone stresses in external fracture fixation devices. *J Orthop Res* 1985;3:341–349.
21. Huiskes R, Chao EY. Guidelines for external fixation frame rigidity and stresses. *J Orthop Res* 1986;4:68–75.
22. Bouvy BM, Markel MD, Chelikani S, et al. Ex vivo biomechanics of Kirschner-Ehmer external skeletal fixation applied to canine tibiae. *Vet Surg* 1993;22:194–207.
23. Wu JJ, Shyr HS, Chao EY, et al. Comparison of osteotomy healing under external fixation devices with different stiffness characteristics. *J Bone Joint Surg Am* 1984;66:1258–1264.
24. Biliouris TL, Schneider E, Rahn BA, et al. The effect of radial preload on the implant-bone interface: a cadaveric study. *J Orthop Trauma* 1989;3:323–332.

25. Chao EY, Aro HT, Lewallen DG, et al. The effect of rigidity on fracture healing in external fixation. *Clin Orthop Relat Res* 1989:24–35.
26. Aro HT, Kelly PJ, Lewallen DG, et al. The effects of physiologic dynamic compression on bone healing under external fixation. *Clin Orthop Relat Res* 1990:260–273.
27. Aro HT, Chao EY. Biomechanics and biology of fracture repair under external fixation. *Hand Clin* 1993;9:531–542.
28. Liu RW, Kim YH, Lee DC, et al. Computational simulation of axial dynamization on long bone fractures. *Clin Biomech* 2005;20:83–90.
29. Lewis DD, Cross AR, Carmichael S, et al. Recent advances in external skeletal fixation. *J Small Anim Pract* 2001;42:103–112.
30. Hopper SA, Schneider RK, Ratzlaff MH, et al. Effect of pin hole size and number on in vitro bone strength in the equine radius loaded in torsion. *Am J Vet Res* 1998;59:201–204.
31. McClure SR, Watkins JP, Ashman RB. In vitro comparison of the effect of parallel and divergent transfixation pins on breaking strength of equine third metacarpal bones. *Am J Vet Res* 1994;55:1327–1330.
32. McClure SR, Watkins JP, Hogan HA. In vitro evaluation of four methods of attaching transfixation pins into a fiberglass cast for use in horses. *Am J Vet Res* 1996;57:1098–1101.
33. Williams JM, Elce YA, Litsky AS. Comparison of 2 equine transfixation pin casts and the effects of pin removal. *Vet Surg* 2014;43:430–436.
34. Seltzer KL, Stover SM, Taylor KT, et al. The effect of hole diameter on the torsional mechanical properties of the equine third metacarpal bone. *Vet Surg* 1996;25:371–375.
35. Les CM, Stover SM, Keyak JH, et al. The distribution of material properties in the equine third metacarpal bone serves to enhance sagittal bending. *J Biomech* 1997;30:355–361.
36. Skedros JG, Dayton MR, Sybrowsky CL, et al. Are uniform regional safety factors an objective of adaptive modeling/remodeling in cortical bone? *J Exp Biol* 2003;206:2431–2439.

37. Skedros JG, Dayton MR, Sybrowsky CL, et al. The influence of collagen fiber orientation and other histocompositional characteristics on the mechanical properties of equine cortical bone. *J Exp Biol* 2006;209:3025–3042.
38. Bigley RF, Gibeling JC, Stover SM, et al. Volume effects on yield strength of equine cortical bone. *J Mech Behav Biomed Mater* 2008;1:295–302.
39. Hawkins DL, Stover SM. Pregnancy-associated changes in material properties of the third metacarpal cortical bone in mares. *Am J Vet Res* 1997;58:182–187.
40. Martin RB, Gibson VA, Stover SM, et al. Residual strength of equine bone is not reduced by intense fatigue loading: implications for stress fracture. *J Biomech* 1997;30:109–114.
41. Gibson VA, Stover SM, Martin RB, et al. Fatigue behavior of the equine third metacarpus: mechanical property analysis. *J Orthop Res* 1995;13:861–868.
42. Burkhart TA, Andrews DM, Dunning CE. Finite element modeling mesh quality, energy balance and validation methods: a review with recommendations associated with the modeling of bone tissue. *J Biomech* 2013;46:1477–1488.
43. Huiskes R, Hollister SJ. From structure to process, from organ to cell: recent developments of FE-analysis in orthopaedic biomechanics. *J Biomech Eng* 1993;115:520–527.
44. Taylor M, Prendergast PJ. Four decades of finite element analysis of orthopaedic devices: Where are we now and what are the opportunities? *J Biomech* 2015;48:767–778.
45. Fish J, Belytschko T. Introduction. In: Fish J, Belytschko T eds. *A first course in finite elements.* Hoboken, NJ: John Wiley; 2007:1-9.
46. Kuo RF, Chao EY, Rim K, et al. The effect of defect size on the stress concentration and fracture characteristics for a tubular torsional model with a transverse hole. *J Biomech* 1991;24:147–155.
47. Hipp JA, Edgerton BC, An KN, et al. Structural consequences of transcortical holes in long bones loaded in torsion. *J Biomech* 1990;23:1261–1268.
48. Wazen RM, Currey JA, Guo H, et al. Micromotion-induced strain fields influence early stages of repair at bone-implant interfaces. *Acta Biomater* 2013;9:6663–6674.

49. Capper M, Soutis C, Oni OO. Comparison of the stresses generated at the pin-bone interface by standard and conical external fixator pins. *Biomaterials* 1994;15:471–473.
50. Les CM, Stover SM, Taylor KT, et al. Ex vivo simulation of in vivo strain distributions in the equine metacarpus. *Equine Vet J* 1998;30:260–266.
51. Chen Q, Thouas GA. Metallic implant biomaterials. *Mater Sci Eng: R*: 2015;87:1–57.
52. Stevenson M, Barkey M, Bradt R. Fatigue failures of austenitic stainless steel orthopedic fixation devices. *Pract Fail Analy* 2002;2:57–64.
53. Anonymous. Product Data Sheet - 316/316L Stainless Steel. 2007. Available at: www.aksteel.com.
54. McClure SR, Glickman LT, Glickman NW, et al. Evaluation of dual energy x-ray absorptiometry for in situ measurement of bone mineral density of equine metacarpi. *Am J Vet Res* 2001;62:752–756.
55. Karunratanakul K, Schrooten J, Van Oosterwyck H. Finite element modelling of a unilateral fixator for bone reconstruction: Importance of contact settings. Med Eng Phys 2010;32:461–467.
56. Karunratanakul K, Kerckhofs G, Lammens J, et al. Validation of a finite element model of a unilateral external fixator in a rabbit tibia defect model. *Med Eng Phys* 2013;35:1037–1043.
57. Dymock DC, Pauwels FET. Investigation into the morphology of the third metacarpal bone in the horse. *N Z Vet J* 2012;60:223–227.
58. Biewener AA. In vivo measurement of bone strain and tendon force. In: Biewener AA ed. *Biomechanics - structures and systems: a practical approach*. Oxford IRL Press, New York. 1992:123–147.
59. Zioupos P, Currey JD, Mirza MS, et al. Experimentally determined microcracking around a circular hole in a flat plate of bone: comparison with predicted stresses. *Philos Trans R Soc Lond, B, Biol Sci* 1995;347:383–396.
60. Taddei F, Cristofolini L, Martelli S, et al. Subject-specific finite element models of long bones: An in vitro evaluation of the overall accuracy. *J Biomech* 2006;39:2457–2467.

61. Schileo E, Taddei F, Malandrino A, et al. Subject-specific finite element models can accurately predict strain levels in long bones. *J Biomech* 2007;40:2982–2989.
62. Schileo E, Taddei F, Cristofolini L, et al. Subject-specific finite element models implementing a maximum principal strain criterion are able to estimate failure risk and fracture location on human femurs tested in vitro. *J Biomech* 2008;41:356–367.
63. Les CM, Keyak JH, Stover SM, et al. Development and validation of a series of three-dimensional finite element models of the equine metacarpus. *J Biomech* 1997;30:737–742.
64. Merritt JS, Burvill CR, Pandy MG, et al. Determination of mechanical loading components of the equine metacarpus from measurements of strain during walking. *Equine Vet J Suppl* 2006:440–444.
65. Merritt JS, Pandy MG, Brown NAT, et al. Mechanical loading of the distal end of the third metacarpal bone in horses during walking and trotting. *Am J Vet Res* 2010;71:508–514.

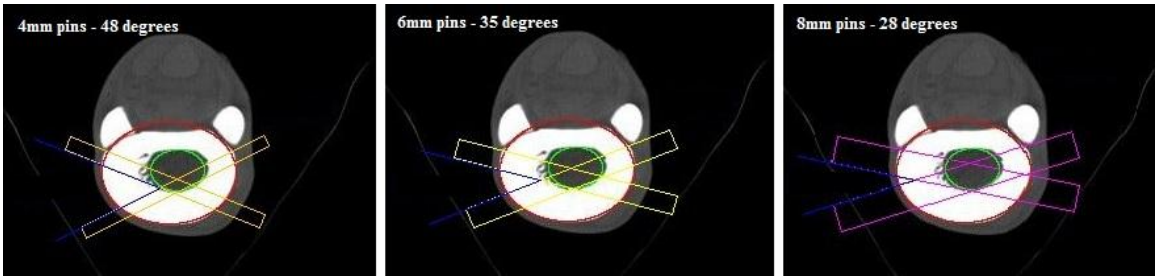

Figure 3.1 Illustration showing the method used to determine the maximum possible angle of deviation from the frontal plane when 4 mm, 6 mm and 8 mm pins are used in an offset pin orientation. Pins outlines were positioned to avoid encroaching on the 2nd or 4th metacarpal bones and the dorsal cortex concurrently.

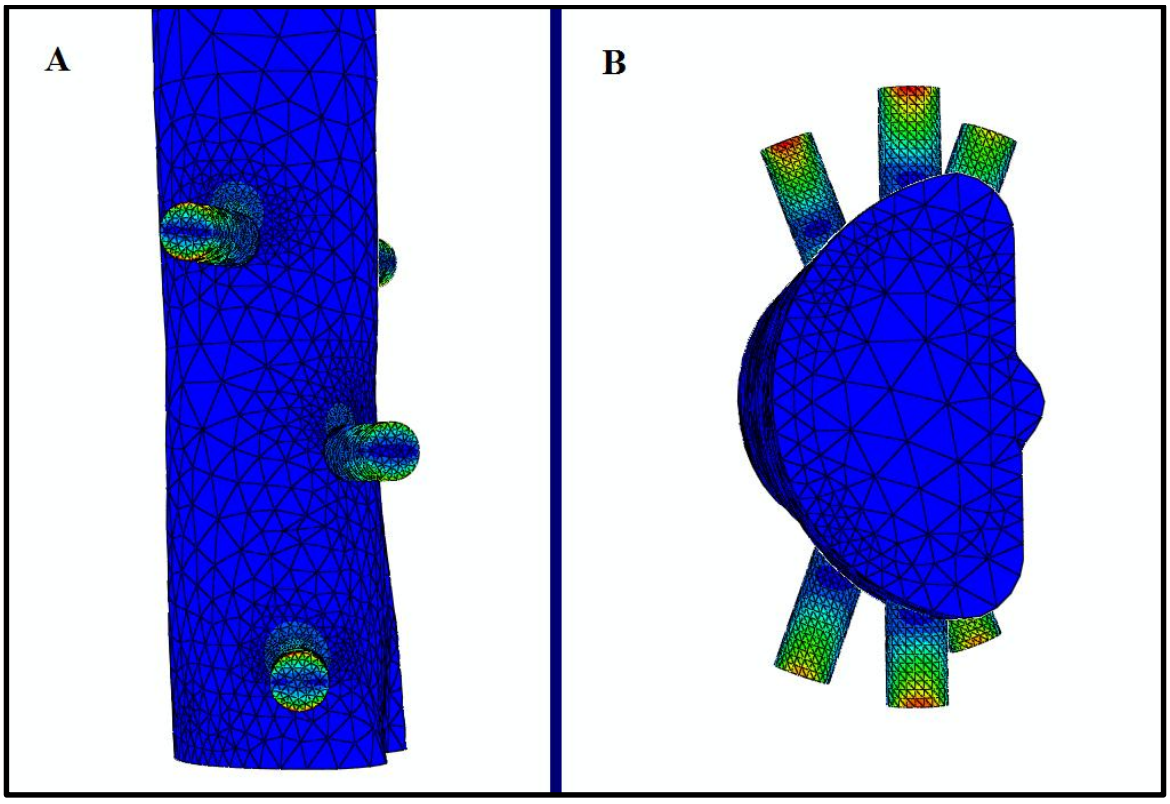

Figure 3.2 A. Image of the corticocancellous bone model with 3 pins (7 mm diameter) in an offset orientation as viewed from the medial aspect of the bone. B. Same model as in A, viewed from the distal aspect of the bone to illustrate the angle of offset between pins.

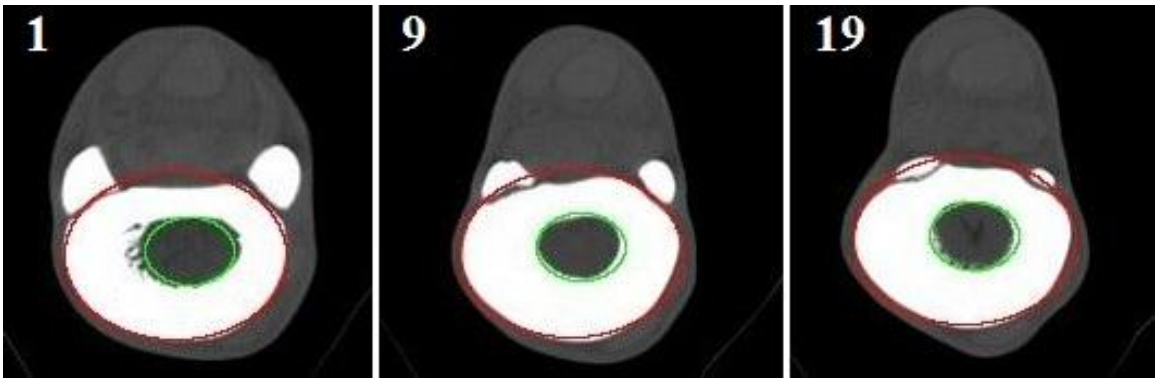

Figure 3.3 Illustration of the shape fitting used on computed tomography slices 1, 9 and 19 of the cortical diaphysis model. The ellipse size for the cortical outline (red) was 30 mm x 40 mm. The ellipse size used for the medullary cavity (green) was 12 mm x 16 mm.

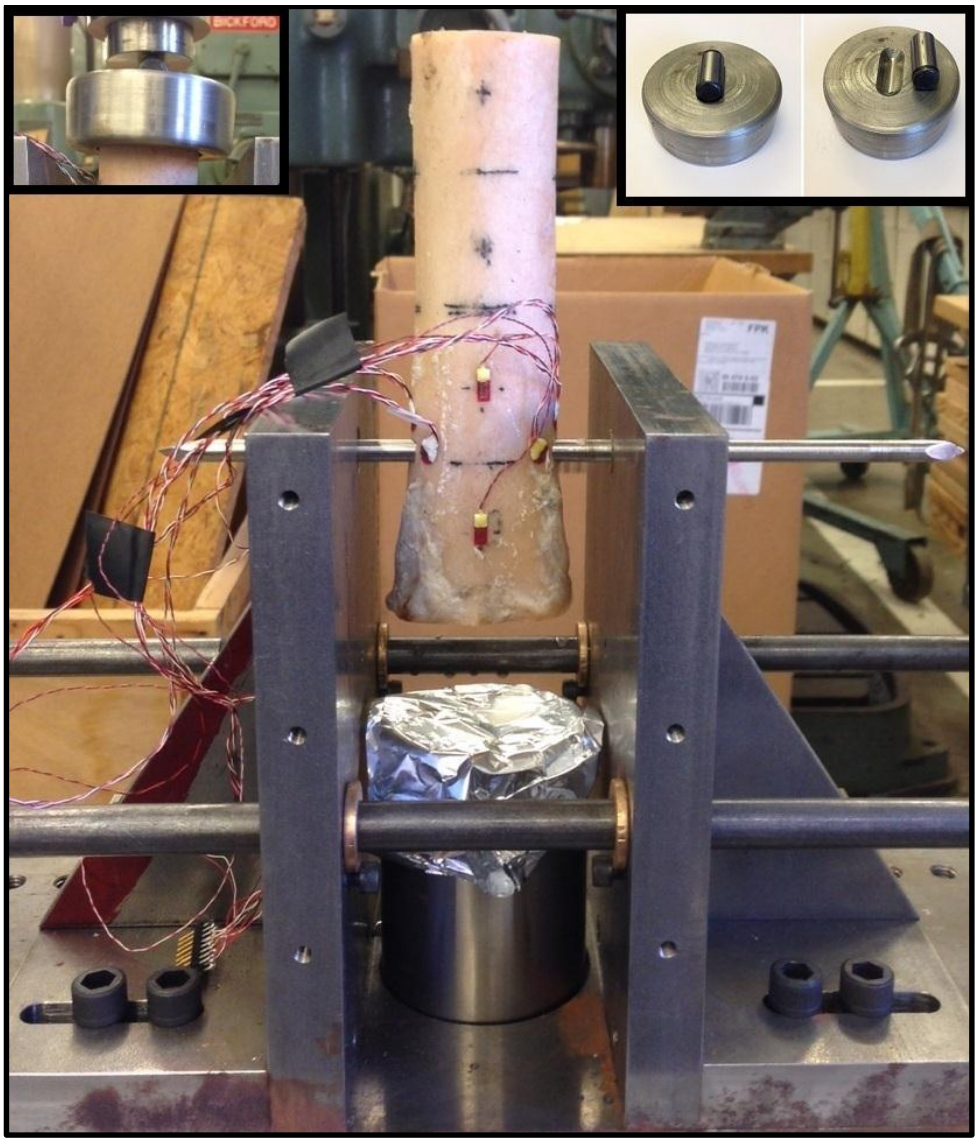

Figure 3.4 Photo of the custom jig used to perform axial compression testing. The bone and pin combination used for validation of the equine MC3 transfixation pin response under 3 separate loading conditions (2500 N, 5000 N and 7500 N) is pictured. The lateral side of the bone is on the left side of the image. Strain gauges are attached to the dorsal bone surface and around both the medial and lateral pin holes. The insets show the loading cap design (right) and positioning on the proximal bone surface (left) with the solid steel cylinder placed for even load transfer across the bone width from the material testing system load cell.

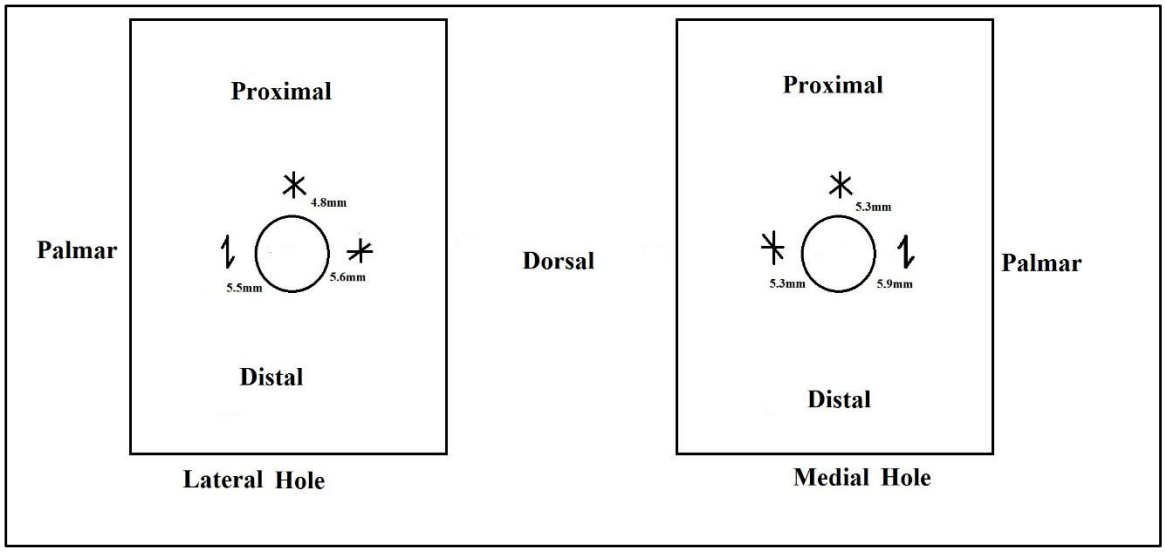

Figure 3.5 Diagram illustrating the positioning of rosette (*****) and single axis (|)strain gauges around the lateral and medial holes of the corticocancellous bone segment used for model validation. The actual measured distance from the center of the gauge to the hole margin is included for each gauge location.

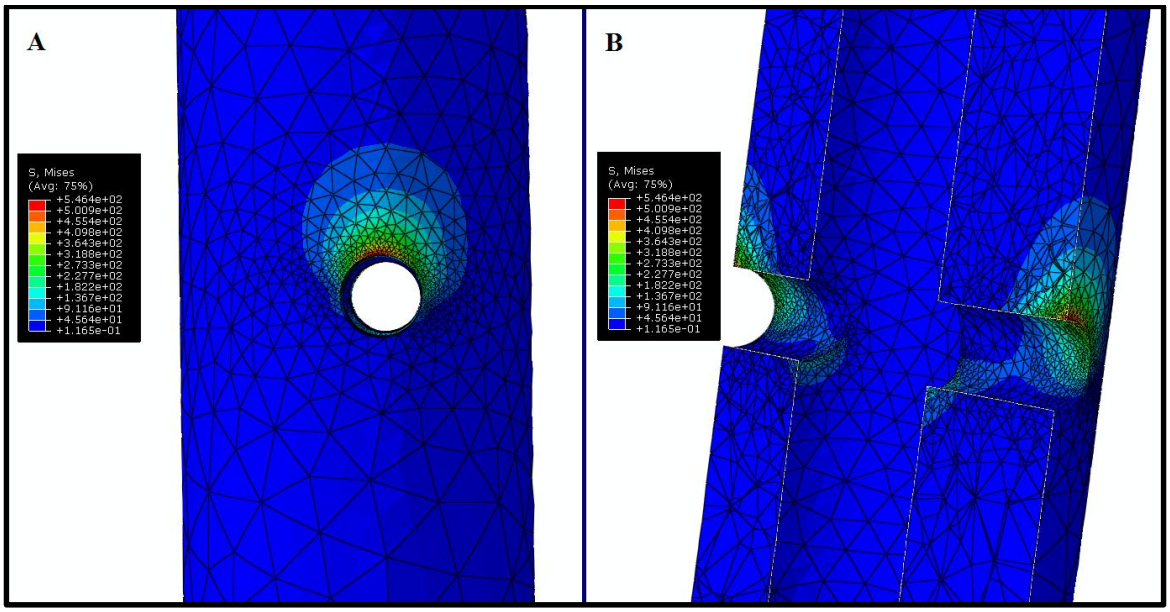

Figure 3.6 Representative images showing the pattern of von Mises stress distribution surrounding a single smooth pin within the cortical diaphysis model. Maximum von Mises stress is found at the proximal outer cortical margin of the pin hole. The legend shows the color scale used to display von Mises stress. A. View from the medial side of the bone directly at the medial pin hole. B. Sectioned view from the dorsal medial aspect of the bone showing the von Mises stress distribution within the medial and lateral cortices.

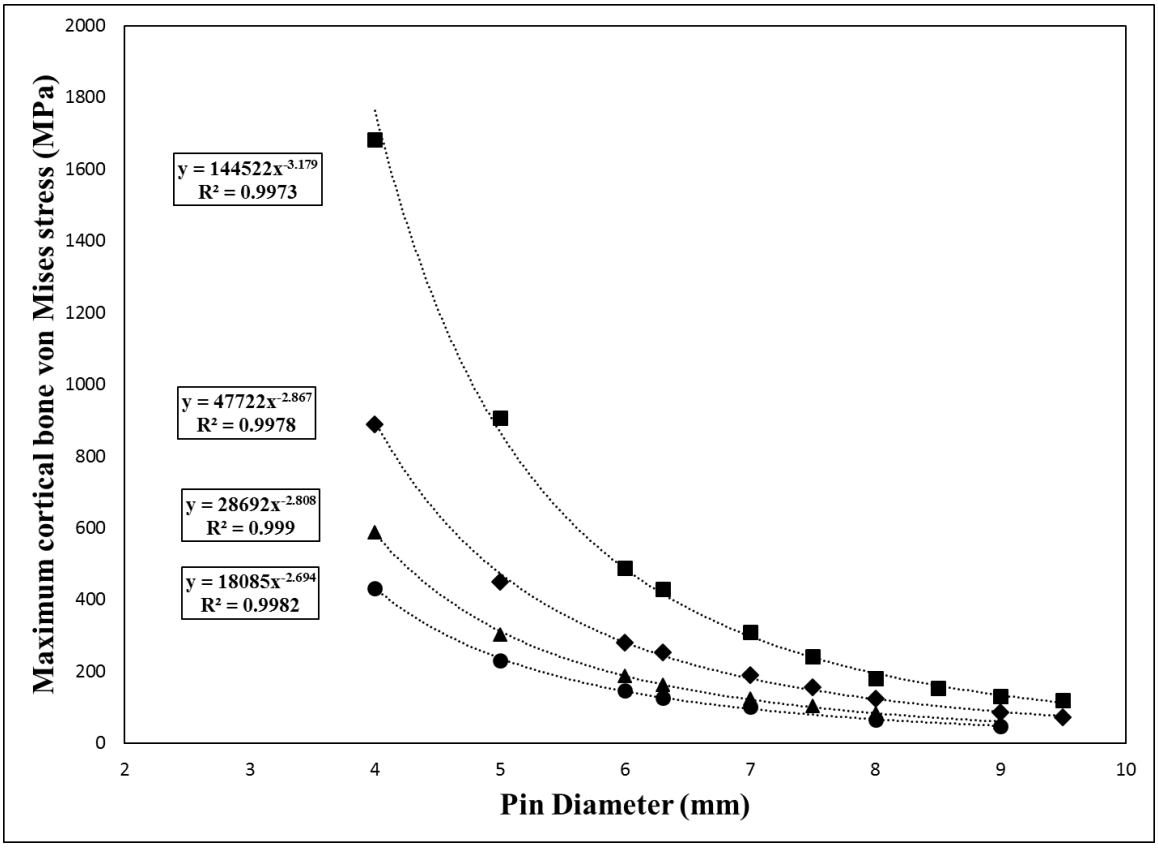

Figure 3.7 Pin diameter versus cortical bone von Mises stress for the cortical diaphysis model. Solid squares = 1 pin models; Solid diamonds = 2 pin models; Solid triangles = 3 pin models; Solid circles = 4 pin models. Fitted power law equations with associated R^2 value (Pearson product moment correlation coefficient) are shown for each pin number.

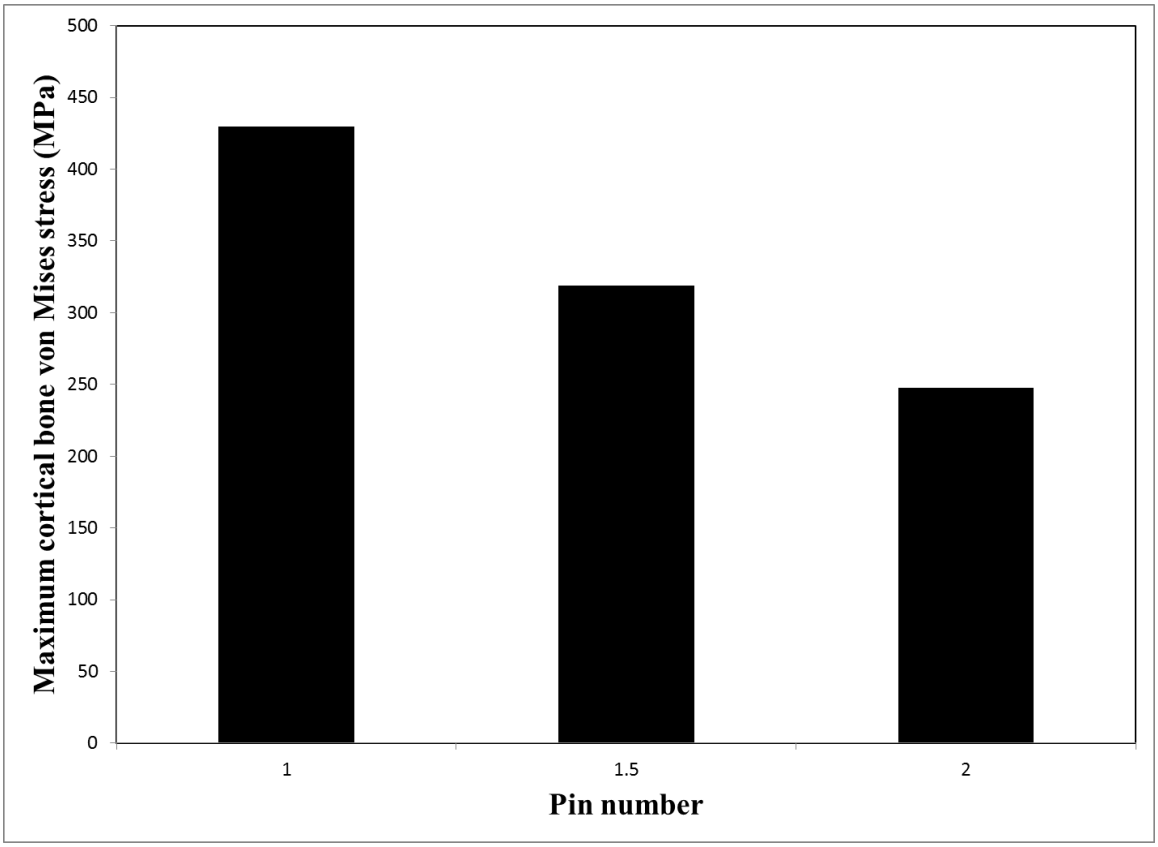

Figure 3.8 Maximum cortical bone von Mises stress for a one, one and a half, and two pin configuration in the cortical diaphysis model. The half pin configuration reduces the maximum von Mises stress value to approximately midway between a one and two pin configuration.

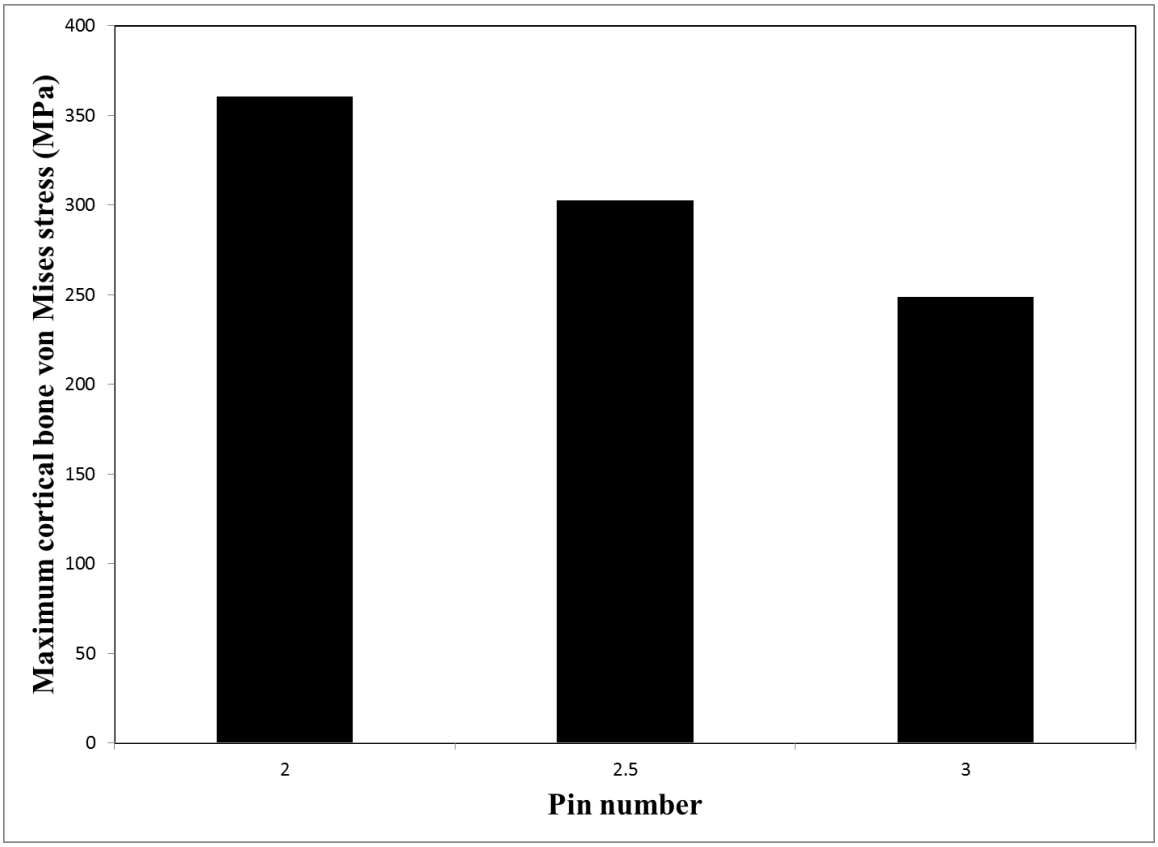

Figure 3.9 Maximum cortical bone von Mises stress for a two, two and a half, and three pin configuration in the corticocancellous bone model. The half pin configuration reduces the maximum von Mises stress value to approximately midway between a 2 and 3 pin configuration.

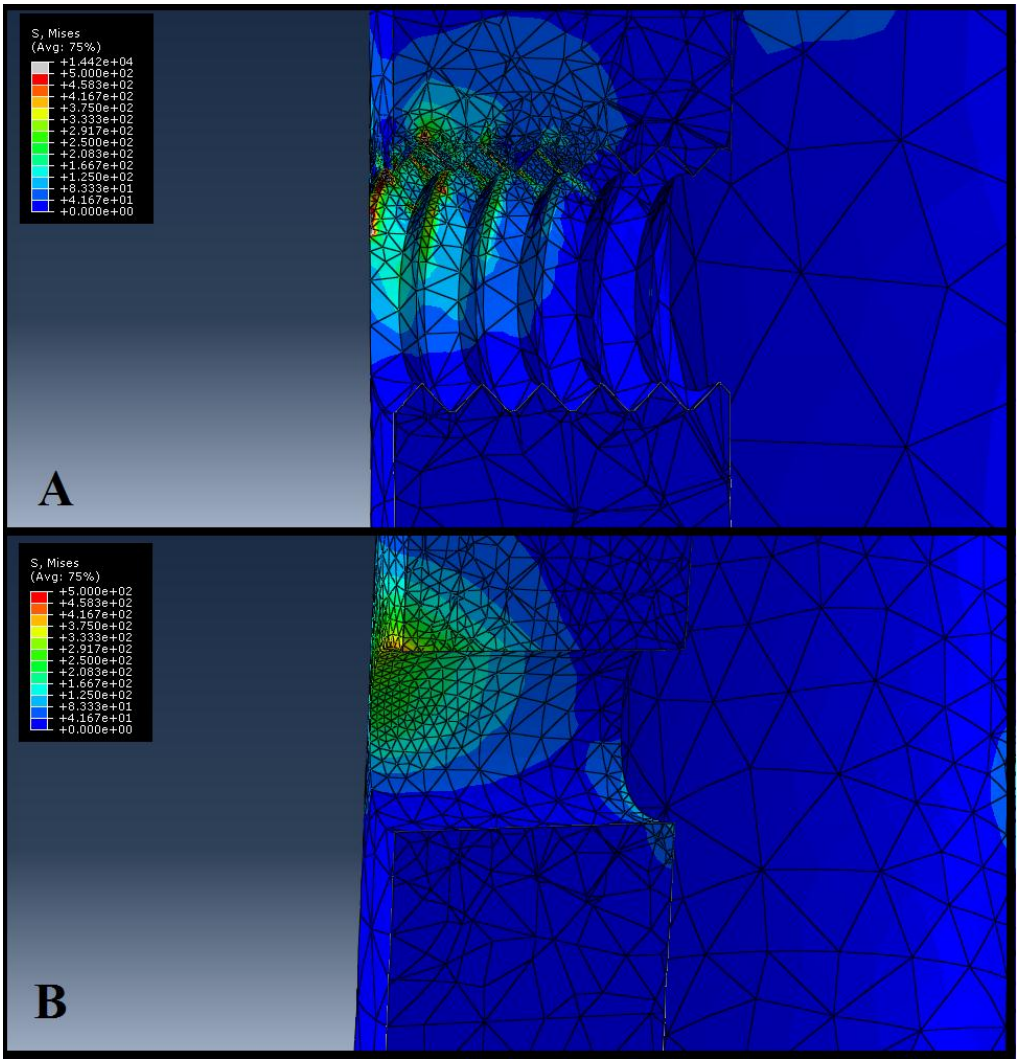

Figure 3.10 Illustration of the cortical bone von Mises stress in the threaded pin (A) compared to the smooth pin (B). The section is taken through the frontal plane of each bone model to show the stresses at the bone-pin interface. The pins have been removed from the view and only cortical bone is present. Large stress values at the trough of the threads are apparent in A, making direct comparison with the smooth pin stresses difficult.

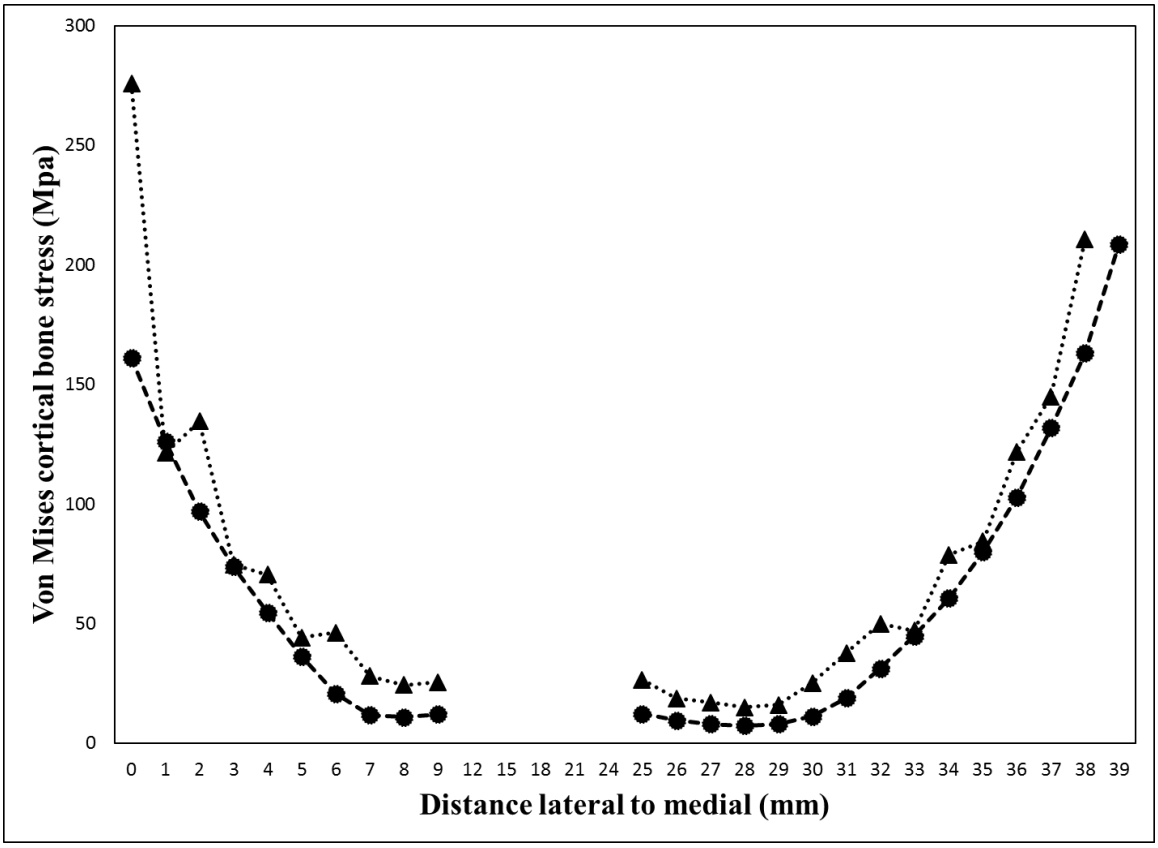

Figure 3.11 Comparison of the cortical bone von Mises stress from lateral to medial a distance of 1 mm from the pin (core). Threaded (solid diamonds and dotted line) and smooth (solid circles and dashed line) pin data are presented from the cortical diaphysis bone model.

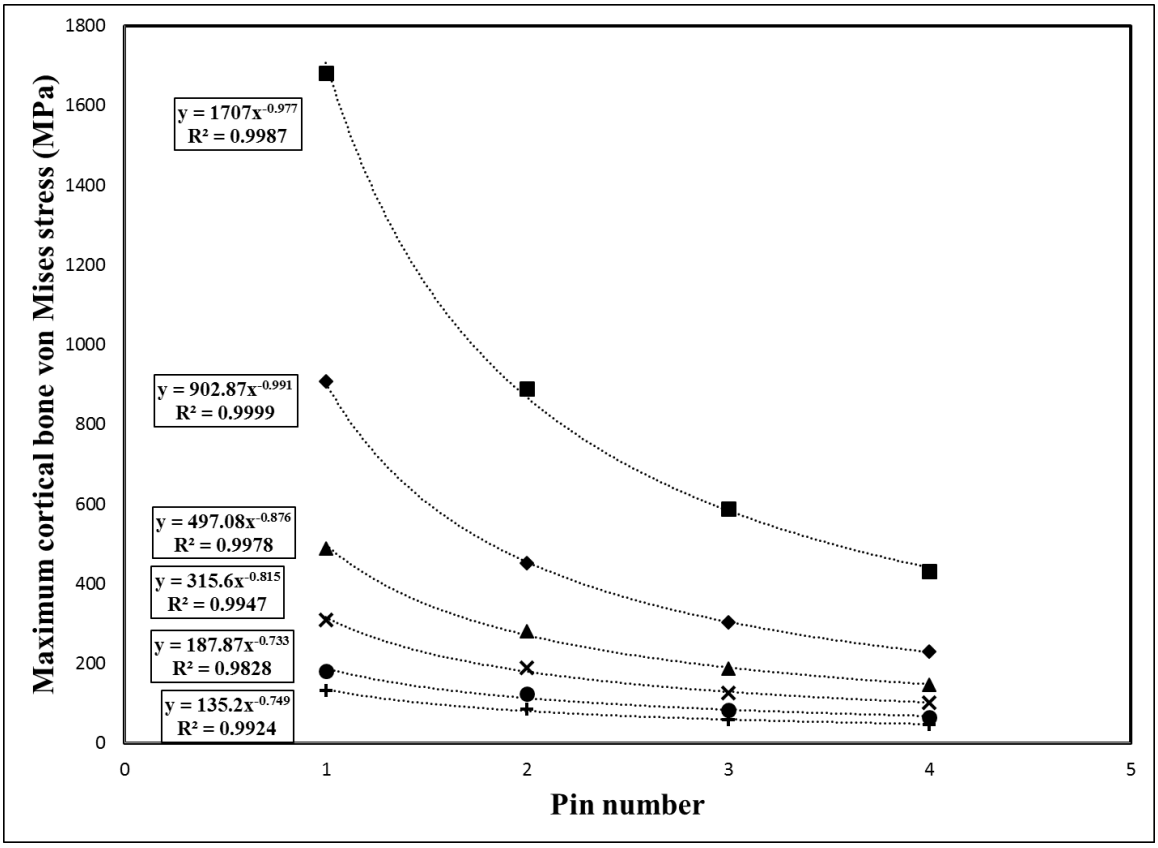

Figure 3.12 Pin number versus maximum cortical bone von Mises stress for the cortical diaphysis bone model. Solid squares = 4 mm pins; Solid diamonds = 5 mm pins; Solid triangles = 6 mm pins; Crosses = 7 mm pins; Solid circles = 8 mm pins; Plus signs = 9 mm pins. Fitted power law equations with associated R^2 value (Pearson product moment correlation coefficient) are shown for each pin size.

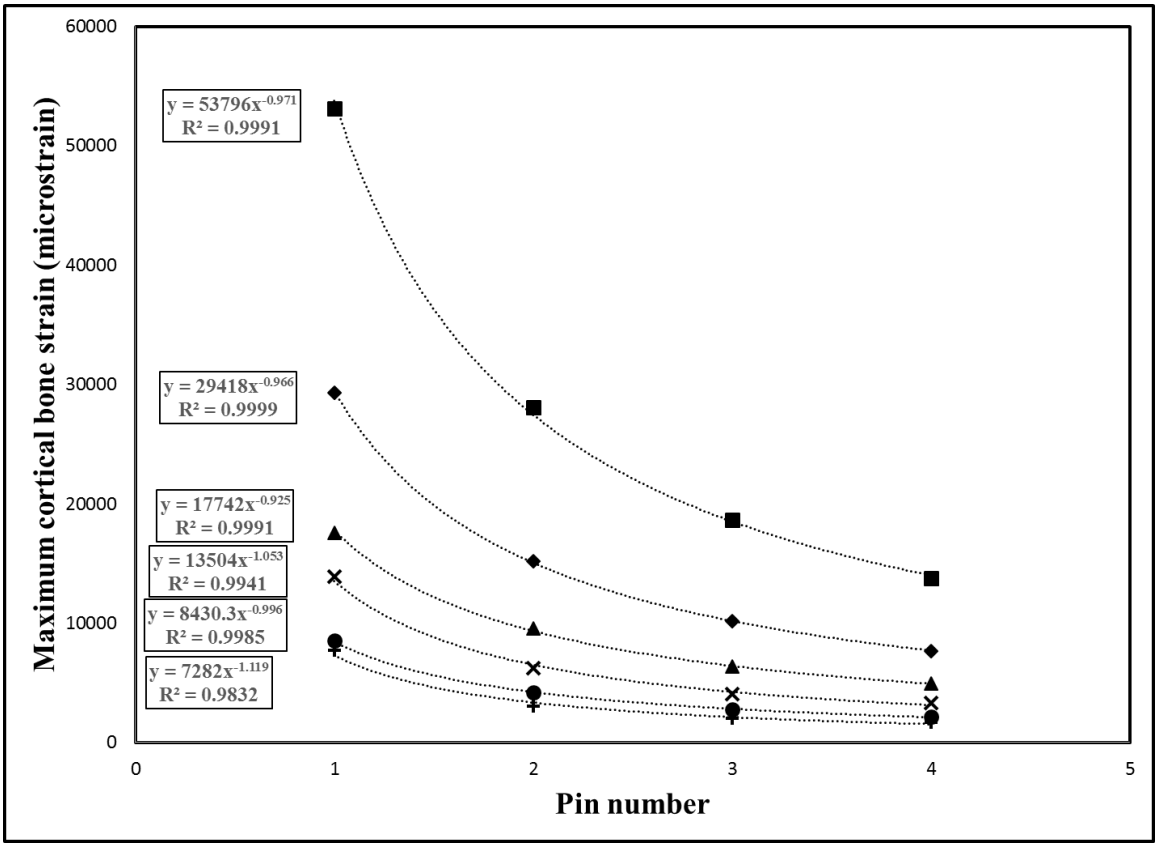

Figure 3.13 Pin number versus maximum cortical bone strain for the cortical diaphysis bone model. Solid squares = 4 mm pins; Solid diamonds = 5 mm pins; Solid triangles = 6 mm pins; Crosses = 7 mm pins; Solid circles = 8 mm pins; Plus signs = 9 mm pins. Fitted power law equations with associated R^2 value (Pearson product moment correlation coefficient) are shown for each pin diameter.

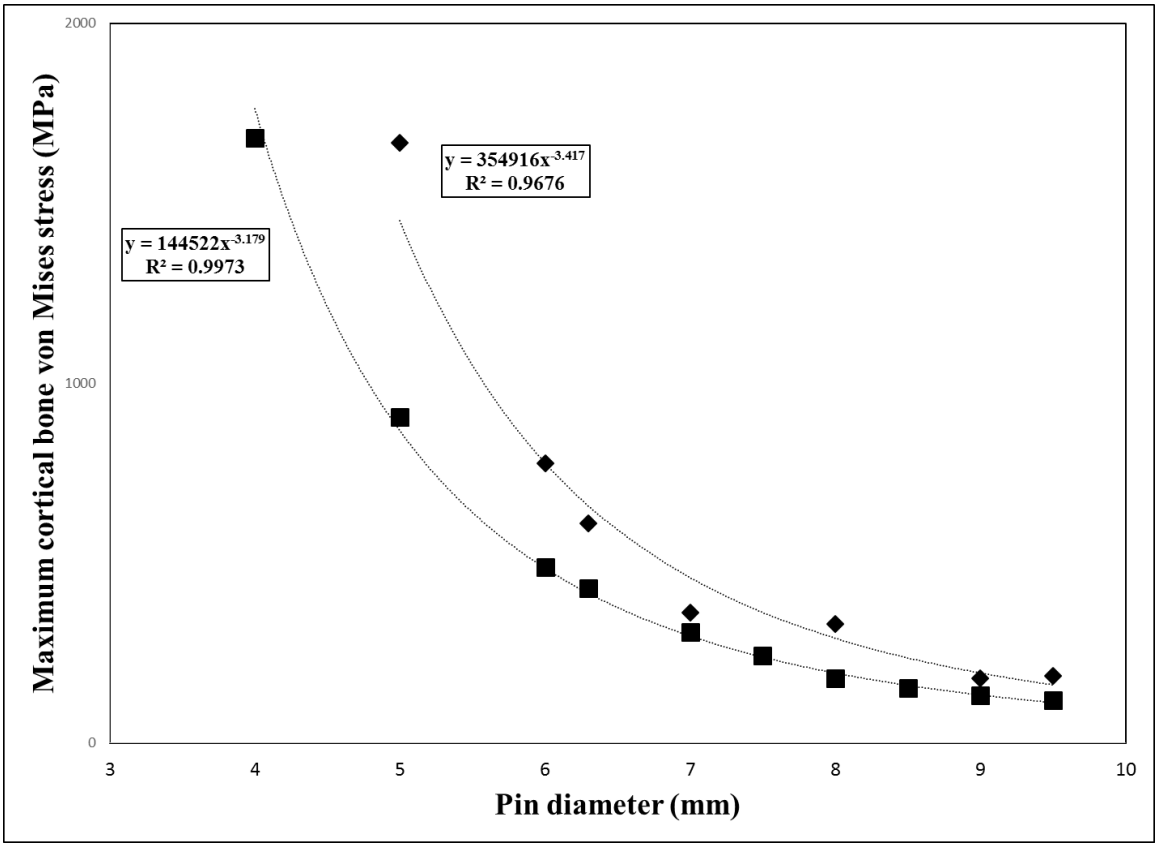

Figure 3.14 Pin diameter versus maximum cortical bone von Mises stress for single 6.3 mm pins in the cortical diaphysis bone model (solid squares) and the corticocancellous bone model (solid diamonds). Fitted power law equations with associated R^2 value (Pearson product moment correlation coefficient) are shown for each model over the range of pin diameters used.

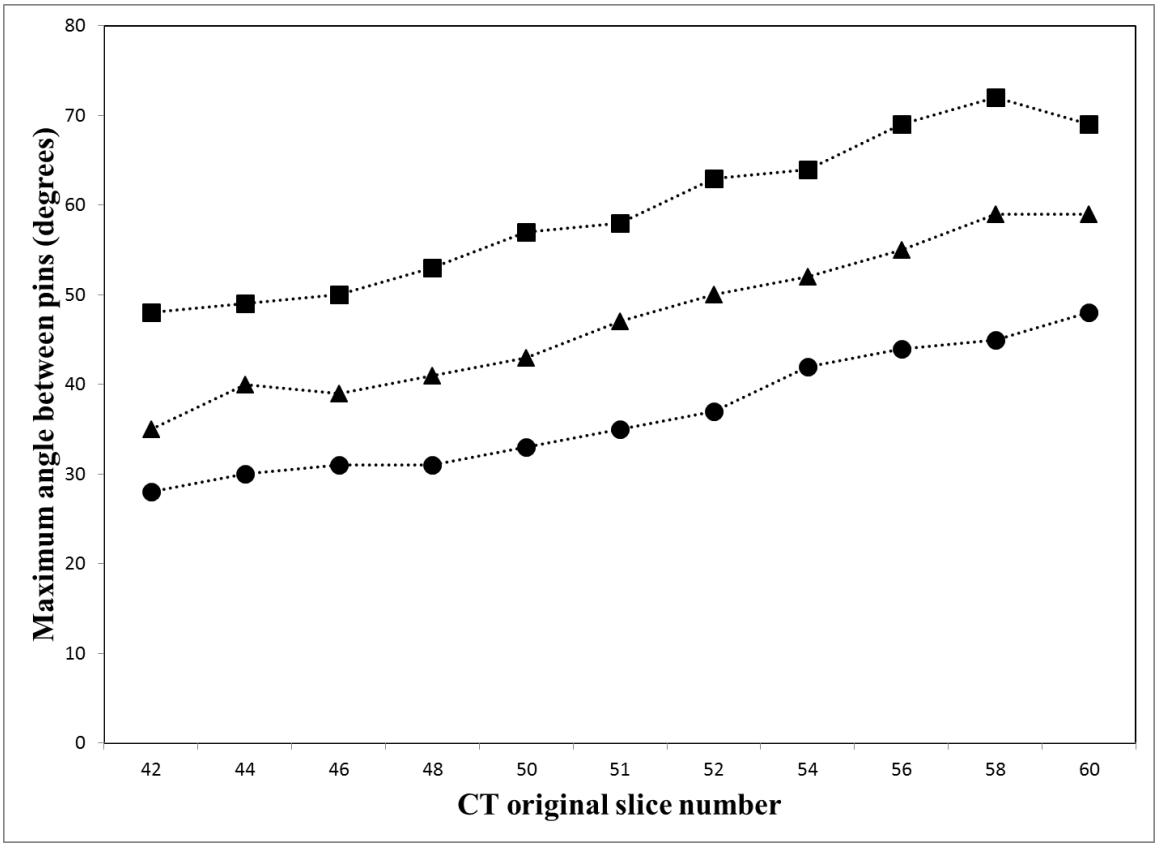

Figure 3.15 Computed tomography slice number of the cortical diaphysis model versus the maximum angle measured between pins positioned within the confines of the 2nd and 4th metacarpal bones and the dorsal cortex of the MC3 (refer to Figure 3.1). Solid squares = 4 mm pins; Solid triangles = 6 mm pins; Solid circles = 8 mm pins.

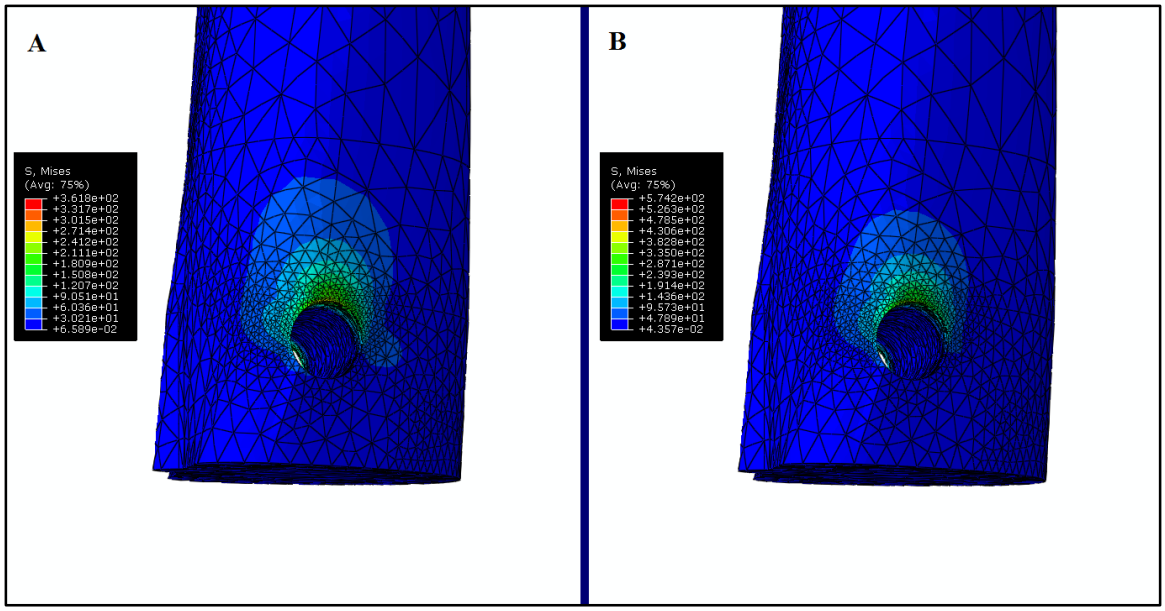

Figure 3.16 Representative image of the von Mises stress pattern observed around the pin hole located just proximal to the physeal scar in the corticocancellous bone model. The pins have been removed from the images to reveal the cortical bone stress pattern as seen from the surface. Dorsal is to the right and distal is down in each image. A. Single, 7 mm stainless steel pin model. B. Single, 7 mm titanium alloy pin model.

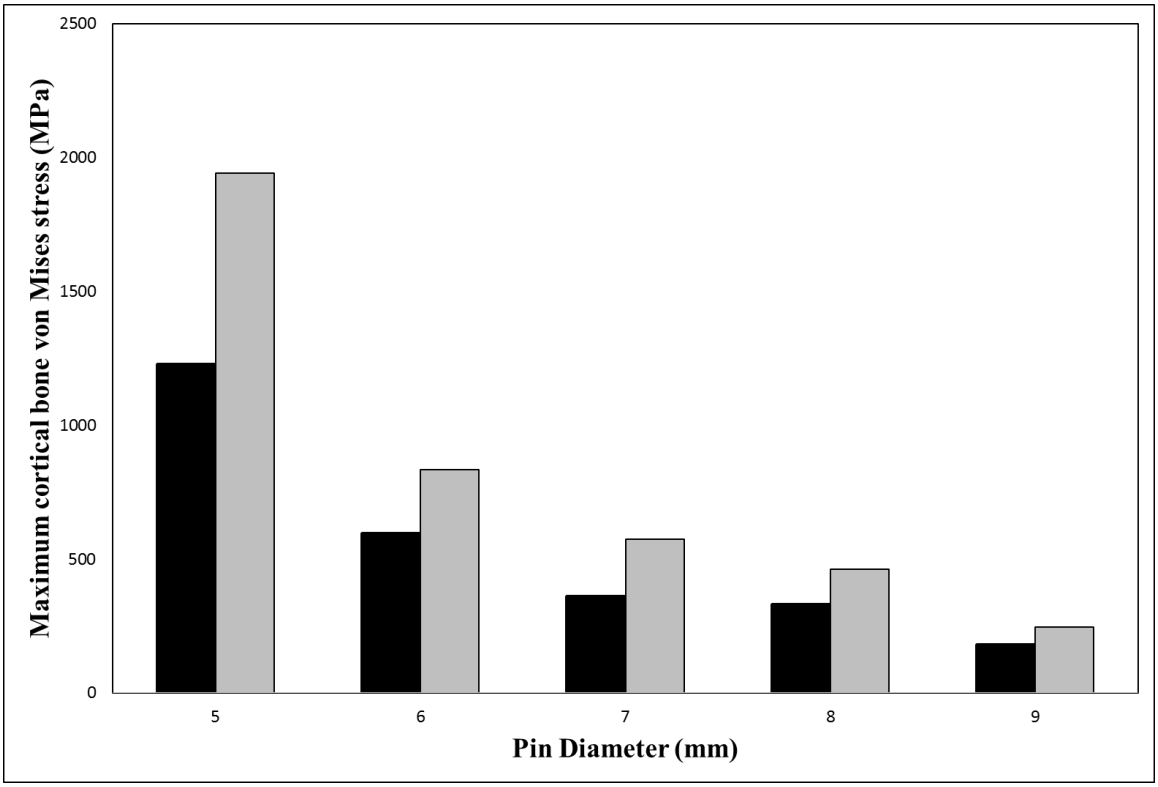

Figure 3.17 Pin diameter versus maximum cortical bone von Mises stress for stainless steel (black bars) and titanium alloy (grey bars) pins. Analysis was performed in the corticocancellous bone model using a single pin positioned at a distal metaphyseal location.

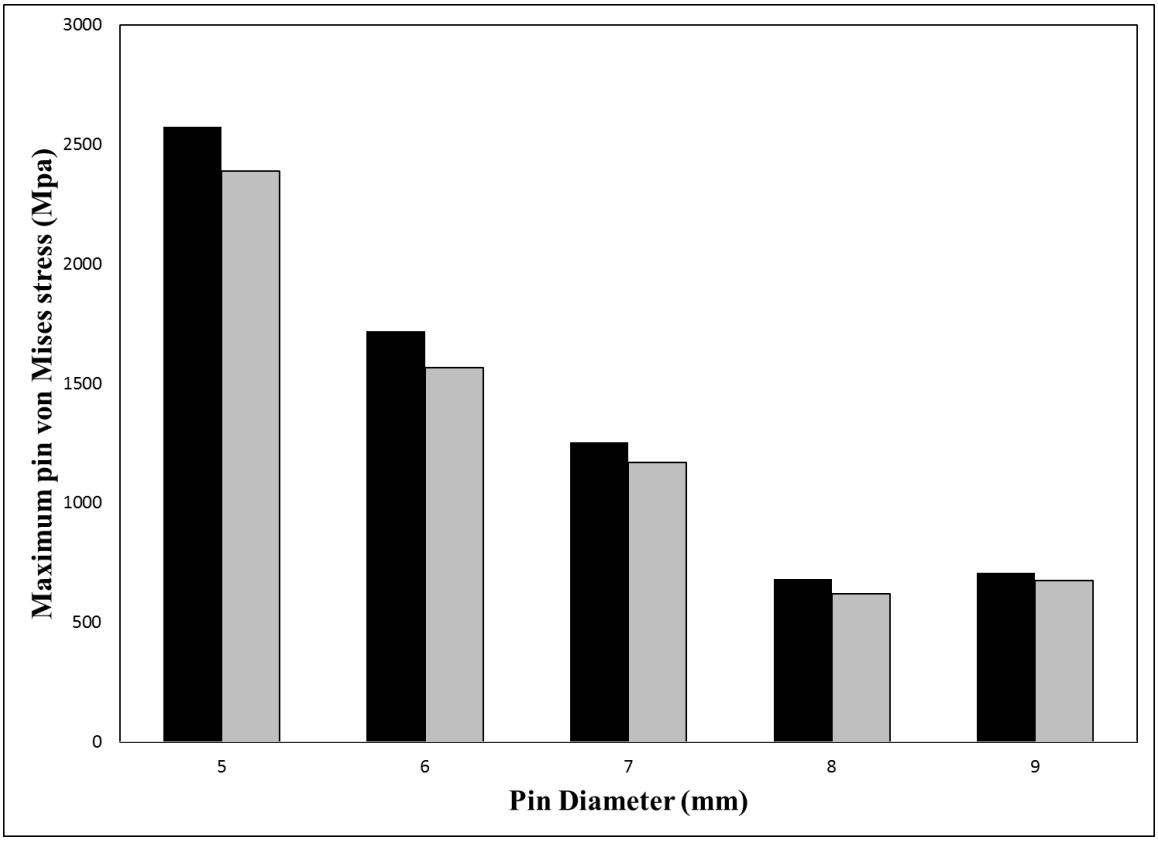

Figure 3.18 Pin diameter versus maximum pin von Mises stress for stainless steel (black bars) and titanium alloy (grey bars) pins. Analysis was performed in the corticocancellous bone model using a single pin positioned at a distal metaphyseal location.

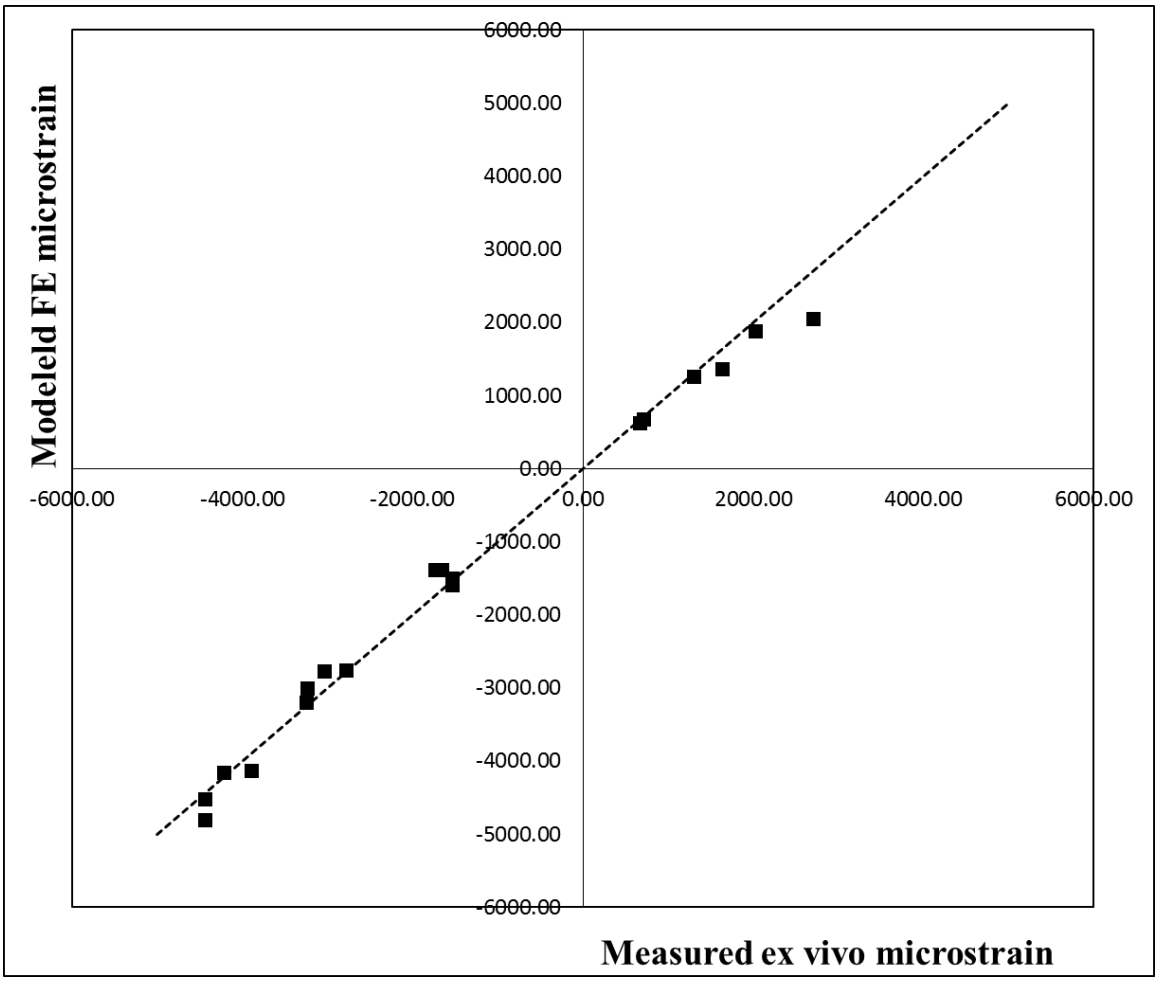

Figure 3.19 Graph showing the comparison of measured ex vivo strain compared to modeled FE strain in the corticocancellous model. Data for longitudinal strain, maximum and minimum principal strains at loading levels of 2500 N, 5000 N and 7,500 N are shown as individual points on the graph. The dashed line is a plot of x = y to illustrate where exact matching between measured and modeled values lies.

Table 3.1 Material properties of bone and metals used for FE modeling of transfixation pin combinations within the equine MC3.[51–54]

	Density (g/cm^3)	**Elastic modulus (GPa)**	**Poisson's ratio**
Cortical bone	2000	17	0.3
Cancellous bone	500	0.5	0.3
Stainless steel	8000	205	0.3
Titanium alloy	4430	114	0.34

Table 3.2 Von Mises stress, maximum principal stress, minimum principal stress, maximum principal strain and minimum principal strain observed in FE analysis using a cortical diaphysis bone model to evaluate pin diameter using one pin. VM = von Mises; MPa = megapascals; Pr. = principal; με = microstrain

Pin Diameter (mm)	Pin number	VM stress max (MPa)	Pr. stress max (MPa)	Pr stress min (MPa)	Pr strain max (με)	Pr strain min (με)
4	1	1682	654.6	-1396	53130	-90360
5	1	907.1	406.9	-740.3	29290	-48300
6	1	489.2	274.8	-382.9	17580	-25460
6.3	1	429.8	242.9	-338	15530	-22460
7	1	309.7	232.9	-251.3	13910	-16410
7.5	1	242.4	198.4	-194.6	11790	-12770
8	1	180.4	137.7	-136.6	8513	-9227
8.5	1	152.6	147.2	-120	8702	-7919
9	1	131.9	131.1	-93.6	7739	-6231
9.5	1	118.9	118.7	-75	6990	-5036

Table 3.3 Von Mises stress, maximum principal stress, minimum principal stress, maximum principal strain and minimum principal strain observed in FE analysis using a cortical diaphysis bone model to evaluate pin diameter using two pins. VM = von Mises; MPa = megapascals; Pr. = principal; με = microstrain.

Pin Diameter (mm)	Pin number	VM stress max (MPa)	Pr. stress max (MPa)	Pr stress min (MPa)	Pr strain max (με)	Pr strain min (με)
4	2	889.5	316	-733.3	28080	-47640
5	2	450.7	185	-356.5	15200	-23590
6	2	281.1	120.7	-220.6	9567	-14660
6.3	2	252.2	104.2	-199.2	8528	-13190
7	2	188.7	100.9	-154.3	6238	-10050
7.5	2	155.9	88.5	-127.5	5371	-8301
8	2	123.1	69.6	-100.1	4193	-6525
9	2	85.3	50.1	-69.7	3013	-4538
9.5	2	71.8	43.8	-58.3	2622	-3807

Table 3.4 Von Mises stress, maximum principal stress, minimum principal stress, maximum principal strain and minimum principal strain observed in FE analysis using a cortical diaphysis bone model to evaluate pin diameter using three pins. VM = von Mises; MPa = megapascals; Pr. = principal; με = microstrain.

Pin Diameter (mm)	Pin number	VM stress max (MPa)	Pr. stress max (MPa)	Pr stress min (MPa)	Pr strain max (με)	Pr strain min (με)
4	3	588.8	207.8	-484.9	18620	-31510
5	3	302.8	119.8	-240.6	10170	-15890
6	3	187.5	76.4	-148	6337	-9804
6.3	3	163.3	67.8	-128.9	5545	-8542
7	3	125.1	64.7	-103.3	4081	-6693
7.5	3	102.9	54	-84.6	3337	-5498
8	3	83.2	44.9	-68.2	2746	-4434
9	3	58.1	33	-47.3	2052	-3087

Table 3.5 Von Mises stress, maximum principal stress, minimum principal stress, maximum principal strain and minimum principal strain observed in FE analysis using a cortical diaphysis bone model to evaluate pin diameter using four pins. VM = von Mises; MPa = megapascals; Pr. = principal; με = microstrain.

Pin Diameter (mm)	Pin number	VM stress max (MPa)	Pr. stress max (MPa)	Pr stress min (MPa)	Pr strain max (με)	Pr strain min (με)
4	4	431.5	152.6	-352.7	13790	-23010
5	4	230.1	87.9	-183	7682	-12080
6	4	146.3	55.3	-115.8	4912	-7665
6.3	4	126.1	48.9	-99.8	4249	-6607
7	4	101.9	49.6	-84.2	3309	-5445
8	4	65.7	34.6	-54	2175	-3507
9	4	47.3	26.9	-38.8	1675	-2520

Table 3.6 Von Mises stress, maximum principal stress, minimum principal stress, maximum principal strain and minimum principal strain observed in FE analysis using a corticocancellous bone model for one pin placed in the metaphysis with pin diameter ranging from 5 mm to 9.5 mm. VM = von Mises; MPa = megapascals; Pr. = principal; με = microstrain.

Pin Diameter (mm)	**Pin number**	**VM stress max (MPa)**	**Pr. stress max (MPa)**	**Pr stress min (MPa)**	**Pr strain max (με)**	**Pr strain min (με)**
5	1	1669	433.6	-1940	32350	-104300
6	1	776.7	276.9	-871.7	16700	-47760
6.3	1	609.8	232.1	-716.4	13940	-37400
7	1	361.8	170.1	-331.7	10910	-20320
8	1	330.6	129.6	-380.7	7666	-20190
9	1	179.2	97.5	-163.2	6000	-9986
9.5	1	186.2	87.6	-177.7	5287	-10690

Table 3.7 Effect of pin orientation within 2 and 3 pin models on von Mises stress, maximum principal stress, minimum principal stress, maximum principal strain and minimum principal strain observed in FE analysis using a cortical diaphysis bone model. VM = von Mises; MPa = megapascals; Pr. = principal; με = microstrain.

Pin orientation	**Pin diameter (mm)**	**Pin number**	**VM stress max (MPa)**	**Pr stress max (MPa)**	**Pr stress min (MPa)**	**Pr strain max (με)**	**Pr strain min (με)**
Inline	6.3	2	247.7	108.8	-194.4	8450	-12920
Offset positive	6.3	2	243.4	127.7	-206.6	8283	-13180
Offset negative	6.3	2	246.3	130.6	-207.6	8475	-13260
Inline	6.3	3	163.3	67.8	-128.9	5545	-8542
Offset positive	6.3	3	166.3	83.5	-140.2	5620	-8989
Offset negative	6.3	3	164.6	84.8	-137.9	5664	-8807

Table 3.8 Effect of pin orientation within 3, 4 and 6 pin models on von Mises stress, maximum principal stress, minimum principal stress, maximum principal strain and minimum principal strain observed in FE analysis using a corticocancellous bone model. VM = von Mises; MPa = megapascals; Pr. = principal; με = microstrain.

Pin orientation	**Pin diameter (mm)**	**Pin number**	**VM Max (MPa)**	**Princ S Max (MPa)**	**Princ S Min (MPa)**	**Princ LE max (με)**	**Princ LE min (με)**
Inline	7	3	134.7	69.3	-118.7	4762	-7331
Offset positive	7	3	141.7	72.9	-127	4687	-7820
Offset negative	7	3	136.3	70.3	-125.7	4391	-7654
Inline	7	4	115.1	49	-95.8	3722	-6170
Offset positive	7	4	116.6	50.2	-96.5	3739	-6236
Offset negative	7	4	121.8	50	-100.8	3911	-6514
Inline	5.5	6	144.8	58.1	-115.5	4834	-7617
Offset positive	5.5	6	145.6	64	-128.4	4609	-7928
Offset negative	5.5	6	140.1	60.9	-119.1	4579	-7615

Table 3.9 Comparison of measured (ex vivo) and modeled (FEM) values for longitudinal strain, maximum principal strain and minimum principal strain for the corticocancellous bone model (CC model) and longitudinal strain for the cortical diaphysis model (CD model). Values for principal strains were calculated using rosette gauge readings obtained proximal to the pin hole on both lateral and medial sides of the bone. Longitudinal strains were measured directly during loading. N = Newtons με = microstrain.

		Lateral hole			**Medial hole**		
CC model	**Load (N)**	**2500**	**5000**	**7500**	**2500**	**5000**	**7500**
Longitudial	**Ex vivo**	-1539	-3239	-4436	-1656	-2788	-3895
strain (με)	**FEM**	-1502	-3008	-4515	-1376	-2751	-4131
	% Difference	*2.4*	*7.2*	*1.8*	*16.9*	*1.3*	*6.1*
Maximum	**Ex vivo**	713	1640	2703	662	1302	2029
principal	**FEM**	685	1370	2055	629	1256	1882
strain (με)	***% Difference***	*3.9*	*16.5*	*23.9*	*4.9*	*3.6*	*7.3*
Minimum	**Ex vivo**	-1540	-3246	-4440	-1734	-3043	-4216
principal	**FEM**	-1593	-3194	-4803	-1383	-2766	-4153
strain (με)	***% Difference***	*3.4*	*1.6*	*8.2*	*20.2*	*9.1*	*1.5*
CD model	**Load (N)**	**2500**	**5000**	**7500**	**2500**	**5000**	**7500**
Longitudial	**Ex vivo**	-414	-997	-2004	-1777	-3309	-4359
strain (με)	**FEM**	-1109	-2183	-3225	-1161	-2285	-3381
	% Difference	*63.0*	*54.0*	*38.0*	*35.0*	*31.0*	*22.0*

CHAPTER 4. A THEORETICAL APPROACH FOR TRANSCORTICAL PIN SELECTION IN TRANSFIXATION CASTING BASED ON THE EQUINE THIRD METACARPAL BONE

4.1 Introduction

Equine transfixation casting has been used for the management of a variety of distal limb fractures in the horse.[1–7] However, complications associated with the transcortical pins and the pin holes contribute to its morbidity and mortality[1,2] and continue to negatively impact equine surgeons' confidence in using this fixation method clinically.[8] A majority of these treatment complications reflect bone failure at the **bone-pin interface (BPI)**, either acutely in the form of secondary pin hole fracture or chronically in the form of pin loosening due to local bone resorption. Analysis of 5 recent studies,[1,2,4,7,8] where equine distal limb fractures were treated using the transfixation cast technique, revealed that 21 out of a total of 77 horses were euthanized during treatment. Eight of the 21 euthanized horses (38%) suffered a secondary pin hole fracture while an additional 2 horses were euthanized for reasons directly related to the transfixation cast technique. In addition to the mortality associated with these treatment complications, the morbidity associated with transfixation casting is primarily related to loosening of the transcortical pins.[1] While it is a simplification of the problem to state that most treatment complications reflect mechanical bone failure at the BPI, as it does not account for the clinical and biological factors that also contribute, it does provide a basis for determining where enhancements in the safety and reliability of transfixation casting may be achieved. Improvements in the success of treating distal limb fractures using the transfixation cast technique require a reduction in the complications associated with the transcortical pins and pin holes.

Bone material failure occurs after the yield stress (strain) for the tissue has been reached or exceeded.[9–11] In the horse, it has been shown that bone failure often occurs soon after or even at the yield point and that this brittle post-yield behavior is more likely in bone with a higher density and elastic modulus.[9] In addition, bone microdamage in the form of microcracking has been shown to occur at the onset of yielding,[12] and results in osteocyte apoptosis and a cascade of signaling events leading to osteoclast recruitment and local bone resorption.[13–16] Reducing BPI stresses below the yield threshold of equine cortical bone should reduce local bone failure and complications associated with transcortical pins and pin holes. The majority of the stress present at the BPI of a transfixation cast, or external fixator, is attributable to the bending moment placed on the pin itself rather than the transverse load applied directly from the bone through the pin. Reduced pin bending results in lower BPI stresses.[17–19] The pin bending moment is a function of the load applied to the pin and the distance from the pin end (the cast connection) to the point where the pin enters the outer bone cortex, also known as the pin working length.[17,18] The ability of a pin to resist bending is related to the properties of the pin material (elastic modulus) and the **pin area moment of inertia (PAMi)**,[17,18] which is proportional to the pin diameter raised to the fourth power. As a result, a larger pin resists bending better than a smaller pin and is expected to result in substantially lower BPI stresses.[17–19] However, the relative size of the pin hole in the bone has been shown to be related to a loss of bone strength.[20–24]

The mechanical advantage of a larger pin diameter must be balanced with the loss of bone strength and increased risk of bone failure through the pin hole. Any bone defect has the potential to reduce bone strength through a stress concentration effect,[25] however, multiple investigations have shown that residual bone strength following drilling is inversely related to the size of the defect.[20–22,26] There have been 2 parameters used to characterize the relative defect size in a bone. The ratio of hole diameter to bone diameter, a 1 dimensional measurement, and the area fraction reduction calculated from the bone cross section area before and after hole creation, a 2 dimensional measurement. The selection of pin diameter and number for equine external fixation has previously been

based on recommendations on the use of external skeletal fixation in small animal and human patients.[22,27–29] Those recommendations have been to use a pin diameter that is approximately 20 - 25% of the width of the bone. This corresponds to a hole to bone diameter ratio of 0.2 to 0.25. Additional recommendations include using at least 3 pins positioned either side of the fracture whenever possible. Early attempts at equine external fixation utilized commercially available human systems which had insufficient strength to withstand weight bearing in the adult horse.[30] Subsequently, a custom designed equine external skeletal fixation device was developed by Nunamaker and colleagues in an attempt to overcome these early failures and allow immediate weight bearing in an adult horse.[30] The initial device used a foot plate below the hoof and 3 centrally threaded 9.6 mm diameter transcortical pins above the fracture to stabilize the limb. This diameter of pin is approximately 30-33% of the dorsal-palmar width of the equine **third metacarpal bone (MC3)**, corresponding to a hole to bone diameter ratio of 0.3 to 0.33.[23] The hole size required for this diameter pin has been shown to reduce the yield and failure torque of the MC3. Bone failure in torsion occurred at the yield point with no post-yield plastic deformation.[23] A high rate of secondary pin hole fractures in the early clinical reports using this device resulted in the introduction of a smaller 7.9 mm diameter pin and a modification which utilized a tapered pin-sleeve between the bone and the sidebar to reduce the effective bending moment of the pin.[19,31] Transfixation casting in the adult horse typically utilizes 2 or 3 threaded 6.35 mm diameter transcortical pins. It is possible to utilize a smaller diameter pin because the pin working length present in a transfixation cast is less than the external skeletal fixation device.[30,32] The rate of secondary pin hole fractures reported clinically is lower for transfixation casts than for the equine external fixation device although it is still unacceptably high at approximately 15%.[1,2,4,7,8]

Previous studies on the mechanical behavior of external fixation pins and fixators have shown that the number of pins and the number of connecting rods in the fixation has an inverse relationship with BPI stress.[17,18] It is unknown how the cast connection between pins of a transfixation cast compares mechanically to a set number of connecting rods. Fiberglass casting material has been reported to have an elastic modulus of 316 MPa,

whereas connecting rods are considerably stiffer, with an elastic modulus similar to transcortical pins at approximately 200 GPa.[17,18,33] However, casting material is located closer to the bone and is continuous between each pin compared to connecting rods which require clamps to connect between pins and must have a finite number of connections within the fixator system. A cast also limits bending forces in the bone directly, an effect that is not present with an external skeletal fixator aside from the influence of the pins through the BPI. The pin diameter has the greatest influence on BPI stress through both a direct linear effect attributable to the available bearing surface of the pin and the more substantial effect of the fourth power relationship associated with the pin area moment.[18] Considering these relationships between pin diameter, pin number and their connections, and BPI stress, and the historical problems of secondary pin hole fracture, in theory, a larger number of small pins could be used in place of a small number of large pins to achieve the same BPI stress if an equivalent resistance to bending is present between those two pin configurations. Given the previously reported high rate of complications when large transcortical pins are used in the horse, determining a combination of pin diameter and number that minimizes both the BPI stress and strain, and the pin hole size required for pin placement, could, in theory, result in an alternative approach to pin selection for transfixation casting in the horse. In support of this approach, a previous investigation of the effect of pin hole size and number in the equine radius found that a larger hole size significantly reduced torsional strength of the bone, whereas an increase in hole number from 1 to 3 to 6 holes did not reduce torsional strength significantly.[24] Similarly, in sheep femora, increasing the hole size significantly reduced torsional strength of the bone although increasing the hole number from 3 to 4 holes had no significant weakening effect.[34] These studies suggest that the bone weakening effect of hole diameter may be more important than the potential weakening effect of a greater number of holes.

In the previous chapter, an FE model of the equine MC3 was developed in which analysis of the effect of different pin diameter and number combinations, as well as other pin parameters, on the predicted stress in the bone surrounding the pin during weight bearing

was performed. A compressive yield strain of -1% and a tensile yield strain of 0.5% were selected as threshold values based on cyclic loading studies of the equine MC3.[35,36] Values below these thresholds for a specific pin diameter and number combination was designated as being a preferred candidate for further ex vivo and in vivo testing based on the parameters considered. Consistent with previous investigations, the finite element models of the equine MC3 used in this work showed that peak bone stress is related to the total pin number and diameter of the pin in the bone.[17,18] Maximum bone strain at the BPI was also influenced by pin diameter and pin number. It was shown that as both the number of pins and the diameter of the pins increased, the strain around each pin during loading decreased.

Considering these previous findings, and the desire to develop pin selection guidelines specifically for the transfixation cast technique, a continued exploration of the relationship between pin diameter and pin number in determining the maximum bone strain surrounding the pins was undertaken. In addition, the relationship between the amount of bone removed when placing transfixation pins and the resultant bone strain during loading was examined. The previously used methods of estimating the impact of hole size on bone strength have been the 1 dimensional ratio hole diameter to bone diameter, and the 2 dimensional parameter bone area fraction reduction. Bone volume removed is a 3 dimensional parameter and in theory more closely reflects the full impact of hole size and number on the bone. The other parameters are essentially estimates of the bone volume removed relative to the bone size and are geometrically related to bone volume removed. Therefore, the aim of this study was to develop a general theory for pin selection in equine transfixation casting that does not exceed a set threshold of peak bone strain surrounding pin holes while minimizing the amount of bone to be removed when placing transfixation pins. A secondary aim was to compare the 3 estimates of bone removal based on their different dimensionality and ease of measurement. Finally, we compared the general theory to previously developed guidelines for determining the compressive bone stress present around the pins of external fixators.[17,18] The first specific objective of this study was to examine the relationship between pin diameter, pin number,

and the predicted bone strain surrounding the pin hole using FE models of the equine MC3. To achieve this, we used the total sum of the PAMi for all pin ends engaging the cast to represent the total resistance to bending of each specific bone pin construct. This approach combined the effect of pin number, pin diameter and the cast into a single parameter for comparisons. The second objective of this study was to use this relationship to determine whether an optimal pin configuration can be predicted that results in maximum BPI strains below set bone yield threshold values while minimizing the volume of cortical bone to be removed during pin insertion. The third objective of this study was to develop a general theoretical approach for determining preferred transcortical pin configurations by examining cortical width, bone width and cortical area fraction at each pin site to determine specific bone parameters or guidelines that may be used to predict an optimal pin configuration that may be applied beyond MC3. We compared our results to a previously developed parametric model of the bone compressive stress predicted during external fixation.

4.2 Materials and Methods

4.2.1 Study design

A previously validated FE model of the equine distal limb transfixation cast was used to construct a series of individual pin configurations within the MC3 from which the parameters of interest were examined. Pin configurations from the previous study were expanded upon to include different pin diameter combinations within the same bone model. Data for maximum cortical bone von Mises stress, maximum and minimum cortical bone principal stress and strain, maximum pin von Mises stress, volume of bone removed and volume of cortical bone removed from each model were recorded. In addition, for each pin in each model, the dorsal-palmar bone diameter, the pin diameter, and the cortical cross sectional area and pin cross sectional area through the cortex were determined. Relationships between the parameters of interest and the output variables were plotted and examined visually. The influence of pin number and pin diameter on the

ability of a constructed model to resist load was combined to create the composite parameter, total PAMi. This was calculated as the sum of the PAMi for each pin end fixed within the construct. In addition to the volume of cortical bone removed, the volume of bone removed, the ratio of pin diameter to dorsal-palmar bone diameter at the specific pin locations and their maximum and mean value, and the cortical area fraction and the pin area fraction for each pin location and their minimum and mean value were calculated for each model. The cortical area fraction was defined as the area of cortical bone cross section remaining following pin insertion divided by the initial cortical bone cross section area through the center of the pin. The pin area fraction was defined as the pin cross sectional area removed divided by the initial cortical bone cross sectional area **(Table 4.1)**.

4.2.2 Finite element model

A model of the equine MC3 was constructed within an FE software program (Abaqus, v.6.12, Dassault Systemes Simulia Corp, RI, USA) to contain both cortical and cancellous segments of the distal 70% (diaphysis and metaphysis) of the bone. The x-axis represented the medial to lateral direction across the bone, the y-axis represented the dorsal to palmar direction and the z-axis the proximal to distal or longitudinal direction of the bone. This process was described in the previous chapter in detail, however, in brief, the geometry of the MC3 of a 10 year old Quarter Horse gelding was constructed using extrusion of specific 2-dimensional cross sections to create a 3-dimensional solid model of the bone. A computed tomography scan of the limb performed using a 64 slice helical scanner (Lightspeed VCT, General Electric, Milwaukee, WI) at a slice thickness of 3.75 mm was used to provide cross sectional images from which the dimensions of the cortical and cancellous portions of the bone were characterized and reproduced within the FE software program. Smooth transfixation pins from 4 mm to 9.5 mm were constructed to be 70 mm in length by similar solid extrusion. Pins were positioned within the bone model and pin holes were created using Boolean operations. A 7500 N distributed axial compressive load was applied to the proximal surface of the bone to simulate an adult

horse walking with the transfixation cast in place. This load and distribution approximates the in vivo mid-diaphyseal surface strains of the MC3 when applied during ex vivo testing.[37] The elastic modulus used for the cortical bone was 17 GPa[38,39] and the density used was 2000 g/cm^3.[40] The cancellous portion of the bone model had an elastic modulus of 0.5 GPa and a density of 500 g/cm^3. Stainless steel pins were used in all models evaluated in this study and an elastic modulus of 205 GPa and a density of 8,000 g/cm^3 was used.[41–43] Automated free meshing algorithms were used for all meshing procedures. All models were meshed using solid quadratic tetrahedral elements (C3D10I) that are formulated for improved surface stress predictions. Adaptive remeshing was performed to refine the mesh for each individual model based upon the output variable von Mises stress. Remeshing was continued until there was a maximum of 2% change in von Mises stress when compared to the previous mesh. The cast-pin attachment was represented by a boundary condition at the end of the pins and was restrained in all 3 axes.[44] All models were evaluated under conditions that would simulate a complete, unstable fracture distal to the MC3 by keeping the distal end of the bone unrestrained in the longitudinal direction (z-axis). Both the lateral to medial (x-axis) and dorsal to palmar (y-axis) directions were restrained to prevent rotation around the pin during loading with single pin models. This was maintained for all models since the primary loading component of the MC3 is axial compression.[45] Non-linear surface to surface contact stiffness was used at the BPI which allows separation of surfaces after contact, sliding between surfaces and prevents overclosure of surfaces under pressure. These conditions were considered representative of the BPI immediately after pin insertion. Global seeds were set for the creation of each mesh, with initial approximate element size ranging from 4 to 6 mm. A virtual topology feature was used prior to meshing to combine faces of the more complex geometries, allowing a smoother mesh to be created during the final meshing procedure.

4.2.3 Data analysis

Data for maximum von Mises stress, maximum and minimum cortical bone stress and strain, maximum pin von Mises stress, bone volume removed and cortical bone volume removed were recorded from each model constructed. Cortical thickness at each pin location in each model was measured and recorded. The equation for the area of an ellipse was used to calculate the total bone cross section area from the dimensions of the outer cortical diameters from both medial to lateral and dorsal to palmar. The same procedure was used to calculate the area of the medullary canal or the cancellous bone region, which was then subtracted from the total bone cross section area to calculate the cortical bone cross section area. The pin area, taken through the center of the pin, corresponding to each cortical bone cross section area was then calculated to derive the cortical area fraction for each pin hole. The pin area fraction of the cortex was also calculated from the pin cross sectional area of the cortex and the cortical cross sectional area. The pin diameter to bone diameter ratio was also calculated for each pin hole. This information was collected and maintained in a computer spreadsheet program (Microsoft Excel 2013, Microsoft Corporation, Redman, WA) along with the calculated total PAMi for each model. Scatter plots were constructed initially to examine the relationships between maximum and minimum stress and strain values and calculated total PAMi and total cortical bone volume removed. Preferred model constructs were based on three selection criteria; 1. Strain values for the model at or below the threshold values of minimum (compressive) and maximum (tensile) strain (-1% and 0.5%, respectively); 2. The maximum of the pin diameter to bone diameter ratio for pins in the model was less than 0.25; and 3. The mean pin diameter to bone diameter ratio for the construct was less than 0.23. The volume of cortical bone removed in each of the pin configurations that met these 3 selection criteria was then compared to select the optimum pin configuration. Data were generated based on the analytical model of Huiskes et al.[18] for compressive bone stress at the BPI from the parameters used in the constructed FE models. The parameters used were load (7500 N), side bar separation (15 mm), cortical thickness (12 mm), intramedullary width (16 mm), sidebar number (2), pin elastic modulus (205 GPa)

and foundation modulus (88200 MPa). Foundation modulus is related to the bone elastic modulus and was kept constant by Huiskes et al. Pin diameter was varied from 4 mm to 9.5 mm and pin number from 3 to 5 to generate data for comparison to the current FE analysis.

4.3 Results

A total of 67 models were constructed and evaluated. All models were remeshed successfully and details of each model are presented in **Table 4.2**. The total PAMi values for the models constructed ranged from 50.4 to 2397.6 mm^4. There was a consistent relationship observed between the stress and strain output variables obtained and total PAMi. A strong negative power law relation was fitted to the data ($R^2 = 0.95$) when total PAMi was plotted against the maximum tensile strain of each model construct **(Figure 4.1)**. The other stress and strain relations with PAMi were similar. There was a steep increase in peak tensile strain observed with total PAMi values lower than 200 mm^4 and a more gradual increase above the threshold value of 5,000 microstrain between total PAMi values of 500 and 200 mm^4. Values of total PAMi larger than approximately 500 mm^4 resulted in marginally lower maximum strain values with a four-fold increase in total PAMi resulting in an approximately 50% decrease in maximum strain.

The mean cortical bone volume removed from each model to create pin holes ranged from 220 to 1,535 mm^3. The relationship between the stress and strain output variables and mean cortical bone volume removed was similar to their relationship with total PAMi **(Figure 4.2).** Mean cortical bone volume removed of less than 400 mm^3 resulted in a sharp increase in the peak tensile strain. A more gradual decrease in tensile strain was observed from 400 to 1500 mm^3. A similar pattern was evident for the peak compressive strain values. The mean pin area fraction ranged from 0.029 to 0.073 **(Figure 4.3)**. Values lower than approximately 0.035 were associated with a sharp increase in the peak tensile and compressive strains. Values of mean pin area fraction larger than 0.035 were associated with more gradual changes in strain values. The mean pin to bone diameter

ratio ranged from 0.14 to 0.34 over the 67 models. The relationship with peak cortical bone strain values was less apparent that with the mean cortical bone volume and the mean pin area fraction **(Figure 4.4)**.

Application of the bone pin construct selection criteria resulted in a total of 9 preferred pin number/diameter combinations based on the total PAMi, with another 5 models being alternative constructs with altered spacing, pin orientation or pin order (for different pin sizes) (**Table 4.3**). None of the preferred transcortical pin configurations had less than 4 pins, with 5 configurations having 5 pins and 6 configurations having 6 pins. From these preferred pin combinations, based on the mean cortical bone volume removed, the mean pin diameter to bone diameter ratio and the mean pin area fraction, a transfixation cast with 4 proximal 4.8 mm pins and 2 distal 6.3 mm pins each spaced 10 mm apart would be the optimal configuration. Based on the total cortical bone volume removed, a transfixation cast with a single proximal 6 mm pin and 3 distal 6.3 mm pins would be optimal.

The mean cortical area fraction had a similar relationship with maximum tensile and compressive cortical bone strain as was observed with the total PAMi and the mean cortical bone volume removed. The mean cortical area fraction is equivalent to the pin area fraction of the cortex subtracted from 1. Therefore the similar findings between these parameters is expected. Similar to total PAMi and total cortical bone volume removed, there was a point observed where further decreases in the cortical area fraction had little effect on lowering the cortical bone strain levels. There was a second order polynomial relationship found between mean cortical bone volume removed and the mean cortical area fraction calculated (**Figure 4.5**).

The maximum pin von Mises stress occurred at the junction with the cast at the pin ends in all cases and approximated the ultimate stress in all of the preferred pin configurations. These values were similar in magnitude to those obtained for currently used conventional transfixation cast pin diameter and number combinations. The location of maximum

cortical bone von Mises stress, and maximum and minimum cortical bone principal stresses and strains are presented in **Table 4.4**. The maximum compressive strain was consistently located at the proximal medial margin of the proximal pin hole (**Figure 4.6**). The maximum compressive stress was at this location in all but 4 of the preferred pin configurations. While these locations were consistent, there were not large differences between the maximum stresses and strains at these locations and at similar locations of the other more distal pin holes. In several of the bone-pin constructs, more distal pins were the site of maximum tensile stresses and strains.

The relationship between total PAMi and compressive stress at the BPI was compared to data generated using the analytical model **(Figure 4.7)**. The shape of the 2 curves are similar but the quantities generated are different despite using similar parameters for generating data.

4.4 Discussion

The results of this study show that there is a negative power law relationship that exists between the total PAMi of a pin construct for transfixation casting and the peak tensile strain that is predicted from FE models. Given that the corticocancellous bone model used in this study has been previously validated with an ex vivo bone model, it is reasonable to expect that this relationship exists and may be reproduced and further defined in additional ex vivo or in vivo studies. This relationship, and the use of bone yield strain and hole size threshold or cutoff values, highlight the balance between bone pin constructs that provide sufficient resistance to bending during loading and constructs that have the smallest bone holes possible to accommodate the pins selected, thereby minimizing secondary fracture risks associated with large pin holes.[3,30] Using a broad series of models of bone-pin constructs for transfixation casting, we used specific selection criteria based on previous studies of equine cortical bone yield and failure,[10,35,36,46,47] as well as information on the relationship between hole size and reduced bone strength,[20–22,26] to select a small set of preferred bone-pin constructs for

transfixation casting in the horse. The principles of this method of selecting bone-pin constructs, based on the balance between their resistance to loading within the transfixation cast, and the anticipated bone hole sizes required to complete the construct, could be used in other locations other than the MC3. Further, using the related variables of mean cortical bone volume removed and mean cortical area fraction for each construct, we arrived at 2 optimal pin configurations that should be further evaluated in an ex vivo setting.

A strain based criterion was preferred over a stress based one for selection of the threshold values used for local bone failure at the pin hole because of evidence that the prediction of failure within bone is more accurate using maximum principal strain.[48] Each of the peak cortical bone tensile strain relationships examined in this study displayed a general power law relationship, including with total PAMi, the total cortical bone volume and the mean cortical bone volume removed. These relationships suggest a point or region within which the balance between the two variables changes. As an example, the peak tensile strain values appear to be very responsive to changes in total PAMi below values of approximately 200 mm^4 while values above 500 mm^4 result in a much less dramatic reduction in peak tensile strain. These relationships form a general working theory that could be used to decide on a combination of pin diameter and number for locations beyond the MC3. Combined with the previously suggested hole diameter to bone diameter ratio of less than 0.25 and a mean cortical area fraction between 0.95 and 0.97, we arrived at 2 optimal bone-pin constructs from a larger group of preferred constructs.

The evaluation of three different methods of estimating the amount of bone tissue removed when placing a transcortical pin merits some discussion. In the literature,[20–22,26] the measures of pin or hole diameter to bone diameter ratio and cortical area fraction have been used to assess bone holes and residual bone strength. These are one and two dimensional parameters, respectively, being used to estimate the removal of a 3 dimensional volume of bone. For this reason, we elected to compare all 3 of these

measures, and their values normalized for pin number in each construct, to assess their relationship with peak bone strain values. A bone volume removed by a drill can be related geometrically to both the area fraction removed and a hole diameter to bone diameter ratio using some assumptions on simplifying the bone shape. It is worth noting that the relationship between cortical bone volume removed and peak cortical strain contained data that was less scattered than both the pin area fraction and the hole to bone diameter ratio.

Finite element analysis requires assumptions to be made in order to provide a complete and solvable set of equations from which to calculate a solution to the physical problem considered. The influence of the assumptions on the results of the models presented here are relative to one another in the context of the overall results presented. One assumption that has been shown to impact FE results is the material property assumptions for bone. While some studies that examined broad scale changes or general implant interactions, such as we did in this study, have used a global estimate of elastic modulus and bone density for FE modeling, an improvement on this approach would be the assignment of a density based elastic modulus. This approach uses the known relationship between bone density and elastic modulus to assign specific material properties to specific regions or elements of the model.[44,49–51] This approach requires a greater degree of computational time and would have made construction of the large number of models used in this analysis considerably more intensive. It has been recently shown that FE models are sensitive to the use of a heterogenous bone material property designation based on microcomputed tomography data for bone mineral density compared to an averaged value and that this has a large impact on the cancellous portion of the model and a lesser impact on cortical bone.[52] We elected to utilize an elastic modulus for bone based on reported values from the literature because our initial intent was to construct a number of general models with which to evaluate a broad range of transfixation casting parameters. While we used a specific subject for creating our bone model geometry and validating it previously, the intent was not to make specific predictions in a subject-specific manner.

Additional assumptions that were made in this study were the fixed boundary conditions assigned to the ends of the pins (all 3 axes) and the distal end of the bone model (x- and y- axes). The unrestricted movement of the distal end of the bone in the proximal to distal direction (z-axis) was also used to simulate a completely unstable fracture, however this is unlikely to be the case with contact between the cast material and the distal portion of the limb providing some resistance to displacement of the bone even when an unstable fracture is present. Further refinement of this model will be required to more accurately represent the boundary condition at the distal end of the bone. In terms of the pin attachments, most investigations of external fixation pin mechanics have assumed a fixed pin end.[17,18,44] This assumption has been shown to introduce significant errors in a half pin fixation,[53] therefore caution should be used in adopting this assumption without further investigation, particularly considering the relative lack of information regarding the role of the cast and how cast material may compare mechanically to more classical external fixator constructs. One final assumption that should be recognized as not being accurate is the friction that likely occurs between the pin and bone at the BPI. While loading forces were only axial in the current model, some frictional influence on pin sliding within the bone hole may be expected.

Our previous validation of the modeling approach used in this study showed that the general parameter comparisons made were consistent with the expected results from previous parametric analyses of external skeletal fixation,[17,18] as well as ex vivo and in vivo studies.[54–57] However, the absolute values for stress and strain provided by the models should be further validated for the specific models selected through ex vivo testing or further refinement of the modeling procedures to assess the full impact of the range of assumptions made. It has been stated that the process of FE modeling is most effective when there is a cycle between analysis and ex vivo and in vivo testing rather than a single stand-alone study.[51,58] Further refinement of the model and theory presented here will be necessary before it is applicable in the clinical setting.

In the present study, we compared the total construct PAMi with data generated using the analytical model proposed by Huiskes et al. for calculating peak compressive stress at the BPI.[18] These results were qualitatively similar but the absolute values calculated for this comparison were much lower from the analytical model than from our current series of FE models. This quantitative difference is likely to be related to the construct set up differences, with pins on both sides of the fracture site considered in calculations with the analytical model while the pins in the FE models used here were only positioned above the theoretical fracture location with the distal end of the MC3 free to move distally. In addition, the analytical model was based on a symmetrical cylinder of bone with set dimensions input into the equation for peak compressive bone stress. The current FE analysis was performed on a model of the distal MC3 resulting in variable cortical thickness and intramedullary width, both input variables for the analytical model. The analytical model was developed using the assumption that BPI stresses and loading would be similar between each of the pins in the model, whereas the FE analysis presented here did not require this assumption. In addition, the derivation of the analytical models used a parameter called the foundation modulus, which was introduced as part of the beam on elastic foundation theory used to develop the equations to account for the interaction of the pin directly on the bone. The foundation modulus was shown to be related to the bone elastic modulus by a factor that was kept constant in the original studies.[17,18] In the FE analysis presented here, the elastic modulus of bone was used directly within the modeling process.

It has been shown previously that cortical bone that is primarily loaded in compression during use, more readily resists failure in compression than a cortex loaded primarily in tension.[59] Microdamage due to compressive loading is different than microdamage due to tensile loading with larger linear microcracks seen following compressive damage while more diffuse smaller cracks are observed with tensile bone damage. The equine MC3 is primarily loaded in compression during the weight bearing phase of the stride at the walk.[45] Loading of transcortical pins results in large compressive stresses within the bone at the BPI. Differences between tensile and compressive bone regions may be relevant to

the placement of transcortical pins when the risk of secondary cortical pin hole fracture is considered. In addition, the fact that regional safety factors vary around the equine MC3 mid-diaphyseal cortex in both tensile and compressive loading modes, means that specific pin placement locations may be at greater risk for secondary fracture regardless of the anticipated stresses.[46] Information such as is provided by the development of FE models of transcortical pins and the stresses and strains that are predicted, may be useful in comparing specific sites for pin positioning. However, considerably more work is needed to elucidate all of the factors that may contribute to the currently high incidence of secondary pin hole fractures during transfixation casting in the horse. For instance, we found that the site of maximum principal bone strain was consistently the most proximal pin hole in the construct although there were exceptions. Williams et al showed that removal of pins from different positions in the MC3 altered the measured strains found distal to the pins. A greater proportion of the stress in these constructs appears to be experienced at the proximal pin hole, which may in itself explain the high rate of occurrence of secondary pin hole fractures in this location, regardless of proximity to the diaphysis of the bone or the top of the transfixation cast.[1,3,60]

The selection of specific pin configurations becomes somewhat arbitrary when the concept of total construct PAMi is used as a single parameter, rather than using the individual components of pin number and pin diameter. When combined with keeping pin diameter below a certain ratio compared to bone diameter, 0.25 in our selection procedure, the result is that constructs with a larger number of smaller pins were required to meet these selection criteria and thresholds. The number of pins that can be used in a particular bone will vary depending upon anatomic limitations. Additional work is also necessary to clarify the role of the cast material on the specific bone stress distribution that occurs within a transfixation cast.

A greater understanding of the factors that contribute to bone failure at the BPI is needed to reduce the morbidity and mortality associated with equine transfixation casting. The reason for investigating the BPI stresses and strains in this study was to develop a

strategy to reduce the likelihood of local acute and chronic bone failure that occurs clinically during transfixation casting. Ultimately this strategy is aimed at improving the safety and reliability of this fracture fixation method in the horse. A series of bone-pin constructs for transfixation casting were assessed using FE analysis and a small group of preferred configurations were selected. Based on the amount of cortical bone removed to place transfixation pins, 2 optimal configurations were selected from this group to go forward into further testing and validation.

4.5 List of References

1. Lescun TB, McClure SR, Ward MP, et al. Evaluation of transfixation casting for treatment of third metacarpal, third metatarsal, and phalangeal fractures in horses: 37 cases (1994-2004). *J Am Vet Med Assoc* 2007;230:1340–1349.

2. Joyce J, Baxter GM, Sarrafian TL, et al. Use of transfixation pin casts to treat adult horses with comminuted phalangeal fractures: 20 cases (1993-2003). *J Am Vet Med Assoc* 2006;229:725–730.

3. Nemeth F, Back W. The use of the walking cast to repair fractures in horses and ponies. *Equine Vet J* 1991;23:32–36.

4. Kraus BM, Richardson DW, Nunamaker DM, et al. Management of comminuted fractures of the proximal phalanx in horses: 64 cases (1983-2001). *J Am Vet Med Assoc* 2004;224:254–263.

5. Easter JL, McClure SR, Honnas CM, et al. Transfixation cast repair of an open cannon bone fracture in a foal. *Equine Pract* 1994;16:16...23.

6. Easter JL, Schumacher J, Watkins JP. Transfixation cast technique for arthrodesis of the distal interphalangeal joint of horses. *Vet Comp Orthop Traumatol* 2011;24:62–67.

7. Rossignol F, Vitte A, Boening J. Use of a modified transfixation pin cast for treatment of comminuted phalangeal fractures in horses. *Vet Surg* 2014;43:66–72.

8. Bischofberger AS, Fürst A, Auer J, et al. Surgical management of complete diaphyseal third metacarpal and metatarsal bone fractures: clinical outcome in 10 mature horses and 11 foals. *Equine Vet J* 2009;41:465–473.

9. Les CM, Stover SM, Keyak JH, et al. Stiff and strong compressive properties are associated with brittle post-yield behavior in equine compact bone material. *J Orthop Res* 2002;20:607–614.

10. Bigley RF, Gibeling JC, Stover SM, et al. Volume effects on yield strength of equine cortical bone. *J Mech Behav Biomed Mater* 2008;1:295–302.

11. Akkus O, Yeni YN, Wasserman N. Fracture mechanics of cortical bone tissue: a hierarchical perspective. *Crit Rev Biomed Eng* 2004;32:379–426.

12. Zioupos P, Currey JD, Mirza MS, et al. Experimentally determined microcracking around a circular hole in a flat plate of bone: comparison with predicted stresses. *Philos Trans R Soc Lond, B, Biol Sci* 1995;347:383–396.
13. Kennedy OD, Herman BC, Laudier DM, et al. Activation of resorption in fatigue-loaded bone involves both apoptosis and active pro-osteoclastogenic signaling by distinct osteocyte populations. *Bone* 2012;50:1115–1122.
14. Kennedy OD, Laudier DM, Majeska RJ, et al. Osteocyte apoptosis is required for production of osteoclastogenic signals following bone fatigue in vivo. *Bone* 2014;64:132–137.
15. Cardoso L, Herman BC, Verborgt O, et al. Osteocyte apoptosis controls activation of intracortical resorption in response to bone fatigue. *J Bone Miner Res* 2009;24:597–605.
16. Herman BC, Cardoso L, Majeska RJ, et al. Activation of bone remodeling after fatigue: differential response to linear microcracks and diffuse damage. *Bone* 2010;47:766–772.
17. Huiskes R, Chao EY. Guidelines for external fixation frame rigidity and stresses. *J Orthop Res* 1986;4:68–75.
18. Huiskes R, Chao EY, Crippen TE. Parametric analyses of pin-bone stresses in external fracture fixation devices. *J Orthop Res* 1985;3:341–349.
19. Nash RA, Nunamaker DM, Boston R. Evaluation of a tapered-sleeve transcortical pin to reduce stress at the bone-pin interface in metacarpal bones obtained from horses. *Am J Vet Res* 2001;62:955–960.
20. McBroom RJ, Cheal EJ, Hayes WC. Strength reductions from metastatic cortical defects in long bones. *J Orthop Res* 1988;6:369–378.
21. Edgerton BC, An KN, Morrey BF. Torsional strength reduction due to cortical defects in bone. *J Orthop Res* 1990;8:851–855.
22. Hipp JA, Edgerton BC, An KN, et al. Structural consequences of transcortical holes in long bones loaded in torsion. *J Biomech* 1990;23:1261–1268.
23. Seltzer KL, Stover SM, Taylor KT, et al. The effect of hole diameter on the torsional mechanical properties of the equine third metacarpal bone. *Vet Surg* 1996;25:371–375.

24. Hopper SA, Schneider RK, Ratzlaff MH, et al. Effect of pin hole size and number on in vitro bone strength in the equine radius loaded in torsion. *Am J Vet Res* 1998;59:201–204.
25. Brooks DB, Burstein AH, Frankel VH. The biomechanics of torsional fractures. The stress concentration effect of a drill hole. *J Bone Joint Surg Am* 1970;52:507–514.
26. Kuo RF, Chao EY, Rim K, et al. The effect of defect size on the stress concentration and fracture characteristics for a tubular torsional model with a transverse hole. *J Biomech* 1991;24:147–155.
27. Palmer RH. External fixators and minimally invasive osteosynthesis in small animal veterinary medicine. *Vet Clin North Am Small Anim Pract* 2012;42:913–934, v–vi.
28. Lewis DD, Cross AR, Carmichael S, et al. Recent advances in external skeletal fixation. *J Small Anim Pract* 2001;42:103–112.
29. Clary E, Roe S. Enhancing external skeletal fixation pin performance - consideration of the pin- bone interface. *Vet Comp Orthop Traumatol* 1995;8:6–13.
30. Nunamaker DM. A new external skeletal fixation device that allows immediate full weightbearing application in the horse. *Vet Surg* 1986;15:345–355.
31. Nunamaker DM, Nash RA. A tapered-sleeve transcortical pin external skeletal fixation device for use in horses: development, application, and experience. *Vet Surg* 2008;37:725–732.
32. McClure S, Honnas CM, Watkins JP. Managing equine fractures with external skeletal fixation. *Comp Cont Educ Pract Vet* 1995;17:1054–1063.
33. Mihalko WM, Beaudoin AJ, Krause WR. Mechanical properties and material characteristics of orthopaedic casting material. *J Orthop Trauma* 1989;3:57–63.
34. Olcay E, Allahverdi E, GüLmez T, et al. Evaluation of the effects of holes of various sizes on fracture rates in sheep femurs. *Kafkas Univ Vet Fak Derg* 2013;19(Suppl-A):A49-A53.
35. Martin RB, Stover SM, Gibson VA, et al. In vitro fatigue behavior of the equine third metacarpus: remodeling and microcrack damage analysis. *J Orthop Res* 1996;14:794–801.

36. Martin RB, Gibson VA, Stover SM, et al. Residual strength of equine bone is not reduced by intense fatigue loading: implications for stress fracture. *J Biomech* 1997;30:109–114.
37. Les CM, Stover SM, Taylor KT, et al. Ex vivo simulation of in vivo strain distributions in the equine metacarpus. *Equine Vet J* 1998;30:260–266.
38. Gibson VA, Stover SM, Martin RB, et al. Fatigue behavior of the equine third metacarpus: mechanical property analysis. *J Orthop Res* 1995;13:861–868.
39. Gibson VA, Stover SM, Gibeling JC, et al. Osteonal effects on elastic modulus and fatigue life in equine bone. *J Biomech* 2006;39:217–225.
40. McClure SR, Glickman LT, Glickman NW, et al. Evaluation of dual energy x-ray absorptiometry for in situ measurement of bone mineral density of equine metacarpi. *Am J Vet Res* 2001;62:752–756.
41. Chen Q, Thouas GA. Metallic implant biomaterials. *Mat Sci Eng R* 2015;87:1–57.
42. Stevenson M, Barkey M, Bradt R. Fatigue failures of austenitic stainless steel orthopedic fixation devices. *Pract Fail Analys* 2002;2:57–64.
43. Anonymous. Product Data Sheet - 316/316L Stainless Steel. 2007. Available at: www.aksteel.com.
44. Brianza S, Brighenti V, Lansdowne JL, et al. Finite element analysis of a novel pin-sleeve system for external fixation of distal limb fractures in horses. *Vet J* 2011;190:260–267.
45. Merritt JS, Burvill CR, Pandy MG, et al. Determination of mechanical loading components of the equine metacarpus from measurements of strain during walking. *Equine Vet J Suppl* 2006:440–444.
46. Skedros JG, Dayton MR, Sybrowsky CL, et al. Are uniform regional safety factors an objective of adaptive modeling/remodeling in cortical bone? *J Exp Biol* 2003;206:2431–2439.
47. Skedros JG, Dayton MR, Sybrowsky CL, et al. The influence of collagen fiber orientation and other histocompositional characteristics on the mechanical properties of equine cortical bone. *J Exp Biol* 2006;209:3025–3042.

48. Schileo E, Taddei F, Cristofolini L, et al. Subject-specific finite element models implementing a maximum principal strain criterion are able to estimate failure risk and fracture location on human femurs tested in vitro. *J Biomech* 2008;41:356–367.
49. Prendergast P. Finite element models in tissue mechanics and orthopaedic implant design. *Clin Biomech* 1997;12:343–366.
50. Schileo E, Dall'ara E, Taddei F, et al. An accurate estimation of bone density improves the accuracy of subject-specific finite element models. *J Biomech* 2008;41:2483–2491.
51. Cristofolini L, Schileo E, Juszczyk M, et al. Mechanical testing of bones: the positive synergy of finite-element models and in vitro experiments. *Philos Trans A Math Phys Eng Sci* 2010;368:2725–2763.
52. Yang H, Butz KD, Duffy D, et al. Characterization of cancellous and cortical bone strain in the in vivo mouse tibial loading model using microCT-based finite element analysis. *Bone* 2014;66:131–139.
53. Drijber FL, Finlay JB, Dempsey AJ. Evaluation of linear finite-element analysis models' assumptions for external fixation devices. *J Biomech* 1992;25:849–855.
54. Aro HT, Chao EY. Biomechanics and biology of fracture repair under external fixation. *Hand Clin* 1993;9:531–542.
55. Chao EY, Aro HT, Lewallen DG, et al. The effect of rigidity on fracture healing in external fixation. *Clin Orthop Relat Res* 1989:24–35.
56. Pettine KA, Chao EY, Kelly PJ. Analysis of the external fixator pin-bone interface. *Clin Orthop Relat Res* 1993:18–27.
57. Aro HT, Markel MD, Chao EY. Cortical bone reactions at the interface of external fixation half-pins under different loading conditions. *J Trauma* 1993;35:776–785.
58. Taylor M, Prendergast PJ. Four decades of finite element analysis of orthopaedic devices: Where are we now and what are the opportunities? *J Biomech* 2015;48:767–778.
59. Reilly GC, Currey JD. The development of microcracking and failure in bone depends on the loading mode to which it is adapted. *J Exp Biol* 1999;202:543–552.
60. Williams JM, Elce YA, Litsky AS. Comparison of 2 equine transfixation pin casts and the effects of pin removal. *Vet Surg* 2014;43:430–436.

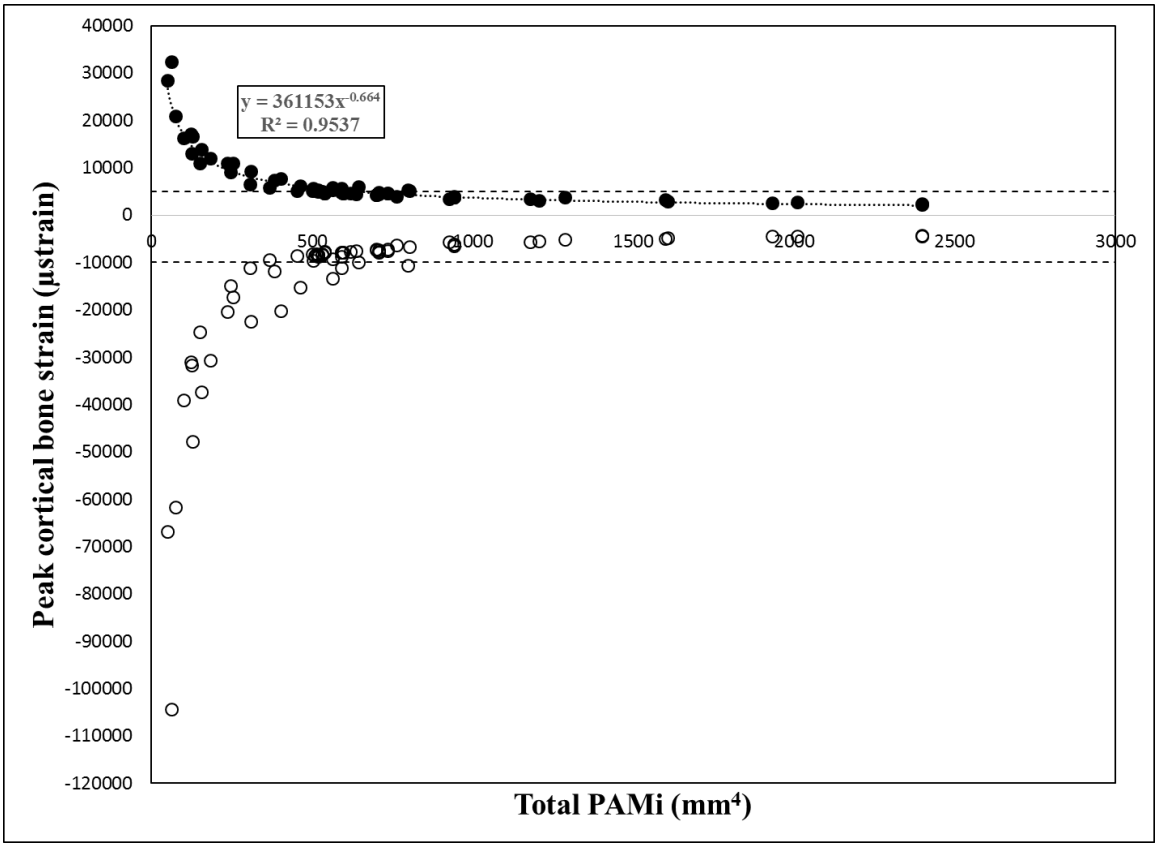

Figure 4.1 Total pin area moment of inertia (PAMi) versus the peak tensile (solid circles) and compressive (open circles) strain calculated for 67 individual finite element models of the equine distal limb transfixation cast. The dashed lines represent the cortical bone yield threshold values of -1.0% for compression and 0.5% for tension used for determining preferred models.

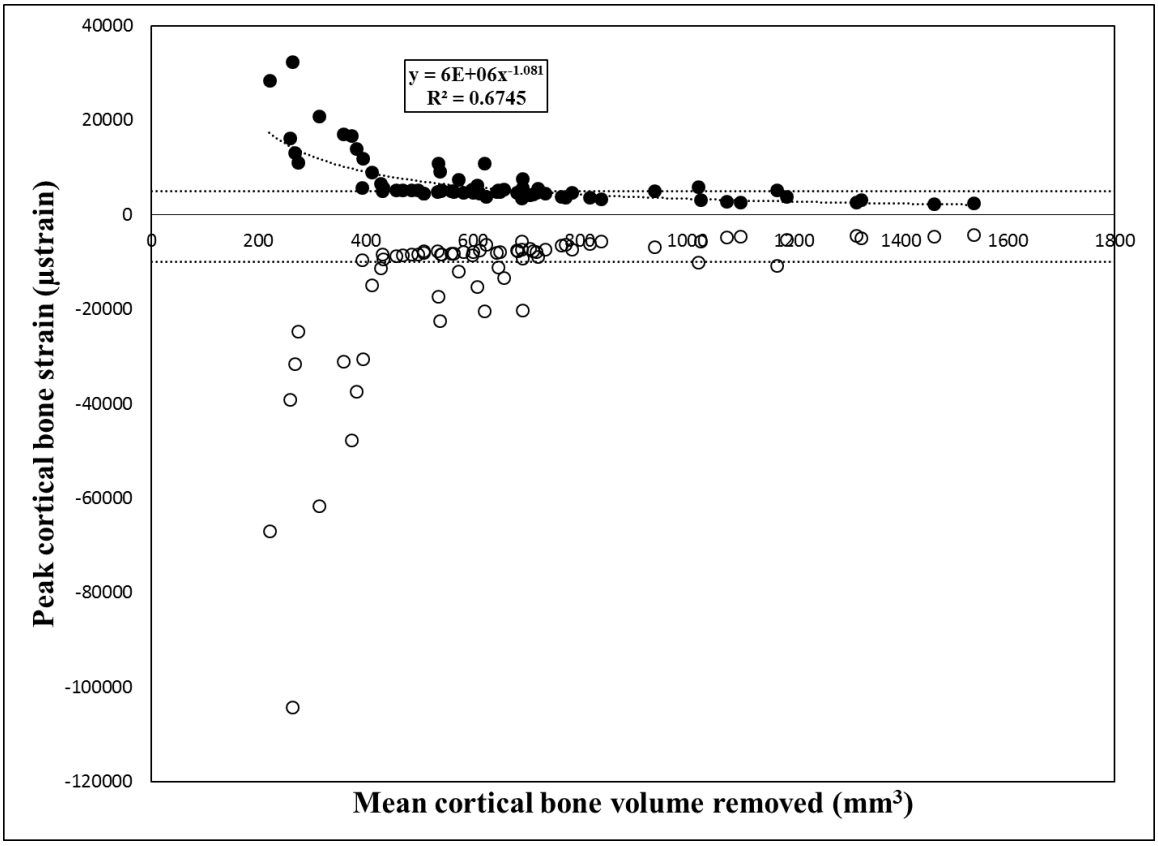

Figure 4.2 Mean cortical bone volume removed versus peak tensile (solid circles) and compressive (open circles) cortical bone strain calculated for 67 individual finite element models of the equine distal limb transfixation cast. The dashed lines represent the cortical bone yield threshold values of -1.0% for compression and 0.5% for tension used for determining preferred models.

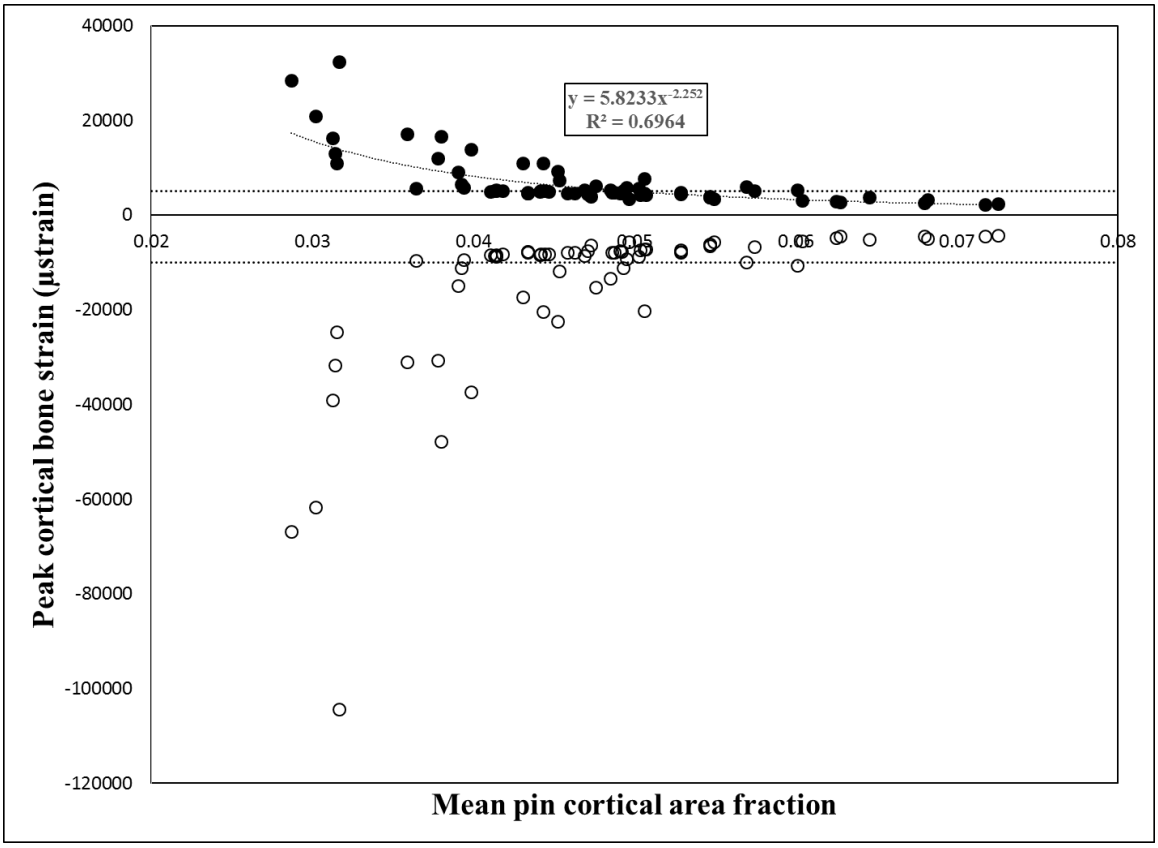

Figure 4.3 Mean pin cortical area fraction versus peak tensile (solid circles) and compressive (open circles) cortical bone strain for 67 individual finite element models of the equine distal limb transfixation cast. The graph shows an elevation in both tensile and compressive peak strain when the mean pin area fraction for the transfixation pin construct becomes less than 0.04. The dashed lines represent the cortical bone yield threshold values of -1.0% for compression and 0.5% for tension used for determining preferred models.

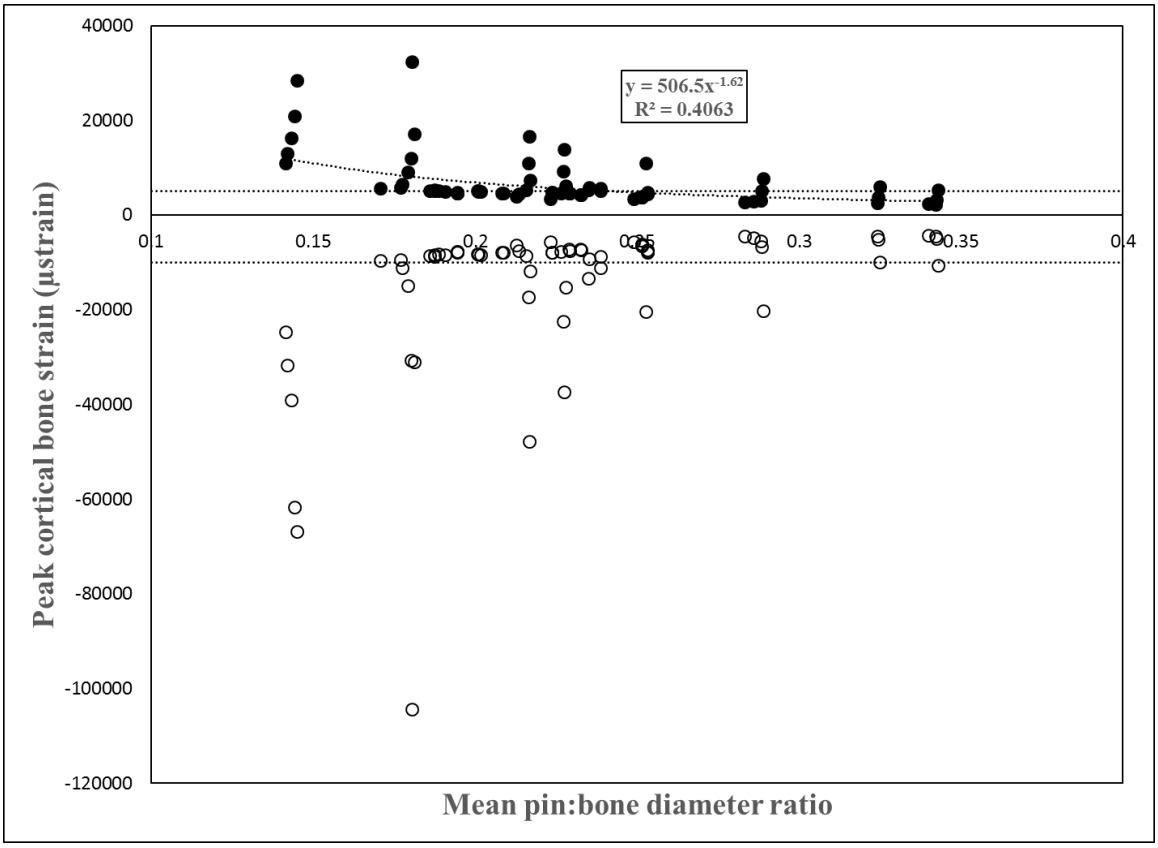

Figure 4.4 Mean pin to bone diameter ratio versus peak tensile (solid circles) and compressive (open circles) cortical bone strain for 67 individual finite element models of the equine distal limb transfixation cast. The dashed lines represent the cortical bone yield threshold values of -1.0% for compression and 0.5% for tension used for determining preferred models.

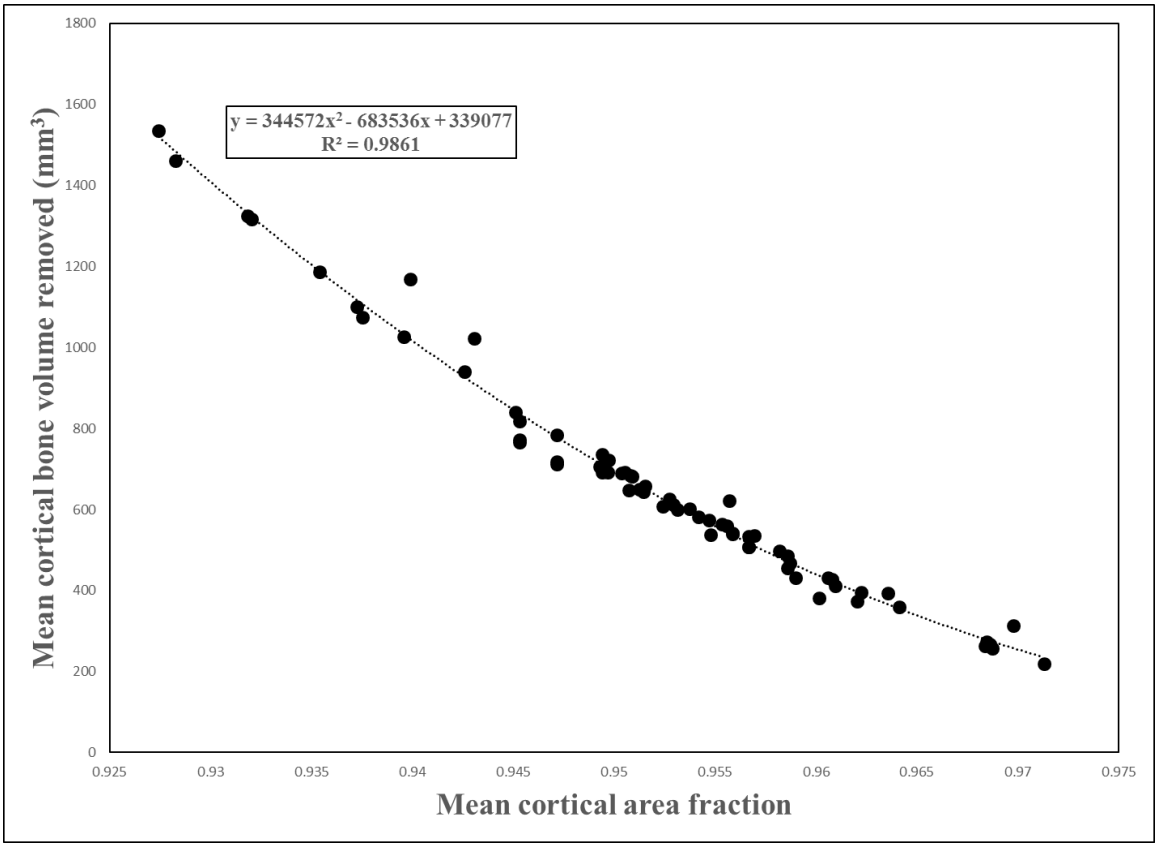

Figure 4.5 Mean cortical area fraction versus mean cortical bone volume removed for 67 individual finite element models of the equine distal limb transfixation cast. A fitted polynomial equation with associated R^2 value (Pearson product moment correlation coefficient) is shown.

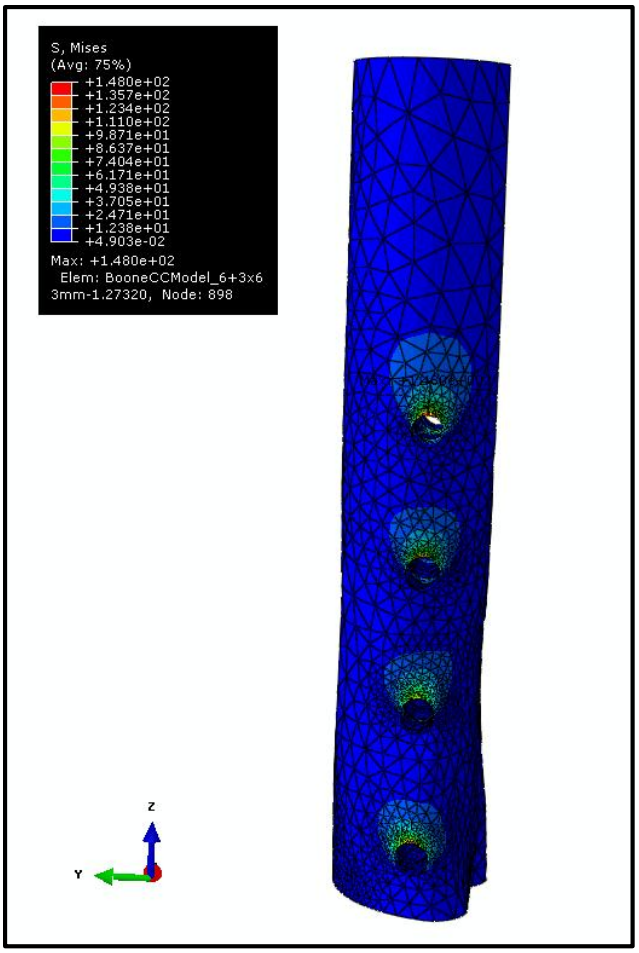

Figure 4.6 Image showing the von Mises stress distribution around the 4 pin holes of a transcortical pin-bone construct as viewed from the medial side of the bone. The legend shows the scale of von Mises stress values represented on the image. Proximal is to the top and dorsal is to the left.

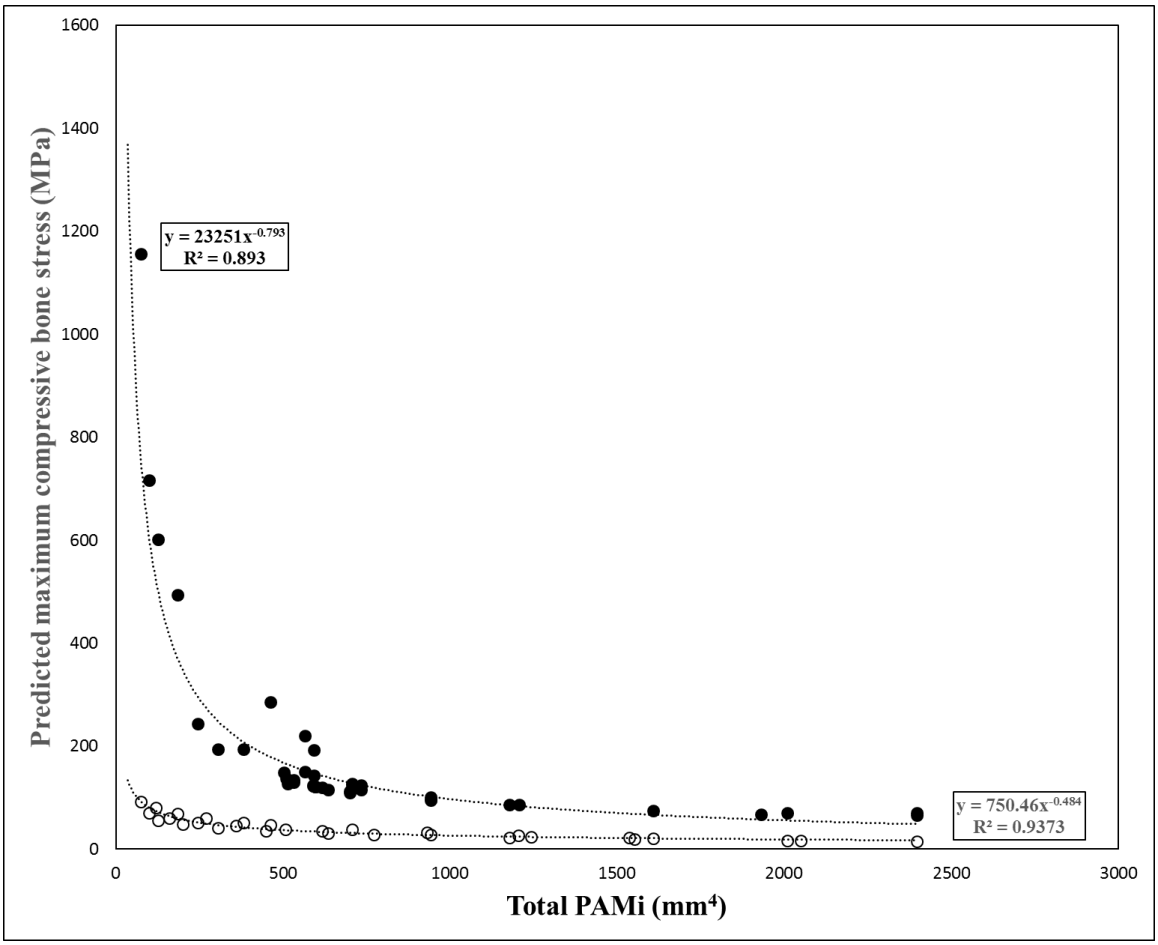

Figure 4.7 Comparison of predicted maximum compressive stress versus total pin area moment of inertia from the present study (solid circles) and calculated using formula from a previous analytic model of the external skeletal fixator (open circles). [Huiskes et al., Parametric analysis of pin-bone stresses in external fracture fixation devices. *J Orthop Res*, 1985] The parameter values used to generate data from the equation proposed by Huiskes et al. were the same as those used in the present study (Load = 7500N; side bar separation (pin working length) = 15 mm; cortical thickness = 12 mm; intramedullary width = 16 mm; sidebar number = 2; pin elastic modulus = 205 GPa; foundation modulus = 88200). Pin diameter was varied from 4 mm to 9.5 mm and pin number from 3 to 5 to generate the displayed data points.

Table 4.1 Definitions and calculations used for the various parameters and output variables described in the present study.

Name	**Definition**	**Method of calculation or measurement**
Bone volume (BV) removed	The volume of bone removed as a result of placing all pins of a construct into the bone	Calculated from specific FE mesh as difference between the original bone model volume and the bone model following pin placement.
Cortical bone volume (CV) removed	The volume of cortical bone removed as a result of placing all pins of a construct into the bone	Calculated from final FE mesh as difference between the CV of the original bone model and the CV of the bone model following pin placement.
Pin area moment of inertia (PAMi)	$=(\pi/64)d^4$; where d is the pin diameter	Directly from pin diameter
Total PAMi	the sum of PAMi for each pin end fixed within the construct	Addition of the PAMi previously calculated for each pin in the construct.
Dorsal palmar bone diameter (D)	Distance from dorsal outer cortical edge to palmar outer cortical edge	Measured directly from computed tomography scans.
Cortical cross sectional (CXS) area	Cross sectional area of cortical bone at a specific pin location	BXS area – MXS area.
Pin cross sectional (PXS) area – cortex	The cross sectional area of cortex removed as a result of pin placement at a specific location	(Lateral cortical width + medial cortical width) X pin diameter.
Bone cross sectional (BXS) area	Bone area at a specific pin location	(Dorsal palmar bone width X lateral medial bone width) X $\boldsymbol{\pi}$
Medullary cross sectional (MXS) area	Medullary area at a specific pin location	(Dorsal palmar medullary width X lateral medial medullary width) X $\boldsymbol{\pi}$
Cortical area fraction	area of cortical bone cross section remaining following pin insertion, divided by the initial cortical bone cross section area	= (CXS area – PXS area) / CXS area
Cortical pin area fraction	The area of a pin centered cortical bone section missing following pin insertion	= PXS area / CXS area.
Pin diameter to bone diameter ratio	The ratio of the pin diameter to bone diameter at a specific pin location	= d/D; where d is the pin diameter and D is the dorsal palmar bone diameter

Table 4.2 Details of 67 finite element models constructed to evaluate the effect of total pin area moment of inertia (PAMi) on output stress and strain values during loading. Consistent loading and boundary conditions as well as material properties for pins and bone were maintained for all models. The order of pin diameters indicated is from proximal to distal in MC3. Abbreviations: No. = number; Cort vol = cortical volume; mm = millimeters; MPa = megapascals; VM = von Mises; Pr = principal; max = maximum; min = minimum; με = microstrain; pos = positive; neg = negative.

Pin diameter (s) / spacing (mm)	Pin no.	Pin offset?	Cort vol removed	Mean Cort Vol removed	Total PAMi (mm^4)	VM stress max (MPa)	Pr. stress max (MPa)	Pr stress min (MPa)	Pr strain max (με)	Pr strain min (με)	Pin VM stress max (MPa)
5	1	No	263	263	61.4	1669	433.6	-1940	32350	-104300	9107
6	1	No	373	373	127.2	776.7	276.9	-871.7	16700	-47760	6669
6.3	1	No	382	382	154.6	609.8	232.1	-716.4	13940	-37400	1596
7	1	No	622	622	235.6	361.8	170.1	-331.7	10910	-20320	1255
8	1	No	693	693	402	330.6	129.6	-380.7	7666	-20190	681.7
9	1	No	1022	1022	643.8	179.2	97.5	-163.2	6000	-9986	706.4
9.5	1	No	1168	1168	799.2	186.2	87.6	-177.7	5287	-10690	2671
4 / 20	2	No	440	220	50.4	1117	433.8	-1225	28440	-66890	2770
5 / 20	2	No	718	359	122.8	531	251.1	-555.3	17070	-31040	1560
6 / 20	2	No	1072	536	254.4	308.9	163.9	-282.3	10910	-17330	1001
6.3 / 20	2	No	1077	538.5	309.2	360.6	135.1	-426.9	9264	-22420	903.6
8 / 20	2	No	1880	940	804	120.9	74.4	-110.7	5099	-6746	370.7
9 / 20	2	No	2373	1186.5	1287.6	101.7	55.2	-78.6	3775	-5194	380.3
9.5 / 20	2	No	2650	1325	1598.4	93.1	50.2	-76.7	3219	-4925	1493

Pin diameter (s) / spacing (mm)	Pin no.	Pin offset?	Cort vol removed	Mean Cort Vol removed	Total PAMi (mm4)	VM stress max (MPa)	Pr. stress max (MPa)	Pr stress min (MPa)	Pr strain max (με)	Pr strain min (με)	Pin VM stress max (MPa)
4 / 20	3	No	941	313.7	75.6	997.2	313.8	-1156	20840	-61640	2045
5 / 20	3	No	1186	395.3	184.2	429.6	182.6	-494.5	11950	-30570	1116
6 / 20	3	No	1720	573.3	381.6	211.1	109.7	-194.3	7388	-11890	690.2
6.3 / 20	3	No	1825	608.3	463.8	248.9	95.2	-285.2	6221	-15170	2227
2x6+7.5 / 20	3	No	1975	658.3	564.8	233.8	82.7	-220	5,370	-13400	556.5
7.5+2x6 / 20	3	No	2079	693	564.8	164.7	86.9	-150.4	5829	-9230	549.2
6+6.3+7.5 / 20	3	No	1943	647.7	592.2	186.8	76.8	-192.3	5209	-11080	539.4
7.5+6.3+6 / 20	3	No	2166	722	592.2	158.1	82.4	-142.7	5606	-8798	530.9
7 / 20	3	No	2354	784.7	706.8	134.7	69.3	-118.7	4762	-7331	473.6
7 / 20	3	Pos	2156	718.7	706.8	141.7	72.9	-127	4687	-7820	499.9
7 / 20	3	Neg	2136	712	706.8	136.3	70.3	-125.7	4391	-7654	494.1
8 / 20	3	No	3079	1026.3	1206	101.8	46.6	-87.1	3125	-5533	279.7
9 / 20	3	No	3951	1317	1931.4	82.1	32.7	-68	2619	-4403	310.6
9.5 / 50	3	No	4606	1535.3	2397.6	78.3	33	-66	2419	-4241	1392
9.5 / 20	3	No	4384	1461.3	2397.6	81.1	30.5	-71	2323	-4480	1221
4 / 20	4	No	1032	258	100.4	633.3	250.2	-716.4	16290	-39090	1603
5 / 20	4	No	1648	412	245.6	265.1	135.9	-243	9063	-14840	843.9
6 / 20	4	No	2397	599.25	508.8	158.2	79.9	-136.9	5403	-8521	515.2
3x6.3+6 / 20	4	No	2603	650.75	591	146.8	71.6	-124.8	4848	-7870	484.8
6+3x6.3 / 20	4	No	2578	644.5	591	148	71	-123.3	4829	-7938	479
6.3 / 20	4	No	2734	683.5	618.4	143.7	63.4	-119.7	4722	-7611	502.1
3x6.3+7 / 20	4	No	2767	691.75	699.4	136.3	61.9	-113.3	4379	-7310	449.7

Pin diameter (s) / spacing (mm)	Pin no.	Pin offset?	Cort vol removed	Mean Cort Vol removed	Total PAMi (mm4)	VM stress max (MPa)	Pr. stress max (MPa)	Pr stress min (MPa)	Pr strain max (με)	Pr strain min (με)	Pin VM stress max (MPa)
7 + 3x6.3 / 20	4	No	2824	706	699.4	132.4	62.6	-110	4273	-7108	461.8
5+6+7+7.5 / 20	4	No	2728	682	734.6	141.4	60.8	-115.4	4635	-7480	453.6
7.5+7+6+5 / 20	4	No	2941	735.25	734.6	136.5	65.2	-124.7	4581	-7231	2044
7 / 20	4	No	3274	818.5	942.4	115.1	49	-95.8	3722	-6170	404.4
7 / 20	4	Neg	3065	766.25	942.4	121.8	50	-100.8	3911	-6514	423.4
7 / 20	4	Pos	3090	772.5	942.4	116.6	50.2	-96.5	3739	-6236	408.8
8 / 20	4	No	4299	1074.75	1608	89.9	35.9	-74.3	2874	-4817	244.4
4 / 20	5	No	1335	267	126	507.5	201.7	-602.3	13070	-31620	1291
5 / 20	5	No	2138	427.6	307	198.4	97	-193.9	6586	-11190	665.8
4x4+8 / 20	5	No	1964	392.8	502.4	177.5	82.2	-149.5	5713	-9585	599.3
4x5.5+6.3 / 20	5	No	2706	541.2	513.8	157	66.2	-127.2	5179	-8291	517.4
6.3+4x5.5 / 20	5	No	2798	559.6	513.8	154.9	66.2	-131.2	5130	-8165	531.9
2x5+2x6 +6.3 / 20	5	No	2703	540.6	531.6	155.4	72.7	-129.6	5008	-8364	506.9
6.3+2x6+2x5 / 20	5	No	2818	563.6	531.6	152	74.1	-134	4941	-8184	501.4
5+3x6+6.3 / 20	5	No	2910	582	597.6	144.9	66	-121.2	4666	-7799	469.7
6.3+3x6+5 / 20	5	No	3006	601.2	597.6	144.8	67.1	-120.8	4637	-7796	478
6 / 20	5	No	3064	612.8	636	139.1	60.3	-115.9	4493	-7477	455.4
7 / 20	5	No	4201	840.2	1178	104.2	42.3	-86.8	3372	-5603	365.4
8 / 20	5	No	5499	1099.8	2010	84.2	32.7	-69.8	2681	-4516	226.3
4 / 20	6	No	1642	273.7	151.2	401.3	168.8	**-464.4**	11070	-24630	1086
5 / 20	6	No	2594	432.3	368	174.1	86	-144.4	5821	-9338	582.2

Pin diameter (s) / spacing (mm)	Pin no.	Pin offset?	Cort vol removed	Mean Cort Vol removed	Total PAMi (mm4)	VM stress max (MPa)	Pr. stress max (MPa)	Pr stress min (MPa)	Pr strain max (με)	Pr strain min (με)	Pin VM stress max (MPa)
3x5+3x5.5 / 20	6	No	2810	468.3	452	160	68.9	-135.9	5221	-8545	539
4x5+2x6 / 20	6	No	2982	497	499.8	157.2	65	-126.1	5203	-8290	530
4x4.8+2x6.3 / 20	6	Pos	2740	456.7	517.6	162.8	68.3	-134.7	5280	-8671	561.3
4x4.8+2x6.3 / 20	6	No	2910	485	517.6	157.4	64.4	-126.5	5186	-8313	534.1
4x4.8+2x6.3 / 10	6	Pos	2590	431.7	517.6	156	73.5	-130.5	5009	-8392	514.8
5.5 / 20	6	No	3206	534.3	538.8	144.8	58.1	-115.5	4834	-7617	494
5.5 / 20	6	Pos	3050	508.3	538.8	145.6	64	-128.4	4609	-7928	494
5.5 / 20	6	Neg	3052	508.7	538.8	140.1	60.9	-119.1	4579	-7615	494.6
6 / 20	6	No	3750	625	763.2	117.8	51.1	-97	3898	-6274	414.4
6.3 / 20	6	No	4146	691	463.8	105.6	46.4	-86.7	3433	-5624	385.7

Table 4.3 Recorded and calculated variables of 14 transcortical pin configurations selected from 67 finite element models of pins placed in the equine MC3. All of these models have a principal maximum strain ≤ ~ 5000 microstrain, a principal minimum strain ≥ ~-10,000 microstrain; a maximum pin to bone diameter ratio of < 0.25 and a mean pin to bone diameter ratio of < 0.23. The order of pin diameters indicated is from proximal to distal in MC3. See legend of table 4.2 for abbreviations.

Pin diameter (s) / spacing (mm)	Pin no.	Pin offset?	Cort vol removed	Mean Cort Vol removed	Total PAMi (mm^4)	Pr strain max (με)	Pr strain min (με)	Max pin diam:bone diam. ratio	Mean pin diam:bone diam. ratio	Mean cort area fraction
3x6.3+6 / 20	4	No	2603	650.75	591	4848	-7870	0.229	0.224	0.9513
6+3x6.3 / 20	4	No	2578	644.5	591	4829	-7938	0.229	0.224	0.9514
6.3 / 20	4	No	2734	683.5	618.4	4722	-7611	0.229	0.226	0.9508
2x5+2x6 +6.3 / 20	5	No	2703	540.6	531.6	5008	-8364	0.227	0.202	0.9559
6.3+2x6+2x5 / 20	5	No	2818	563.6	531.6	4941	-8184	0.218	0.201	0.9553
5+3x6+6.3 / 20	5	No	2910	582	597.6	4666	-7799	0.227	0.209	0.9542
6.3+3x6+5 / 20	5	No	3006	601.2	597.6	4637	-7796	0.218	0.208	0.9537
6 / 20	5	No	3064	612.8	636	4493	-7477	0.218	0.213	0.9529
4x4.8+2x6.3 / 10	6	Pos	2590	431.7	517.6	5009	-8392	0.227	0.191	0.959
5.5 / 20	6	No	3206	534.3	538.8	4834	-7617	0.2	0.195	0.9567
5.5 / 20	6	Pos	3050	508.3	538.8	4609	-7928	0.2	0.195	0.9567
5.5 / 20	6	Neg	3052	508.7	538.8	4579	-7615	0.2	0.195	0.9567
6 / 20	6	No	3750	625	763.2	3898	-6274	0.218	0.213	0.9527
6.3 / 20	6	No	4146	691	463.8	3433	-5624	0.229	0.223	0.9504

Table 4.4 Hole location of peak cortical bone von Mises, tensile and compressive stresses and strains among 14 preferred transfixation cast configurations. Hole locations were numbered from proximal to distal in each construct such that the proximal hole was always number 1. Abbreviations: No. = number; mm = millimeters; VM = von Mises; Pr = principal; max = maximum; min = minimum; pos = positive; neg = negative; Prox = proximal; Md = medial; Lat = lateral; Pa = palmar; Ds = Dorsal.

Pin diameter (s) / spacing (mm)	**Pin no.**	**Pin offset?**	**Total PAMi (mm^4)**	**VM stress max**	**Pr. stress max**	**Pr stress min**	**Pr strain max**	**Pr strain min**
3x6.3+6 / 20	4	No	591	Prox. Md - 1	Ds. Prox. Md - 4	Prox. Md - 4	Prox. Md - 1	Prox. Md - 1
6+3x6.3 / 20	4	No	591	Prox. Md - 1	Prox. Md - 4	Prox. Md - 1	Prox. Md - 1	Prox. Md - 1
6.3 / 20	4	No	618.4	Prox. Md - 1	Prox. Md - 3	Prox. Md - 4	Prox. Md - 3	Prox. Md - 1
2x5+2x6 +6.3 / 20	5	No	531.6	Prox. Md - 1	Prox. Md - 3	Prox. Md – 1	Prox. Md - 3	Prox. Md - 1
6.3+2x6+2x5 / 20	5	No	531.6	Prox. Md - 1	Prox. Md - 4	Prox. Md – 1	Prox. Md - 1	Prox. Md - 1
5+3x6+6.3 / 20	5	No	597.6	Prox. Md - 1	Prox. Md - 4	Prox. Md – 1	Prox. Md - 1	Prox. Md - 1
6.3+3x6+5 / 20	5	No	597.6	Prox. Md - 1	Prox. Md - 4	Prox. Md - 1	Prox. Md - 1	Prox. Md - 1
6 / 20	5	No	636	Prox. Md - 1	Prox. Md - 4	Prox. Lat - 5	Prox. Md - 4	Prox. Md - 1
4x4.8+2x6.3 / 10	6	Pos	517.6	Prox. Md - 1	Ds. Prox. Md - 6	Prox. Md - 1	Prox. Md - 1	Prox. Md - 1
5.5 / 20	6	No	538.8	Prox. Md - 1	Pa. Prox. Md - 5	Prox. Lat - 6	Prox. Md - 1	Prox. Md - 1
5.5 / 20	6	Pos	538.8	Prox. Md - 1	Ds. Prox. Md - 6	Prox. Md – 1	Prox. Md - 1	Prox. Md - 1
5.5 / 20	6	Neg	538.8	Prox. Md - 1	Ds. Prox. Md - 6	Prox. Md – 1	Prox. Md - 1	Prox. Md - 1
6 / 20	6	No	763.2	Prox. Md - 1	Pa. Prox. Md - 1	Prox. Md – 1	Prox. Md - 1	Prox. Md - 1
6.3 / 20	6	No	463.8	Prox. Md - 1	Prox. Md - 1	Prox. Md – 1	Prox. Md - 1	Prox. Md - 1

Chapter 5: An evaluation of the effect of cast material properties and pin attachment on bone pin interface stresses in a finite element model of the equine distal limb transfixation cast

Manuscript to be submitted to the American Journal of Veterinary Research.

CHAPTER 5. AN EVALUATION OF THE EFFECT OF CAST MATERIAL PROPERTIES AND PIN ATTACHMENT ON BONE PIN INTERFACE STRESSES IN A FINITE ELEMENT MODEL OF THE EQUINE DISTAL LIMB TRANSFIXATION CAST

5.1 Introduction

Transfixation casting is an alternative method of external fixation typically used in the horse for managing distal limb fractures that are not suited to internal fixation.[1–4] The major complications of transfixation casting arise at the **bone-pin interface (BPI)** in the form of pin loosening and secondary pin hole fracture. These complications are related to mechanical overload at the pin hole resulting from stresses which exceed the local yield and failure stresses of the bone.[5] Currently, there is a paucity of information available on the BPI stresses present during transfixation casting[6] although information can reasonably be extrapolated from what is known about external skeletal fixation pins and their use in humans and small animals. Various models of external fixation have been developed as a means of understanding the stresses at the BPI. These models aim to represent the actual situation, enabling relevant information regarding unmeasured or unmeasurable aspects of the system to be extrapolated. Assumptions typically need to be made regarding boundary conditions and material behavior during the modeling process. Previous attempts to model the mechanics of an external fixator generally assume that the clamp attachment between the pin and the side bar is rigidly fixed and stable.[7–9] It has been shown that the validity of this assumption is questionable, particularly within unilateral fixators, and can significantly affect the overall stiffness of the construct and the accuracy of modeling predictions.[10–12] Previous attempts to model the equine transfixation cast using finite element analysis, including our own, have also assumed that there is

perfect stability between the pin and the cast.[6] In light of previous findings in external fixators this assumption warrants investigation, as it may not be an accurate representation of the actual clinical situation.

In contrast to external fixation, where pins are attached to sidebars using specifically designed clamps, transfixation casting utilizes fiberglass cast material to incorporate the pins and act as their external attachment during fixation. There are three key mechanical differences between the connections of a side bar in external fixation and the fiberglass cast material used for a transfixation cast. First, properly applied cast material acts as a solitary unit for the transfixation cast while connecting rods and side bars are connected to each other in a specific configuration. Second, the distance from the inner surface of the cast to the BPI, or the pin working length, is considerably shorter than the distance from the side bar to the BPI in an external fixator.[13] Finally, side bars and connecting rods are made from materials which have a relatively high modulus of elasticity compared to fiberglass cast material, and as such contribute to construct stiffness.[7,8] Previous investigators have examined how altering the method of attachment at the **cast-pin interface (CPI)** affects the stiffness of a transfixation cast construct by modifying the exposed pin ends with additional attachments.[13] This study showed that the axial stability of the transfixation cast is primarily determined by the properties of the fiberglass casting material itself.[13] However, it is currently unknown how the stability at the CPI or the stiffness of the cast affect the overall stiffness of the transfixation cast construct and the stresses observed at the BPI.

We have developed a **finite element (FE)** model of the equine distal limb transfixation cast in order to systematically evaluate modifiable parameters within the system. Considering the lack of information available regarding the stability of the pin embedded within the cast, and the importance of the assumptions made on the accuracy of FE models, the purpose of the study reported here was to determine the effect of CPI stability and cast stiffness on BPI stresses in the equine third metacarpal bone during transfixation casting. We hypothesized that increasing the stability of the CPI will decrease the BPI

stresses in the equine third metacarpal bone. In addition, we hypothesized that increasing the stiffness of the cast will decrease the BPI stresses in the equine third metacarpal bone. We tested these hypotheses using a previously developed FE model of preferred pin-bone constructs for the equine distal limb transfixation cast. The models were used to compare the predicted BPI stresses resulting from different pin-cast attachment settings and cast properties.

5.2 Materials and Methods

5.2.1 Study design

An FE model of the distal limb transfixation cast in the horse was used to evaluate the effect of altering cast attachment and cast stiffness on BPI stresses. The model comprised the distal 70% of the equine **third metacarpal bone (MC3)**, transcortical pins positioned within the bone and the cast positioned around the bone to engage the pin ends. Bone-pin constructs used for analysis were a 4 pin construct using one 6 mm pin with three 6.3 mm pins and a 6 pin construct using 6.3 mm pins. All pins were aligned within the frontal plane in both constructs. For each bone-pin construct, 2 alternate settings for CPI stability were modeled and compared to full constraint of the pin ends in all 3 axes. Cast stiffness was evaluated by altering both the value of Young's modulus for the cast material and by changing the thickness of the cast applied over the pins. The maximum cortical bone von Mises stress in each model was compared to evaluate the effect of changes in the CPI on predictions of BPI stress.

5.2.2 Finite element modeling

5.2.2.1 Bone and pins

All modeling procedures were performed within an FE software program (Abaqus, v.6.12, Dassault Systemes Simulia Corp, RI, USA). The MC3 model was developed from a computed tomography scan (Lightspeed VCT, General Electric, Milwaukee, WI) of the distal limb of a 10 year old Quarter Horse gelding which was performed with a slice thickness of 3.75 mm. Slice images of the scan were used to manually map geometric information regarding both the cortical bone and the cancellous bone envelopes into the FE software program. Thirty-nine slice images of interest were imported into image processing software (Image J, v1.46r, National Institutes of Health, http://imagej.nih.gov/ij) to perform measurements and manual shape fitting procedures on each slice. Measurements of cortical and medullary thickness were made for each slice at dorsal, palmar, lateral and medial aspects of the bone. Shape fitting procedures involved fitting of an ellipse to either the cortical or the cancellous envelope and then modifying this basic shape to visually match the slice image. The second and fourth metacarpal bones were not included in the shape fitting or modeling process. Lofting or extrusion procedures were performed to create the solid shape from the slice data directly within the FE software. The cancellous portion of the metaphysis was formed using Boolean operations following creation of the cortical envelope and the creation of a model of the medullary canal to perform subtraction. The final bone model represented the distal 70% of the MC3 excluding the metacarpal condyles. Construction of the bone model in this way allowed the use of solid quadratic tetrahedral elements to be used for FE analysis and an improved surface stress formulation that is available within the FE software program. The MC3 model was retained as a part within the model database. Smooth pins of either 6 or 6.3 mm diameter (depending on the construct), 70 mm in length, were constructed directly within the FE software program and inserted into the bone model using Boolean procedures. Contact interactions, load and boundary

conditions, meshing and remeshing were then performed to create the final meshed model for analysis.

A 9 mm distance from the outer cortical bone margin to the pin end contact with the cast (pin working length) was used for all models. A static analysis was used with a 7500 N distributed axial compressive load applied to the proximal surface of the MC3. This load and distribution has been shown to approximate the in vivo mid-diaphyseal surface strains of the MC3 when applied during ex vivo testing.[14] Materials were all modeled as isotropic with a Poisson's ratio of 0.3. The Young's modulus was set for cortical bone, cancellous bone, and stainless steel pins at 17, 0.5 and 205 GPa, respectively.[15–17] Free meshing algorithms were used for all meshing procedures. All models were meshed using solid quadratic tetrahedral elements (C3D10I), formulated for accurate surface stress predictions with enforced pressure continuity across material boundaries. Adaptive remeshing was performed to refine the MC3 mesh for each of the pin constructs based upon the output variable von Mises stress. A maximum of 2% difference from one mesh to the next was used to establish convergence and stop the adaptive remeshing procedure. The bone end distal to the pins was restrained in the x- and y- axes (transverse) but allowed to move freely proximal to distal in the z-axis. This was used to simulate the most extreme transfixation casting situation where a fracture is completely unstable under axial load. For the BPI, a non-linear surface to surface contact stiffness was applied for all models. Separation of surfaces after contact and sliding between surfaces was allowed. Any overclosure of surfaces under pressure was prevented. These conditions were intended to model the BPI soon after pin insertion. It has been shown that a fully bonded interface will result in an overestimation of the fixator stiffness and that these contact settings are important in the overall accuracy of the model.[11,12] Global seeds were set for the creation of each bone mesh, with approximate element size ranging from 4 to 6 mm.

5.2.2.2 Cast

The casts were constructed in a manner similar to the pins using extrusion of the cast shape to create an elliptical cylinder and a solid base. The cast material Young's modulus was set at 0.3 GPa based on 2 available values in the literature.[13,18] This value was used for all analyses except when modulus was examined as an independent variable. In order to restrict the analysis to axial compression and remove any bending or buckling effects of the cast, the outer cast wall was restrained in the transverse axes (x and y) in all models. In this way the variable of cast thickness primarily affected the compressive stiffness of the cast. The ground surface of the cast was restrained in all 3 axes.

Two methods of modeling the attachment of the pin within the cast were examined. To simulate the conventional transfixation casting method of creating slits in the cast material to allow it to be applied over the pins,[1,13,19] a sliding surface to surface contact was used, similar to the conditions applied at the BPI. This mode of attachment allows the pin and cast surfaces to slide and separate during loading, but does not allow overclosure of the surfaces by enforcing pressure continuity across the surface. In order to simulate the situation where the pin is firmly attached by wrapping cast material around the pin and completely embedding pins in the cast with reinforcement, as has been suggested with a modified transfixation casting approach,[3] the pin end was tied to the cast material at the surface to surface contact nodes. This mode of attachment does not allow separation of the pin from the cast material during loading. For all analyses the ends of the pins were restrained along their long axis (x-axis). During contact surface designation, all pin surfaces were set as master surfaces and cast and bone surfaces set as slave surfaces as it relates to the enforced behavior at the contact surface, due to the greater stiffness of the stainless steel pin material than the bone and the cast material.

Two methods were used to alter the stiffness of the cast in the model. The modulus of elasticity of the cast material was varied from 300 MPa to 1,000 MPa while keeping the

other parameters of the model unchanged. In addition, the thickness of the cast was changed from a thin cast to a thick cast. The thick cast had dimensions of 12 mm wall thickness and a 20 mm base. The thin cast had dimensions of 4 mm wall thickness and a 10 mm base. The same contact conditions were used between casts and the ends of the pins were only restrained along their long axis. To maintain the same distance along each pin from the inner cast wall to the bone surface, the thin cast had the pins ends protruded 1 mm beyond the outer margin of the cast, whereas the thick cast extended over the pin ends (**Figure 5.1**).

5.2.3 Data analysis

From each of the models constructed a series of data were collected and compared directly. The maximum cortical bone von Mises stress was used as the primary outcome variable of interest to compare the different model conditions evaluated. Other outcome variable of interest were maximum and minimum cortical bone principal stress and strain and their locations and maximum pin von Mises stress. The construct stiffness, calculated as the applied load divided by the axial displacement for each model was also compared.

5.3 Results

The maximum cortical bone von Mises stress was reflective of the other output variables collected, namely maximum and minimum principal stress and strain values, and is presented to illustrate the overall trends observed **(Table 5.1)**. Changing the CPI attachment from fixed pin ends as a boundary condition in the model to either a sliding surface contact with only x-axis pin end restraint, or a tied surface contact with only x-axis pin end restraint, resulted in an increase in the predicted maximum cortical bone von Mises stress at the BPI in both the 4 pin and 6 pin constructs **(Figure 5.2)**. The thick cast models had an average 21% lower cortical bone von Mises stress than the thin cast

models. The sliding contact condition resulted in an average 17% decrease in maximum cortical bone von Mises stress compared to the tied surface contact condition. Both of these conditions resulted in higher von Mises stress than having fixed pin ends as a boundary condition.

Increasing the cast stiffness by utilizing a thicker 12 mm cast resulted in a reduction in predicted maximum cortical bone von Mises stress at the BPI in both the 4 pin and 6 pin constructs compared to the thin cast with 4 mm walls. However, the von Mises stress values for the thicker cast construct were still higher than the fixed pin ends boundary condition, illustrating an underestimation of stresses when an assumption of fixed pin ends was made compared to when CPI attachment settings were included in the modeling process. The pin ends visibly separated from the cast material during loading when a sliding surface contact condition was examined, which was more obvious in the thin cast models than the thick cast models **(Figure 5.3)**. There was a relatively small decrease in predicted maximum cortical bone von Mises stress at the BPI when increases in cast modulus were used to increase the overall construct stiffness. A 5-fold increase in cast material modulus, from 200 MPa to 1000 MPa, resulted in only an 8% decrease in the maximum cortical bone von Mises stress in the 4 pin construct and a 10% decrease in the 6 pin construct **(Figure 5.4)**. There was a linear increase in construct stiffness with the increase in cast modulus applied with a 5-fold increase in modulus resulting in an approximately 4-fold increase in overall construct stiffness for the thin cast models of both bone pin constructs.

A different pattern of stress (and strain) distribution between the pin holes was observed when the fixed pin end boundary condition was replaced with either of the CPI surface contact conditions. Higher stresses surrounded the lower pin holes when the cast and CPI attachment conditions were included in the model **(Figure 5.5)**.

5.4 Discussion

The results of this study showed that the assumption of having a rigid and stable fixed pin end as a boundary condition in an FE model of the equine transfixation cast resulted in an underestimation of the maximum BPI stresses by approximately 20%. Finite element modeling results of 2 methods of simulating non-fixed CPI attachment showed that the sliding surface contact resulted in 17% lower BPI stresses on average than the tied surface contact. Increasing the overall stiffness of the construct by increasing the Young's modulus of the cast material 5-fold from 200 to 1000 MPa, reduced BPI stresses by an average of only 9% across the models evaluated. A fixed pin end boundary condition also had a different pattern of stress distribution between pins, with higher stresses at the more proximal pins compared to when a cast with CPI attachment conditions was included in the models. Taken together, these findings show that the assumption of using a fixed pin end in modeling the transfixation cast should be viewed with caution, as both quantitative and qualitative differences in maximum bone stress at the BPI are likely if the real conditions within the cast are not perfectly rigid. These findings support both of our original hypotheses.

Based on the results of this study, a cast that is applied to allow sliding of pins within the cast material but at the same time solid support on which the pin will pivot and bend during loading appears to be the most favorable for lowered BPI stresses. It is highly unlikely that the pin ends are fixed and rigid within the transfixation cast and so an effect of uneven pin loading throughout the cast when seen clinically may be a function of how well the pins are supported by the cast material at the CPI.

The study reported here is unable to conclude which method of modeling is closest to the real situation within a transfixation cast and further ex vivo and in vivo evaluation of the stability of the CPI is necessary. We did not account for friction in the contact surface

conditions studied and so the real situation may well be between the two simulations of sliding and tied surfaces. However, clinical observations would generally support that the CPI is not perfectly stable during transfixation casting. Both cracking and separation of cast material around pins and of synthetic polymethylmethacrylate used to cover pin ends has been observed, along with migration of pins relative to the cast during clinical use of the transfixation cast in horses.[1,20] These observations would also support that the sliding contact surfaces condition is likely to be closer to the real situation than the fully tied surface, even when efforts are made to wrap the casting tape around pin ends.[3]

The sliding contact surfaces condition allowed for pins to separate from the cast material during loading, making the cast material supporting the pin a base or pivot point from which the pin end could bend and move within. The tied contact surface condition resulted in the pin ends moving with the cast material and flexing less during loading. It was expected that the tied contact surface condition would result in a more stable pin end and be closer to the fixed pin end boundary condition. However, being tied to the cast material resulted in the entire pin end moving with the cast material as it deformed during loading. The result was a higher construct stiffness, higher pin and bone stresses when compared to the sliding contact surface. Further work is needed to elucidate the best fitting contact conditions for the pin ends within a transfixation cast to be modeled accurately to investigate these phenomena further.

Fiberglass casting material has changed the ease of use of casts in the horse when compared to plaster of Paris.[21] Fiberglass casting material is faster to cure, lighter weight, less susceptible to breakdown in a fluid environment, stiffer and stronger than plaster of Paris.[18] The modulus of elasticity of fiberglass casting material has been estimated to be 316 MPa in a tensile material test.[18] A compressive modulus of 256 MPa was reported by McClure et al in an in vitro study evaluating methods of attachment of transfixation pins to fiberglass casting material.[13] In comparison, typical sidebar material for external skeletal fixators has a considerably higher modulus of elasticity at approximately 200

GPa.[8] We used a baseline cast modulus value of 300 MPa but chose to evaluate modulus values from 200 to 1000 MPa in each model to assess whether altering the cast material itself would be expected to achieve a more stable construct overall since current and future technologies may be utilized to produce a cast material with higher stiffness. The results of the present study show that even several fold increases in the modulus of the cast material will only have a marginal effect on lowering the BPI stresses within a transfixation cast. In support of previous conclusions by McClure et al, increasing the number of pins within the cast, and consequently the surface area for load distribution, did result in a slightly higher construct stiffness for the 6 pin models when compared to the 4 pin models with concurrently lower BPI stresses.[13]

Apart from the mechanical differences between external skeletal fixation and transfixation casting outlined earlier, as they relate to the performance of a sidebar compared to a cast, a fourth difference between external fixators and the transfixation cast is the resistance to bending that a cast provides independently of the transcortical pins. A multiplanar external fixator provides good bending resistance in multiple directions through the sidebar connections to the pins. A transfixation cast provides bending resistance of the entire limb in multiple directions through the stiffness of the cast material and its proximity to the limb surface in a conforming multilayered shell. Transfixation casts have been shown to effectively reduce axial displacement below the pins and for this reason are effective when used to manage axially unstable fractures which are not amenable to internal fixation. The results of the present study highlight the need to closely examine assumptions that are made from external fixation mechanics and applied to transfixation casting. The overall constructs are sufficiently different to raise caution in accepting many of the modeling assumptions that are made.

Limitations of the present study include the lack of validation of our findings with ex vivo or in vivo studies of the true CPI interactions and stability. However, our purpose was to determine the effect of changing CPI conditions on BPI stresses in the MC3. We have previously validated the model used in the present study with a single pin loaded in

axial compression. The conclusions of the current study would be expected to remain consistent even if the quantitative values for the conditions examined change. Other limitations include those inherent with any modeling process, with multiple assumptions made to allow simplified modeling procedures to cover a broad range of constructs and to examine several CPI attachment scenarios. The findings presented here provide an initial point from which to work towards a more complete and accurate model. Our results show that the CPI attachment is an important area of future work if more accurate FE models are to be generated for transfixation casting in the horse.

In conclusion, the results presented here show that BPI stresses within a model of the equine transfixation cast are increased when CPI attachments are modeled as being sliding contact surfaces or tied contact surfaces as opposed to an idealized fixed pin end. In addition, it was shown that increasing the stiffness of the cast decreased the BPI stresses in the equine MC3, which should be confirmed with further ex vivo and in vivo investigation.

5.5 List of References

1. Lescun TB, McClure SR, Ward MP, et al. Evaluation of transfixation casting for treatment of third metacarpal, third metatarsal, and phalangeal fractures in horses: 37 cases (1994-2004). *J Am Vet Med Assoc* 2007;230:1340–1349.

2. Joyce J, Baxter GM, Sarrafian TL, et al. Use of transfixation pin casts to treat adult horses with comminuted phalangeal fractures: 20 cases (1993-2003). *J Am Vet Med Assoc* 2006;229:725–730.

3. Rossignol F, Vitte A, Boening J. Use of a modified transfixation pin cast for treatment of comminuted phalangeal fractures in horses. *Vet Surg* 2014;43:66–72.

4. Kraus BM, Richardson DW, Nunamaker DM, et al. Management of comminuted fractures of the proximal phalanx in horses: 64 cases (1983-2001). *J Am Vet Med Assoc* 2004;224:254–263.

5. Pettine KA, Chao EY, Kelly PJ. Analysis of the external fixator pin-bone interface. *Clin Orthop Relat Res* 1993:18–27.

6. Brianza S, Brighenti V, Lansdowne JL, et al. Finite element analysis of a novel pin-sleeve system for external fixation of distal limb fractures in horses. *Vet J* 2011;190:260–267.

7. Huiskes R, Chao EY, Crippen TE. Parametric analyses of pin-bone stresses in external fracture fixation devices. *J Orthop Res* 1985;3:341–349.

8. Huiskes R, Chao EY. Guidelines for external fixation frame rigidity and stresses. *J Orthop Res* 1986;4:68–75.

9. Aro HT, Chao EY. Biomechanics and biology of fracture repair under external fixation. *Hand Clin* 1993;9:531–542.

10. Drijber FL, Finlay JB, Dempsey AJ. Evaluation of linear finite-element analysis models' assumptions for external fixation devices. *J Biomech* 1992;25:849–855.

11. Karunratanakul K, Schrooten J, Van Oosterwyck H. Finite element modelling of a unilateral fixator for bone reconstruction: Importance of contact settings. *Med Eng Phys* 2010;32:461–467.

12. Karunratanakul K, Kerckhofs G, Lammens J, et al. Validation of a finite element model of a unilateral external fixator in a rabbit tibia defect model. *Med Eng Phys* 2013;35:1037–1043.
13. McClure SR, Watkins JP, Hogan HA. In vitro evaluation of four methods of attaching transfixation pins into a fiberglass cast for use in horses. *Am J Vet Res* 1996;57:1098–1101.
14. Les CM, Stover SM, Taylor KT, et al. Ex vivo simulation of in vivo strain distributions in the equine metacarpus. *Equine Vet J* 1998;30:260–266.
15. Chen Q, Thouas GA. Metallic implant biomaterials. *Mater Sci Eng: R* 2015;87:1–57.
16. Stevenson M, Barkey M, Bradt R. Fatigue failures of austenitic stainless steel orthopedic fixation devices. *Pract Fail Analy* 2002;2:57–64.
17. Anonymous. Product Data Sheet - 316/316L Stainless Steel. 2007. Available at: www.aksteel.com.
18. Mihalko WM, Beaudoin AJ, Krause WR. Mechanical properties and material characteristics of orthopaedic casting material. *J Orthop Trauma* 1989;3:57–63.
19. McClure S, Honnas CM, Watkins JP. Managing equine fractures with external skeletal fixation. *Comp Cont Educ Pract Vet* 1995;17:1054–1063.
20. Lescun TB, Baird DK, Oliver LJ, et al. Comparison of hydroxyapatite-coated and uncoated pins for transfixation casting in horses. *Am J Vet Res* 2012;73:724–734.
21. Janicek JC, McClure SR, Lescun TB, et al. Risk factors associated with cast complications in horses: 398 cases (1997-2006). *J Am Vet Med Assoc* 2013;242:93–98.

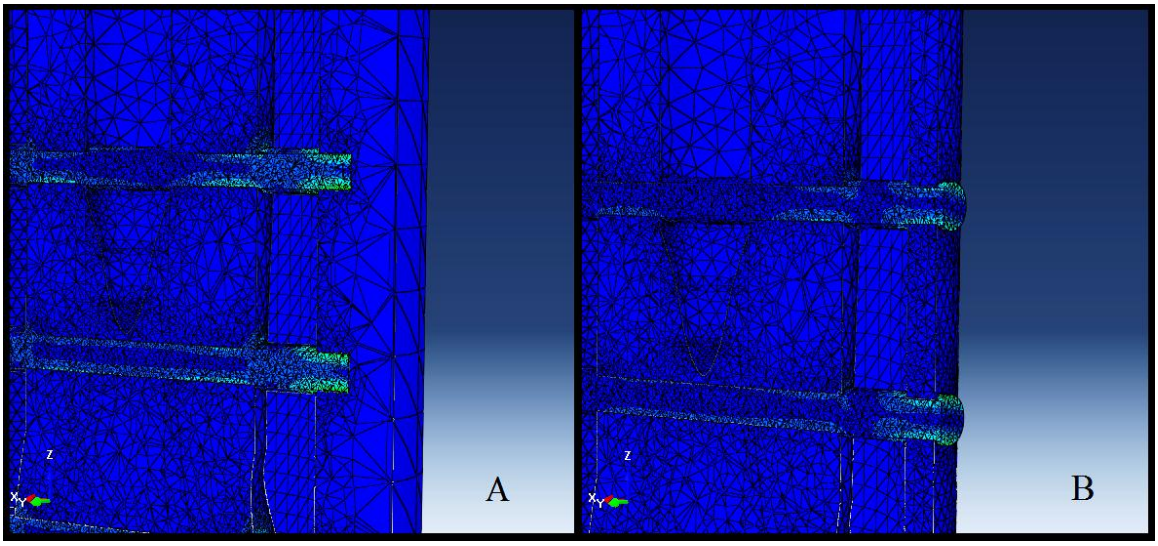

Figure 5.1 Image of the 2 cast thicknesses modeled by finite element analysis in the study. A. The thick cast was 12 mm and enclosed the end of the pin on each side of the bone. B The thin cast was 4 mm and did not enclose the pin end. For both casts, pins were restrained along their long axis, so movement from side to side within the cast and bone was not possible.

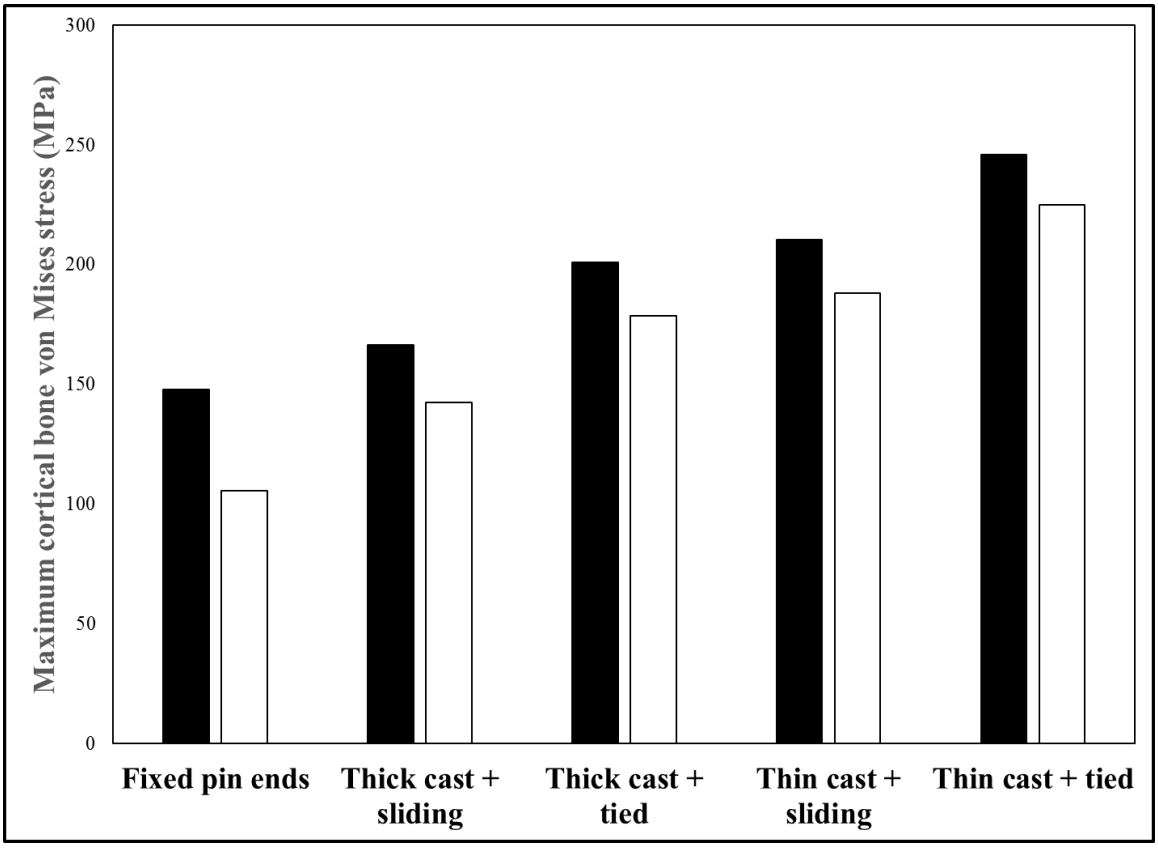

Figure 5.2 Bar chart showing the maximum cortical bone von Mises stress under a range of different cast pin interface modeling conditions. Values are shown for both a 4 pin construct (black bars) and a 6 pin construct (white bars). Fixed ends = pin ends are fixed in all three axes; Thick cast = a 12 mm cast wall. Thin cast = a 4 mm cast wall. Sliding = surface to surface contact which allows sliding and separation of surfaces during loading. Tied = surface to surface contact which ties contacted surfaces of the cast and pin during loading. All pins were held fixed in the x-axis so that they could not move along the pin length within either the bone or the cast.

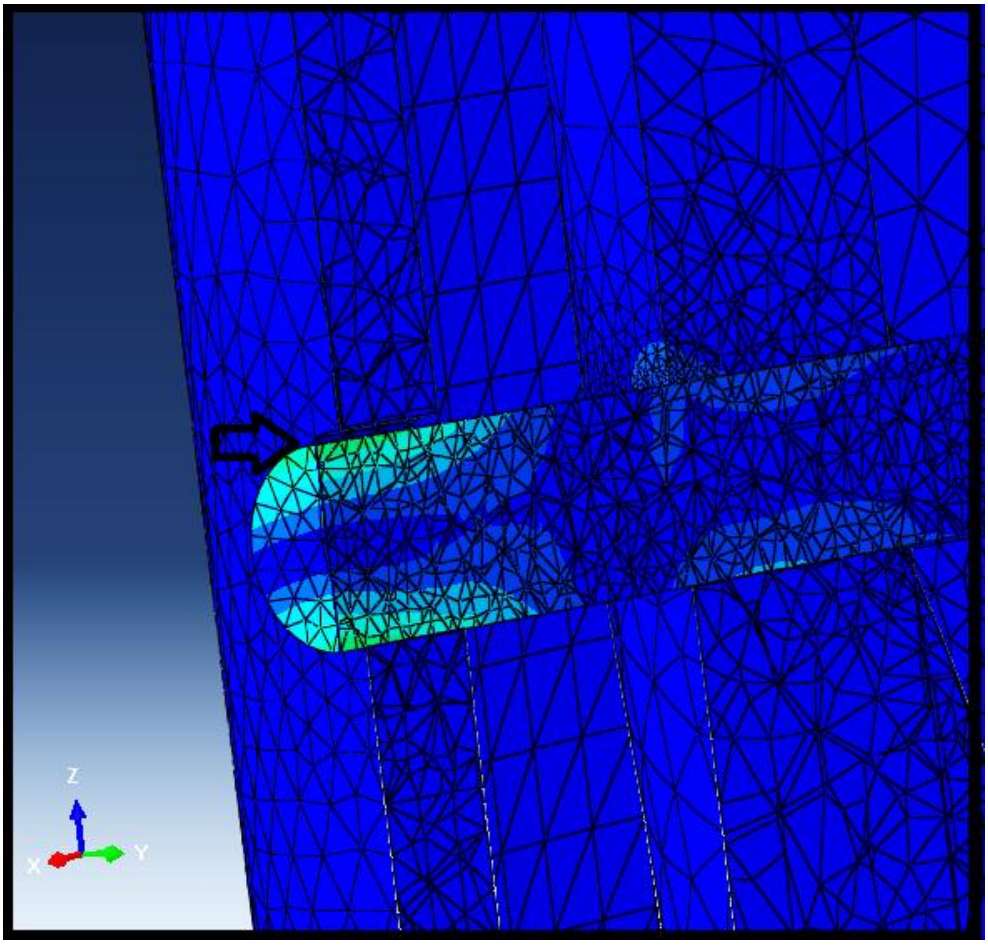

Figure 5.3 Image of the bone pin interface (right side) and cast pin interface (left side) in the thin cast model with sliding surface contact condition, showing separation of the pin from the cast material during loading (open black arrow). The thick cast model with sliding contacts also had separation of surfaces during loading.

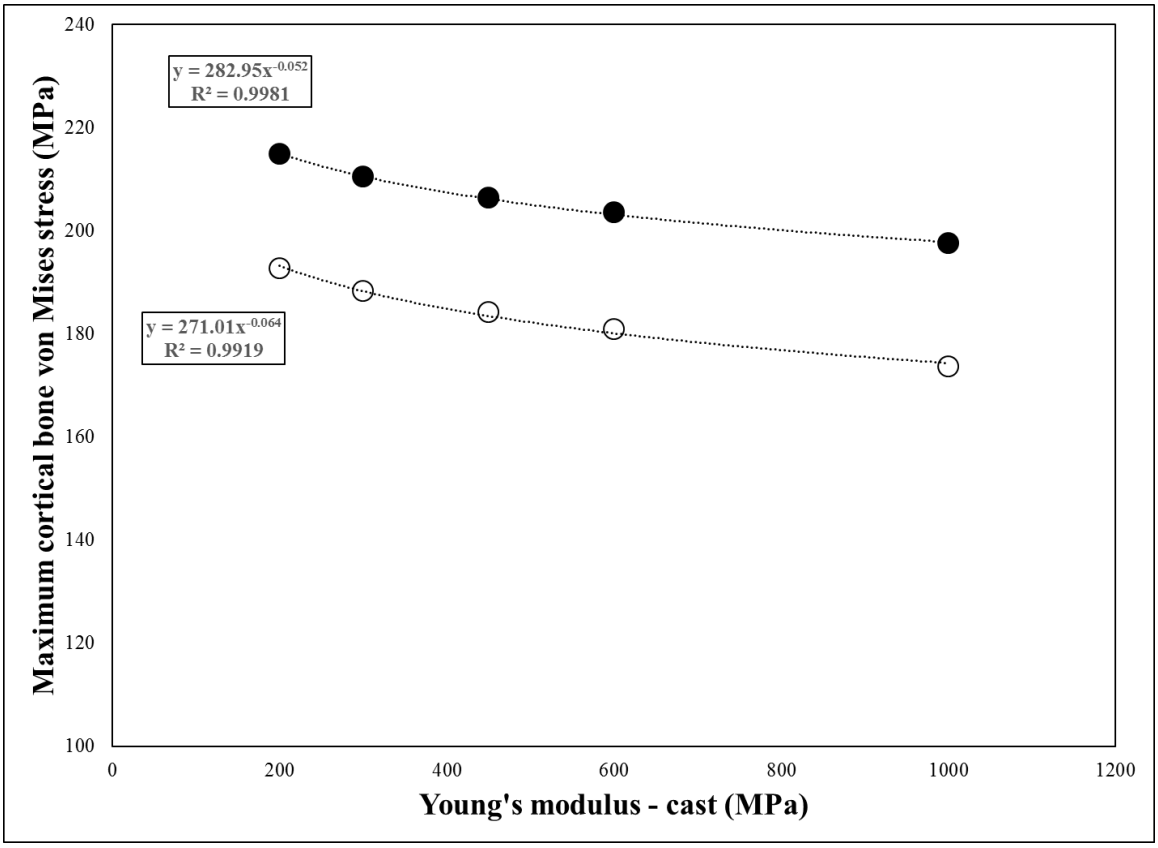

Figure 5.4 Cast material Young's modulus versus the maximum cortical bone von Mises stress for a 4 pin construct (solid black circles) and a 6 pin construct (open circles). Fitted power law equations with associated R^2 value (Pearson product moment correlation coefficient) are shown for pin bone construct.

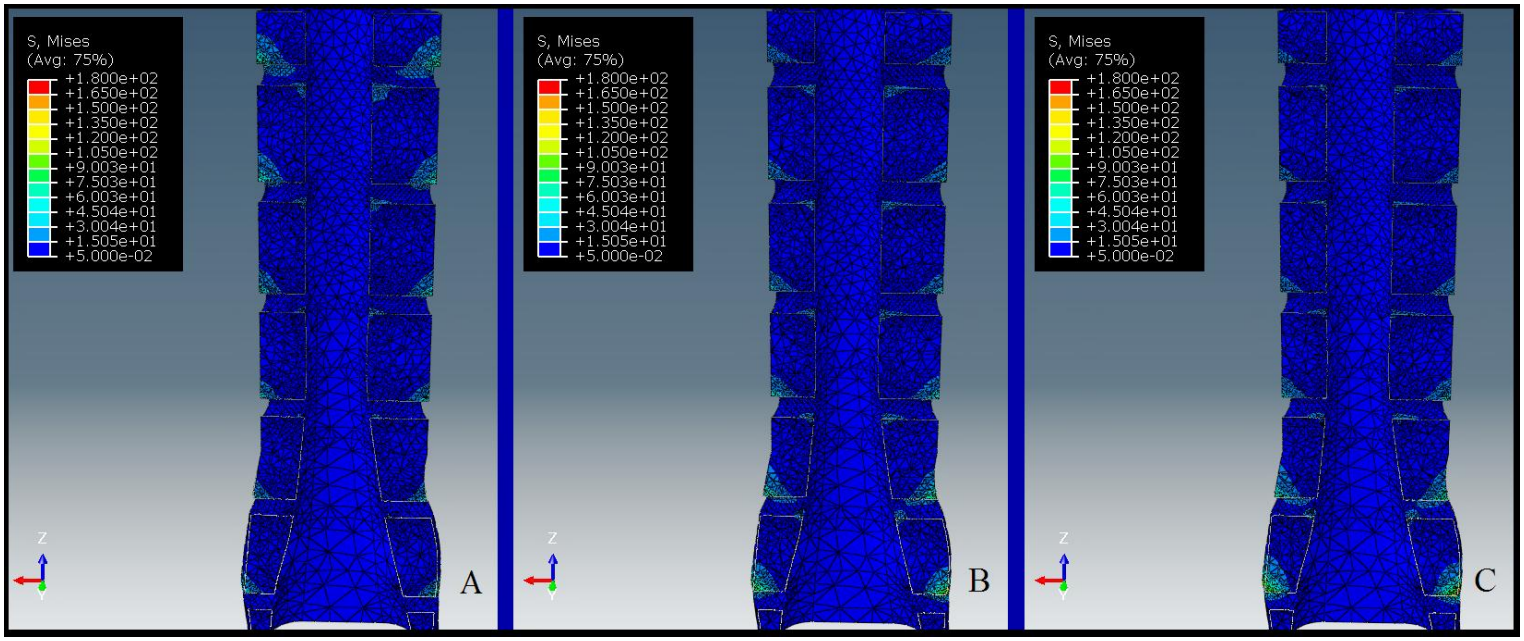

Figure 5.5 Image showing the overall cortical bone von Mises stress pattern in the third metacarpal bone for three different methods of modeling the cast pin interface in a 6 pin transfixation cast construct. The section is taken through the frontal plane of the third metacarpal bone. The pins and cast are not shown. A = pin ends were fixed in all 3 axes as a boundary condition of the model. B = pin ends were allowed free movement in y and z axes and sliding contact with cast. C = pin ends allowed free movement in y and z axes and have tied contact with the cast. The legend in the upper left hand corner shows the color scale and values for von Mises stress and is the same scale between images. Notice that the stress distribution among pin holes is different in Images B and C, compared to Image A, with higher stresses occurring at the lower pin holes in Images B and C where the cast pin interface contact conditions were applied.

Table 5.1 Results from FE analysis of 2 different bone pin constructs for a distal limb transfixation cast using 3 different methods of modeling the cast pin interface attachment and 2 different cast thicknesses. Abbreviations: VM = von Mises stress; MPa = megapascals; µstrain = microstrain (10^{-6} strain).

		Bone VM	**Principal stress (MPa)**		**Principal strain (µstrain)**		**Pin VM**	**Construct**
		(MPa)	**Maximum**	**Minimum**	**Maximum**	**Minimum**	**(MPa)**	**stiffness (N/mm)**
4 pins constructs								
Fixed pin ends		148	71	-123.3	4829	-7938	479	57,383
Thick cast	Sliding	166.5	87.7	-152	5453	-9361	456.3	8,182
	Tied	201	103.9	-183	6440	-11280	571.1	10,362
Thin cast	Sliding	210.4	108.8	-191.5	6744	-11810	527.3	4,213
	Tied	245.9	126.6	-223.7	7855	-13800	585.7	4,870
6 pin constructs								
Fixed pin ends		105.6	46.4	-86.7	3433	-5624	385.7	92,822
Thick cast	Sliding	142.3	79.6	-127.6	4876	-7895	426.2	9,141
	Tied	178.8	98.3	-159.8	6074	-9899	558.8	10,949
Thin cast	Sliding	188.2	103.7	-168.2	6402	-10420	514.3	4,358
	Tied	225	123.6	-201	7642	-12460	583	4,957

Chapter 6: The effect of altered distal loading conditions within the equine transfixation cast on bone pin interface stresses in the equine third metacarpal bone.

Manuscript to be submitted to the American Journal of Veterinary Research.

CHAPTER 6. THE EFFECT OF ALTERED DISTAL LOADING CONDITIONS WITHIN THE EQUINE TRANSFIXATION CAST ON BONE PIN INTERFACE STRESSES IN THE EQUINE THIRD METACARPAL BONE

6.1 Introduction

The equine distal limb transfixation cast effectively reduces the strain within the proximal phalanx by greater than 80%, and displacement of experimental osteotomies over 6-fold when compared to a standard short limb cast.[1,2] The effectiveness of the transfixation cast in diverting weight bearing loads away from the skeleton distal to the transcortical pins is the primary reason it is an effective method for managing severely comminuted proximal and middle phalanx fractures in the horse.[3–5] This effective load transfer from the proximal skeleton through the transcortical pins and cast to the ground results in substantial stress at the **bone pin interface (BPI)**.[6] Complications observed during transfixation casting in the horse are related to both the large stresses at the BPI and the extent of load transfer away from the skeleton below the transfixation pins. These complications include pin loosening, secondary pin hole fracture, radiographic osteopenia, pathologic fractures of the proximal sesamoid bones and delayed mineralization of fractures.[3–5]

The concept of dynamization of external skeletal fixation, whereby alterations in the fixation construct are made during fracture healing in order to alter the stresses at the fracture site, results in improved callus remodeling, particularly after the early stages of fracture healing have occurred.[7–13] Recently, the effect of staggered removal of pins from a transfixation cast was evaluated and it was shown that removing the top pin or pins, depending on whether a 2 or 4 pin construct was used, resulted in an up to 10%

increase in strain on the dorsal surface of P1.[14] Staggered pin removal is an attractive approach to apply the principles of fracture dynamization due to the ease with which it can be accomplished. However, reducing the number of pins in a construct is known to increase the stresses at the BPI for the remaining pins,[15,16] and so could increase the risk of complications such as secondary pin hole fracture in the horse.

As a result of the unique configuration of the transfixation cast compared to external skeletal fixation, whereby the cast surrounding the foot acts as the distal support of the fixation, increasing the stresses at the fracture site may be achieved by altering the loading conditions between the foot and the cast. However, it is currently unknown how the loading conditions distal to the transcortical pins affect local bone stresses and the BPI stresses. In addition, the stiffness of the tissues at the fracture site change during the course of fracture healing. Markel et al examined the material properties of the bone healing tissue within osteotomies over a 12 week period.[17] They found that the gap tissue gradually increases in stiffness over the course of healing whereas periosteal and endosteal tissue became no stiffer after 8 weeks. At 2 weeks, all three of the tissue types had less than 5% of the stiffness of cortical bone, by 4 weeks they were all still less than 7% and by 8 weeks this percentage had risen to 33%, 15% and 17% for periosteal, gap, and endosteal tissue, respectively. Understanding how alterations in the loading distal to the transcortical pins affect the stress and strain environment at the fracture site and the BPI would allow the development of methods to improve the fracture healing environment during transfixation casting in the horse. Therefore, the purpose of this study was to determine how changing the stiffness of tissues distal to the transcortical pins within the transfixation cast will affect local stresses at the BPI and within the bone segments distal to the transcortical pins. We used a previously developed **finite element (FE)** model of the equine distal limb transfixation cast to examine these concepts by altering the stiffness of a composite tissue block in the gap between the transcortical pins and the foot of the cast. In addition the presence of a material pad of fixed material properties between the foot and the cast was evaluated in terms of the contact pressure experienced between the pad and the cast. We hypothesized that increasing tissue

stiffness distal to the transcortical pins would increase stresses in bone distal to the pins and decrease the BPI stresses. In addition, we hypothesized that the stress patterns surrounding the BPI would be altered by an increase in the tissue stiffness and contact pressure between the foot and the cast.

6.2 Materials and Methods

6.2.1 Study design

A previously developed and validated model of the equine distal limb transfixation cast with transcortical pins positioned in the **third metacarpal bone (MC3)** was used to investigate the influence of alterations in the stiffness of the tissues between the base of the cast and the end of MC3 on BPI stresses and bone stresses distal to the transcortical pins. The stiffness of the tissues was represented by a composite tissue block within the cast and altered to mimic various time points during the fracture healing process. These were immediately following transfixation cast application, soft tissue only (0 - 250 MPa),[18,19] early (2-4 weeks) fracture healing tissue properties (250 – 1000 MPa) and late (8 weeks) fracture healing tissue properties (2500 MPa).[17] Loading of the proximal MC3 was performed at 7500 N to reflect loads expected in this bone during walking.[20] Output variables examined included maximum cortical bone von Mises stress, maximum and minimum cortical bone principal stress and strain, maximum pin von Mises stress, maximum displacement of the proximal bone surface and von Mises stress 10 mm distal to the most distal transcortical pin in the bone segment. The composite stiffness was calculated from the loading force and the maximum displacement value. Output values were compared to the modulus of the composite tissue block positioned between the cast and the distal MC3. In addition, a material pad of fixed properties was positioned between the base of the composite tissue block and the foot of the cast. Alterations in contact pressure between the pad and the cast were recorded and the effect of not having the pad in place was also assessed.

6.2.2 Finite element modeling approach

An FE model of the equine MC3, developed from a computed tomography scan as described previously, was combined with six smooth stainless steel transcortical pins of 6.3 mm diameter within an FE software program (Abaqus, v.6.12, Dassault Systemes Simulia Corp, RI, USA). The bone was aligned within the co-ordinate system such that the lateral to medial direction across the bone was the x-axis, the dorsal to palmar direction was the y-axis and the proximal to distal direction was the z-axis. Following positioning, bone was removed by placing pins in a line within the bone in a lateral to medial direction and within the frontal plane and performing Boolean subtraction to create pin holes. Pins were spaced 20 mm apart (edge to edge) beginning at a location 10 mm from the MC3 physeal scar and positioned proximally into the cortical bone of the diaphysis. Pins were centered in the bone and were all 70 mm in length. A cast was constructed that was 12 mm in thickness with a 20 mm base at the ground surface. The cast extended 154 mm beyond the distal end of MC3 based on the original CT scan of the limb used to create the MC3 model. The pin ends were enclosed by the cast following its positioning around the bone and distal limb segment. The distance from the pin contact with the bone surface and their contact with the inner cast surface was 9mm. The distal limb segment of the cast was filled with a composite tissue block, consisting of 14 sections 10 mm in thickness and one 4 mm in thickness. A foot pad 10 mm in thickness was positioned to occupy the space between the distal end of the composite tissue block and the cast. The Young's modulus of the composite tissue block was varied between 0 (suppressed in model) and 2500 MPa while all other parameters of the model remained unchanged. For comparison to a homogenous tissue block, the modulus of the composite tissue was also adjusted to simulate a comminuted fracture of the proximal phalanx by assigning a very low stiffness value to a 60 mm length (6 of the sections) of the block while maintaining the remainder at a stiffness equal to cortical bone. The Young's modulus of the foot pad was 100 MPa. The material properties of the bone and pins used for the models were based on previous studies.[21–23] The cortical bone was assigned a Young's modulus of 17 GPa and a density of 2000 g/cm^3. Cancellous bone was assigned

a Young's modulus of 0.5 GPa and a density of 500 g/cm^3. The stainless steel pins were assigned a Young's modulus of 205 GPa and a density of 8000 g/cm^3. The cast material was assigned a Young's modulus of 0.3 GPa and a density of 1080 g/cm^3. All materials were considered isotropic with linear elastic behavior. Free meshing algorithms were used for each of the parts of the model. Solid quadratic tetrahedral elements (C3D10I) formulated for accurate surface stress predictions were used. Mesh refinement using an adaptive remeshing procedure for each individual model was based upon the output variable von Mises stress. Remeshing was continued until no more than a 2% change in von Mises stress was present from the previous mesh. While the pins were embedded in the cast, they were also restrained from movement within their long axis (x-axis). All surface to surface contacts within the model were treated in the same manner, including the BPI, the cast pin interface and the interfaces between the composite tissue block, the foot pad, and the cast. The surface contacts were sliding contacts in which overclosure was prevented. This type of contact allows sliding between surfaces and separation with gap formation. The cast was restrained from buckling and bending by using a boundary condition on the wall in both the x- and y- axes. The cast was allowed to deform in the axial loading direction according to its material property assignment.

6.3 Results

Increasing the Young's modulus of the composite tissue block between the distal end of MC3 and the cast base resulted in a decrease in von Mises stress around the transcortical pins **(Figure 6.1)**, a decrease in the maximum and minimum principal strain around the transcortical pins **(Figure 6.2)**, an increase in von Mises stress distal to the transcortical pins **(Figure 6.3)**, an increase in the contact pressure on the foot pad between the cast and the composite tissue block **(Figure 6.4)**, and a decrease in the maximum pin von Mises stress **(Figure 6.5)**. There was a linear relationship between the increase in von Mises stress in the distal bone segment and the maximum contact pressure observed on the foot pad. There was also an increase in the construct stiffness observed as the composite tissue block modulus increased. The bone pin interface was always the location of the

maximum stresses and strains when the composite tissue modulus was below 500 MPa. Increases in tissue modulus from 500 to 2500 MPa moved the location of maximum principal stresses and strains away from the bone pin interface. Results for the maximum compressive and tensile principal stress values reflected the strain patterns in both quantitative changes and the strain distribution patterns observed.

For the simulated comminuted proximal phalanx fracture, lower maximum stress and strain values were observed compared to the homogenous composite tissue block set with the same modulus value as the simulated fracture segment. These results were similar whether the foot pad was in place or not. The cortical bone von Mises stress pattern surrounding the pin holes became less focal **(Figure 6.6)** and the maximum values at the BPI decreased as the modulus of the composite tissue block increased **(Figure 6.7)**. The maximum pin von Mises stress decreased from 426 MPa when there was no contact between the distal bone segment and the cast, to 63 MPa when the material block modulus was 500 MPa. Material block modulus values higher than 500 MPa resulted in a small increase in the maximum pin von Mises stress with a change in the location of the maximum from the proximal edge of the distal most pin to the distal edge of the distal most pin.

6.4 Discussion

The results of the present study support both of our hypotheses. In the distal limb transfixation cast model presented, increases in the stiffness of a composite tissue block between the distal end of the MC3 and the cast base resulted in an increase in the bone stress present in the segment distal to the transcortical pins, and a corresponding decrease in the maximum BPI stresses. Additionally, with increasing contact pressure and tissue stiffness below the pins, the stress pattern surrounding the transcortical pins was altered, displaying less focally increased stresses at the BPI and a more evenly distributed stress among the 6 transcortical pins used in this study.

The overall objective of this study was to explore the relationship between altered tissue stiffness in the fracture location during healing and the stress present in bone distal to and around the transcortical pins within a distal limb transfixation cast. The primary motivation was to determine whether it may be feasible, mechanically, to impact the stresses at the fracture site, and in bone tissue distal to the transcortical pins, during the transfixation casting period. Our results suggest that it may be possible, and provide a basis from which to develop such a system.

Significant morbidity has been observed following periods of transfixation casting with secondary pathologic proximal sesamoid bone fractures, radiographically observable osteopenia, cartilage thinning, poor fracture healing and slow callus mineralization.[4,5,24] Within a short period of transfixation casting, such as 4 weeks, that might avoid some of the complications attributable to the large stress reductions present distal to the pins, fracture stability is often insufficient to remove the pins. Periods of 6-8 weeks are currently recommended for the duration of transfixation casting.[4,5] Manipulating the loading in the distal portion of the cast below the transcortical pins could increase fracture stress (and strain) to improve fracture healing and minimize the other associated co-morbidities. It is proposed that this approach would be safer than staggered pin removal as it would, in theory, decrease BPI stresses. It has been previously shown for external fixation pins that reducing the number of pins is expected to increase the BPI stresses around those remaining.[16] We have also recently shown this with the FE model used for the present study.

A secondary motivation for this study was to determine, in a qualitative manner, how changes in the tissue stiffness during the fracture healing process, may affect BPI stresses within the transfixation cast. We used values of tissue modulus extrapolated from the study by Markel et al who looked at healing tissue within osteotomized tibiae of dogs.[17] The indentation modulus from that study, expressed as a percentage of the cortical tissue value similarly measured, was then used to calculate an estimated tissue modulus value from the cortical bone modulus of 17 GPa used here for equine bone. In this way, early

fracture callus from 2-4 weeks was represented by a tissue modulus of between 250 and 1000 MPa, while fracture callus at 8 weeks would have a tissue modulus of approximately 2500 MPa. This method of extrapolating the healing tissue modulus may be overestimating the true situation present in the healing fracture with a transfixation cast due to the stress protection that this study and others have shown to be present below the transcortical pins, at least early in the course of treatment. Regardless, understanding that increases in fracture stiffness should reduce BPI stresses during the course of transfixation casting may be important for tailoring different approaches to better stimulate fracture healing. Considering fracture healing biology, prior experience with external fixators and dynamization, and the results of the present study, the first cast change around 3-4 weeks would be the earliest recommended time to attempt to alter loading within the cast.

An additional aspect of transfixation casting that is supported by the results of the present study is the application of additional implants, such as cortical screws placed in lag fashion, where possible, to supplement the fracture fixation. While this is logical and has been recommended in terms of fracture fragment alignment, compression and fracture healing, it is also expected to be beneficial by reducing stresses at the BPI by providing greater stiffness of the fractured tissues, even if it is not sufficient for axial loading. In addition, even modest increases in the fractured tissue stiffness may increase stresses experienced in the bone distal to the transcortical pins, including the fracture site, thereby reducing the risk of secondary complications and improving the fracture healing environment.

There are several limitations of the present study that warrant discussion. As with all modeling approaches, moving into ex vivo validation and calibration of a load altering system will be essential prior to clinical adoption of this concept. This study was not designed with specific parameters in mind but rather as a proof of concept and an initial point from which to build and refine our data. The present study used an unsophisticated method of representing changes in tissue stiffness for the purposes of evaluating fracture

healing effects. The use of a focal fracture zone such as the 60mm length of the composite tissue block would appear to be a closer representation than the homogenous composite tissue block models. The focal fracture zone model resulted in a further transfer of loading away from the pins and towards the distal tissue segment. The logical location to adjust contact pressure and distal loading is beneath the foot in the transfixation cast, however this presents its own set of challenges such as hoof distortion with pressure inside a solid cast resulting in soft tissue damage as well as the ongoing hoof growth which occurs inside the cast. Incidentally, this hoof growth may result in stress and contact pressure changes in the current, unaltered transfixation cast. Our MC3 and transcortical pin model has been validated through the collection of surface strain data corresponding to a single pin location in the metaphyseal region of the bone. More extensive validation of the model, taking into account the cast pin interface attachments and altered loading beneath the distal bone segment, for the purpose of examining the changes seen in this study would help consolidate the findings when this work moves into ex vivo and in vivo phases. Further refinement of the current model could also be achieved by using a model that takes into account the viscoelastic properties of the soft tissues rather than using simple linear elastic material properties. The static, generalized analysis performed here was undertaken to proof the concept and consider both a controllable spacer beneath the hoof as well as changes in the tissue material properties during the fracture healing process.[17] More precise modeling of the relationship between soft tissue changes and progression through fracture healing within a transfixation cast could expand upon these initial results.

In this study, an FE model of the equine distal limb transfixation cast was constructed to explore the question of whether the increasing tissue modulus expected during fracture healing would alter loading conditions and affect bone stresses distal to the transcortical pins. We have shown that this was the case and that the BPI stresses were lower with higher modulus values in the tissues. We have also shown that the stress patterns were altered to be less focal around the pin holes with increasing tissue stiffness. These findings, while a preliminary concept, should help clinicians appreciate that

manipulations following the early fracture healing period may be beneficial in reducing bone pin interface stresses and to increase stresses at the fracture site to improve healing and reduce secondary complications. In addition, efforts to improve fracture alignment and skeletal stiffness, even if insufficient for weight bearing, may reduce the risk of secondary BPI complications and improve fracture healing through a less profound transfer of loading forces through the transcortical pins and cast.

6.5 List of References

1. McClure SR, Watkins JP, Bronson DG, et al. In vitro comparison of the standard short limb cast and three configurations of short limb transfixation casts in equine forelimbs. *Am J Vet Res* 1994;55:1331–1334.

2. Schneider RK, Ratzlaff MC, White KK, et al. Effect of three types of half-limb casts on in vitro bone strain recorded from the third metacarpal bone and proximal phalanx in equine cadaver limbs. *Am J Vet Res* 1998;59:1188–1193.

3. Kraus BM, Richardson DW, Nunamaker DM, et al. Management of comminuted fractures of the proximal phalanx in horses: 64 cases (1983-2001). *J Am Vet Med Assoc* 2004;224:254–263.

4. Joyce J, Baxter GM, Sarrafian TL, et al. Use of transfixation pin casts to treat adult horses with comminuted phalangeal fractures: 20 cases (1993-2003). *J Am Vet Med Assoc* 2006;229:725–730.

5. Lescun TB, McClure SR, Ward MP, et al. Evaluation of transfixation casting for treatment of third metacarpal, third metatarsal, and phalangeal fractures in horses: 37 cases (1994-2004). *J Am Vet Med Assoc* 2007;230:1340–1349.

6. McClure S, Honnas CM, Watkins JP. Managing equine fractures with external skeletal fixation. *Comp Cont Educ Pract Vet* 1995;17:1054–1063.

7. Wu JJ, Shyr HS, Chao EY, et al. Comparison of osteotomy healing under external fixation devices with different stiffness characteristics. *J Bone Joint Surg Am* 1984;66:1258–1264.

8. Chao EY, Aro HT, Lewallen DG, et al. The effect of rigidity on fracture healing in external fixation. *Clin Orthop Relat Res* 1989:24–35.

9. Aro HT, Kelly PJ, Lewallen DG, et al. The effects of physiologic dynamic compression on bone healing under external fixation. *Clin Orthop Relat Res* 1990:260–273.

10. Aro HT, Chao EY. Biomechanics and biology of fracture repair under external fixation. *Hand Clin* 1993;9:531–542.

11. Liu RW, Kim YH, Lee DC, et al. Computational simulation of axial dynamization on long bone fractures. *Clin Biomech* 2005;20:83–90.
12. Claes L, Blakytny R, Göckelmann M, et al. Early dynamization by reduced fixation stiffness does not improve fracture healing in a rat femoral osteotomy model. *J Orthop Res* 2009;27:22–27.
13. Claes L, Blakytny R, Besse J, et al. Late dynamization by reduced fixation stiffness enhances fracture healing in a rat femoral osteotomy model. *J Orthop Trauma* 2011;25:169–174.
14. Williams JM, Elce YA, Litsky AS. Comparison of 2 equine transfixation pin casts and the effects of pin removal. *Vet Surg* 2014;43:430–436.
15. Huiskes R, Chao EY, Crippen TE. Parametric analyses of pin-bone stresses in external fracture fixation devices. *J Orthop Res* 1985;3:341–349.
16. Huiskes R, Chao EY. Guidelines for external fixation frame rigidity and stresses. *J Orthop Res* 1986;4:68–75.
17. Markel MD, Wikenheiser MA, Chao EY. A study of fracture callus material properties: relationship to the torsional strength of bone. *J Orthop Res* 1990;8:843–850.
18. Pai S, Ledoux WR. The compressive mechanical properties of diabetic and non-diabetic plantar soft tissue. *J Biomech* 2010;43:1754–1760.
19. Bartel DL, Davy DT, Keaveny TM. Tissue Mechanics II Soft tissue. In: Bartel DL, Davy DT, Keaveny TM eds. *Orthopaedic biomechanics : mechanics and design in musculoskeletal systems*. Upper Saddle River, NJ. Pearson/Prentice Hall; 2006:121–167.
20. Les CM, Stover SM, Taylor KT, et al. Ex vivo simulation of in vivo strain distributions in the equine metacarpus. *Equine Vet J* 1998;30:260–266.
21. Chen Q, Thouas GA. Metallic implant biomaterials. *Mater Sci Eng: R* 2015;87:1–57.
22. Stevenson M, Barkey M, Bradt R. Fatigue failures of austenitic stainless steel orthopedic fixation devices. *Pract Fail Analy* 2002;2:57–64.
23. Anonymous. Product Data Sheet - 316/316L Stainless Steel. 2007. Available at: www.aksteel.com.
24. Lescun TB, Baird DK, Oliver LJ, et al. Comparison of hydroxyapatite-coated and uncoated pins for transfixation casting in horses. *Am J Vet Res* 2012;73:724–734.

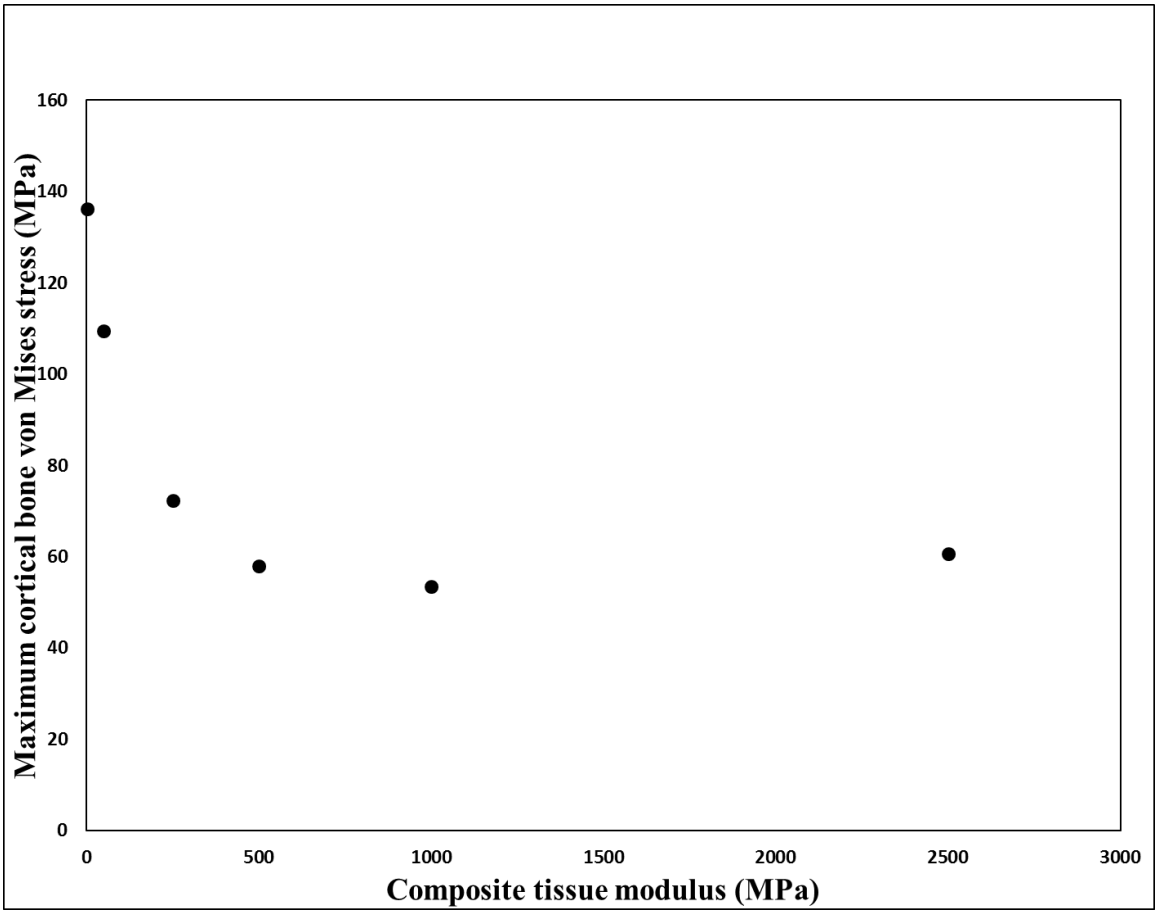

Figure 6.1 Plot of the Young's modulus of a composite tissue block and maximum cortical bone von Mises stress. The composite tissue was a section representing the distal limb segment below transcortical pins in MC3 down to the foot of the transfixation cast. For modulus values of 1000 MPa and higher the maximum von Mises stress in the model was not at a bone-pin interface.

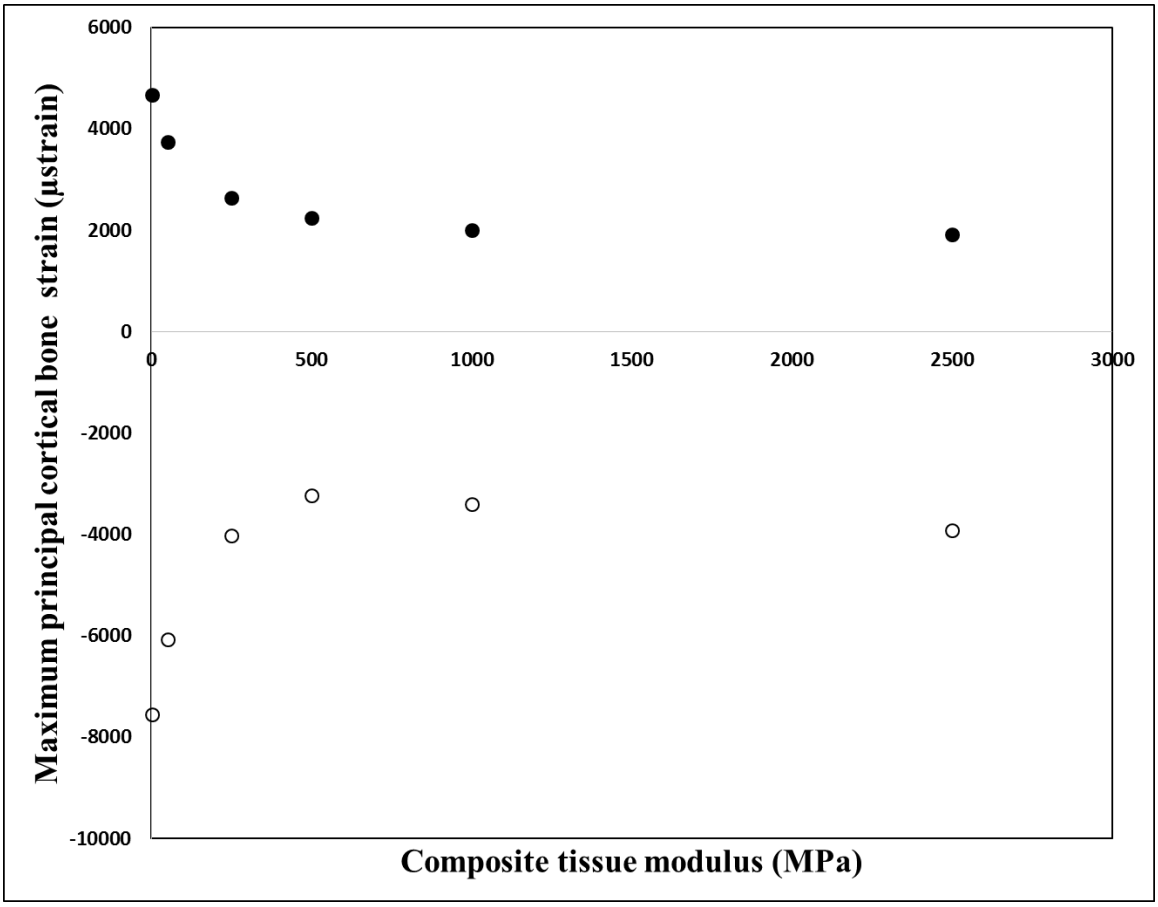

Figure 6.2 Plot of the composite tissue modulus versus maximum (solid circles) and minimum (open circles) principal cortical bone strain. The composite tissue was a section representing the distal limb segment below transcortical pins in MC3 down to the foot of the transfixation cast. For modulus values of 1000MPa and higher the minimum principal strain location was not at a bone-pin interface. For the modulus value of 2500 MPa, the maximum principal strain location was not at a bone-pin interface.

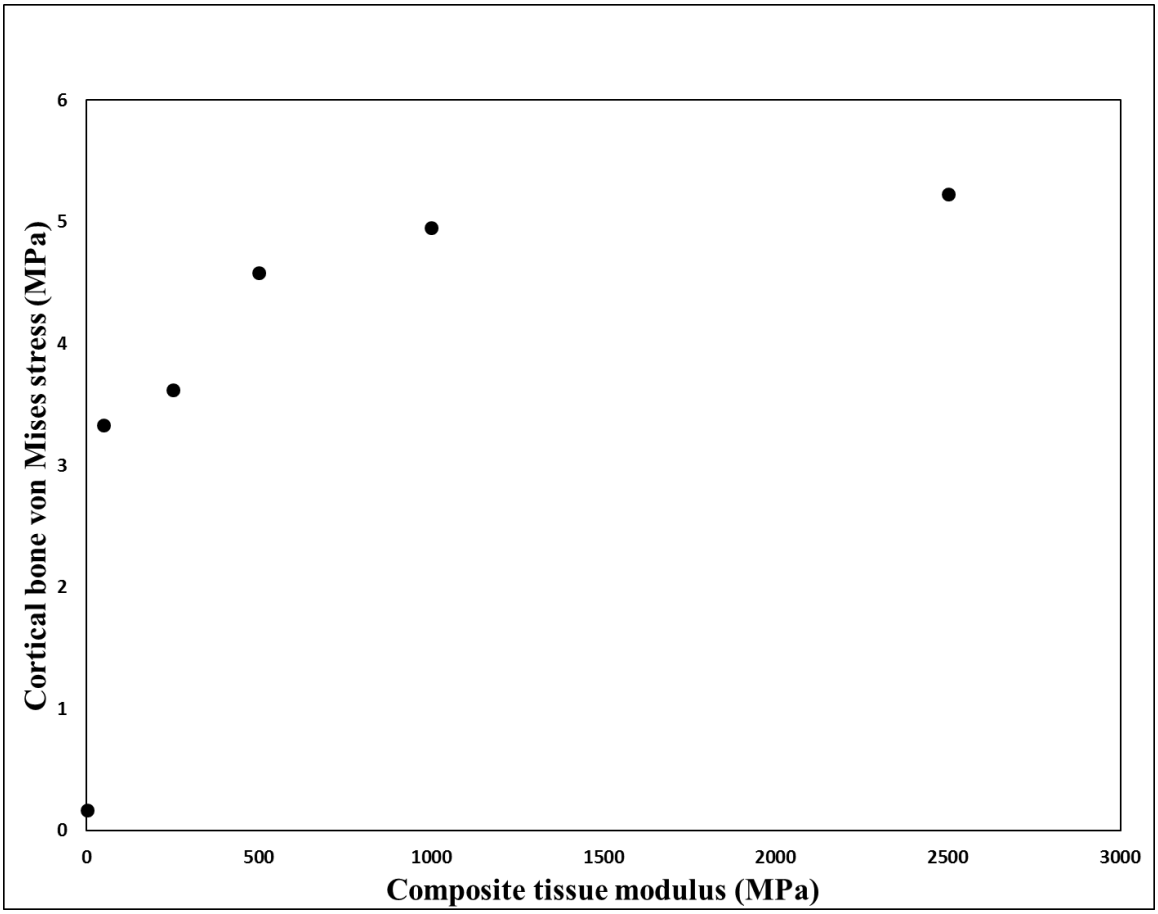

Figure 6.3 Plot of the composite tissue modulus versus cortical bone von Mises stress at a midline point on dorsal MC3 distal to the transcortical pins. The location was in the dorsal cortex, 10mm distal to the distal pin. The composite tissue was a section representing the distal limb segment below transcortical pins in MC3 down to the foot of the transfixation cast.

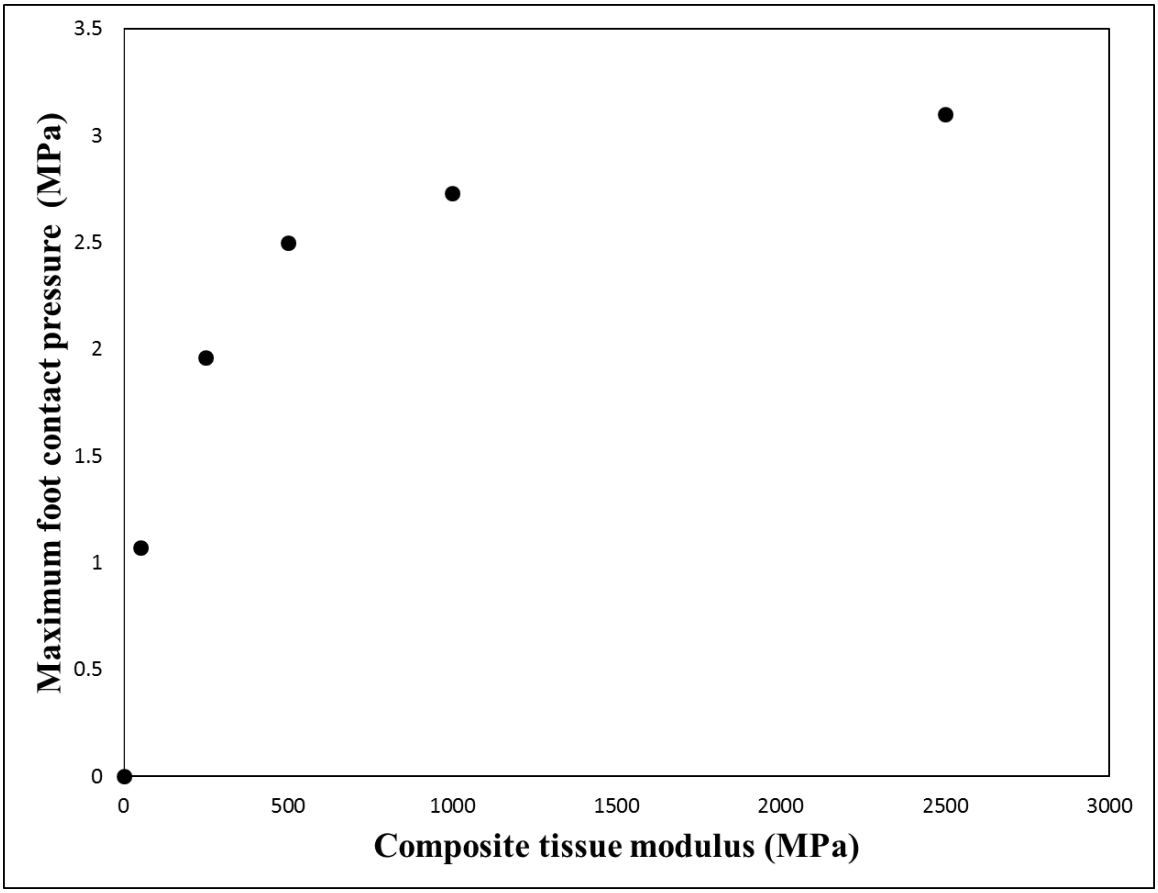

Figure 6.4 Plot of the composite tissue modulus versus maximum foot contact pressure. The composite tissue was a section representing the distal limb segment below transcortical pins in MC3 down to the foot of the transfixation cast. The foot pad was located between the composite tissue section and the cast.

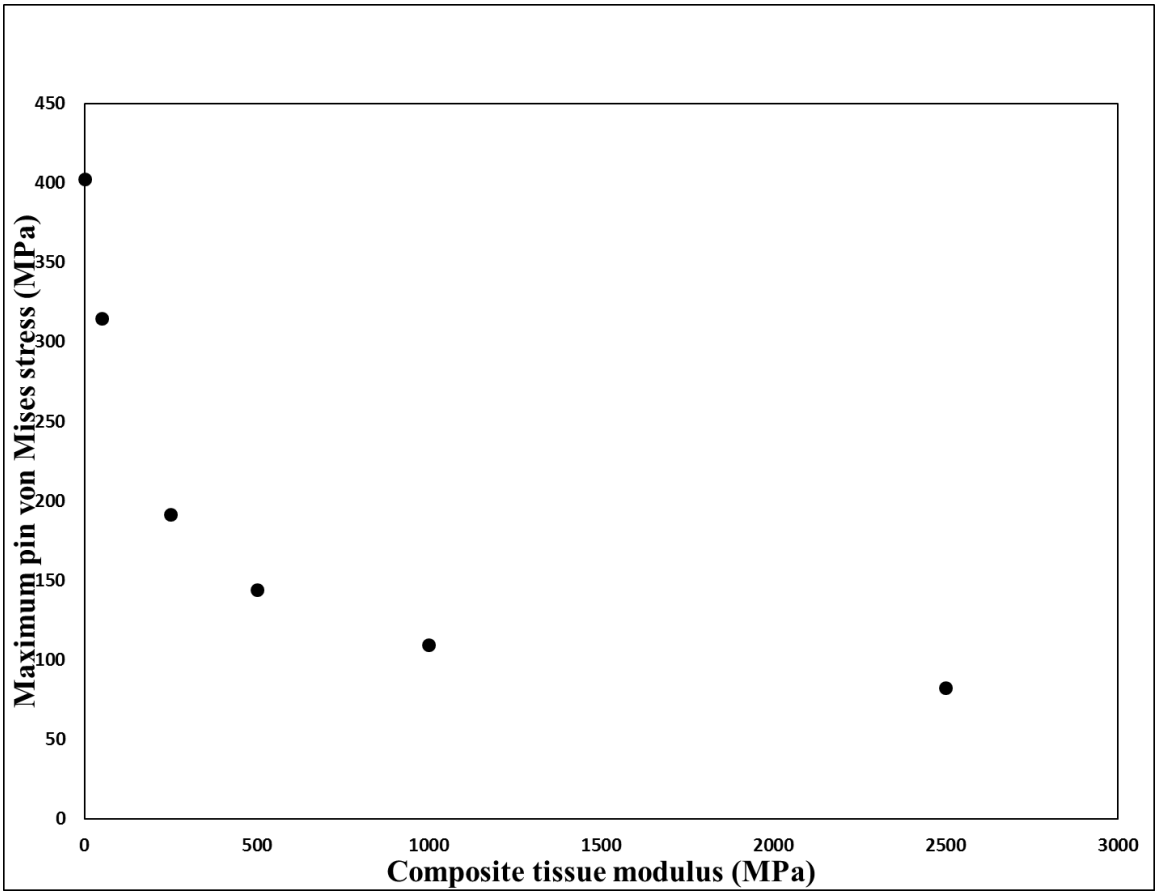

Figure 6.5 Plot of the composite tissue modulus versus maximum pin von Mises stress. The composite tissue was a section representing the distal limb segment below transcortical pins in MC3 down to the foot of the transfixation cast. A foot pad was located between the composite tissue section and the cast.

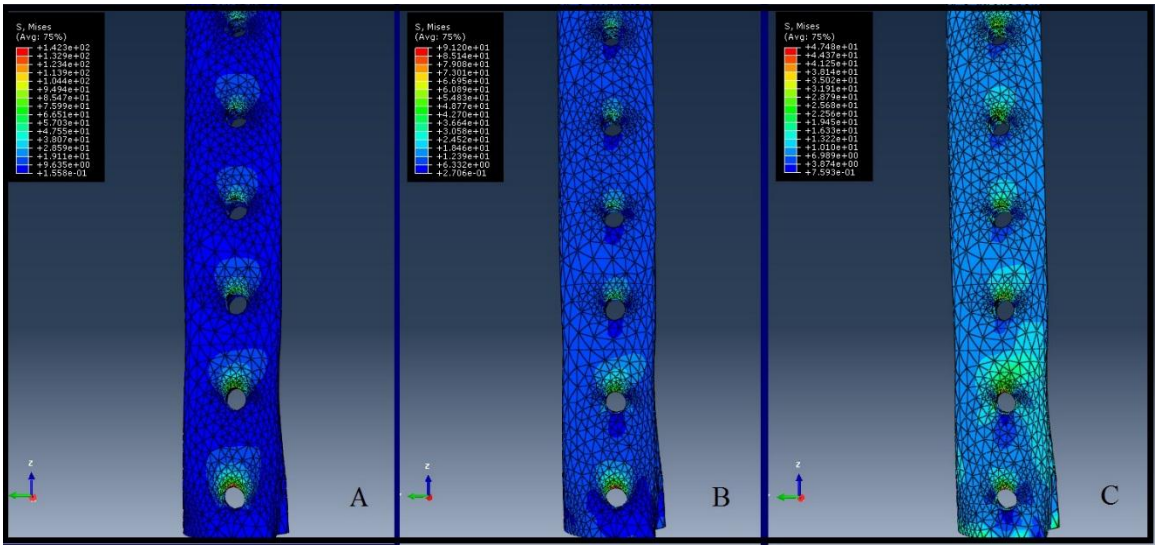

Figure 6.6 Representative images of the cortical bone segment of the third metacarpal bone illustrating the distribution of von Mises stress on the bone and around the pin holes. The results from three different levels of modulus in a material block below the distal bone segment are shown. A. Composite tissue modulus = 0 (suspended). B. Composite tissue modulus = 50 MPa (soft tissue/immediate fracture). C. Composite tissue modulus = 500 MPa (early fracture healing). Note that the legend values in the upper left corner of the images are not the same. Stress distribution can be compared between images, not absolute stress levels.

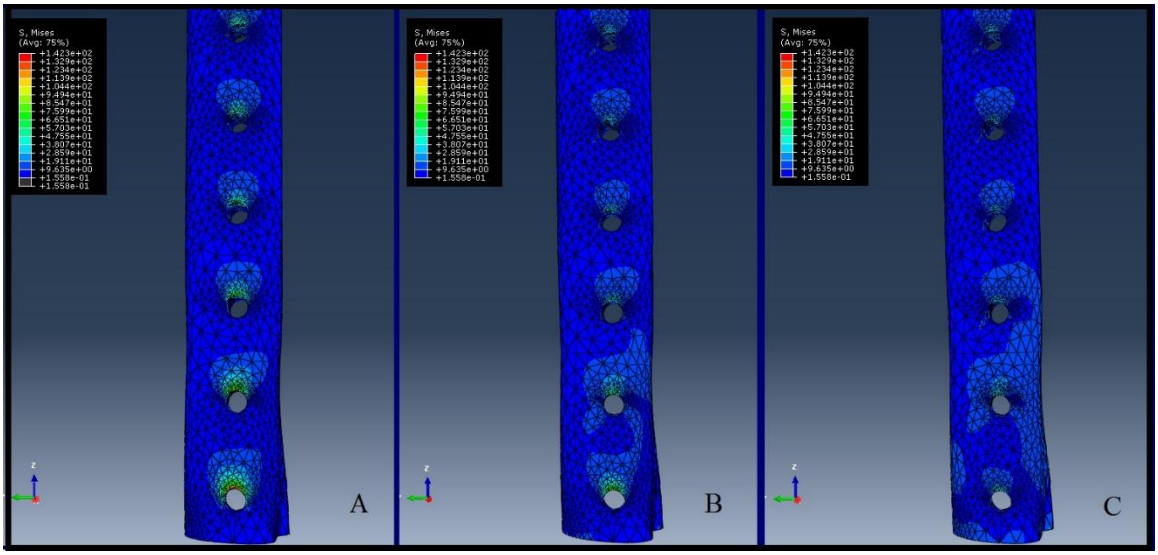

Figure 6.7 Representative images of the cortical bone segment of the third metacarpal bone illustrating the distribution of von Mises stress on the bone and around the pin holes. The results from three different levels of modulus in a material block below the distal bone segment are shown. A. Composite tissue modulus = 0 (suspended). B. Composite tissue modulus = 50 MPa (soft tissue/immediate fracture). C. Composite tissue modulus = 500 MPa (early fracture healing). Note that the image shown is the same as in Figure 6.3 but the legend values in the upper left corner of the images are all the same, allowing direct comparison of stress values between images.

CHAPTER 7. CONCLUSIONS

7.1 Discussion

The **finite element (FE)** models developed in this work were utilized to answer several research questions related to the equine distal limb transfixation cast and specifically the **bone-pin interface (BPI)**. Since bone failure in this location is the underlying mechanism for the most common and clinically significant complications of transfixation casting, the focus of our analysis was predicted stress and strain at the BPI. While not absolute, due to the clinical and biologic factors that always play a role in complications, achieving BPI stress and strain below previously documented cortical bone yield stress and strain values was the underlying assumption used to select preferred bone-pin construct models that would minimize the risk of BPI failure when employed clinically. The ***long term goal*** of this area of study is to improve the safety and reliability of transfixation casting in the horse. The ***central hypothesis*** was that the safety and reliability of equine distal limb transfixation casting with transcortical pins placed in the **third metacarpal bone (MC3)** will ultimately be improved through the use of preferred pin configurations, the promotion of pin stability within the cast, and an approach to control the stress environment within the cast. The 4 specific research goals were:

Research goal #1: To utilize FE models of the equine distal limb transfixation cast to determine transcortical pin configurations which result in BPI stress predictions below the expected yield stress of the equine MC3. Examination of a range of pin parameters, including pin diameter, number, type, spacing, orientation and location within the bone, and material properties found that pin spacing and orientation within the bone had only minor effects on BPI stresses; location within the bone, the type of pin used and the

pin material used had a moderate influence on BPI stresses, while the pin diameter and number were found to be the dominant influences BPI stresses. These findings were consistent with previously reported studies regarding external fixation pins.

Research goal #2: To develop a general approach for determining preferred transcortical pin configurations in anatomic locations other than the MC3 of horses. The unique aspect of transfixation casting compared to external fixation is the manner in which the cast is used to connect all of the transcortical pins into one unit. This prompted an examination of a parameter called total **pin area moment of intertia (PAMi)**. This parameter was found to have a strong relationship with the predicted bone stresses and strains in the FE models developed and it was proposed that this parameter represents the ability of a transfixation cast to resist axial loading. In this way, the total PAMi can be used to compare one transfixation cast construct to another and potentially predict expected bone stress at sites other than MC3 when bone dimensions are considered. A negative power law relationship was found to fit the total PAMi versus maximum bone strain relationship quite well. Taking this relationship further, we used it to help determine preferred bone pin constructs by considering different parameters reflecting the size of the holes required to place the pins, and used these to further refine our selection process.

Research goal # 3: To determine, using preferred transcortical pin configurations, the effect of **cast pin interface (CPI)** stability on BPI stresses in the equine third metacarpal bone. An examination of the CPI and the manner in which it is modeled in the transfixation cast revealed that it has a clear impact on the predicted BPI stresses. Predictions of BPI stresses based on completely fixed pin ends as a boundary condition are likely to underestimate the BPI stress present within the transfixation cast. The sliding surface contact model appears to be the most likely contact condition to represent the true mechanism of interaction between the pin and the cast material. It was concluded that the CPI is an important consideration in the modeling of the equine transfixation cast.

Research goal #4: To determine, using an FE model of the equine distal limb transfixation cast, how changing the loading conditions within the cast distal to the transcortical pins will affect local stresses at the BPI. We used a composite tissue section distal to the transcortical pins to show that increases in tissue stiffness associated with fracture healing decreases the BPI stresses in MC3.

7.2 Future Directions

This work was undertaken in an attempt to answer some of the key questions regarding the mechanics of transfixation casting in the horse. While the conclusions will be helpful in guiding current clinical practice, the study also serves as a starting point for further examination of the transfixation cast BPI as well as the CPI. Additional ex vivo validation studies, in vivo testing of promising bone pin constructs and methods to improve the transfixation cast in terms of BPI stresses will be essential to complete the sketch that has been started here.

Specific future work directly related to the present study should determine which of the parameters evaluated or assumed conditions used were most influential on BPI stresses. A sensitivity analysis could be performed from the data generated here and combined with a more complete validation of specific pin configurations. Future work could also investigate a pin surface that may resist the propensity for loosening by promoting osseointegration. The findings of this study could make the potential for success higher in developing an osseointergating pin the horse through reductions in BPI stresses and lower interfacial strains. The advantages of osseointegration of temporary transcortical pins can be questioned, however improved patient comfort and cortical bone density maintenance surrounding the pins rather than its loss, would both offer significant advantages to the horse. In considering the entire fracture healing process that occurs when transfixation casting is employed a future area of investigation may be to examine, using the current FE models, whether fracture dynamization or strain based control of loading is feasible in the clinical patient. While rigid fixation is beneficial early in the healing process,

modulation of the strain environment at the fracture site later in the healing process would be desirable. This could be achieved with a better understanding of the transfixation cast mechanics and may be addressed through the use of FE models developed in the present study.

VITA

VITA

Timothy B. Lescun

GENERAL INFORMATION

Current Address

Department of Veterinary Clinical Sciences
College of Veterinary Medicine, Purdue University
625 Harrison Street, West Lafayette, IN 47907-2026
Telephone: (765) 494-6653
E-mail: tlescun@purdue.edu

Academic Record

2009-Present	Ph.D. candidate, Purdue University
	Passed preliminary examination, April 2012
2007	Educational Commission for Foreign Veterinary Graduates (ECFVG) certification
2002	M.S., Purdue University
1994	B.V.Sc. (Hons), University of Melbourne, Australia

Specialty Certification

2000	Board Certified in Surgery, American College of Veterinary Surgeons (ACVS)

Employment

Academic Appointments

July 2008-Present	Associate Professor, Department of Veterinary Clinical Sciences, College of Veterinary Medicine, Purdue University, West Lafayette, IN
Jan. 2002-June 2008	Assistant Professor, Department of Veterinary Clinical Sciences, College of Veterinary Medicine, Purdue University, West Lafayette, IN
July 1999-June 2000	Visiting Instructor, Large Animal Surgery, Department of Veterinary Clinical Sciences, College of Veterinary Medicine, Purdue University, West Lafayette, IN

Other Professional Appointments

July 2000-Dec. 2001	Associate Veterinarian, Goulburn Valley Equine Hospital, 905B Goulburn Valley Highway, Congupna, Victoria 3633, Australia
July 1996-June 1999	Resident, Large Animal Surgery, Department of Veterinary Clinical Sciences, College of Veterinary Medicine, Purdue University, West Lafayette, IN
Dec. 1994-June 1996	Intern, Goulburn Valley Equine Hospital, 905B Goulburn Valley Highway, Congupna, Victoria 3633, Australia

Awards and Honors

2012	The Weedon Faculty Recognition Award, PVM
2010, 2005	Student Recognition for Excellence in Teaching, PVM
2004	Best Podium Presentation, Veterinary Orthopedic Society Annual Meeting, Big Sky, MT
1999	Second Place, Osborne Clinical Investigator Award, Phi Zeta Honorary Society, Omicron Chapter

1999	Gamma Sigma Delta Honorary Society
1998	Finalist, Mark Bloomberg Award, Veterinary Orthopedic Society Annual Meeting, Snowmass, CO
1998	Phi Zeta Honorary Society for Veterinary Medicine, Omicron Chapter
1992, 1991	Newman College Academic Scholarship
1989	Xavier High School Dux (Highest Academic Score)
1989	Caltex All Rounder Award (Achievement in all areas of school)

Licenses

2007-Present	Indiana (USDA Federal accreditation - Category II)
1994-2002	Victoria, Australia

Memberships in Academic, Professional, and Scholarly Societies

1998-Present	Phi Zeta Honor Society (Omicron Chapter)
2000-Present	American College of Veterinary Surgeons (ACVS)
2002-Present	American Veterinary Medical Association (AVMA)
2003-Present, 1998-2001	Veterinary Orthopedic Society
2005-Present	Indiana Veterinary Medical Association
2007-Present	American Association of Equine Practitioners (AAEP)
1993-1996	Australian Veterinary Association
1994-1996	Australian Equine Veterinary Association